

**An Experimental and Modelling Investigation of the  
Rheological Properties of Water/Oil/Gas Hydrate Mixtures**

By

**Hossein Moradpour**

Submitted for the degree of **Doctor of Philosophy** in  
**Petroleum Engineering**

**Heriot-Watt University**  
**Institute of Petroleum Engineering**  
**November 2011**

The copyright in this thesis is owned by the author. Any quotation from the thesis or use of any of the information contained in it must acknowledge this thesis as the source of the quotation or information.

## ABSTRACT

In the search for new conventional oil and gas reserves, operators are moving into more challenging reservoirs. The move of the oil and gas industry into increasingly deeper and colder locations and/or production from mature reservoirs, in which water cut can be relatively high, has faced the industry with a major challenge, because the traditional hydrate prevention methods are very expensive (i.e., high CAPEX and/or OPEX) and even, in some cases, unfeasible. In this context, hydrate management may be more economical than hydrate avoidance. Forming dispersed hydrate particles using Anti-agglomerants (AAs) is currently an attractive option for overcoming hydrate blockage problems, especially for long tieback and high subcooling systems.

This study mainly focuses on the rheological behaviour of hydrate slurry in high water-cut systems (from 60 to 80%), as these are probably the most difficult conditions for managing flow assurance issues using conventional techniques.

To engineer a controlled formation of slurry flow made up of hydrate particles in high water cut systems, it is critical that the flow characteristics of water-oil emulsions and the hydrate slurries are well understood.

In high water cut systems, by converting a certain amount of water phase into hydrate particles, the behaviour of hydrate slurry will be strongly dependent on the water-oil emulsion which acts as a carrier fluid to the hydrate particles. In this case, the behaviour of water-oil emulsions can depend on many parameters, such as the presence of natural surfactants, AAs, salt and even hydrate particles, might affect the morphology of the emulsions. So far, however, in terms of hydrate slurries, there has been very little research on the morphology of water-oil emulsions in the presence of AAs and hydrate particles. This work is initially focused on the effect of these parameters on the stability of water-in-oil (W/O) emulsions, oil-in-water (O/W) emulsions and phase inversion from W/O to O/W and vice versa.

The rheological study of hydrate slurries is a difficult subject and to date there has been little study on this issue. Most of these studies have focused on low water cut systems and there is a lack of data specifically relating to hydrate slurries in high water cut systems. In this research work, which concentrates on the rheological behaviour of hydrate slurries in

high water cut systems, the agglomeration of hydrate particles has been shown to be responsible for the rheological behaviour of water/oil/hydrate mixtures through viscosity measurements from an in-house high pressure Helical Tube Impeller (HTI) viscometer and pressure drop measurements from a pilot-scale flow loop. The effect of oil composition, AA concentration, water cut, shear rate and salt concentration has been investigated on the rheological behaviour of hydrate slurries in high water cut systems.

Existing models to predict viscosity of hydrate slurry do not consider the effect of water-oil emulsion, which acts as a carrier fluid for transporting hydrate particles. It will lead to deviations between model and experimental data specifically relating to hydrate slurry in high water cut systems. In this study a model has been developed to predict the viscosity of water-oil emulsion in the presence of hydrate particles in high water cut systems using the concept of a bimodal mixture. In the model, water-oil emulsion and hydrate aggregates in the liquid continuous phase are treated separately as unimodal models. A new modification of Mills' (1985) equation has been applied to describe the viscosity of unimodal hydrate suspension. The model has been validated using experimental data acquired by the HTI viscometer for water/oil/hydrate mixtures in the presence of different AA concentrations and different oil compositions. The predictions of the proposed model are in good agreement with experimental data for both experiments performed with oil-in-water and water-in-oil emulsions.

*I dedicate this thesis to my lovely son **Parsa** and my wife **Dr. Panteha Ghahri** who has always helped me and believed that I could do it.*

## **ACKNOWLEDGEMENTS**

It is with immense gratitude that I acknowledge the support and help of my principal supervisor, Professor Bahman Tohidi. I have always benefited from his expertise supervision, brilliant ideas, valuable advice and extensive knowledge. His careful editing contributed enormously to the production of this thesis. I truly like my time working with him.

I greatly appreciate Dr. Antonin Chapoy for his constructive guidance, generous support and inspired suggestions on this thesis.

I am also very grateful to my examiners, Dr. Roar Larsen and Dr. Jingsheng Ma for taking their time to read my thesis and sharing their valuable comments and suggestions.

My deepest thanks go to my wife Dr. Panteha Ghahri and my lovely son Parsa. I cannot thank them enough for their love, support and their belief in me.

I would like to thank Mr. Rod Burgass for his support, fruitful comments and discussions. Additionally, I am indebted to all of my colleagues in the Centre for Gas Hydrate Research who supported me during this study.

The financial support of the Institute of Petroleum Engineering, Heriot-Watt University, through the award of a full scholarship to conduct this work is sincerely acknowledged.

# Table of Contents

<b>ABSTRACT .....</b>	<b>ii</b>
<b>ACKNOWLEDGEMENTS .....</b>	<b>v</b>
<b>Table of Contents.....</b>	<b>vi</b>
<b>List of Figures .....</b>	<b>ix</b>
<b>List of Tables.....</b>	<b>xiii</b>
<b>List of Publications .....</b>	<b>xiv</b>
<b>CHAPTER 1 INTRODUCTION.....</b>	<b>1</b>
1.1 INTRODUCTION.....	1
1.2 REFERENCES .....	5
<b>CHAPTER 2 GAS HYDRATE INHIBITION AND MANAGEMENT-LITERATURE STUDY .....</b>	<b>6</b>
2.1 BACKGROUND.....	6
2.2 MOLECULAR STRUCTURE OF GAS HYDRATES .....	6
2.3 PHASE EQUILIBRIUMS OF GAS HYDRATES.....	9
2.4 GAS HYDRATE PROBLEMS IN OIL AND GAS INDUSTRY.....	11
2.5 STRATEGIES FOR SOLVING GAS-HYDRATE PROBLEMS.....	13
2.5.1 Current Methods Of Preventing Gas Hydrate Blockage.....	14
2.5.1.1 Physical Methods .....	14
2.5.1.2 Thermodynamic Inhibitors.....	15
2.5.1.3 Low Dosage Hydrate Inhibitors.....	17
2.6 HYDRATE MANAGEMENT -COLD FLOW TECHNOLOGY.....	23
2.6.1 The NTNU Cold Flow Technology (Gudmundsson's Concept) .....	24
2.6.2 The SINTEF-BP's Cold Flow Technology.....	26
2.6.3 HYDRAFLOW: A Novel 'Wet Cold Flow' Concept Suggested by Heriot Watt University ..	28
2.6.3.1 Loop Concept.....	29
2.7 REFERENCES.....	32
<b>CHAPTER 3 WATER-CRUDE OIL EMULSIONS WITH APPLICATION TO GAS HYDRATES ..</b>	<b>37</b>
3.1 INTRODUCTION.....	37
3.2 CHEMISTRY AND CLASSIFICATION OF CRUDE OILS.....	38
3.3 BIODEGRADATION OF CRUDE OIL .....	43
3.4 FUNDAMENTALS OF WATER-OIL EMULSIONS.....	44
3.4.1 Classification And Formation Of Emulsions .....	44
3.4.2 Stability of Emulsions.....	46
3.4.3 Film Drainage and Interfacial Viscosity .....	49
3.4.4 Factors Affecting Surface Films and Stability.....	50
3.5 HYDRATE FORMATION AND AGGLOMERATION IN EMULSIONS .....	54
3.6 NATURAL ANIT-AGGLOMERANT COMPONENTS IN CRUDE OIL .....	56
3.7 REFERENCES.....	60
<b>CHAPTER 4 EXPERIMENTAL APPARATUS .....</b>	<b>66</b>
4.1 INTRODUCTION.....	66
4.2 DETECTION OF EMULSION TYPE .....	66
4.3 PHASE INVERSION POINT MEASUREMENT SETUP.....	67
4.4 RHEOLOGICAL STUDY OF HYDRATE SLURRIES USING HIGH PRESSURE AUTOCLAVE CELL EQUIPPED WITH HELICAL TUBE IMPELLER (HTI).....	68

4.4.1. High pressure Autoclave Cell- Small Scale Viscometer .....	70
4.5 FLOW LOOP SYSTEM.....	72
4.5.1 Design.....	73
4.5.2 Main Pump .....	73
4.5.3 Storage Tank.....	76
4.5.4 Seal Unit System .....	76
4.5.5 Gas Make-Up System.....	77
4.5.6 Cooling System.....	78
4.5.7 Instrumentation and Data Acquisition .....	78
4.6 REFERENCES.....	80

## **CHAPTER 5 MORPHOLOGY OF WATER-OIL EMULSIONS WITH AND WITHOUT HYDRATES..... 82**

5.1 INTRODUCTION.....	82
5.2 MORPHOLOGY OF WATER-OIL EMULSIONS WITHOUT HYDRATES .....	83
5.2.1 Emulsion Stability Measurements .....	83
5.2.1.1 Experimental Set-Up and Material .....	84
5.2.1.2 Measurements of the Stability of the Prepared Emulsions.....	85
5.2.1.3 Results and discussion .....	86
5.2.2 Phase Inversion in Liquid-Liquid Dispersions .....	91
5.2.2.1 Experimental setup and materials .....	92
5.2.2.2 Phase inversion point determination .....	92
5.2.2.3 Results and discussion .....	93
5.3 EFFECT OF HYDRATE FORMATION ON PHASE INVERSION IN HIGH WATER CUT SYSTEMS .....	103
5.3.1 Experimental Set-Up and Materials.....	104
5.3.2 Experimental Procedure.....	105
5.3.3 Results and Discussion .....	106
5.4 CONCLUSIONS .....	111
5.5 REFERENCES.....	113

## **CHAPTER 6 EXPERIMENTAL INVESTIGATION ON RHEOLOGICAL BEHAVIOUR OF HYDRATE SLURRIES IN HIGH WATER CUT SYSTEMS..... 116**

6.1 INTRODUCTION.....	116
6.2 EXPERIMENTAL EQUIPMENT .....	118
6.3 MATERIALS .....	118
6.4 RHEOLOGICAL STUDY OF HYDRATE SLURRIES IN HIGH WATER CUT SYSTEMS.....	118
6.4.1 Results and Discussion .....	119
6.4.1.1 Evaluation of the performance of AAs in high water cut systems .....	119
6.4.1.2 High water cut experiments with oil (A).....	122
6.4.1.3 High water cut experiments with oil (B) and oil (C).....	127
6.4.1.4 Comparison of hydrate transportability of high water cut systems with different oil compositions .....	130
6.4.1.5 Effect of mixer speed/shear rate on rheological behaviour of water/oil/hydrate mixtures in high water cut systems .....	135
6.5 EFFECT OF OIL BLENDING ON RHEOLOGICAL BEHAVIOUR OF HYDRATE SLURRIES.....	138
6.6 EFFECT OF HYDRATE FORMATION AND DISSOCIATION ON EMULSION STABILITY IN HIGH WATER CUT SYSTEMS .....	141
6.7 EXAMINATION OF THE EFFECT OF SALT (NaCl) CONCENTRATION ON THE PERFORMANCE OF AAS IN HIGH WATER CUT SYSTEMS .....	144
6.7.1 Materials and Experimental Procedure.....	144
6.7.2 Results and Discussion .....	145
6.8 SHUT-IN AND START-UP .....	147
6.8.1 Experimental Procedure.....	148
6.8.2 Results and Discussion .....	148
6.8.2.1 No hydrate before shut-in .....	148

6.8.2.2	Hydrates present before shut-in .....	149
6.9	CONCLUSIONS .....	151
6.10	REFERENCES .....	153
<b>CHAPTER 7 EXPERIMENTAL STUDY USING A SATURATED FLOW LOOP .....</b>		<b>157</b>
7.1	INTRODUCTION .....	157
7.2	EXPERIMENTAL EQUIPMENT .....	158
7.3	MATERIALS .....	158
7.4	OPERATIONAL PROCEDURE .....	158
7.5	RESULTS AND DISCUSSION.....	159
7.5.1	Effect of AA Concentration .....	160
7.5.2	Effect of Salt on AA Performance .....	162
7.5.3	Effect of Pump Speed/ Shear Rate .....	165
7.5.4	The Effect of Water Cut .....	166
7.5.5	Comparison of Flow Loop and Small Scale Results.....	167
7.6	CONCLUSIONS .....	170
7.7	REFERENCES .....	172
<b>CHAPTER 8 BIMODAL MODEL FOR PREDICTING THE EMULSION- HYDRATE MIXTURE VISCOSITY IN HIGH WATER CUT SYSTEMS.....</b>		<b>173</b>
8.1	INTRODUCTION .....	173
8.2	APPLICATION OF THE BIMODAL MODEL TO PREDICT THE VISCOSITY OF A WATER/OIL/HYDRATE MIXTURE .....	174
8.2.1	Bimodal Suspensions.....	174
8.2.2	Unimodal Suspension -Viscosity of Hard-Sphere Suspensions.....	177
8.2.3	Unimodal Suspension -Viscosity of Pure Emulsion .....	178
8.2.4	Development of a New Viscosity Equation for the Relative Viscosity of Hydrate Slurry ....	180
8.3	MODEL DESCRIPTION.....	182
8.4	RESULTS AND DISCUSSION.....	185
8.4.1	Comparison of Existing Hard-Sphere Models with Experimental Data .....	186
8.4.2	Effect of Anti-Agglomerant Concentrations.....	188
8.4.3	Effect of Liquid Hydrocarbon Compositions .....	194
8.4.4	Correlation for the Trapped Liquid Factor, $K_v$ .....	196
8.5	CONCLUSIONS .....	199
8.6	REFERENCES .....	200
<b>CHAPTER 9 CONCLUSIONS AND RECOMMENDATIONS .....</b>		<b>203</b>
9.1	INTRODUCTION .....	203
9.2	CONCLUSIONS .....	203
9.2.1	Experimental Study to Investigate Morphology of Water-Oil Emulsions .....	203
9.2.2	Rheological Study of Water/Oil/Hydrate Mixtures Using HTI Viscometer and Flow Loop.	204
9.2.3	Proposed model to predict apparent viscosity of water/oil/hydrate mixture.....	206
9.3	RECOMMENDATIONS .....	207
9.4	REFERENCES .....	209



## List of Figures

Figure 2. 1 Simple illustration of a gas molecule encapsulated by a framework of water. Image taken from the homepage of Hydrate Group at Heriot Watt University .....	7
Figure 2. 2 The three most common hydrate unit crystal structures (Sloan, 2003). .....	8
Figure 2. 3 Phase Diagrams of Different simple natural gases hydrocarbons that form hydrates. (modified by Sloan (2008) from the plot developed by (Katz et al., 1959)).....	10
Figure 2. 4 Phase diagram of a multi-component hydrocarbon mixture that form hydrates (Sloan and Koh, 2008). .....	11
Figure 2. 5 Typical pipeline conditions from wellhead towards platform with intrusion into the hydrate stability zone (Sloan and Koh, 2008). .....	12
Figure 2. 6 Hydrate accumulation retrieved at the pig-catcher of a Petrobras rig (Photo courtesy of Petrobras) (Clark et al., 2008). .....	12
Figure 2. 7 Structure of good quaternary ammonium or phosphonium hydrate growth inhibitors, where M=N or P and at least two of the R groups are n-butyl, n-pentyl, or isopentyl. Figure taken from Kelland (2006).....	21
Figure 2. 8 Structure of Shell's quaternary AA chemicals, ( $R_1$ =long chain hydrocarbon tail; $R_2$ =n-butyl, n-pentyl, or isopentyl; M=N or P; X is an optional spacer group). Figure taken from Kelland (2006).....	21
Figure 2. 9 Schematic of AA interactions on a hydrate crystal. ....	22
Figure 2. 10 Hydraulic gradient for 32% hydrate-in-water slurry plotted against Reynolds number (Andersson, 1999).....	25
Figure 2. 11 Hydraulic gradient for 12.7 % hydrate-in-oil (diesel fuel) slurry plotted against Reynolds number (Andersson, 1999).....	25
Figure 2. 12 Schematic description on the field implementation of NTNU concept (Gudmundsson, 2002). .	25
Figure 2. 13 Agglomeration of hydrate particles in the bulk fluid and on the pipe wall (Lund and Larsen, 2000). .....	27
Figure 2. 14 A schematic description of the hydrate reactor, SINTEF- BP (Larsen et al., 2001). ....	28
Figure 2. 15 Illustration of the <i>HYDRAFLOW</i> pipeline 'loop' concept (Haghighi et al., 2007).....	30
Figure 3. 1 Surface active components in crude oils can adsorb to hydrate surfaces and change the wettability which reduces the agglomeration of hydrate particles (Erstad, 2009) .....	38
Figure 3. 2 Schematic of SARA fractionation of crude oils (Auflem, 2002). ....	40
Figure 3. 3 Example of asphaltene molecule (Langevin et al., 2004).....	41
Figure 3. 4 Resin solvated asphaltene aggregate (Spiecker, 2001).....	42
Figure 3. 5 Common destabilization mechanisms of water-in-oil emulsion (Aichele, 2009). ....	47
Figure 3. 6 Some mechanisms of emulsion stability(Zerpa et al., 2011).....	48
Figure 3. 7 Gibbs-Marangoni effect at oil-water interface (Aske, 2002).....	50
Figure 3. 8 Accumulation of asphaltene aggregates at the oil-water interface (Spiecker, 2001).....	52
Figure 3. 9 Droplet stabilization by very fine solids (Kokal, 2006) .....	53
Figure 3. 10 Wetting behaviour of fine solid in the water-oil interface (Kokal, 2006). ....	54
Figure 3. 11 Conceptual picture for a) hydrate plug formation from a water-in-oil emulsion      b) conversion of a water droplet to hydrate (Balakin, 2010) .....	55
Figure 3. 12 Summary of adhesion forces between cyclopentane hydrates particles for Caratinga crude oil in unmodified, deasphalted, and pH-14extracted conditions (Dieker et al., 2009) .....	59
Figure 4. 1 Setup for hydrate free phase inversion point measurement experiments. ....	68
Figure 4. 2 Flow diagram of the high pressure autoclave cell. ....	71
. Figure 4. 3 The overall view of the saturated flow loop.....	74
Figure 4. 4 Flow diagram of the saturated flow loop.....	75
Figure 4. 5 Flow diagram of the main pump seal unit. ....	77
Figure 5. 1 Appearance of the samples used in the bottle tests for W/O emulsion of oil (A) after 24 hrs when the aqueous phase is; a) pure deionised water, b) deionised water with 1.0 wt. % AA, c) deionised water with 1.0 wt. % AA and 5 wt. % NaCl. ....	87
Figure 5. 2 Bottle test results for W/O emulsions of oil (B) for different AA and salt concentrations. ....	88
Figure 5. 3 Appearance of the samples used in the bottle tests for W/O emulsions of oil (B) a) untreated water after 135 minutes, b) treated with 0.3 wt. % AA after 105 minutes, c) treated with 1 wt. % AA after 85 minutes, d) treated with 1 wt. % AA and 5 wt. % NaCl after 52 minutes.....	89
Figure 5. 4 Anti-agglomerants displace the natural surfactants in the interface film. ....	90
Figure 5. 5 Variation of the emulsion conductivity through a dynamic inversion produced by an increase in internal phase ratio, Arrows indicate the direction of change (Becher, 1988). ....	91

Figure 5. 6 Oil (A) emulsion with about 85% water cut turned into a thick paste. Aqueous phase is deionised water. Figure (b) shows the water cannot be dissolved into the emulsion and it remained as a separate phase. ....	94
Figure 5. 7 Oil (B) emulsion with about 83% water cut turned into a soft gel. Aqueous phase is pure deionised water. Figure (b) shows the water cannot be dissolved in the emulsion and it remained as a separate phase. ....	94
Figure 5. 8 Motor current as a function of water cut for different AA concentrations (W/O to O/W emulsion). The phase inversion occurs when the motor current approach a maximum value and suddenly drops off. ....	96
Figure 5. 9 Motor current and conductivity as a function of water cut. Phase inversion point occurs when conductivity/mixer power change abruptly. ....	96
Figure 5. 10 Phase inversion point as a function of AA concentration in the aqueous phase (oil (A)). ....	97
Figure 5. 11 The phase inversion point as a function of AA concentration in the aqueous phase (oil (B)). ....	98
Figure 5. 12 Water cut at phase inversion point from W/O to O/W emulsion as a function of AA concentration in the presence or absence of 5 wt. % NaCl (oil (A)). ....	99
Figure 5. 13 Water cut at phase inversion point from W/O to oil-in water emulsion as a function of AA concentration in the presence or absence of 5 wt. % NaCl (oil (B)). ....	99
Figure 5. 14 Motor current and electrical resistance of emulsion as a function of oil volume fraction (O/W to W/O emulsion). Phase inversion results in a sharp increase in motor current and electrical resistance. ....	101
Figure 5. 15 Phase inversion point as a function of AA concentration for O/W to W/O emulsion (in the presence and absence of salt). ....	101
Figure 5. 16 Comparison of phase inversion point for two types of W/O and O/W emulsions as a function of AA concentration in the presence and absence of salt. ....	102
Figure 5. 17 W/O emulsion stability characterised based on separated water as a function of time. ....	105
Figure 5. 18 Effect of emulsion type on the mixture viscosity as a function of hydrate volume fraction (60% water cut, 5 wt% NaCl, 1.0 wt% AA), oil (A). ....	107
Figure 5. 19 Effect of emulsion type on the mixture viscosity as a function of hydrate volume fraction (60% water cut, 5 wt% NaCl, 1.0 wt% AA), oil (B). ....	107
Figure 5. 20 Effect of emulsion type on the mixture viscosity as a function of hydrate volume fraction for oil (A) (60% water cut, 5 wt% NaCl, 0.3-2.0 wt% AA). ....	109
Figure 5. 21 Effect of emulsion type on the mixture viscosity as a function of hydrate volume fraction for oil (B) (70% water cut, 5 wt% NaCl, 0.3-2.0 wt% AA). ....	109
Figure 5. 22 Hydrate volume fractions at phase inversion point $\phi_h^{inv}$ from water continuous to oil continuous emulsions as a function of AA concentration, 60% water cut. ....	110
Figure 6. 1 Apparent viscosity of water/oil/hydrate mixture as a function of hydrate volume fraction to evaluate performance of different AAs (1 wt% AA) in 60% water cut. ....	121
Figure 6. 2 Hydrates in crude oil (A) with 60% water cut. The hydrate value represented by arrows in the figure indicates the hydrate volume fractions at which the apparent viscosity is about 600 cP. ....	124
Figure 6. 3 Hydrates in crude oil (A) with 70% water cut. The hydrate value represented by arrows in the figure indicates the hydrate volume fractions at which the apparent viscosity is about 600 cP. ....	124
Figure 6. 4 Hydrates in crude oil (A) with 80% water cut. The hydrate value represented by arrows in the figure indicates the hydrate volume fractions at which the apparent viscosity is about 600 cP. ....	125
Figure 6. 5 Hydrate volume fractions at about 600 cP as a function of AA concentration for different water cuts. ....	128
Figure 6. 6 Hydrates in crude oil (B) with 60% water cut at different AA concentrations. ....	129
Figure 6. 7 Hydrates in crude oil (C) with 60% water cut at different AA concentrations. ....	129
Figure 6. 8 Apparent viscosity of water/oil/hydrate mixture as a function of hydrate volume fraction for 60% water cut and 0.3 wt. % AA. ....	132
Figure 6. 9 Apparent viscosity of water/oil/hydrate mixture as a function of hydrate volume fraction for 60% water cut and 0.6 wt. % AA. ....	132
Figure 6. 10 Apparent viscosity of water/oil/hydrate mixture as a function of hydrate volume fraction for 60% water cut and 1 wt. % AA. ....	133
Figure 6. 11 Apparent viscosity of water/oil/hydrate mixture as a function of hydrate volume fraction for 60% water cut and 2 wt. % AA. ....	133
Figure 6. 12 Final water conversions versus AA concentration for different water-oil emulsions with 60% WC. ....	134

Figure 6. 13 Comparison of required AA concentration to transport a certain hydrate volume fraction for different oil-water emulsion systems, 60% water cut. ....	134
Figure 6. 14 Apparent viscosity of water/oil/hydrate mixture as a function of hydrate volume fraction for two different mixer speeds of 200 and 400 RPM. Water cut is 60% with 0.3 wt. % AA. ....	136
Figure 6. 15 Apparent viscosity of water/oil/hydrate mixture as a function of hydrate volume fraction for two different mixer speeds of 200 and 400 RPM. Water cut is 60% with 2.0 wt. % AA. ....	137
Figure 6. 16 Water conversion rates for tests with 60% water cut and 0.3 wt. % AA at different mixer speeds. ....	137
Figure 6. 17 Water conversion rates for tests with 60% water cut and 2.0 wt. % AA at different mixer speeds. ....	138
Figure 6. 18 Hydrate transport for blends of crude oil (A) and diesel oil (C) with ratio of 20/80. Water cut is 60% and AA concentrations are 0.6 wt. % of aqueous phase. ....	140
Figure 6. 19 Hydrate transport for blends of crude oil (A) and diesel oil (C) with ratio of 20/80. Water cut is 60% and AA concentrations are 2.0 wt. % of aqueous phase. ....	140
Figure 6. 20 Emulsion samples taken from a) Step1, before hydrate formation (2 hours after sampling) b) Step 4, after hydrate dissociation (3.5 minutes after sampling). ....	142
Figure 6. 21 Schematic representation of phase inversion from W/O to O/W emulsion for 70% water cut system tested in this study during the hydrate formation and dissociation process. Adapted from Greaves et al. (2008). ....	143
Figure 6. 22 Effect of salt concentration on the mixture viscosity as a function of hydrate volume fraction. ....	146
Figure 6. 23 Hydrate volume fractions for the mixture viscosity at 600 cP as a function of NaCl concentration. ....	147
Figure 6. 24 Shut-in and restart test when no hydrate present before shut-in. ....	149
Figure 6. 25 Shut-in and restart test when about 11 vol. % hydrates have formed before shut-in. ....	150
Figure 6. 26 Shut-in and restart test when about 24 vol. % hydrates have formed before shut-in. ....	151
Figure 7. 1 Pressure drop across the Moineau pump as a function of the hydrate volume fraction for different AA concentrations: Tests 3 and 4 with 60% water cut and pump speed of 150 RPM. ....	161
Figure 7. 2 Water conversion rate for systems with different AA concentrations: Tests 3 and 4 with 60% water cut and pump speed of 150 RPM. ....	162
Figure 7. 3 Pressure drop across the Moineau pump and the rate of hydrate formation during the test without salt: Test 1 with 60% water cut, 0.6 wt. % AA and pump speed of 300 RPM. ....	163
Figure 7. 4 Pressure drop across the Moineau pump as a function of the hydrate volume fraction for tests without and with 5 wt. % salt: Tests 1 and 2 with 60% water cut and pump speed of 300 RPM. ....	164
Figure 7. 5 Water conversion rate for systems with different salt contents: Tests 1 and 2 with 60% water cut and pump speed of 300 RPM. ....	164
Figure 7. 6 Pressure drop across the Moineau pump as a function of the hydrate volume fraction for different pump speeds: Tests 2 and 3 with 60% water cut and 0.6 wt. % AA. ....	166
Figure 7. 7 Pressure drop across the Moineau pump as a function of the hydrate volume fraction for different water cut: Tests 4 and 5 with 1 wt. % AA and pump speed of 150 RPM. ....	167
Figure 7. 8 Comparison of small scale and flow loop test with 60% WC, 0.6 wt. % AA, and 5 wt. % salt. Flow loop pump speed and high pressure autoclave cell mixer speed were kept constant during the tests at 150 RPM and 200 RPM respectively. ....	169
Figure 7. 9 Comparison of small scale and flow loop test with 60% WC, 1 wt. % AA and 5 wt. % salt. Flow loop pump speed and high pressure autoclave cell mixer speed were kept constant during the tests at 150 RPM and 200 RPM respectively. ....	169
Figure 7. 10 Calibration curve for flow loop to covert pressure drop to viscosity for a constant pump speed of 150 RPM. ....	170
Figure 8. 1 Conceptual model of a hydrate aggregate enclosed by the dashed circle; the hydrate shells covering the hydrate particles, denoted by "S"; unconverted water inside hydrate particles, denoted by "U" and emulsion trapped in the void space of the fractal structure, denoted by "E". ....	181
Figure 8. 2 Comparison between experimental data and existing models for solid spheres: Test 1, 50% water cut and 1 wt. % AA, water-in-oil (A) emulsion. ....	187
Figure 8. 3 Comparison between experimental data and existing models for solid spheres: Test 2, 70% water cut and 1 wt. % AA, water-in-oil (A) emulsion. ....	187
Figure 8. 4 Comparison between experimental data and proposed model for Tests 3 and 4, 60% water cut, water-in-oil (A) emulsion. ....	189
Figure 8. 5 Comparison between experimental data and proposed model for Test 5, 60% water cut and 0.6 wt. % AA, water-in-oil (A) emulsion. ....	191

Figure 8. 6 Comparison between experimental data and proposed model for Test 6, 60% water cut and 1 wt. % AA, water-in-oil (A) emulsion.....	191
Figure 8. 7 Comparison between experimental data and proposed model for Test 7, 60% water cut and 2 wt. % AA, water-in-oil (A) emulsion.....	192
Figure 8. 8 Comparison between experimental data and proposed model for Test 8, 80% water cut and 0.3 wt. % AA, oil (A) -in-water emulsion.....	192
Figure 8. 9 Comparison between experimental data and proposed model for Test 9, 80% water cut and 0.6 wt. % AA, oil (A) -in-water emulsion.....	193
Figure 8. 10 Comparison between experimental data and proposed model for Test 10, 80% water cut and 1 wt. % AA, oil (A) -in-water emulsion.....	193
Figure 8. 11 Comparison between experimental data and proposed model for Test 11, 80% water cut and 2 wt. % AA, oil (A) -in-water emulsion.....	194
Figure 8. 12 Comparison between experimental data and proposed model for Test 13, 60% water cut and 1 wt. % AA, water-in-oil (B) emulsion.....	195
Figure 8. 13 Comparison between experimental data and proposed model for Test 13, 60% water cut and 2 wt. % AA, water-in-oil (B) emulsion.....	195
Figure 8. 14 Trapped Liquid factor, $K_v$ , as a function of AA concentration for 60% water cut, Tests 3-7, water-in-oil (A) emulsion.....	198
Figure 8. 15 Trapped liquid trapped factor, $K_v$ , as a function of AA concentration for 80% watercut, Tests 8-11, oil (A) -in-water emulsion.....	198

## List of Tables

Table 2. 1 Average cavity radius ( $\text{\AA}$ ) of three different hydrate structures (Sloan, 1998).....	9
Table 2. 2 Comparison of Methanol and MEG (Bai and Bai, 2005). ....	16
Table 3. 1 Elemental composition of petroleum (Erstad, 2009; Speight, 2007). ....	39
Table 3. 2 Examples of emulsion in the petroleum industry (Schramm, 1992).....	45
Table 5. 1 Properties of crude oils .....	85
Table 5. 2 Emulsion stability results for oil (A) .....	87
Table 5. 3 Emulsion stability results for oil (B) .....	88
Table 5. 4 Determination of phase inversion point from water continuous to oil continuous emulsion as a function of vol. % of hydrate (total volume of the cell) for oil (A) .....	110
Table 6. 1 Experimental matrix for Oil (A) .....	122
Table 6. 2 Experimental matrix for Oil (B) and Oil (C) .....	127
Table 6. 3 Experimental matrix for studying the effect of mixer speed, oil (C). ....	136
Table 6. 4 Experimental matrix for blended oils. ....	139
Table 6. 5 Viscosity changes during hydrate formation and dissociation processes. ....	141
Table 6. 6 Experimental matrix for studying the effect of salt on AA performance. ....	145
Table 6. 7 Results of second scenario before shut-in and after restart.....	150
Table 7. 1 Test matrix for flow loop experiments in high water cut.....	160
Table 8. 1 Summary of oil/water/hydrate slurry systems considered in the present work.....	186
Table 8. 2 Calculated $K_v$ and $R^2$ for the systems presented in this work .....	197

## List of Publications

- **Moradpour H.**, Chapoy A., Tohidi B., 2011. Bimodal model for predicting the emulsion-hydrate mixture viscosity at high water cut systems, *Fuel*, volume 90, 11, p. 3343-3351.
- **Moradpour H.**, Chapoy A., Tohidi B., 2011. Phase Inversion in Water-Oil Emulsions with and without Gas Hydrates. *Energy & Fuels*, DOI: 10.1021/ef201374v
- **Moradpour H.**, Chapoy A., Tohidi B., 2011. Controlling Hydrate Slurry Transportability by Optimizing Anti-Agglomerant Usage in High Water Cut Systems. *OTC 22485*, Proc. Offshore Technology Conference, Rio de Janeiro, Brazil, 4–6 October, 2011
- **Moradpour H.**, Chapoy A., Tohidi B., 2011. Transportability of Hydrate Particles at High Water Cut Systems and Optimisation of Anti-Agglomerant Concentration. Proceedings of the 7th International Conference on Gas Hydrates (*ICGH 2011*), Edinburgh, U.K., 17-21 July, 2011

## **CHAPTER 1 INTRODUCTION**

### **1.1 INTRODUCTION**

Gas hydrates are crystalline inclusion components composed largely of water (Sloan and Koh, 2008). They form when a sufficient amount of water is present, a hydrate former is present, and the right combination of temperature or pressure is encountered (hydrate formation is favoured by low temperature and high pressure). Under the right conditions hydrates can form anytime and anywhere that the above conditions are met.

Oil and natural gas productions are typically accompanied with the production of water from the well. Water production becomes a major problem as these oilfields mature. Higher levels of water production lead to an increase in the amounts of the gas hydrate which may eventually result in pipeline/well shut-in for untreated oil and gas production systems (with associated mitigation/work-over costs). Recent studies have focused on the formation of the dispersed hydrate particles and controlling viscosity of the hydrate slurry instead of the traditional methods of hydrate prevention. Therefore, an understanding of the rheology of hydrate slurries in oil and gas piping and production facilities is important to avoid plugging in deepwater operations especially for mature oilfields which are facing high water cut problem.

The rheology of hydrate slurries is a difficult subject and so far there has been little discussion of this issue. To the best of our knowledge there are only a few groups (IFP, Ecole des Mines de Saint-Etienne, CSM) that have made significant contributions to the study of rheological properties of hydrate slurries (Sum et al., 2009). Moreover, to date there has not been any standard instrument and methodology for measuring viscosity of hydrate slurries and almost all equipments used by some researcher groups are custom-built with particular requirements (Azarinezhad, 2010).

This thesis presents experimental and modelling study regarding water-oil emulsion formation and the rheological behaviour of hydrate slurries in high water cut systems, which are probably the most difficult conditions for managing flow assurance issues. In order to produce transportable hydrate slurries, different concentrations of commercial Anti-Agglomerant (AA) have been added to the aqueous phase. The thesis has been

organised as details in the followings: the main goal of Chapter 2 is to review the state-of-the-art of hydrate prevention, detailing hydrate structure, conditions and mechanisms of formation, and developing methods from the conventional hydrate prevention and inhibition to managing hydrate formation and transportation. Its focus on low dosage hydrate inhibitors (LDHI), including a review of form, function, development, selection and applications, highlights gaps in current knowledge. A special attention has been given to describing different types of anti-agglomerants, the mechanism of their actions on water/oil or hydrate/oil interfaces because they have been widely used in this study to produce transportable hydrate slurries in high water cut systems. In the last section there is more attention on cold flow, which is an alternative technology on hydrate agglomeration prevention in pipelines at deepwater productions allowing hydrates to form and suspending as dispersed solid particles without forming blockages. Different concepts have been developed for cold flow technology which is explained in details.

Chapter 3 reviews basic concepts of water-oil emulsion and surface chemistry, two main subjects of interfacial phenomena for identifying the tendency of hydrate particles to agglomerate and plug the oil and gas pipelines. This chapter starts with brief explanations of the composition of crude oils in order to understand the nature of natural surfactants existing in the crude oil. Depending on water cut and system conditions, different type of water-oil emulsions may form during the production of crude oil, as co-produced water is mixed with the oil from reservoir to separation facilities. In case of hydrate formation, such emulsions in the presence of gas phase at right pressure and temperature may introduce technical challenges, as they must be resolved to provide the specified product quality. Asphaltenes and resins indigenous to the crude oil are acknowledged as the most important components in respect to stabilization of the interface against droplets coalescence and also hydrate particles agglomeration. The basic concepts of water-oil emulsions and mechanism by which asphaltenes and resins stabilize the emulsions will be described in Section 3.4. The last two sections of Chapter 3 focus on a review of fundamental concepts of surface chemistry for identifying interfacial phenomena and surface chemistry interactions involved in gas hydrate formation and agglomeration. Moreover, these sections attempt to elucidate the most recent findings covering the challenge of isolation and identification of natural inhibiting compounds in crude oils which have been recognised to display hydrate anti-agglomerating effects.



Chapter 4 describes all the experimental accessories used in this study. The first two sections of this chapter demonstrate the experimental setups and visual techniques which are used to determine the type of emulsions and also phase inversion points. It follows with a description of a purpose-built apparatus called Helical Tube Impeller (HTI) setup designed and built in-house with particular aim of studying the rheological behaviour of hydrate slurries at pressures much higher than usual atmospheric levels. Finally, the chapter attempts to describe in detail the new saturated flow loop which has been designed, installed and commissioned during this study to investigate the rheological behaviour of hydrate slurry during hydrate formation in a real pipeline.

Chapter 5, which is devoted to the study of morphology of water-oil emulsions in the presence of anti-agglomerate and also hydrate particles, starts with measuring stability of water-in-oil (W/O) and oil-in-water (O/W) emulsions in the presence of different concentrations of AA and salt at ambient temperature and atmospheric pressure. The influence of existence of natural surfactants such as asphaltenes and resins will be discussed on the stability of emulsions. Section 5.3.1 describes the effect of AA and salt concentrations on the phase inversion point of water-oil emulsions during a mixing process when the dispersed phase is added to the emulsion. Finally, the effect of hydrate formation on the morphology of initial water-oil emulsions in high water cut systems will be presented in Section 5.4. In this section the effect of liquid hydrocarbon phase compositions will be also studied on the phase inversion point of O/W emulsions during hydrate formation process.

Chapter 6 presents the results of rheological study of hydrate slurries in high water cut systems at different test conditions. In the first part of this chapter, the results of experimental studies carried out using the HTI set-up to investigate the effect of water cut, AA and salt concentrations and the nature of liquid hydrocarbon phase on the rheological properties of hydrate slurries will be discussed. The second part describes the effect of hydrate formation and dissociation on emulsion stability. The last part of this chapter presents the results of shut-in and restart condition for two different scenarios i) with no hydrate before shut-in condition ii) with different amounts of hydrate formed before shut-in condition.

In order to investigate the rheological behaviour of hydrate slurries in pipelines, and to transfer the results of the small scale experiments from Chapter 6 to the real pipeline

condition, several experiments have been conducted in a saturated flow loop in high water cut systems. The results of these studies will be presented in Chapter 7. This chapter also discusses the results of comparison between the pressure drops measurements from the flow loop and the viscosity measurements from the small scale helical tube viscometer (HTI).

The fundamental rheological characterization of hydrate slurries is today mainly an art in that no general theoretical methods are available to describe the behaviour of such systems in advance without specific examinations. To describe the rheological behaviour of hydrate slurries in high water cut systems, that is, concentrated hydrate-liquid mixtures, a new slurry model is introduced and discussed in details in Chapter 8. Unlike previous models which consider only oil as continuous phase, this model will incorporate water-oil emulsion as continuous phase to predict the viscosity of the ternary water, oil and hydrate systems using a bimodal mixture concept. The chapter starts with a review of fundamentals of the bimodal model to aid the reader who is not familiar with its application to predict the viscosity of ternary systems. Water-oil emulsion and hydrate particles in the liquid continuous phase are treated separately as unimodal models. A modification is applied to the Mills (1985) model to calculate the viscosity of unimodal hydrate suspensions, which will be discussed in Sections 8.2 and 8.3. The last part of this chapter validates the application of the proposed model using the experimental data collected from HTI viscometer in Chapter 6 for water/oil/hydrate mixtures in the presence of different AA concentrations and different liquid hydrocarbon compositions.

The main conclusions of this thesis are presented in Chapter 9. This chapter also includes some recommendations for further investigations of the research areas discussed in this work.

## 1.2 REFERENCES

Azarinezhad, R., 2010. A chemical based wet cold flow approach for addressing hydrate flow assurance problems, PhD Thesis, Heriot-Watt University, Edinburgh.

Mills, P., 1985. Non-Newtonian behaviour of flocculated suspensions. *Journal de Physique Lettres*, 46(7): 301-309.

Sloan, E.D. and Koh, C.A., 2008. *Clathrate hydrates of natural gases*. 3<sup>th</sup> ed. CRC Press, New York.

Sum, A.K., Koh, C.A. and Sloan, E.D., 2009. Clathrate hydrates: From laboratory science to engineering practice. *Industrial & engineering chemistry research*, 48(16): 7457-7465.

## **CHAPTER 2    GAS HYDRATE INHIBITION AND MANAGEMENT- LITERATURE STUDY**

### **2.1 BACKGROUND**

It is believed that gas hydrates were first discovered in the laboratory in 1810 by Sir Humphrey Davy (Englezos, 1993; Sloan and Koh, 2008) when he cooled an aqueous solution saturated with chlorine gas below 9 °C to yield a crystal/ice like material. It was later determined that Davy had discovered chlorine hydrate. However, for over 100 years after Davy's findings, studies in this field were purely academic (Englezos, 1993), until the early years of the 20th century that oil and gas became an important world energy source. Hydrate plugging in the oil and gas pipelines was identified first by Hammerschmidt (1934), whose studies showed that pipeline plugging was not due to ice formation, as it was occurring above the melting point of ice. He attributed the phenomenon to hydrate formation in the pipeline. This discovery made gas hydrates a topic of considerable interest for oil and gas industry. Since that time, numerous studies have attempted to better understand hydrate formation in production equipment during oil and gas productions. Further in the 1960s, it was recognized that large volumes of natural gas hydrates exist in the nature and being mostly discovered in deep oceans and permafrost regions (Makogon, 1965).

### **2.2 MOLECULAR STRUCTURE OF GAS HYDRATES**

Gas hydrates are ice-like solids with guest molecules trapped in the frameworks of hydrogen-bonded water molecules (Sloan and Koh, 2008) as illustrated in Figure 2.1. There are no direct chemical bonds between host water molecules and guest molecules. Without the inclusion of the trapped molecules in the cavities, these frameworks cannot be stabilized and would undergo significant strain and then dissociate. The guest molecules are linked to the framework by adding extra van der Waals forces, which stabilise the framework. Gas hydrates can be classified within a special class of non-stoichiometric compounds called "clathrates". The word "clathrate" derives from the Latin word

“clathratus”, which means “to encage” (Mooijer-Van Den Heuvel, 2004). Methane, ethane, propane, iso-butane, normal butane, nitrogen, carbon dioxide and hydrogen sulphide are the most common guest molecules occupying the cavities in the lattice, with methane occurring most abundantly in natural gas hydrates.

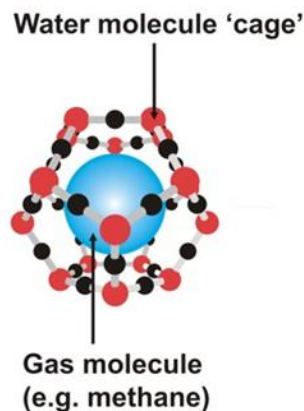


**Figure 2. 1 Simple illustration of a gas molecule encapsulated by a framework of water. Image taken from the homepage of Hydrate Group at Heriot Watt University**

The type of hydrate structure is generally determined by the guest or trapped molecules. Common natural gas hydrates belong to three crystal structures, known as structure I, structure II, and structure H. X-ray hydrate crystal diffraction experiments by Von Stackelberg and co-workers between 1949 and 1956 resulted in the determination of two hydrate crystal structures I and II (Song et al., 2008). More recently, structure H, was discovered by Ripmeester et al. (1987). These three structural types are illustrated in Figure 2.2.

The structures of hydrates exhibit a water skeleton. The pentagonal dodecahedron, designed by the notation  $5^{12}$ , is a basic building block cavity, i.e., 12 faces with five sides per face.

The space cannot be completely filled with dodecahedra and thus in order to form the hydrate structure, dodecahedra is necessarily associated with other types of polyhedron such as  $5^{12}6^2$  (tetrakaidecahedron),  $5^{12}6^4$  (hexakaidecahedron),  $4^35^66^3$ , and  $5^{12}6^8$ . The structure I basic unit is a body centred cubic constructed of  $5^{12}$  and  $5^{12}6^2$  cages, in a ratio of 2:6. Hydrates with structure I commonly contain natural gas including molecules smaller than propane (Sloan, 1998). The most common hydrate formers of structure I are methane, ethane and  $\text{CO}_2$  (Sloan, 2003). Structure II type hydrate is a diamond lattice formed by  $5^{12}$

and  $5^{12}6^4$  cages in a ratio of 16:8. This type of hydrate structure generally forms from molecules larger than ethane, but smaller than pentane (Sloan, 1998). The most common hydrate formers of Structure II hydrates are propane and iso-butane (Sloan, 2003). Structure H crystals have the largest volume capacity. They are made up three types of cages,  $5^{12}$ ,  $4^35^66^3$  and  $5^{12}6^8$  in the ratio of 3:2:1. In order to stabilize their structures, structure H hydrates need to include both small and large guest molecules (Mehta and Sloan, 1999). The small cages of the structure are occupied by small guest molecules, referred to as help gases (i.e. methane,  $H_2S$ , xenon) that increase the stability of the structure (Mehta and Sloan, 1999). The most common hydrate formers of structure H hydrate are methane + neo-hexane and methane + cycloheptane molecules (Sloan, 2003). Figure 2.2 shows three different hydrate structures and their cavity structures.

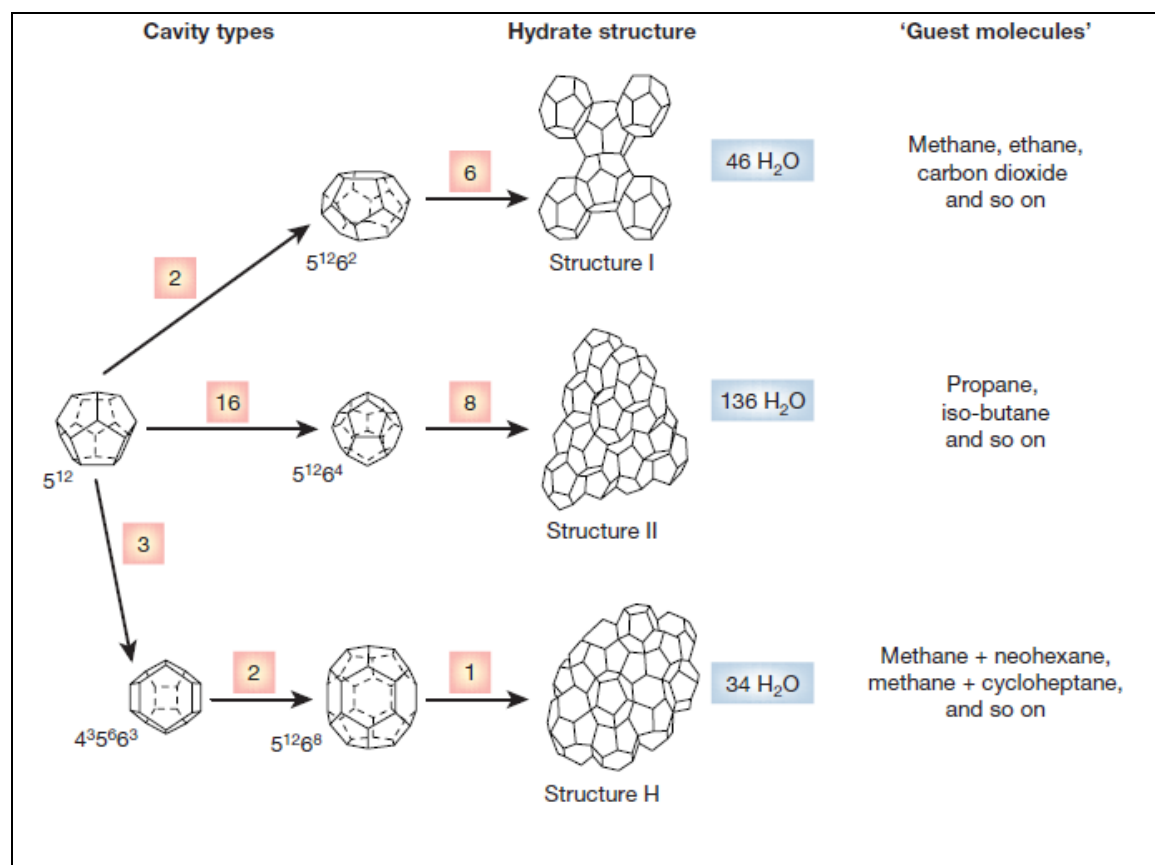


**Figure 2. 2 The three most common hydrate unit crystal structures (Sloan, 2003).**

It has been reported that all three hydrate structures could include 85 mol% water and 15 mol% guest molecules, when their cavities are completely occupied by guest molecules (Sloan,

1998). The values of average cavity radius ( $\text{\AA}$ ) of three different hydrate structures are given in Table 2.1.

**Table 2. 1 Average cavity radius ( $\text{\AA}$ ) of three different hydrate structures (Sloan, 1998).**

	<b>I</b>		<b>II</b>		<b>H</b> (from geometric models)		
cavity	Small	Large	Small	Large	Small	Medium	Large
description	$5^{12}$	$5^{12}6^2$	$5^{12}$	$5^{12}6^4$	$5^{12}$	$4^35^66^3$	$5^{12}6^8$
average cavity radius ( $\text{\AA}$ )	3.95	4.33	3.91	4.73	3.91	4.06	5.71

### 2.3 PHASE EQUILIBRIUMS OF GAS HYDRATES

The formation of hydrate crystals occur when water and at least one hydrate former exist within the pressure and temperature region of hydrate formation. Thermodynamic properties of gas hydrates have been studied extensively since it was identified as a problem for oil and gas production by Hammerschmidt (1934). If the composition of a produced fluid is known, it is now very easy to predict its hydrate phase equilibrium with a reasonable degree of accuracy using computer programs such as HydraFLASH or PVTsim. These computer programs can also estimate with an acceptable accuracy the quantity of the required inhibitors which are needed to ensure safe operation. Figure 2.3 shows phase diagrams of different natural gas components that can form gas hydrate. Gas hydrates are stable to the left of the equilibrium curves.  $L_{HC}$ ,  $L_W$ , I, H and V refer to liquid hydrocarbon, liquid water, ice, hydrate and vapour phases, respectively. There are two quadruple points, namely  $Q_1$  (I-  $L_W$ - H- V), the lower hydrate quadruple point and  $Q_2$  ( $L_W$ - H- V-  $L_{HC}$ ), the upper quadruple point. The values of  $Q_1$  and  $Q_2$  for each hydrate former are unique and give a quantitative classification for hydrate components of natural gases (Sloan and Koh, 2008). Temperature at quadruple point  $Q_1$  is about 273 K for all hydrate formers in the presence of distilled water though the quadruple pressure varies. With decreasing temperature from  $Q_1$ , the hydrate formation mechanism is changed from liquid water and vapour to ice and vapour. The  $L_W$  -H-V line is the most interesting region of temperature and pressure in the oil and gas industry.  $Q_2$  displays the intersection point of the vapour pressure line of the hydrate former with the  $L_W$  -H-V line. This point indicates

the upper limit of temperature for hydrate formation for pure compounds as the  $L_W-H-L_{HC}$  line rises almost vertically with very large pressure increases for small temperature increases (Sloan and Koh, 2008).

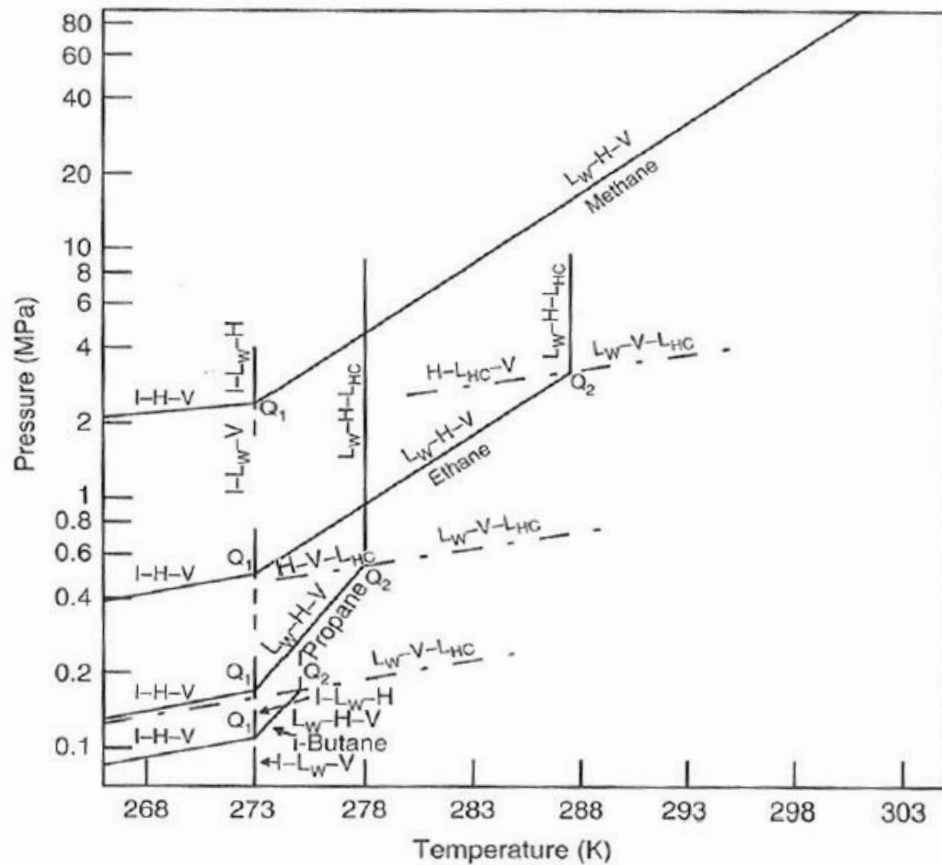


**Figure 2. 3 Phase diagrams of different simple natural gases hydrocarbons that form hydrates. (modified by Sloan (2008) from the plot developed by (Katz et al., 1959)).**

When there is more than one component that forms hydrate, the equilibrium curves slightly changes. Figure 2.4 indicates phase diagram of a multi-component mixture of hydrocarbons that forms gas hydrate. In the figure the curve ECFKL presents the phase envelope of the gas mixture and it is superimposed on the hydrate formation line (Sloan and Koh, 2008). It is clear that the line KC in the multi-component system replaces with the upper quadratic point  $Q_2$  in the single component systems (Sloan and Koh, 2008).



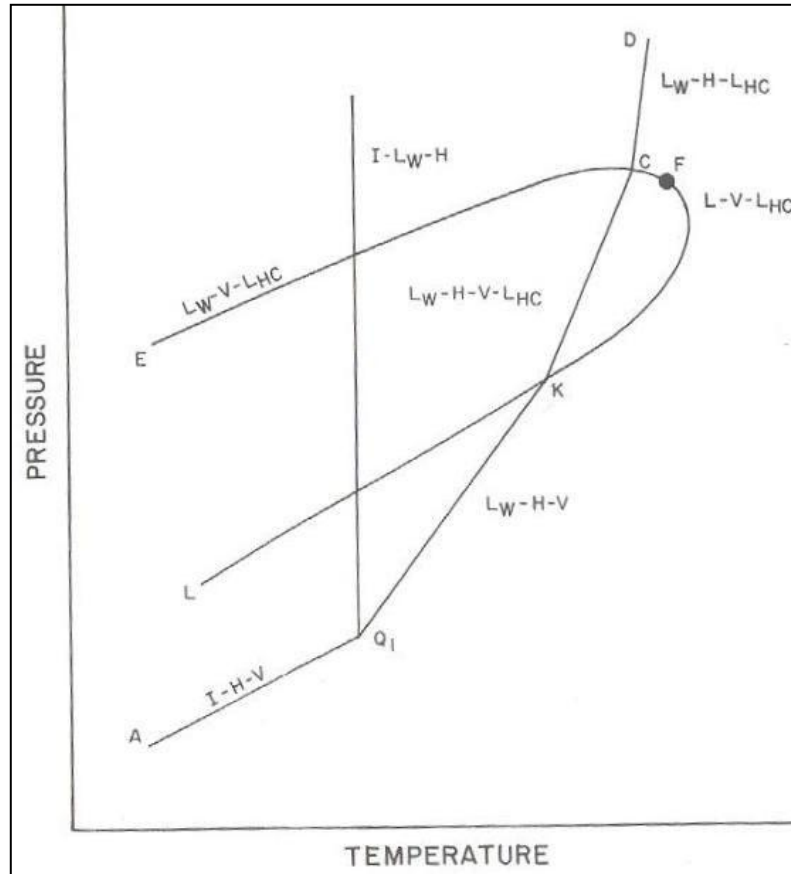


**Figure 2. 4 Phase diagram of a multi-component hydrocarbon mixture that form hydrates (Sloan and Koh, 2008).**

## 2.4 GAS HYDRATE PROBLEMS IN OIL AND GAS INDUSTRY

The most severe operational hazards of oil and gas production pipelines are the risks associated with the transportation of multiphase fluids at high pressure and low temperature. A survey of 110 energy companies showed that flow assurance is the major concern in offshore energy development (Sloan, 2005). When water, oil and gas are flowing inside a pipeline simultaneously, there are potential problems that may lead to formation of hydrate and block the pipeline and eventually shut down of production facilities. Although precipitation of wax and asphaltenes is still a challenge in oil and gas production lines, hydrate issue is a major flow- assurance concern to the oil and gas industry (Mehta and Klomp, 2005). The oil and gas industry is moving towards deepwaters and expanding new fields with multiple subsea and long tiebacks.

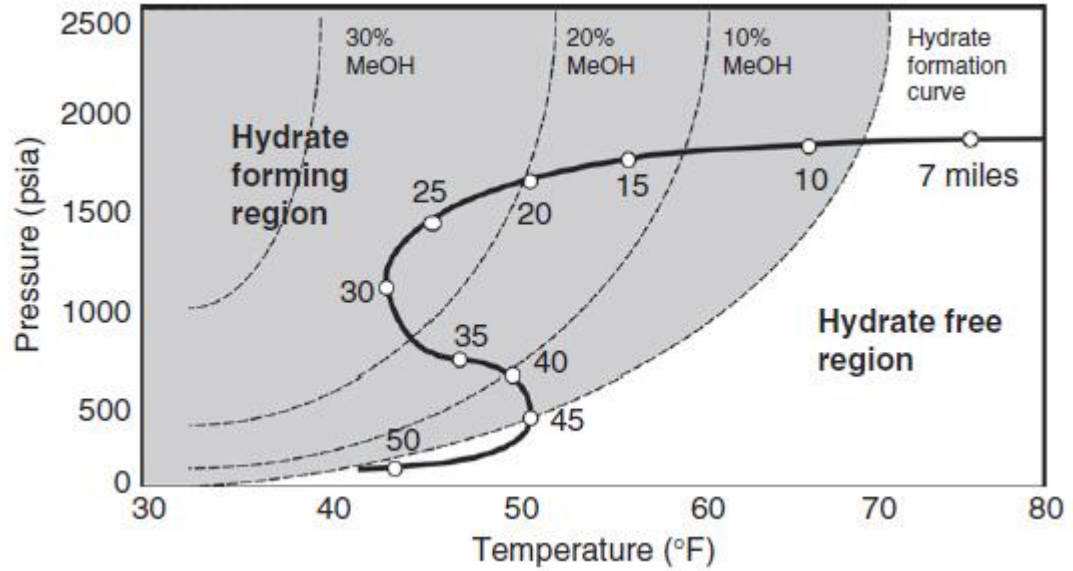


**Figure 2. 5 Typical pipeline conditions from wellhead towards platform with intrusion into the hydrate stability zone (Sloan and Koh, 2008).**



**Figure 2. 6 Hydrate accumulation retrieved at the pig-catcher of a Petrobras rig (Photo courtesy of Petrobras) (Clark et al., 2008).**

Fluids produced from wells are often warm but during production, depending on outside temperature, the fluid stream temperature is reduced and may enter the hydrate stability zone. Figure 2.5 presents the fluid stream conditions in a pipeline simulated with a multiphase program as the fluid conditions superimposed on hydrate stability curves

(Sloan and Koh, 2008). At the beginning the fluid stream remains its reservoir temperature. With flowing in the pipeline, ocean water cools the fluid stream, and it enters the hydrate stability region. Formation of solid hydrates can plug up subsea risers, choke valves, kill lines, and blowout preventers. It is well understood that hydrate blockages in flow lines can have very high cost consequences (Sloan 2000). Figure 2.6 shows hydrate accumulations removed from a subsea pipeline.

Unfortunately, unexpected shut-in conditions may occur in a well's productive life at some point, as the inherent heat of well products is insufficient to prevent hydrate formation even for relatively short pipelines. Other conditions may result in gas hydrate formation; e.g. when gas passes through a choke valve, resulting in Joule-Thompson cooling (Pickering et al., 2001). Thus, controlling hydrates formation is not always easy.

Recent study has indicated that plug formation can vary between cases, and the nature of gas and liquid trapped in pores of hydrate aggregates may determine hydrate plug formation characteristics (Austvik et al., 2000). Hydrate plugging of a pipeline is accompanied by an increasing pressure drop from the well-head. Trying to dissociate and remove hydrate plugs can be a challenging task. It is well known that hydrate dissociation takes place from the pipe-wall toward the centre of the flow line (Kini et al., 2005; Palermo et al., 2004). Once hydrate plugs detach from inside the pipe-wall, they can move at high speed and cause serious mechanical damage at downstream locations where restrictions (control valve), obstructions (closed valve) or sharp change of direction (elbow, tee) exist. Moreover, even safe procedures for removing hydrate plugs could take several weeks (Kashu et al., 2004; Mokhatab et al., 2007). Hydrate plug formation is therefore a complicated subject which it is poorly understood, with ongoing focus on hydrate agglomeration and plugging. Therefore, it is crucial to prevent hydrate plugging in the pipelines effectively and economically to ensure that pipeline operates safely.

## **2.5 STRATEGIES FOR SOLVING GAS-HYDRATE PROBLEMS**

Hydrate plug dissociation and remediation can be a costly and time consuming process and result in restrictions on system operations. Moreover, there are various safety concerns when hydrates are formed in pipelines. Hydrate plugs may take days to months to remove

depending on the system conditions and the remediation actions taken. Therefore, the issue of hydrate plug prevention and, if needed, remediation is very important.

The hydrate inhibition approach selected has to ensure hydrates will not form, or that the hydrates remain transportable during steady state, transient and shut-in conditions. The petroleum industry has been using different approaches to avoid hydrate formation such as chemical or physical methods; however, the complicated and expensive nature of hydrate prevention methods for harsh locations like deepwater productions has persuaded the oil and gas industry to adopt new technologies to deal with hydrates before, during or after their formation. There are different techniques in the open literature for preventing hydrate plugging of pipelines which can be categorise in two main groups:

- Current methods of preventing gas hydrate blockage
- Hydrate management -Cold flow technology

### **2.5.1 Current Methods Of Preventing Gas Hydrate Blockage**

In the oil and gas industry, many methods have been reported as having been used to prevent pipeline blockage due to hydrate formation. The most common methods are

1. Physical methods
2. Thermodynamic inhibitors
3. Low dosage hydrate inhibitors

#### **2.5.1.1 Physical Methods**

In these methods hydrate formation is prevented by controlling pressure, temperature, and hydrate former components in the system. By controlling temperature and pressure of the system it is possible to retain the fluid condition out of the hydrate stability area. Depressurization of the pipeline is the general technique to remove a hydrate plug (Clark et al., 2008; Kashu et al., 2004). However, controlling pressure is not always practical or possible, because pressure is required to transport fluid in pipelines.

Controlling temperature is possible for preventing hydrate formation. To keep the flowing mixture outside the hydrate formation zone, direct heating and/or pipe insulation is employed (Hansen et al., 1999; Nysveen et al., 2007). However, controlling temperature cannot prevent the system entering hydrate stability zone for long period of shutdowns. This method can be practical and economically feasible for some subsea systems,

depending upon the fluid condition and the length of the pipeline. The temperature of pipeline can be controlled by, for example, insulating, pipe-in-pipe heating, or electrical heating of the entire pipeline length. This method can become extremely expensive and its application in subsea installations is limited by the tie back distance. Insulation and heating are usually employed for pipes a few kilometres up to 50 km long (Nysveen et al., 2007). In addition to the high cost of the insulation, the pipeline insulation has a negative impact on blockage remediation. It may require on the order of months or years to dissociate hydrate blockages in a highly insulated pipeline, depending on the temperature driving force, insulation thickness and the extent of depressurization (Kini et al., 2005).

The permanent solution to the hydrate plugging problem is removal of water as hydrate forming component prior to pipeline transportation. Separation of gas from liquid contents using a separator or molecular sieve and transferring the liquid and gas phase separately has been suggested. However it is not known whether such a method has ever been conducted and separation of water phase before pipeline transportation is impractical for subsea applications (Pickering et al., 2001).

#### **2.5.1.2 Thermodynamic Inhibitors**

Injecting high concentrations of thermodynamic Inhibitors (THIs) have been the most common practical method for the prevention of hydrate formation in oil and gas production systems. The most common thermodynamic inhibitors are, methanol (MeOH) and mono-ethylene glycol (MEG), although ethanol and other glycols and salts are also used successfully (Mehta and Klomp, 2005). THIs change the chemical potential of water and reduce the temperature at which hydrate forms (Bai and Bai, 2005) and their effects are similar to adding anti-freeze to water to reduce the freezing point. Figure 2.5 shows that addition of MeOH effectively eliminates the risk of hydrate formation and shifts the hydrate stability zones to low temperatures.

It has been reported that different types of THIs have been used across the world. For example, methanol is mostly used in the Gulf of Mexico and West Africa while MEG is favoured in North sea and Asia-Pacific regions; whereas ethanol has been more widely used by the Brazilian oil and gas sector due to its wide availability (Mehta and Klomp, 2005).

Many parameters need to be considered for selecting either MEG or methanol, including capital and operating costs. Site conditions such as pipeline operating temperature and pressure, an operator's previous favourable or unfavourable experience might also influence the selection. An important parameter when selecting an inhibitor is whether or not it is able to be recovered, regenerated and re-injected. The operating cost for inhibitor make-up may be an important parameter for systems that use methanol, mainly for high gas and/or high water cuts. Table 2.2 summarizes the technical advantages and disadvantages of methanol and MEG (Bai and Bai, 2005).

**Table 2. 2 Comparison of Methanol and MEG (Bai and Bai, 2005).**

	Advantages	Disadvantages
Methanol	<ul style="list-style-type: none"> <li>• Move hydrates formation temperature more than MEG in a mass basis;</li> <li>• Less viscous;</li> <li>• Less likely to cause salt precipitation;</li> <li>• Relative cost of regeneration system is less than MEG;</li> <li>• Approximate GoM cost of 1.0 \$/gal;</li> </ul>	<ul style="list-style-type: none"> <li>• Losses of methanol to gas and condensate phases can be significant, leading to a lower recovery (&lt;80%);</li> <li>• Impact of methanol contamination in downstream processing;</li> <li>• Low flash point;</li> <li>• Environmental limitation on overboard discharge.</li> </ul>
MEG	<ul style="list-style-type: none"> <li>• Easy to recover with recovery of 99%</li> <li>• Low gas &amp; condensate solubility</li> <li>• Approximate GoM cost of 2.5 \$/gal</li> </ul>	<ul style="list-style-type: none"> <li>• High viscosity, impacts umbilical and pump requirements;</li> <li>• Less applicable for restarts, stays with aqueous phase at bottom of pipe;</li> <li>• More likely to cause salt precipitation.</li> </ul>

Since the required dosage of THIs depends on the amount of free water in the system, plus the amount of inhibitor lost to the vapour and liquid hydrocarbon phases larger quantities are usually required for safe operation. One example states that if a well is producing 50,000 barrels/day and the water cut increases to 50 vol %, then there is a need to inhibit 25,000 barrels/day of produced water. To prevent hydrate formation, roughly 25,000 barrels/day of methanol is required (Kini et al., 2005) illustrating the enormous costs and safety issues for transporting and organizing such large quantities.

Inorganic salts such as NaCl and MgCl<sub>2</sub> can be characterized as naturally occurring THIs in co-produced water, at concentrations ranging from hundreds of ppm up to saturation (Masoudi et al., 2006). The strong bond of salt ions with water molecules leads to hydrate inhibition because water is more strongly attached to the ion than to the hydrate structure

(Sloan and Koh, 2008). It was reported that Gulf of Mexico fields produce highly saline waters which prevent hydrate formation effectively (Kini et al., 2005).

### **2.5.1.3 Low Dosage Hydrate Inhibitors**

Although the efficiency of THIs has been highlighted, there are still concerns that large quantity of inhibitor are required for the prevention of hydrate formation. Thus, it is an economically necessary for the oil and gas industry to find cost-efficient and environmentally sustainable inhibitors which can work with the same efficiency of THIs, but at low concentrations.

A new class of inhibitor that showed promise over the traditional means has been under study for almost two decades. These new hydrate inhibitors, called low dosage hydrate inhibitors (LDHIs), consist of two types: kinetic hydrate inhibitors (KHI) and anti-agglomerants (AA).

The purpose of LDHIs is dealing with interfacial and surface properties rather than bulk-phase properties. LDHIs do not change the thermodynamic of hydrate formation but, rather act at the early stages of hydrate formation by controlling the kinetics and/or rheological properties of the system (Mokhatab et al., 2007; Siquin et al., 2004). LDHIs are effective at much lower dosage than THIs. Previous studies have involved LDHIs ranging between 0.1-1.0 wt% based on the water phase, whilst others range from 0.5 to 3 wt% (Alapati et al., 2008). In contrast, 10–50 wt% is needed for thermodynamic inhibitors for the same efficiency.

The field application for the two types of LDHIs uses different ranges, depending on performance, operational conditions, fluid properties and the properties of the additives. KHIs is generally believed to delay hydrate formation whereas an efficient AA allows hydrates to form but prevents hydrates from agglomerating and accumulating into large lumps. Moreover, AAs produce transportable non-sticky slurry of solid hydrates dispersed in the liquid phase.

#### ***LDHI: kinetic hydrate inhibitors (KHIs)***

In the early 1990s, Shell became aware of certain species of fish, which doesn't freeze in subzero sea temperatures due to their producing proteins and glycoproteins which bind themselves to prevent microscopic ice crystals from growth (Kelland, 2006). This

phenomenon sparked invention of KHIs. KHIs are generally water-soluble polymers preventing or delaying hydrate nucleation, although most of them also delay the growth of gas hydrate crystals. Therefore, KHIs allow the systems to transport hydrate-forming fluids, while they operate in the hydrate stability zone, for a certain period of time (induction time) before hydrates formation onset (Kelland, 2006). The induction time is the period that is required for the formation of the first hydrate crystals at a specific level of subcooling (the difference between the system operating temperature and the temperature at which hydrates would form at the same operating pressure within the hydrate stability zone) (Sloan and Koh, 2008). From a practical point of view, using KHIs should be controlled so that its induction time is always greater than the residence time of produced fluids in the hydrate stability zone of the production process to effectively prevent hydrate formation.

Poly (N-vinylpyrrolidone) (PVP) was the first KHIs to show promise in inhibiting hydrate formation. It consists of the five-ring member of the series of polyvinyl lactams, which are manufactured by ISP and BASF (Kelland, 2006; Lederhos et al., 1996). Its performance was investigated using a ball-stop rig and THF/water solution as a model mixture. The time recorded before the ball trapped by hydrate formation indicated the performance of the inhibitor (Lederhos et al., 1996). The earlier generation of KHIs was able to prevent hydrate formation up to 8 °C subcooling for an induction time of approximately 24-hours. New generations of KHIs have been produced to extend the restrictions of subcooling as they are able to operate effectively up to 12 °C for days or weeks depending on the subcooling (Clark et al., 2008). One of the main advantages of KHIs is that their performance is independent of the water cut in the produced fluids. However, KHIs have many limitations as they perform poorly at shut-in conditions or at high operating subcoolings. The greater the degree of pipeline subcooling, the more KHI product is required and the shorter the times for which hydrate formation is controlled. A large number of offshore pipelines exist which need to operate under levels of subcoolings of the order of 20 °C, and even higher subcoolings that can be found in ultra-deepwater pipelines (Clark et al., 2008). In such systems KHIs are clearly unable to work and therefore the oil and gas industry has moved to develop anti-agglomerant hydrate inhibitors.



***LDHI: anti-agglomerants (AAs)***

Fluid production from offshore wells is crucial for flow assurance and the conventional approaches to mitigate the risk of hydrate plugging are very limited. Currently there is interest in preventing formation of solid hydrate particles using the second type of LDHI, anti-agglomerants (AAs). In recent years, AAs have been studied more extensively and it have been demonstrated to be one of the best choices for reducing the risk of hydrate plugging in the deepwater production facilities and pipelines.

AAs have been investigated in a large and growing body of literature (Anklam et al., 2007; Frostman, 2000a; Huo et al., 2001; Oskarsson et al., 2005). They will allow hydrate formation, but discourage hydrate particle agglomeration (Kelland, 2006). The main function of AAs is to disperse hydrate particles in the continuous liquid phase. Ideally, an efficient AA should allow hydrates particles to be transported as non-agglomerated slurry, without any viscosity increase.

With reducing interfacial tension between water and oil phases, AAs may emulsify water droplets into the oil phase and produce a stable water-in-oil emulsion in relatively low water cut systems (York and Firoozabadi, 2009; Zerpa et al., 2011). However, the emulsification property is not a sufficient requirement for an efficient AA, as several studies have revealed that some good emulsifiers have been proven to be poor AAs (Huo et al., 2001; York and Firoozabadi, 2009; Zanota et al., 2005; Zerpa et al., 2011). Moreover, a number of studies have found that AAs have resulted in demulsification of several black oil emulsions (Frostman, 2000b).

The actual performance of AAs varies from one system to another. Several factors can affect the performance of AAs. The composition of the liquid hydrocarbon phase affects the AA performance (Kelland et al., 2006), but only a limited research has been conducted in this area. The salinity effect on AA performance are well known (York and Firoozabadi (2009)). Whereas the effect of salts is always clear from the literature and need to be fundamentally and systematically investigated.

The mechanism of hydrate agglomeration and plug formation is still a mystery. Although hydrate particle agglomeration occurs in the growth phase, some previous studies have reported that agglomeration may occur among meta-stable nuclei (Lederhos et al., 1996).

There is no limitation for AAs on the system pressure and temperature (Kelland, 2006). In contrast to KHIs, AAs can retain their effectiveness for longer periods (Alapati et al.,

2008). One major restriction of AAs compared to KHIs and THIs is that they are limited to water-oil emulsions of 50% water cut or less (Kelland, 2006). Above this water cut, the hydrate volume fraction in the system significantly changes the rheological behaviour of the hydrate slurry, leading to flow problems and unwanted pressure drop in the pipeline (Colombel et al., 2009; Sloan, 2005). Despite this limitation, AAs were successfully applied in a field trial with a water cut of more than 50%. However, how they prevent hydrate formation and blockage is not well-understood (Harun et al., 2008). There is currently a great interest in the study of the application of AAs in high water cut systems (Alapati et al., 2008; Azarinezhad et al., 2008a; Gao, 2009).

Previous studies have reported that quaternary ammonium salts may have a kinetic inhibition quality, i.e., they may increase the induction time and/or decrease the hydrate crystal growth rate (Arjmandi et al., 2005; Karaaslan and Parlaktuna, 2000).

The structure of AAs plays an important role in their performance. To date two different mechanisms have been known for operation of AAs which are directly related to AA structure, although they are not yet fully understood. The first mechanism has been more commonly reported in the journal publications that focus on production of water-in-oil emulsions, in which either AAs is added to or naturally exist in the crude oils. In this mechanism AAs produce a special kind of water-in-oil emulsion. These chemicals which were discovered by workers at IFP are called dispersant additives, which form water-in-oil emulsion where hydrates formation is confined within the water droplets, and the hydrates do not agglomerate and are transported in the form of transportable slurry.

In 1992, the use of dispersant additives with concentrations of 0.5-2.0 wt% was claimed; however, later IFP showed successful results of an AA at 0.8 wt% (Kelland, 2006). The first AA compounds patented by IFP covered diethanolamides, dioctylsulfosuccinates, sorbitans, ethoxylated polyols, ethoxylated fatty acids, ethoxylated amines, and polymeric surfactants based on polyalkenyl succinic anhydride, although they basically claimed all surface-active compounds in their patents. In the mid-1990s, IFP started a project whose aim was to act as springboard for IFPs emulsion AA technology. Over the almost a decade of laboratory research, IFP reduced largely the selection of AAs to polymeric surfactants. For example, Emulfip 102b is a 50% solution of polymerized fatty acids and amides in rapeseed oil.

The second mechanism discovered by Shell U.S. team is the use of surfactants (i.e., AAs) that are attached to hydrate crystal surfaces (Kelland et al., 2006). These AAs are generally quaternary ammonium salts, and recent evidence indicates that they are currently the most successful in industrial testing and field applications (Kelland, 2006; Kelland et al., 2006). However, this type of AA is not environmentally friendly, and the industry is seeking for greener alternatives. After a short period of research, Shell found that salts with two or more *n*-butyl, *n*-pentyl, and isopentyl groups were the best at delaying the growth of hydrate crystals (Figure 2.7).

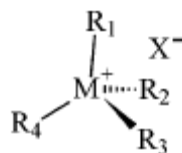


**Figure 2. 7 Structure of good quaternary ammonium or phosphonium hydrate growth inhibitors, where M=N or P and at least two of the R groups are *n*-butyl, *n*-pentyl, or isopentyl. Figure taken from Kelland (2006)**

In the next stage they generated very effective AAs with compounds of quaternary ammonium or phosphonium salts, whose structures are shown in Figure 2.8. The key to these AAs are two or three medium-chained alkyl groups chosen from *n*-butyl, *n*-pentyl, or isopentyl and one or two longer hydrophobic tails typically of 8-18 carbons that branch from the head.

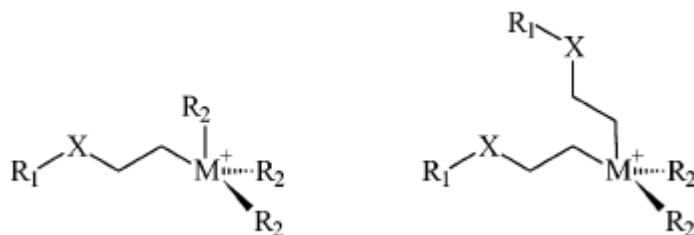


**Figure 2. 8 Structure of Shell's quaternary AA chemicals, ( $R_1$ =long chain hydrocarbon tail;  $R_2$  =*n*-butyl, *n*-pentyl, or isopentyl; M=N or P; X is an optional spacer group). Figure taken from Kelland (2006).**

Shell's quaternary AAs is different from IFP's water-in-oil emulsifying AAs. Quaternary AAs contain a hydrophilic head group and a hydrophobic tail. The AAs move toward the water-oil interface, where hydrate starts to form. The hydrophilic head group, which is the quaternary centre, firmly attaches to the hydrate surface. The butyl/pentyl groups occupy the open cavities on the hydrate surface and can even become embedded in the surface

structure as the hydrate grows around the alkyl groups. The hydrophobic tails alter the surface wettability from water-wet to the oil-wet and prevent hydrate growth on the surface by steric repulsion (Aspenes et al., 2009). Figure 2.9 shows a schematic of the postulated interaction of AAs with a hydrate surface.

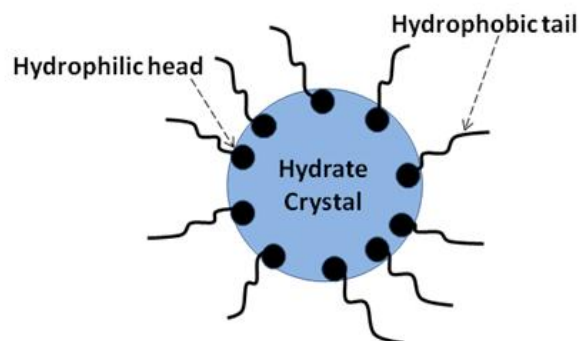


**Figure 2. 9 Schematic of AA interactions on a hydrate crystal.**

Once the enough AA molecules have accumulated on the hydrate surface, the hydrate particle can be easily dispersed in the hydrocarbon phase. The hydrophobic tails inhibit hydrate agglomeration and prevent hydrates to be attached to the inside wall of the pipe.

Gas well AAs (GWAAs) were developed by BJ Service Company (Kelland, 2006). These types mainly include quaternized polyetherpolyamines and are predominantly used for hydrate inhibition in gas wells and flow lines, although quaternization leads to dual antiagglomerants/kinetic hydrate inhibitor function (Pakulski and Hurd, 2005). Quaternized polyetherpolyamines include one or more amine end-groups separated by various lengths and combinations of ethylene oxide and propylene oxide linkages. Laboratory studies and field applications revealed that presence of GWAAs in the gas flow systems led to the formation of dispersed hydrates in the free water phase (unconverted water) (Kelland, 2006). It has been observed that this type of AA does not alter wettability of hydrate surfaces (Pakulski and Hurd, 2005) but prevents the hydrate particles from agglomeration by inhibiting further growth in the associated water on the hydrate surfaces (Azarinezhad, 2010). Since Gas well AAs have not been confirmed at full water conversion in the presence of liquid hydrocarbon, they are not regarded as AAs in the gas and oil sector (Kelland, 2006).

## **2.6 HYDRATE MANAGEMENT -COLD FLOW TECHNOLOGY**

In the search for new conventional oil and gas reserves, operators are moving into more challenging reservoirs such as deepwater production areas. Deepwater flow assurance is a major technical concern in the energy sector, as fluids produced from deep-sea wells are exposed to the relatively low seabed temperature of -2 to 4 °C (Gudmundsson, 2002). The produced fluids require being at high pressures to guarantee adequate potential energy to transport them through long pipelines and tall production risers to the platform or onshore facilities. Moreover, high seafloor hydrostatic pressures increase the pressure by 1 bar for every 10 m of depth; equivalent to 150 bars a water depth of 1,500 meters. In this context, crude oil may congeal immediately in an ordinary pipeline due to hydrate formation. Consequently, deepwater production presents complex engineering challenges as conventional methods such as chemical injections not only have environmental impact but may also not be economical and/or logistically practical. In this context, hydrate management may be more economical than avoidance (Sloan, 2005) and as result, operators are forced to seek innovative approaches to tackle these technical challenges.

One new alternative is Cold Flow technology which is a potential emerging alternative way of dealing with hydrate blockage in harsh and challenging environments such as sub-sea pipeline applications. The main concept of this technology is to engineer a controlled formation of slurry of hydrate particles. It is based on elimination of piping insulation and heating and injection of chemicals for normal operating conditions (Ilahi, 2005; Larsen et al., 2001). The concept of cold flow was first invented by the hydrate R&D group at NTNU (Norwegian University of Science and Technology) studying on the storage and transport of natural gas through hydrate slurry formation and the flow of hydrate particles in water and oil phases. The technology has acceptable cost and good environmental performance and a few research groups are working in this field. SINTEF-BP, NTNU (Norwegian University of Science and Technology) and Heriot Watt University are the main research groups working on cold flow technology. Other research groups, such as IFP and CSIRO/IFP have studied their own versions of cold flow but there are no publications on their results in the open literature (Azarinezhad et al., 2008a).

### **2.6.1 The NTNU Cold Flow Technology (Gudmundsson's Concept)**

A Natural Gas Hydrate (NGH) laboratory was built at NTNU where natural gas hydrate could be continuously produced at various experimental conditions. The laboratory has a flow loop equipped with a viscometer to estimate the viscosity of hydrate slurries through pressure drop measurements. The flow loop consisting of four main units: a continuously stirred tank reactor, a separator, a shell-and-tube heat exchanger and a centrifugal circulation pump.

In this laboratory, Andersson (1999) produced water - hydrate and oil-hydrate slurries using the flow loop to investigate their flow properties. The hydrate particles were first prepared in the reactor and then circulated in the flow loop where hydrate formation was stopped due to eliminating extra gas or water in the system. The experimental results revealed that for hydrate-in-water slurries, the effective viscosities are greater than that of liquid water in the laminar flow regime. However, in the turbulent flow regime, the pressure drops in pipelines carrying hydrate-in-water slurries are the same as the pressure drop in pipelines carrying liquid water. These results were not as would be expected from conventional understanding, and similar results were observed for hydrate in diesel fuel slurries (Andersson, 1999; Gudmundsson, 2002) (Figures 2.10 and 2.11). Such results have significant implications for subsea production of oil and gas, as the experimental work showed that when the water phase is converted to hydrate particles before they enter the pipeline there was no tendency to hydrate agglomeration and hydrate deposition in the flow loop during normal operation conditions.

The results suggest that hydrate technology can be used to achieve cold flow from wellhead to processing facilities. Mainly, the liquid water produced with the oil and gas would have to be converted to hydrate particles before they enter in the pipeline.

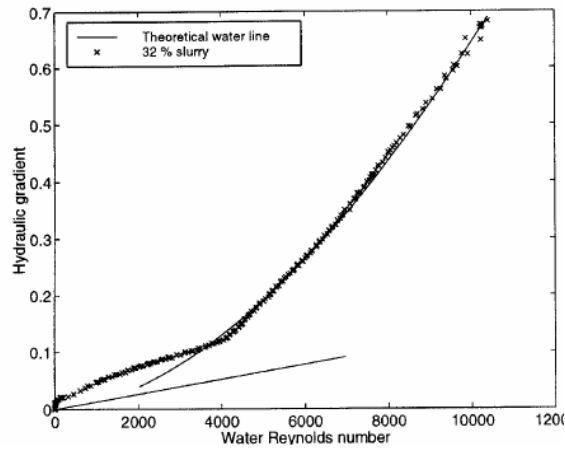


**Figure 2. 10 Hydraulic gradient for 32% hydrate-in-water slurry plotted against Reynolds number (Andersson, 1999)**

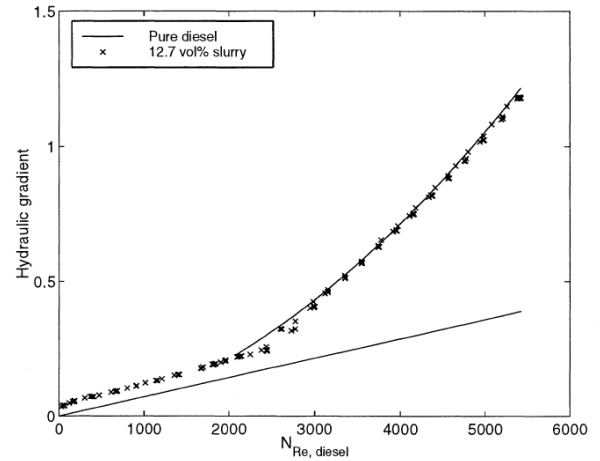


**Figure 2. 11 Hydraulic gradient for 12.7 % hydrate-in-oil (diesel fuel) slurry plotted against Reynolds number (Andersson, 1999).**

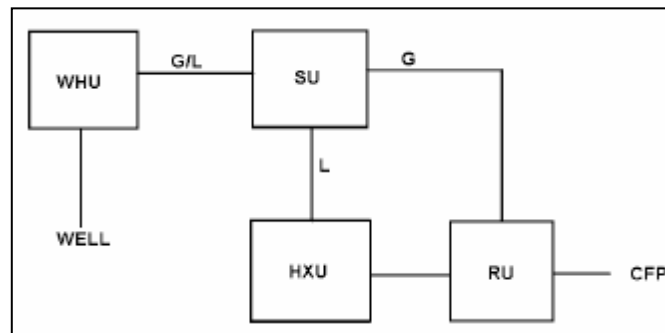


**Figure 2. 12 Schematic description on the field implementation of NTNU concept (Gudmundsson, 2002).**

Gudmundsson (2002) developed the concept of cold flow technology based on the pressure drop results presented by Andersson (1999). In this concept called NTNU Cold flow technology, the objective is to form small hydrates particles from the associated gas and water before they enter the pipeline. The flow diagram of field completion of the NTNU system is shown in Figure 2.12.

The flow enters from a wellbore (WELL) and leaves through a cold flow pipeline (CFP). A gas-liquid mixture is shown flowing from wellhead unit (WHU) to separator unit (SU).

The gas-liquid mixture is separated, the liquid phase flowing to heat-exchanger unit (HXU) and the gas phase to reactor unit (RU). The cooled liquid phase and the gas phase are brought together in RU, where hydrate formation occurs. Depending on the water content WC, the gas/oil ratio GOR and other fluid properties, more than one set of SU+HXU+RU may be required. The system with large GOR and large water cut will make transportation of fluid difficult due to high concentration of hydrate particles in the system. The amount of free water in the system can be controlled through a free water knock out unit put between the wellhead unit and the separator unit.

It is clear that the NTNU system can in itself become a large unit that needs to be placed on the seabed. Therefore, extensive engineering work is needed to make a finished unit. However, the NTNU cold flow technology has been planned to eliminate the chemical injection process. That is, eliminating the need for expensive infrastructure to inject chemicals.

### **2.6.2 The SINTEF-BP's Cold Flow Technology**

SINTEF (Norway), in partnership with BP, were also developing a Cold Flow technology (Larsen et al., 2001; Lund and Larsen, 2000; Wolden et al., 2005). The aim was to develop a very robust procedure for long-distance transportation of unprocessed well fluid including water, by converting the water to very stable and transportable hydrate slurry. The Cold Flow technology is a novel concept entirely owned by SINTEF and patent protection has been applied for and awarded in all important markets in the world (Bai and Bai, 2005).

SINTEF has developed the concept of CONWHYP (CONversion of Water to HYdrate Particles) to create transportable “inert” hydrate particles in a fluid flow. This concept was firstly suggested by Lund et al. (1999). The basis of this concept is to convert all free water to transportable dry hydrate particles without use of any chemical additives as the hydrate particles flow freely along with oil and gas. However, the water content should be no more than 20% (a free water -knockout drum can be employed to reduce the water content) to avoid any problems caused by hydrate deposition on the pipe wall, hydrate agglomeration at stop or start conditions and also viscosity increases due to high volume fraction of hydrate formed in the system (Ilahi, 2005).



In normal operation the initial hydrate formation usually forms as a shell around water droplets and remains unconverted water inside the droplets for long times (Sugaya and Mori, 1996). This water trapped inside the water/hydrate droplets may lead to possible deposition and blocking of the pipeline. When these droplets collide with each other or with, e.g., a pipe wall, the trapped water from the droplet interior will spread to the outer hydrate surface acting as “glue” for agglomeration of the droplets to bigger lumps or to attach to the pipe wall by converting to hydrates (Lund and Larsen, 2000) (Figure 12.3).

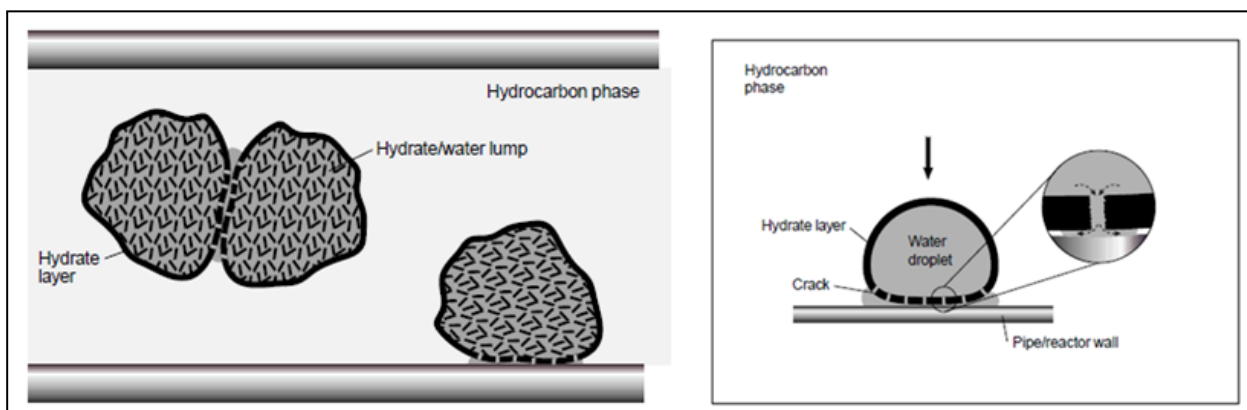


**Figure 2. 13 Agglomeration of hydrate particles in the bulk fluid and on the pipe wall (Lund and Larsen, 2000).**

With hydrate growth from the inside and outwards, the CONWHYP concept eliminates the existence of the trapped water inside the hydrate particles. This concept forms the base of SINTEF’s cold flow technology (Larsen et al., 2001) which is illustrated schematically in Figure 2.14. After water separation (if necessary), the fluid from a subsea well is cooled rapidly towards hydrate stability temperature as it passes through un-insulated pipe. Once the fluid enters the hydrate reactor, further cooling occurs and hydrate formation is improved by mixing the cooled fluid containing dry hydrate particles from a downstream stripper. The exiting water in the production fluid will cover the dry hydrate particle surfaces and is converted to hydrate well before it reaches the splitter. Subsequently, the hydrate particles which are dry, non-depositing and non-agglomerating, flow into the main pipeline.

SINTEF-BPs cold flow technology needs large and expensive infrastructure. In terms of fundamental basis for this technology, there are many concerns regarding the applicability

of the approach, such as: avoiding extreme viscosities that may lead to pipeline plugging; adjusting the recycle fluid flow rate and mixing pattern; effective formation of dry hydrate particles; dimensions and operation of a subsea pump required for the recirculation fluid; cooling process, presence of salt, effect of flow rate, etc.

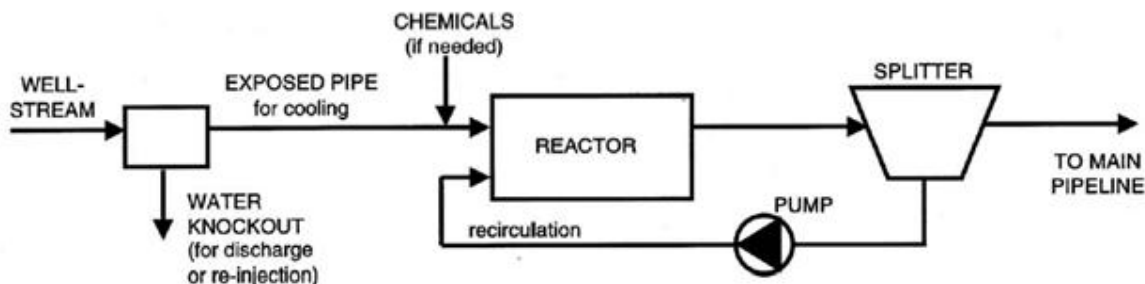


**Figure 2. 14 A schematic description of the hydrate reactor, SINTEF- BP (Larsen et al., 2001).**

### 2.6.3 HYDRAFLOW: A Novel ‘Wet Cold Flow’ Concept Suggested by Heriot Watt University

HYDRAFLOW is a novel ‘wet cold flow’ concept, similar to that of SINTEF-BP and NTNU concepts and breaks from the tradition of straightforward hydrate prevention. The first phase of the research on the HYDRAFLOW concept started in September 2005 with support from the Scottish Enterprise (SE) Proof of Concept Programme. In this first phase of the project, an extensive experimental programme was conducted using a small scale autoclave cell to simulate various production scenarios and fluid systems. The results were all very promising and showed that the concept is feasible at least on the laboratory scale (Haghighi et al., 2007). The second phase which is a Joint Industrial Project (JIP) was planned to generate additional data using a high pressure autoclave cell equipped with helical tube impeller and a large-scale flow loop to enable roll out of this opportunity from mature and water flooded reservoirs.

Although HYDRAFLOW has parallels with other proposed cold flow concepts (e.g. the SINTEF-BP ‘dry hydrates’ approach), it is distinct in that all free water is not converted into hydrates. It is based on allowing gas hydrate formation in the presence of excess water, but preventing hydrate particles agglomeration using low doses (few mass%) of

AAs where necessary. The objective is to minimise or completely eliminate the gas phase by converting gas into hydrates through reaction with formation water (as opposed to other concepts which aim to eliminate all water phase into the dry hydrate particles). If the amount of water in the system is insufficient to convert the gas phase, the HYDRAFLOW suggests adding excess water (e.g. seawater, from other sources or recycle all or part of the liquid/aqueous phase as part of a ‘Loop’ concept). Thus, it is reasonable to describe the HYDRAFLOW concept as “wet cold flow” rather than dry cold flow as used in SINTEF-BP and NTNU concepts.

### **2.6.3.1 Loop Concept**

One of the main benefits of the HYDRAFLOW is its application to a loop production pipeline as it is possible to recycle part or all of the aqueous phase into the system from the surface facilities. Therefore, the recycled fluid plays a significant role in the system and can act as a carrier fluid to transfer hydrate particles towards receiving facilities. Figure 2.15 indicates a typical loop pipeline that collects produced fluids (usually mixture of water-oil emulsion and gas phase) from various wells (each well can be linked to the loop at different points). When the system pressure and temperature enter the gas hydrate stability zone, the water phase converts to the dispersed hydrate particles in the presence of adequate anti-agglomerant concentration. The dispersed hydrate particles are transported as a mixture of water/oil/hydrate to the surface facilities through the recycled fluid. In the receiving facilities, the aqueous phase and gas phase (if present) can be separated easily. Depending on the operational conditions, there are various options for dealing with the oil/hydrate slurry. One can separate hydrate and transport it as a mixture of dry hydrate, or hydrate in water (add water as carrier fluid), or hydrate in oil slurry; or it can be stored as a source of gas (as 1 m<sup>3</sup> of hydrate may contain 150-180 m<sup>3</sup> of gas). Hydrate can also be dissociated, and the oil and gas phase are transported separately.

The proposed HYDRAFLOW approach should reduce or eliminate the risks of hydrate blockage. Low doses of AA chemicals (if necessary) are used to prevent agglomeration and reduce slurry viscosity. By converting the gas phase into hydrates, the density difference between phases (e.g. water, oil, hydrates) will be greatly reduced, which should help to alleviate pipeline slugging problems, thus lowering OPEX/CAPEX. HYDRAFLOW could also reduce pipeline costs by eliminating the need for

heating/insulation, and reducing operating pressures (or increasing capacity). Furthermore, it could have the extra benefit of reducing chemical and disposed water treatment costs (including other chemicals, e.g., corrosion, scale, wax, asphaltene inhibitors) through aqueous phase recycling; which also helps reduce the environmental impact.

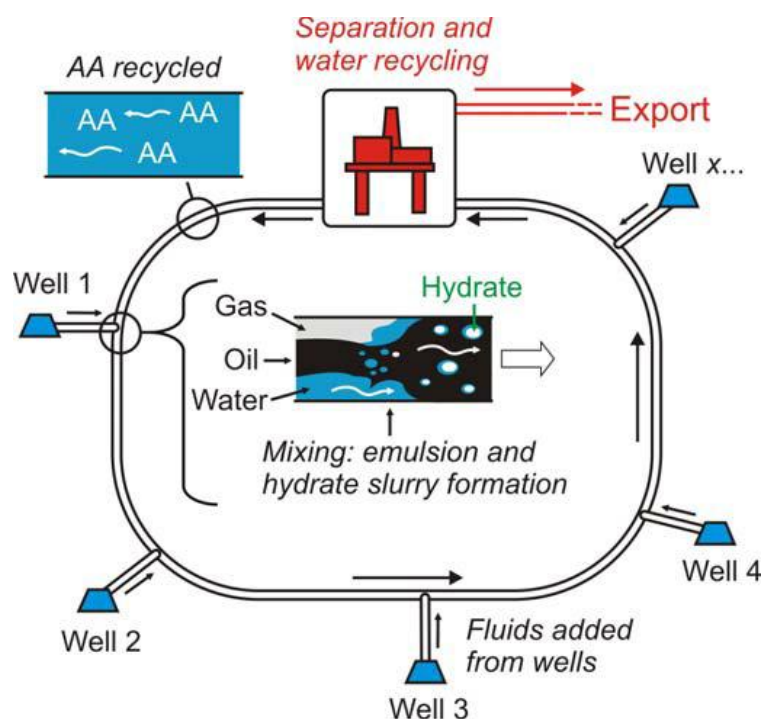


**Figure 2. 15 Illustration of the *HYDRAFLOW* pipeline ‘loop’ concept (Haghighi et al., 2007).**

Recent experimental results have shown that after hydrate dissociation almost all anti-agglomerants remained in the aqueous phase and there was no significant difference observed in the performance of the re-used anti-agglomerants (Azarinezhad et al., 2008b). An additional benefit of the HYDRAFLOW concept is that it could also potentially reduce wax deposition problems by: i) maintaining the pipeline temperature for longer, through exothermic hydrate formation reaction ii) providing solid seeds for wax nucleation in the flowing liquid phase rather than on pipeline walls iii) abrasion of deposited wax by fast moving hydrate particles. Finally, for those interested in gas transportation in the form of

hydrates, HYDRAFLOW could eliminate the need for a hydrate reactor, with the subsea pipeline acting as the reactor with producing hydrates in oil and/or water slurries.

It is obvious that in mature and water-flooded reservoirs the HYDRAFLOW technology may be a more feasible approach compared to alternative techniques available for mitigating the risk of hydrate plugging in pipelines.

The economics of HYDRAFLOW technology compared to other techniques proposed for hydrate management have been evaluated by Azarinezhad (2010) to which the reader is directed for detailed information.

## 2.7 REFERENCES

- Alapati, R., Lee, J. and Beard, D., 2008. Two field studies demonstrate that new LDHI chemistry is effective at high water cuts without impacting oil/water quality, Offshore Technology Conference, OTC 19505, Houston, Texas.
- Andersson, V., 1999. Flow Properties of Hydrate in Water Slurries, PhD Thesis, Norwegian University of Science and Technology.
- Anklam, M.R., York, J.D., Helmerich, L. and Firoozabadi, A., 2007. Effects of anti-agglomerants on the interactions between hydrate particles. *AIChE J.*, 54: 565-574.
- Arjmandi, M., Ren, S.R. and Tohidi, B., 2005. Anti-agglomerant and synergism effect of quaternary ammonium zwitterions, Proceedings of the Fifth International Conference on Gas Hydrates, Trondheim, Norway.
- Aspenes, G., H iland, S., Barth, T. and Askvik, K., 2009. The influence of petroleum acids and solid surface energy on pipeline wettability in relation to hydrate deposition. *Journal of Colloid and Interface Science*, 333(2): 533-539.
- Austvik, T., LI, X. and Gjertsen, L.H., 2000. Hydrate plug properties: formation and removal of plugs. *Annals of the New York Academy of Sciences*, 912(1): 294-303.
- Azarinezhad, R., 2010. A chemical based wet cold flow approach for addressing hydrate flow assurance problems, PhD Thesis, Heriot-Watt University, Edinburgh.
- Azarinezhad, R., Chapoy, A., Anderson, R. and Tohidi, B., 2008a. HYDRAFLOW: A multiphase cold flow technology for offshore flow assurance challenges, OTC 19485, Offshore Technology Conference, Houston.
- Azarinezhad, R., Chapoy, A., Anderson, R. and Tohidi, B., 2008b. Hydraflow: a novel approach in addressing flow assurance problems, Proceedings of the 6th International Conference on Gas Hydrates (ICGH 2008), Vancouver, British Columbia, CANADA.
- Bai, Y. and Bai, Q., 2005. Subsea pipelines and risers. Elsevier Science.
- Clark, L., Anderson, J. and Petrolite, B., 2008. Guap3 scale dissolver and scale squeeze application using kinetic hydrate inhibitor (KHI), Proceedings of the 6th International Conference on Gas Hydrates (ICGH 2008), Vancouver, British Columbia, CANADA.
- Colombel, E., Gateau, P., Barré, L., Gruy, F. and Palermo, T., 2009. Discussion of agglomeration mechanisms between hydrate particles in water in oil emulsions. *Oil & Gas Science and Technology-Revue de l'IFP*, 64(5): 629-636.
- Englezos, P., 1993. Clathrate hydrates. *Industrial & engineering chemistry research*, 32(7): 1251-1274.

Frostman, L., 2000a. Anti-Agglomerant Hydrate Inhibitors for Prevention of Hydrate Plugs in Deepwater Systems, SPE 63122, Society of Petroleum Engineers, Houston, Texas.

Frostman, L., 2000b. Anti-agglomerant hydrate inhibitors for prevention of hydrate plugs in deepwater systems, SPE Annual Technical Conference, SPE 63122, Dallas, Texas.

Gao, S., 2009. Hydrate risk management at high watercuts with anti-agglomerant hydrate inhibitors. *Energy & Fuels*, 23(4): 2118-2121.

Gudmundsson, J.S., 2002. Cold flow hydrate technology, 4<sup>th</sup> International Conference on Gas Hydrates Yokohama pp. 912.

Haghighi, H., Azarinezhad, R., Chapoy, A., Anderson, R. and Tohidi, B., 2007. HYDRAFLOW: Avoiding gas hydrate problems, SPE 107335, Presented at the SPE Europec/EAGE Annual Conference and Exhibition, London.

Hammerschmidt, E., 1934. Formation of gas hydrates in natural gas transmission lines. *Industrial & Engineering Chemistry*, 26(8): 851-855.

Hansen, A., Clasen, T. and Bass, R., 1999. Direct impedance heating of deepwater flowlines, OTC 11037, Offshore Technology Conference, Houston, Texas.

Harun, A., Blanchard, T. and Erdogmus, M., 2008. Managing Hydrate Risks for a Black Oil Long Subsea Tie-Back When Water Cut Predictions Exceed Original Design Basis, SPE-111138, Marrakech, Morocco.

Huo, Z., Freer E., Lamar M., Sannigrahi B., Knauss D. M., E. D. Sloan Jr., 2001. Hydrate plug prevention by anti-agglomeration. *Chemical Engineering Science*, 56: 4979–4991.

Ilahi, M., 2005. Cold Flow Concepts Compared, Master Thesis, Norwegian University of Science and Technology (NTNU), Trondheim, Norway.

Karaaslan, U. and Parlaktuna, M., 2000. Surfactants as hydrate promoters? *Energy & Fuels*, 14(5): 1103-1107.

Kashu, S., Matthews, P. and Subramanian, S., 2004. Gulf of Mexico Export Gas Pipeline–Hydrate Plug Detection and Removal, Offshore Technology Conference, OTC 16691, Houston, Texas, U.S.A., pp. 3-6.

Katz, D.L.V., 1959. Handbook of natural gas engineering. McGraw-Hill New York.

Kelland, M.A., 2006. History of the development of low dosage hydrate inhibitors. *Energy & Fuels*, 20(3): 825-847.

Kelland, M.A., Svartaas, T.M., Ovsthus, J., Tomita, T. and Mizuta, K., 2006. Studies on some alkylamide surfactant gas hydrate anti-agglomerants. *Chemical Engineering Science*, 61(13): 4290-4298.

Kini, R.A., Matthews, P.N., Subramanian, S. and Creek, J., 2005. Change the focus of hydrate plug prevention in the oil industry, Presented at 5th International Conference on Gas Hydrate, Trondheim, Norway, pp. 1215.

Larsen, R., Lund, A., Andersson, V. and Hjarbo, K., 2001. Conversion of Water to Hydrate Particles, SPE 71550-MS, presented at the 2001 SPE Annual Technical Conference and Exhibition, New Orleans, Louisiana.

Lederhos, J., Long, J., Sum, A., Christiansen, R. and Sloan, E., 1996. Effective kinetic inhibitors for natural gas hydrates. *Chemical Engineering Science*, 51(8): 1221-1229.

Lund, A. and Larsen, R., 2000. Conversion of water to hydrate particles-theory and application, presented at 14th (2000) Symposium on Thermophysical Properties, Boulder.

Lund, A., Lysne, D., Larsen, R. and Hjarbo, K.W., 1999. Method and system for transporting a flow of fluid hydrocarbons containing water. patent application PCT/NO99/00293.

Makogon, Y., 1965. Hydrate formation in gas bearing strata under perma frost. *Gazov Prom-st*, 5: 14–15.

Masoudi, R., Tohidi, B., Danesh, A., Todd, A. and Yang, J., 2006. Measurement and Prediction of Salt Solubility in the Presence of Hydrate Organic Inhibitors. *SPE Production & Operations*, 21(2): 182-187.

Mehta, A. and Klomp, U., 2005. An industry perspective on the state of the art of hydrates management, *Proceedings of the Fifth International Conference on Gas Hydrates*, Trondheim, Norway.

Mehta, A. and Sloan, E., 1999. Structure H hydrates: Implications for the petroleum industry. *SPE Journal- SPE* 53450 4: 3-8.

Mokhatab, S., Wilkens, R. and Leontaritis, K., 2007. A review of strategies for solving gas-hydrate problems in subsea pipelines. *Energy Sources, Part A: Recovery, Utilization, and Environmental Effects*, 29(1): 39-45.

Mooijer-Van Den Heuvel, M.M., 2004. Phase Behaviour and Structural Aspects of Ternary Clathrate Hydrate Systems The Role of Additives, PhD Thesis, Delft University of Technology Delft, The Netherlands.

Nysveen, A., Kulbotten, H., Lervik, J. K., Børnes, A. H., 2007. Direct Electrical Heating of Subsea Pipelines—Technology Development and Operating Experience. *Industry Applications, IEEE Transactions on*, 43(1): 118-129.



- Oskarsson, H., Nobel, A., Lund, A., Hjarbo, K.W., 2005. New Technique for Evaluating Antiagglomerate Gas-Hydrate Inhibitors in Oilfield Applications, SPE 93075, Society of Petroleum Engineers, Houston, Texas.
- Pakulski, M. and Hurd, D., 2005. Uncovering a Dual Nature of Polyether Amines Hydrate Inhibitors, Proceedings of the Fifth International Conference on Gas Hydrates, Trondheim, Norway.
- Palermo, T., Mussumeci, A. and Leporcher, E., 2004. Could hydrate plugging be avoided because of surfactant properties of the crude and appropriate flow conditions?, OTC 16681, Presented in the Offshore Technology Conference, Houston, Texas.
- Pickering, P., Edmonds, B., Moorwood, R., Szczepanski, R. and Watson, M., 2001. Evaluating new chemicals and alternatives for mitigating hydrates in oil & gas production, In IIR Conference Aberdeen, Scotland, pp. 1-15.
- Ripmeester, J.A., Tse, J.S., Ratcliffe, C.I. and Powell, B.M., 1987. A new clathrate hydrate structure. *Nature*, 325(6100): 135-136.
- Sinquin, A., Palermo, T. and Peysson, Y., 2004. Rheological and flow properties of gas hydrate suspensions. *Oil & Gas Science and Technology*, 59: 41-57.
- Sloan, E.D., 1998. Gas hydrates: review of physical/chemical properties. *Energy & Fuels*, 12(2): 191-196.
- Sloan, E.D., 2003. Fundamental principles and applications of natural gas hydrates. *Nature*, 426(6964): 353-363.
- Sloan, E.D., 2005. A changing hydrate paradigm--from apprehension to avoidance to risk management. *Fluid Phase Equilibria*, 228: 67-74.
- Sloan, E.D. and Koh, C.A., 2008. Clathrate hydrates of natural gases. 3<sup>th</sup> ed. CRC Press, New York.
- Song, D., Zhang, W., Melby, E.G. and Gupta, R.K., 2008. An instrumented mixer setup for making tackifier dispersions used to make pressure-sensitive adhesives. *Measurement Science and Technology*, 19: 045801.
- Sugaya, M. and Mori, Y.H., 1996. Behavior of clathrate hydrate formation at the boundary of liquid water and a fluorocarbon in liquid or vapor state. *Chemical Engineering Science*, 51(13): 3505-3517.
- Wolden, M., Lund, A., Oza, N., Makogon, T., Argo, C.B., Larsen, R., 2005. Cold flow black oil slurry transport of suspended hydrate and wax solids, *Proceedings of the Fifth International Conference on Gas Hydrates*, Trondheim, Norway.

York, D. and Firoozabadi, A., 2009. Effect of Brine on Hydrate Antiagglomeration. *Energy & Fuels* 23: 2937–2946.

Zanota, M.L., Dicharry, C. and Graciaa, A., 2005. Hydrate Plug Prevention by Quaternary Ammonium Salts. *Energy & Fuels* 19: 584-590.

Zerpa, L.E., Salager, J.L., Koh, C.A., Sloan, E.D. and Sum, A.K., 2011. Surface Chemistry and Gas Hydrates in Flow Assurance. *Industrial & engineering chemistry research*, 50: 188–197.

## **CHAPTER 3      WATER-CRUDE OIL EMULSIONS WITH APPLICATION TO GAS HYDRATES**

### **3.1 INTRODUCTION**

In deepwater exploration and production, where long tieback multiphase pipelines are preferred economic option, gas hydrate blockages are posing serious problems for flow assurance to produce hydrocarbon with high water cuts because the traditional techniques, such as insulation, heating or injection of thermodynamic inhibitors, often becomes economically and logistically impractical. For this reason, the potential of transporting hydrate slurry is one of the most attractive scenarios to the industry for hydrate plug prevention.

The important properties of hydrate slurry are their flow properties, in other words their rheology. The rheological behaviour of hydrate slurries not only depends on the concentration of hydrate particles or hydrate aggregates, but on the rheological behaviour of the fluid which is used as carrier fluid for hydrate particles. These carrier fluids are most often an emulsion of water and oil. Therefore, the rheological behaviour of emulsion and its relation with hydrate particles are of great interest not only for fundamental scientific understanding but also for practical industrial applications.

Several studies have revealed that the presence of some natural components in the crude oils can have a mitigating effect on the plugging tendency of the hydrates and cause hydrate suspensions to be transported easily as slurry flow, although this transportability is somewhat limited by the viscosity of the hydrate slurry at high hydrate volume fractions (Ekott and Akpabio, 2010; Fandes, 1996; Fotland et al., 2011; Leporcher et al., 1998). One suggestion is that those natural components act like surfactants and adsorb on the hydrate surface. Formation of surfactant film on hydrate particles makes an "oil-wet" surface with low tendency to agglomeration and plugging (Figure 3.1). A better knowledge of natural components in the crude oil that influence hydrate anti-agglomeration behaviour can give a precious tool to hydrate plug assessment and can provide positive economic and environmental effects. Motivated by the above observations, this chapter starts with an overview of compositions and existing natural surfactants in crude oils. Additionally, this

chapter will focus on a review of fundamental concepts of water-oil emulsions and surface chemistry, two main subjects of interfacial phenomena, identifying hydrate formation and agglomeration in oil and gas systems.

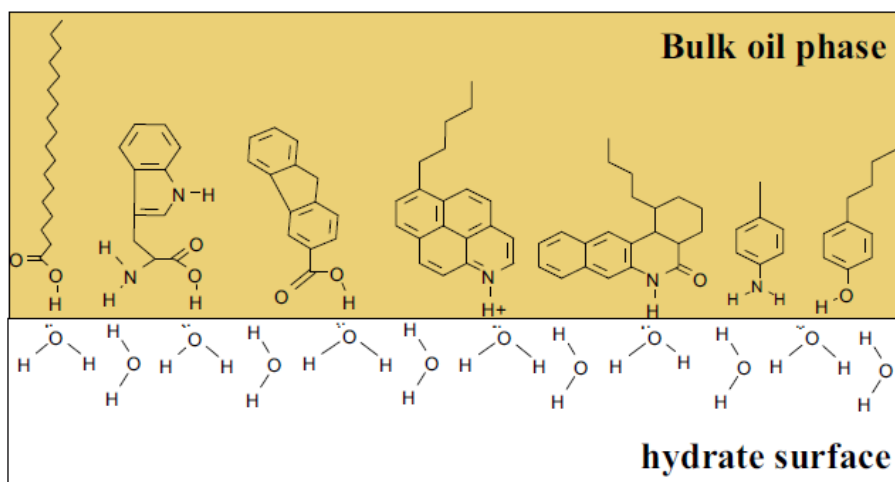


**Figure 3. 1 Surface active components in crude oils can adsorb to hydrate surfaces and change the wettability which reduces the agglomeration of hydrate particles (Erstad, 2009).**

### 3.2 CHEMISTRY AND CLASSIFICATION OF CRUDE OILS

Crude oil is a complex mixture of many different components and depending on location and age of the field might have completely different physical and chemical properties. Composition of crude oils consists mainly of organic compounds (hydrocarbons) with minor amounts of inorganic non-hydrocarbon compounds. The elemental composition of crude oil sources from all over the world is given in Table 3.1 (Erstad, 2009; Speight, 2007).

**Table 3. 1 Elemental composition of petroleum (Erstad, 2009; Speight, 2007).**

Element	%
Carbon	83.0-87.0
Hydrogen	10.0-14.0
Nitrogen	0.1-2.0
Oxygen	0.05-1.5
Sulphur	0.05-6.0
Metals (Ni and V)	<1000 ppm

Crude oils have complex composition and it is impossible to characterize the crude oils by the individual molecular types. Therefore, elemental analysis of crude oils is not desirable since it gives only a limited understanding of the composition of crude oil due to the uniformity of elemental composition. The precise chemical composition of crude oil components especially that of the heavy end of the system, is still speculative. Instead, hydrocarbon group type analysis is commonly employed (Aske et al., 2001). The SARA-separation is an example of such group type analysis, separating heavy end of a crude oil into four distinct fractions namely saturates (S), aromatics (A), resins (R), and asphaltenes (A). Figure 3.2 indicates the SARA-separation scheme (Aske et al., 2001).

The saturates (aliphatics) are non-polar hydrocarbons, without double bonds, but including straight or branched chains (paraffins), as well as containing one or more cyclic structures (naphthenes). Cycloalkanes contain one or more rings, which may have several alkyl side chains. Saturates commonly are the lightest fraction of hydrocarbons and their proportion usually decreases with increasing molecular weight fractions. Wax is a sub-class of saturates, consisting primarily of straight-chain alkanes, mainly ranging from C<sub>20</sub> to C<sub>30</sub>.

The aromatic series is an unsaturated closed-ring series, based on the benzene compound. These ring systems may be linked up with naphthene rings and/or aliphatic side chains. They are usually classified as mono-, di-, and tri-aromatics depending on the number of aromatic rings present in the molecule. The closed ring structure gives aromatics a greater stability than open compounds where double or triples bounds occur. Polar, higher molecular weight aromatics may fall in the resin or asphaltene fraction.

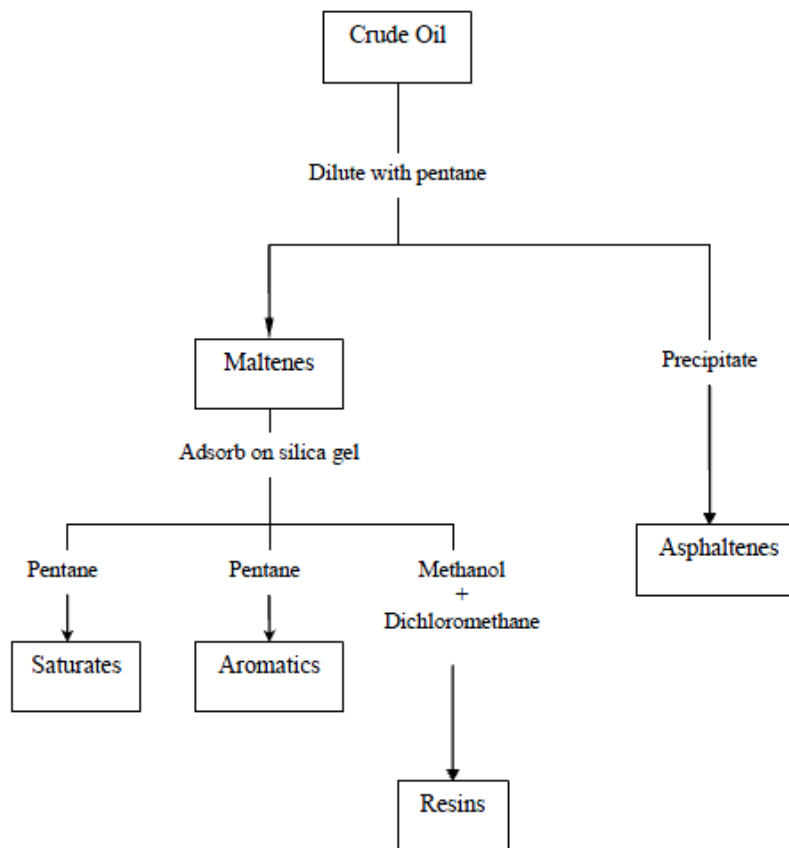


**Figure 3. 2 Schematic of SARA fractionation of crude oils (Auflem, 2002).**

The polar compounds in the crude oil containing hetero atoms such as nitrogen, oxygen or sulphur are often called NSO-compounds or resins. The resin fraction is operationally characterized, and it is generally described as the fraction which is soluble in light alkanes such as pentane and heptane, but insoluble in liquid propane. H/C ratio of resins is relatively higher than asphaltenes, 1.2-1.7 compared to 0.9-1.2 for the asphaltenes (Auflem, 2002). Resins and asphaltenes exhibit similarities in chemical structure but molecular weight of resins is smaller (<1000 g/mole). It has been documented that resins can be adsorbed on to the asphaltene aggregates and keeps them dispersed in the crude oil medium (Aske et al., 2002).

The asphaltene content in crude oils is an important aspect of fluid processability. Asphaltenes, like resins are characterized as a solubility class of crude oil, rather than a chemical class. They are the fraction of the crude oil precipitating in light alkanes like pentane, hexane or heptanes and are soluble in aromatic solvents like toluene and benzene.

Asphaltenes are polar molecules and they are structurally similar to resins, but with higher molecular weight, typically 500–1500 g/mole. Asphaltene fractions are the heaviest and most polar molecules in the crude oil, containing the largest percentage of hetero atoms (N, S, O, metals) than the rest of the components in the crude oil (Aske et al., 2002). It is now believed that the structure of the asphaltenes consist of polycyclic aromatic clusters, substituted with varying alkyl side chains (Sjöblom et al., 2003). Figure 3.3 shows a hypothetical asphaltene monomer molecule.

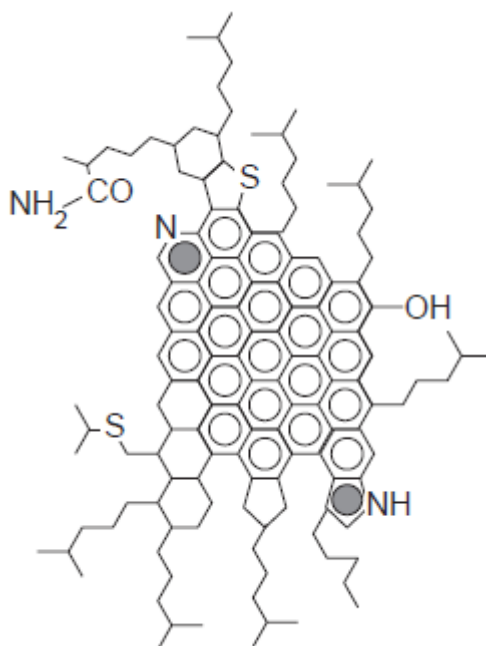


**Figure 3. 3 Example of asphaltene molecule (Langevin et al., 2004).**

Asphaltenes tend to attract each other to form agglomerates. It is believed that asphaltenes suspend as aggregates in the crude oil and the size of the aggregate structures has been suggested to lie between 2 and 25 nm in diameter (Auflem, 2002; Burya et al., 2001; Ravey et al., 1988). The most common theory of asphaltene stability in crude oil suggests that naturally occurring resin molecules form a steric repulsive layer around asphaltene particles. Previous studies have reported that the presence of resins in the crude oil is essential in preventing asphaltene precipitation through dissolving the asphaltenes. Resins are believed to attach to the asphaltene aggregates with their polar groups, and stretch their

aliphatic groups outward to form a steric-stabilisation layer around asphaltenes (Auflem, 2002; Koots and Speight, 1975; Leontaritis and Mansoori, 1987). Resins are needed to suspend the asphaltene aggregate; hence the aggregate is a complex of asphaltene-resin. It is believed that asphaltenes are polycyclic molecules with disc shape and have a tendency to form stacked aggregates (Langevin et al., 2004). Using X-ray diffraction measurements, Yen et al. (1961) showed that dry asphaltenes contain a core of fused aromatic flat rings with an aliphatic periphery (Figure 3.4). Asphaltene aggregates approximately consist of four to five of these flat rings held together with  $\pi$ -bonds, hydrogen bonds, and electron donor-acceptor bonds (Aske, 2002; Spiecker, 2001).

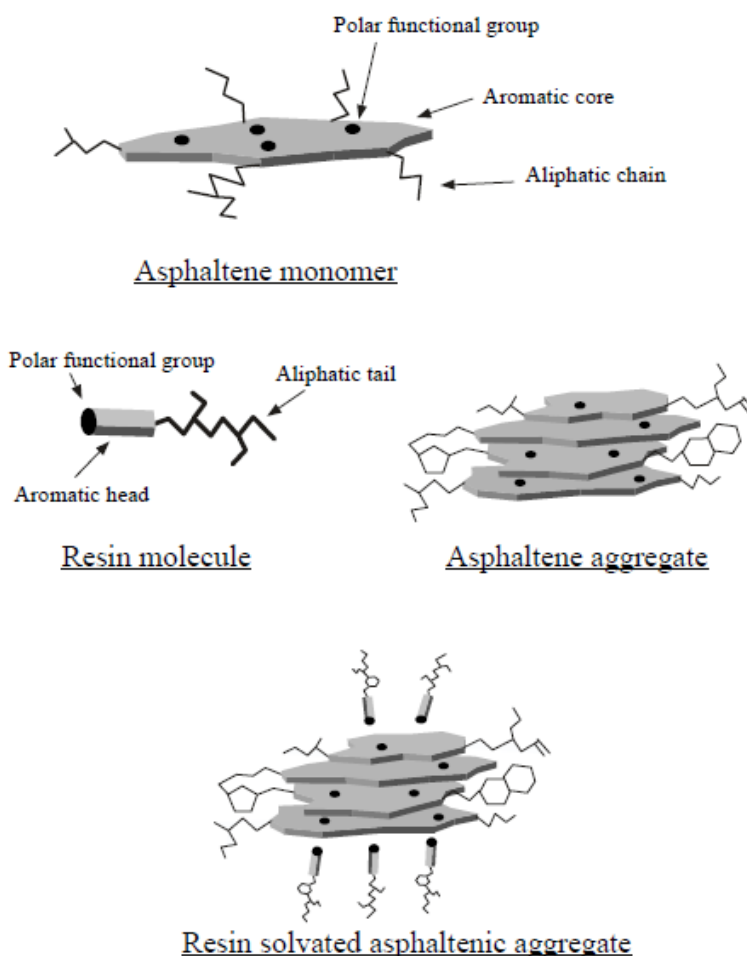


Figure 3. 4 Resin solvated asphaltene aggregate (Spiecker, 2001).



If the concentration of resins is insufficient to cover the surface of the asphaltene particles, then the asphaltene will precipitate out of the solution (Auflem, 2002; Sjöblom et al., 2003).

### **3.3 BIODEGRADATION OF CRUDE OIL**

Biodegradation process, which is a microbial alteration, leads to substantial composition change of crude oil by living organisms (Aspenes, 2009; Borgund, 2007; Head et al., 2003). The existence of bacteria can degrade some of the compounds in crude oil under certain conditions, using them as a source of carbon. The n-alkanes, a major group in crude oil, are readily biodegraded first, followed by branched and cyclic hydrocarbons (Borgund, 2007).

It has been reported that biodegradation (requires oxygen) takes place mainly at the oil-water interfaces, because the bacteria usually lives in the water phase and consume components from the oil phase (Borgund, 2007). Therefore, the presence of water phase is necessary for degradation of the crude oils. Sufficient temperature of petroleum reservoir is another parameter that needs to be achieved for the biodegradation process. Generally the degradation level decrease with increasing temperature up to 80 °C (usually for shallow reservoirs) (Head et al., 2003; Larter et al., 2003).

Biodegradation process makes the crude oil increasingly heavier and results in the reduction of the quality and economic of crude oils and can cause some problems for both the oil recovery and refining process. Biodegradation of the lighter hydrocarbons can lead to formation of heavy polar compounds in the crude oil like asphaltenes (Borgund, 2007). Oxidation of hydrocarbons in the crude oil (C6+ components) during biodegradation process result in reduction in saturated hydrocarbon content and API gravity, a measure that correlates with economic value, but it leads to an increase in oil density, sulphur content, acidity, viscosity and metal content (Borgund, 2007; Head et al., 2003).

The rheological behaviour of hydrate slurry is influenced by the crude oil composition, and therefore, the process of biodegradation seems to be of great importance. It has conclusively been shown that plugging oils are usually non-biodegraded crude oils whereas the majority of non-plugging crude oils are biodegraded (Aspenes, 2009; Erstad,

2009). These occurrences have been attributed to the presence of heavy polar components and relatively large amount of acids in the crude oils during the biodegradation process (Borgund et al., 2008; Fadnes, 1996; Leporcher et al., 1998).

### **3.4 FUNDAMENTALS OF WATER-OIL EMULSIONS**

#### **3.4.1 Classification And Formation Of Emulsions**

Emulsions can be found in almost every part of the petroleum production and recovery process and can be encountered at many stages during drilling, production, transport and processing. Formation of an emulsion requires at least two immiscible liquid phases in the presence of an emulsifying agent. The emulsifier can either exist naturally in one phase, or can be added to one of the phases or both. In emulsion systems, one of the phases is dispersed as globules in the other. The type of emulsion can be characterized according to different physical criteria. In the petroleum industry, the type of emulsions consisted of two immiscible liquids are commonly water-in-oil or oil-in-water emulsions (Schramm, 1992; Zerpa et al., 2011).

If the ratio of phase volumes in an emulsion is very large or very small, then the phase having the larger volume is frequently the continuous phase. If the phase volume ratio is approaching the 1:1 ratio, then other parameters characterize the type of emulsion. Table 3.2 indicates some simple examples of type of crude oil emulsions.

The morphology of emulsion means its presence as either W/O, O/W or multiple emulsions. There are two basic rules that mark the two different approaches to emulsion morphology. The first rule stated by Ostwald who explained that the morphology of an emulsion strongly depends on the volume fraction of the dispersed phase (Aichele, 2009; Vaessen, 1996). He showed that the volume fraction of dispersed phase could not exceed the maximum closed packing for a face centred cubic lattice which is 0.74. Both W/O and O/W emulsions may occur when the volume fraction of dispersed phase is between 0.26 and 0.74. If this fraction exceeds 0.74, it will likely result in a phase inversion in the emulsion. This rule shows an ambivalence range for phase inversion from W/O to O/W and vice versa.

**Table 3. 2 Examples of emulsion in the petroleum industry (Schramm, 1992).**

Occurrence	Usual Type <sup>1</sup>
<b>Undesirable Emulsions</b>	
Well-head emulsions	W/O
Fuel oil emulsions (marine)	W/O
Oil sand flotation process, froth	W/O or O/W
Oil sand flotation process, diluted froth	O/W/O
Oil spill mousse emulsions	W/O
Tanker bilge emulsions	O/W
<b>Desirable Emulsions</b>	
Heavy oil pipeline emulsion	O/W
Oil sand flotation process slurry	O/W
Emulsion drilling fluid, oil-emulsion mud	O/W
Emulsion drilling fluid, oil-base mud	W/O
Asphalt emulsion	O/W
Enhance oil recovery in situ emulsions	O/W

<sup>1</sup> W/O means water-in-oil; O/W means oil-in-water

Secondly, Bancroft (1915) indicated that the phase solubility of a surfactant also contributes to the emulsion type (Aichele, 2009). He explained that the liquid in which the surfactant is most soluble becomes the continuous phase. As a result, an oil-soluble surfactant tends to form water-in-oil emulsion, whereas a water soluble surfactant tends to form oil-in-water emulsion. This concept is a useful empirical method of determining the emulsion morphology in which a surfactant will potentially stabilise (O/W or W/O); however, it is clear that Bancroft's rule cannot predict any hysteresis effects.

The following are the essential factors which are needed to prepare water in oil emulsions (Langevin et al., 2004; Schramm, 1992; Zerpa et al., 2011):

1. Two immiscible liquids must be brought in contact
2. Surface active component must present as the emulsifying agent
3. Sufficient mixing or agitating effect must be provided in order to disperse one liquid into another as droplets

In emulsions, large amount of interfacial area is created resulting in a thermodynamically unstable state in the system. As the immiscible phases separate over time, the interfacial area and therefore the free energy of the dispersion are reduced. It means that the

characteristics of the emulsion (drop size distribution, mean drop size and other properties) may not be constant with time. Therefore, the stability of an emulsion refers to the ability of the dispersion to preserve its properties within a given timeframe. Sufficient mixing effect must be applied in order to overcome the surface energy and to disperse one liquid into another as the dispersed droplets. Indeed, this energy used to overcome the drop's Laplace pressure  $\Delta P$ , which is the difference between the pressure inside and outside the droplet, is given by (Schramm, 1992):

$$\Delta P = \sigma \left( \frac{1}{R_1} + \frac{1}{R_2} \right)$$

where  $\sigma$  is the interfacial tension between water and oil phases and  $R_1$  and  $R_2$  are the principal radii of curvatures. For spherical droplets in an emulsion, the equation reduces to

$$\Delta P = \frac{2\sigma}{R}$$

To deform droplets, an external force, that is large enough to overcome the Laplace pressure, must be applied on the emulsion (e.g. mechanical agitation). The Laplace equation demonstrates that higher external stress is needed to deform small droplets. This external stress decreases with reduction of interfacial tension. Reh binder equation explains that formation of new surface in the emulsion requires work as given in the following equation (Ganiev et al., 2009):

$$W_E = \sigma \Delta A$$

where  $\Delta A$  is forming surface area. It shows that two immiscible liquid thermodynamically prefer to minimise the energy of system by separating into separate phases, hence reducing the surface area.

### 3.4.2 Stability of Emulsions

In an emulsion, the dispersed droplets can come together in very different ways. Emulsion instability may involve a number of processes which take place simultaneously or consecutively, depending on the system conditions. Figure 3.5 indicates three common destabilization mechanisms of water-in-oil emulsions. Sedimentation (the opposite of creaming) arises due to density differences between the two liquid phases and results in a droplet concentration gradient, which produce a close packing of the dispersed droplets.

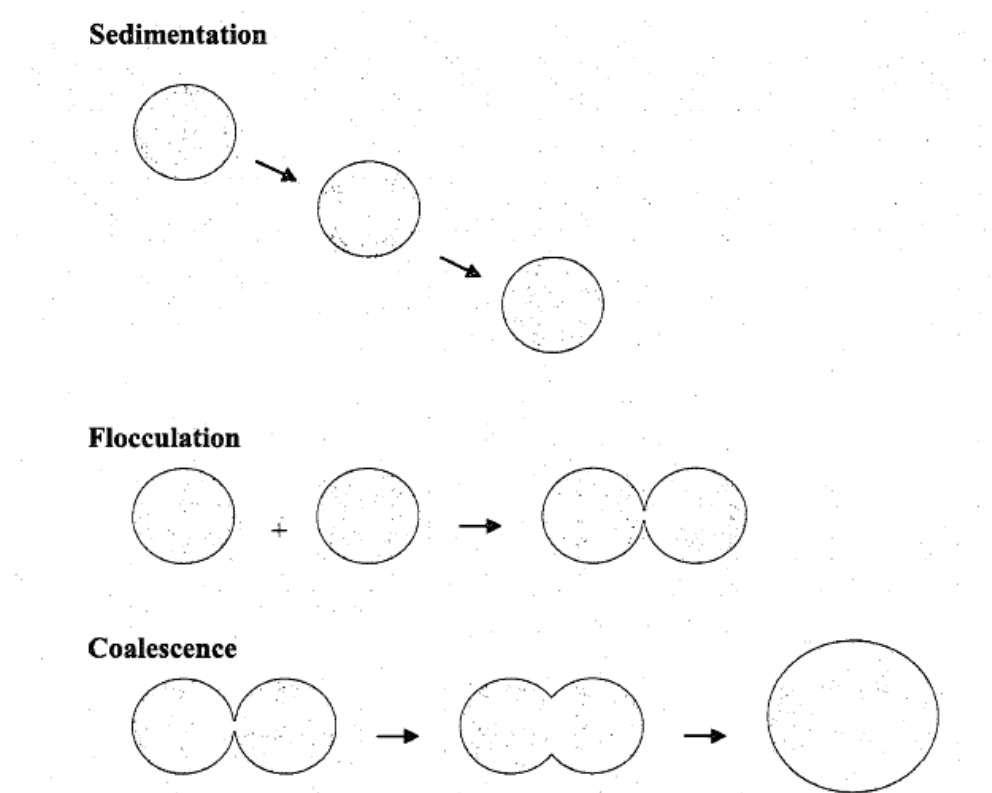
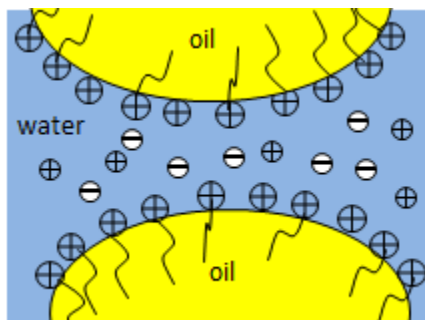


**Figure 3. 5 Common destabilization mechanisms of water-in-oil emulsion (Aichele, 2009).**

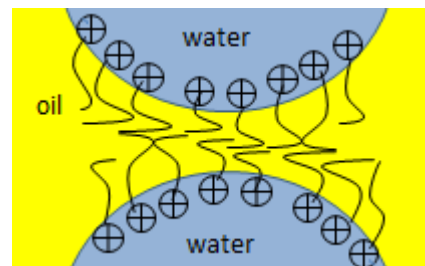
Flocculation (aggregation) occurs when two or more droplets stick together with touching only at certain points, but there is still a separating liquid film between droplets. In the flocculation process, total surface area of the dispersed phase does not almost change. This process can promote coalescence of small droplets and the formation of larger droplets. In coalescence, the thin liquid film between droplets breaks and small droplets combine together to form a larger droplet with a reduced total surface area. Thus, it can be concluded that the stability of emulsions is mostly affected by the nature of the interfacial film and surfactant adsorption mechanisms (Aichele, 2009; Auflem, 2002; Kokal, 2008; Kokal, 2006).

Figure 3.6 illustrates some mechanisms that influence the stability of an emulsion system. Figure 3.6a shows the distribution of electrical charges at the thin liquid film between droplets caused by the adsorption of ionic surfactants. When two charged droplets come

close to each other and their electric double layers overlap, an effective repulsive force is created that significantly stabilize the emulsion system. The effect of electrical repulsive force is more pronounced in oil-in-water emulsions because the electric double-layer thickness is much greater in water than in oil (Schramm, 1992; Zerpa et al., 2011).



(a) Electrostatic repulsion between charged interfaces



(b) Steric repulsion between interfaces with nonionic surfactants

**Figure 3.6 Some mechanisms of emulsion stability (adopted from Zerpa et al., 2011).**

The second mechanism that may affect the stability of an emulsion system, so called steric repulsion, from the root "stereo" which is associated with the idea of volume or three-dimensional effect (Salager, 1994). Figure 3.6b demonstrates the steric repulsion for dispersed droplets in an emulsion system stabilised by physical barriers of adsorbed material such as polymer or surfactant chains (Salager, 1994; Schramm, 1992; Zerpa et al., 2011). For example, when two interfaces are approached, these barrier layers bump one against the other, and the actual distance between the droplet surfaces may not reach the minimum required for the cohesion/adhesion force to take over. This kind of steric stabilization is probably responsible for the stability of water-in-oil emulsions in the crude oil production; where the steric repulsion comes from the bulky hydrophobic groups of natural surfactants in the emulsion system such as asphaltenes and resins or the surfactants added on purpose (Kokal, 2006).

### 3.4.3 Film Drainage and Interfacial Viscosity

The coalescence process of two collided droplets strongly depends on the drainage of the film formed between them (Ekott and Akpabio, 2010; Kokal, 2006). Due to the presence of the surfactant (either added on purpose or existing naturally in the system) collected on the water-oil interface; rigid interfacial films are formed that encapsulate the water droplets. These interfacial films stabilize an emulsion by lowering the IFT and increasing their interfacial viscosity (Kokal, 2006). The interfacial viscosity is the viscosity of the fluid film at the water-oil interface. It is well documented that the interfacial viscosity plays a very important role in determining the stability of emulsions (Campanelli and Cooper, 1989; Kokal, 2008; Kokal, 2006; Wasan et al., 1979; Wasan and Mohan, 1977). Emulsion stability has been correlated with the mobility of interfacial films. Surfactants that modify the rigidity of the film can affect demulsification considerably. High interfacial viscosities significantly slow the liquid drainage rate and thus have a stabilizing effect on the emulsion. Wasan and Mohan (1977) and Wasan et al. (1979) have shown that surfactants which lower the interfacial viscosity also destabilize crude oil-water emulsions. In contrast, surfactants which maximize interfacial viscosity maximize emulsion stability (Campanelli and Cooper, 1989).

As two droplets come together, their external surfaces are stretched. When an interface with adsorbed surfactant is stretched, it resists the stretching due to its viscoelastic behaviour, resulting in a surfactant concentration gradient (Figure 3.7). This surfactant gradient on the oil/water interface will result in a subsequent interfacial tension gradient: relatively low interfacial tension on the edge and relatively high interfacial tension on the centre. Such an interfacial tension gradient will produce a counter-flow along the surface. This is the so-called Gibbs-Marangoni effect. The counter-flow may compensate the drainage flow and the interface can be considered as a rigid film. Physical cross-linking of asphaltenic aggregates will also contribute to this resistance to coalescence (Aske et al., 2002).

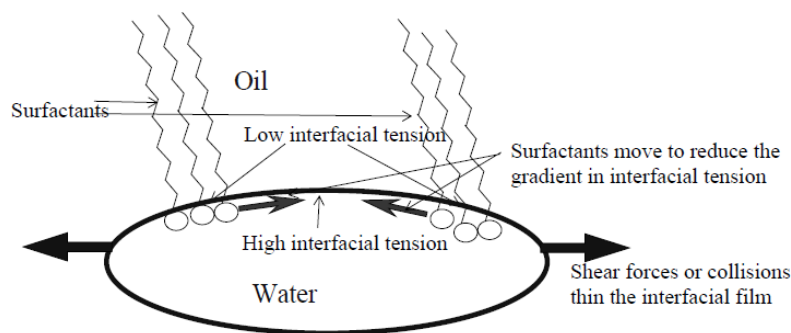


**Figure 3. 7 Gibbs-Marangoni effect at oil-water interface (Aske, 2002).**

#### 3.4.4 Factors Affecting Surface Films and Stability

A number of studies have found that the formation of interfacial films with elastic or viscous properties is responsible to the stability of water-in-oil emulsions (Auflem, 2002; Kokal, 2008; Kokal, 2006; Zerpa et al., 2011). These interfacial films result from the adsorption of high molecular weight hydrocarbons and behave like surfactants at the water-oil interfaces. They improve the stability of an emulsion by increasing the interfacial viscosity. Highly viscous interfacial films retard the rate of film drainage during the coalescence of the water droplets by providing a mechanical barrier to coalescence, resulting in a reduction in the rate of the droplets coalesce.

The interfacial film mobility have been classified into two categories; rigid or solid films and mobile or liquid films (Jones et al., 1978; Kokal, 2006). Rigid films are characterized by very high interfacial viscosity and cover the water droplets with an insoluble layer like solid skin. They provide a structural barrier to droplet coalescence and increase emulsion stability. On the contrary, mobile films are characterized by low interfacial viscosities and they are less stable than rigid films. Adding a demulsifier, for example, may alter a rigid film into a mobile film.

The main parameters that are believed to affect quality of interfacial films are heavy polar fractions in the crude oil such as asphaltens and resins. The nature of asphaltenes in the crude oil is still a subject of debate (Kokal, 2006). Asphaltenes are believed to be dispersed in the oil phase by the resinous components (Auflem, 2002; Kokal, 2006; Spiecker, 2001). In fact, resins are thought to act as peptizing agents for asphaltenes and together form



clusters called micelles (the terms “aggregate” and “micelle” are often used interchangeably in the literature) (Kokal, 2006) (Figure 3.8a).

In many studies, the interfacial film and emulsion forming behaviour have been related to the crude oil asphaltenes and their interplay with resins as a solubilizing agent (Eley et al., 1988; Johansen et al., 1989; Long, 1981; Siffert et al., 1984; Spiecker, 2001; Strassner, 1968; Van der Waarden, 1958). Kilpatrick and Spiecker (2001) published a paper in which they described that the resins are unnecessary in the stabilisation of the asphaltenic film. Once water is added to the crude oil, the asphaltenic aggregates in the oil phase adsorb to the interface film (Figure 3.8b). Although resins are crucial factors to create asphaltenic aggregates and prevent asphaltene precipitation in the crude oil, Kilpatrick and Spiecker (Kilpatrick and Spiecker, 2001) reported that resins are likely shed and do not participate in the stabilising film.

Long et al. (1981) found that once resins were removed from the crude oil by adsorption chromatography, the remaining oil phase could no longer stabilise the asphaltenes. Eley et al. (1988) indicated that the stability of water-in-crude oil emulsions depended on the asphaltene precipitation point and when the asphaltenes were on the edge of precipitation or above, higher emulsion stability was observed.

Van der Waarden(1958) conducted experiments with formation of a water-in-oil emulsion prepared by asphaltenes dissolved in a model oil system. His results indicated that the most stable emulsions typically formed when asphaltenes were near their solubility limit in aliphatic-aromatic mixtures typically. The flocculation of asphaltenes can be prevented for solvents of high aromaticity. Moreover, Van der Waarden(1958) carried out experiments to study the rheological behaviour of interface film using a torsion oscillation method where the oscillation amplitude of a glass disk suspended at the oil-water interface was monitored in the presence of asphaltenes. His findings showed that asphaltenes at or near the point of flocculation exhibited a viscous film and that emulsion stability was facilitated by the adsorption of the coherent asphaltene layer.

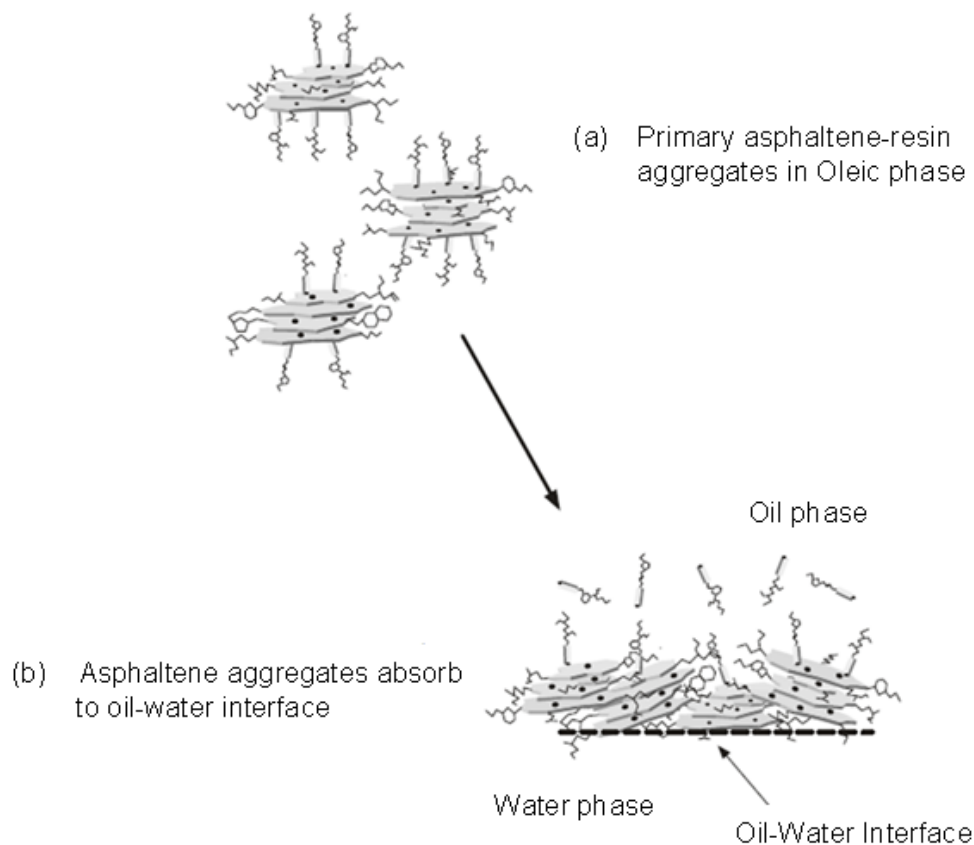


**Figure 3. 8 Accumulation of asphaltene aggregates at the oil-water interface (Spiecker, 2001).**

Asphaltenes are very large and complex molecules and as it reported certain types of compounds in the asphaltenes and/or resins with surfactant properties possibly play a major role in producing stable emulsions. Lee's study (1999) indicated that within the asphaltene fraction, the nickel porphyrins seem to play a significant role in formation of stable emulsions. He reported that compounds with higher solubility in the oil phase than in the aqueous phase are the most likely emulsifying agents to produce stable water-in-oil emulsions. Numerous studies have attempted to explain the emulsifying and stability behaviour of crude oil-water systems. These studies often showed that the asphaltene constituents in crude oils are responsible for film formation and stabilization of water-crude oil emulsions (Cairns et al., 1974; Shetty et al., 1992; Spiecker, 2001).

Wax particles were also found in microscope studies of emulsions produced by North Sea crude oil (Lee, 1999; Thompson et al., 1985). It has been reported that waxes are soluble in crude oils but cannot work by themselves as surface active agents to create stable

emulsions. However, they may act in combination with resins and asphaltenes to stabilize oil-in-water emulsions (Lee, 1999).

It has been found that finely divided insoluble solid particles, which may present in the crude oils, can adsorb at the droplet surface and act as a barrier preventing droplets from coalescing (Kokal, 2005; Tambe and Sharma, 1994; Yan et al., 2001). However, the role of these fine solid particles in stabilizing emulsions and the mechanisms involved depends upon several factors including particle size; inter particle interactions, and the wettability of the particles. Solid particles must be located on the interfacial surface with sufficient particle density. Therefore, the size of solid particles must be much smaller than the size of the dispersed droplets to act as emulsion stabilizer. For example, in the paper published by Yan et.al (2001), they used solid particles with a 12 nm diameter while water droplets were 2  $\mu\text{m}$ . However, if the size of the dispersed droplets in an emulsion is sufficiently smaller than solids, the emulsion is the continuous phase for the solids (Yan et al., 1991). Therefore, the solids cannot treat the dispersed droplets even if the size and size distribution of the solids are similar to the dispersed droplets. The effectiveness of finely divided solid particles in stabilizing emulsions also depends mainly on the formation of a densely packed layer of solid particles at the interfacial surface. This solid layer creates steric hindrance to the coalescence of water droplets (Figure 3.9).

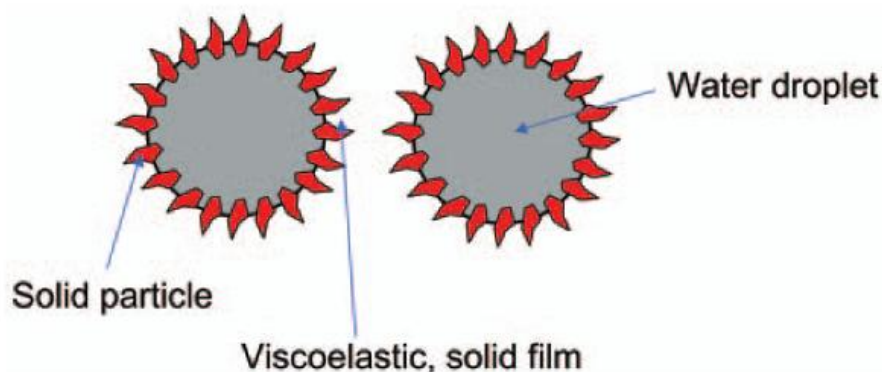


**Figure 3. 9 Droplet stabilization by very fine solids (Kokal, 2006).**

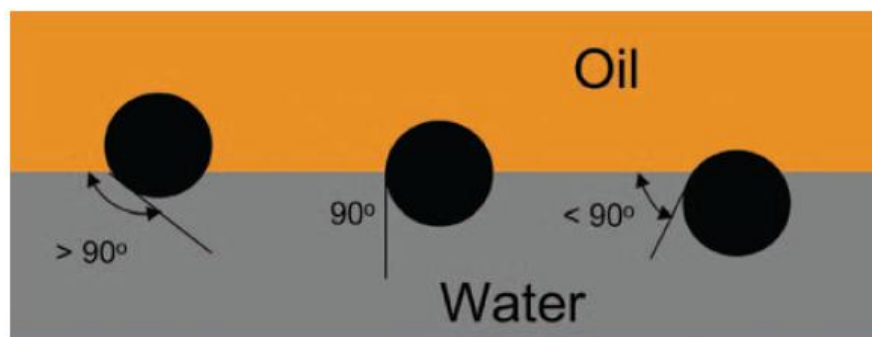


**Figure 3. 10 Wetting behaviour of fine solid in the water-oil interface (Kokal, 2006).**

The other key factor of fine solid particles as a stabilizing agent is their wetting by the two liquids. The wettability is explained as the degree to which a solid is wetted by oil or water when both are present. In the case of very fine solid particles which adsorb to water-oil interfaces, the relevant parameter is the contact angle which the particle makes with the interface. Figure 3.10 presents the three cases of wettability in terms of the contact angle. For water-wet particles, e.g. inorganic scales ( $\text{CaCO}_3$ ,  $\text{CaSO}_4$ ), clays, sand, and corrosion products,  $\Theta$  measured into the aqueous phase is normally less than  $90^\circ$ , and a larger fraction of the particle surface resides in water than in the oil phase. However, when  $\Theta$  is greater than  $90^\circ$ , the solid is preferentially oil-wet and the particle resides more in oil than in water. Contact angles close to  $90^\circ$  result in an intermediately wetted solid. Only particles with intermediate wettability could produce very stable water-in-oil emulsions (Yan et al., 2001). It means that when solid particles can be wetted by the oil and water, they tend to be placed at the interfacial surface. To coalesce of the droplets, these solid particles must be repositioned into either the oil or water phases, but this process requires energy and provides a barrier to coalescence. It is apparent that if the solid particles remain entirely in the oil or water phase, it will not be an emulsion stabilizer (Kokal, 2006).

### 3.5 HYDRATE FORMATION AND AGGLOMERATION IN EMULSIONS

Gas hydrates, waxes, asphaltenes, and scale formation and deposition are the main concerns of flow assurance that may result in pipeline plugging. Because of rapid

formation of massive hydrates, gas hydrates are considered as a serious and common problem in subsea production compared to other solid deposits (Sloan, 2005a).

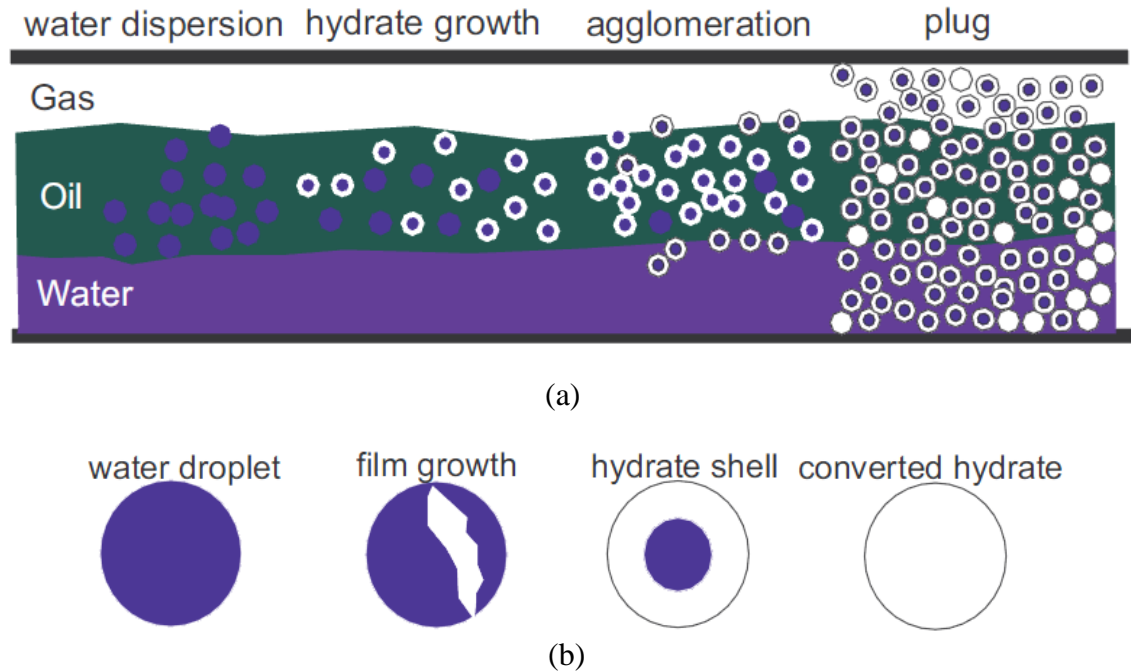


**Figure 3. 11 Conceptual picture for a) hydrate plug formation from a water-in-oil emulsion b) conversion of a water droplet to hydrate (Balakin, 2010).**

Figure 3.11 shows a proposed model of hydrate formation in an oil-dominated systems and a conceptual picture of hydrate shell formation around a water droplet. The figure indicates that for oil dominate systems water phase dispersed well in the oil phase where the size of water droplets is typically tens of microns ( $\mu\text{m}$ ). In the hydrate stability zone, gas hydrates form on the surface of the water droplets (a thin layer perhaps smaller than  $6 \mu\text{m}$  thick) (Sloan and Koh, 2008). Because gas hydrates are an interfacial phenomenon, hydrate formation occurs at the interface between water and liquid hydrocarbon saturated with gas. Hydrate shells covered water droplets form a diffusion barrier between hydrate former components and the water trapped inside the hydrate particles. In this stage presence of free water in the system lead to capillary forces, formed by a liquid bridge, hold the particles together (Austvik et al., 2000). The capillary bridge theory explains that the capillary force between two hydrate particles is proportional to the interfacial tension between the liquid water and the continuous oil phase. A simple estimate of this capillary force is given by (Anklam et al., 2008):

$$\frac{F_S}{R^*} = 2\pi\sigma\cos\theta_p$$

Where  $R^*$  is harmonic mean radius of the two particles,  $\sigma$  is the interfacial tension between the water and the oil phases, and  $\theta_p$  is the contact angle of the water on the hydrate particle.

It is important to note that hydrate agglomeration does not occur due to cohesive/capillary forces between the hydrate particles. However, hydrate agglomerates form and grow due to the contact between a hydrate particle and a water droplet, followed by an immediate crystallization of the water droplet (Palermo et al., 2005). Once hydrates form the concentration of salt in the remaining water phase increases due to the exclusion of salt from the hydrate phase (Davies et al., 2010; Husebø et al., 2009; Larsen et al., 2001). This process causes a decrease in the hydrate equilibrium temperature, slowing down or stopping hydrate formation. Thus, for an emulsion system with saline water, there is always a free water phase during or after the hydrate formation process. Although the presence of such free water will result in capillary force between hydrate particles, theoretically, this does not cause hydrate agglomeration. The problem with free water only arises when it is capable of forming hydrate (thereby gluing hydrate particles together or to the wall) (Larsen et al., 2001).

Flowing hydrate particles may aggregate, leading to a further increase of the slurry viscosity. Formation of hydrate aggregate traps a volume of liquid phase (includes oil and water) that present an effective volume fraction higher than the real volume fraction of particles and droplets (Colombel et al., 2009; Le Ba et al., 2010). Finally the agglomerates become adequately large to increase the effective viscosity of the system so that the flow is stopped.

### **3.6 NATURAL ANIT-AGGLOMERANT COMPONENTS IN CRUDE OIL**

The presence of natural surfactants in crude oil can lead to a change in the rheological properties of fluid flow, when the crude oil comes in contact with one or several other phases, like water or solid particles. Surfactants are of special interest regarding the hydrate plugging concern in the oil and gas industry (Hoiland et al., 2005). For instance, new methods have started to change the philosophy toward hydrate management from the

often more expensive hydrate prevention (Sloan, 2005b). Therefore, a better understanding of natural surfactant components in the crude oil can be helpful for the hydrate management strategy for oil companies, and may lead to both economical savings and environmental improvements. Natural surfactants are effective anti-agglomerant compounds that occur naturally in crude oils. Resins and asphaltenes, including naphthenic acids and phenols, are examples of crude oil components that exhibit such properties (Dieker et al., 2009; Fadnes, 1996; Fotland et al. 2011; Leporcher et al., 1998). Previous works have shown that natural surfactants in crude oils in some cases are able to produce transportable hydrate slurry with low or no risk of plugging (Erstad, 2009; Fadnes, 1996; Leporcher et al., 1998; Palermo et al., 2004). There is evidence that such conditions take place in pipelines in Brazil, where sufficient natural surfactants are present in crude oils (Palermo et al., 2004).

Leporcher et al (1998) attempted to investigate the effect of natural surfactants (asphaltenes and resins) on the transportability of hydrate slurry. Tests were carried out at different water cuts with different crude oil enriched or not with natural surfactants. Their experimental results revealed that hydrate transportability of the water-in crude oil emulsions significantly improved with increasing asphaltene contents. The composition and properties of natural surfactants strongly depends on physico-chemical properties of the crude oil. In the case of hydrate transportability, Leporcher et al (1998) explained that the nature of asphaltene is probably as important as the concentration of this surface active agent. It was concluded that although asphaltenes are proactive species in water in oil emulsion stabilization, other factors such as resins, waxes, aromatics, water quality, etc need to be assessed.

Other studies emphasize that naphthenic acids are also the main component that can affect the transportability of hydrate slurries. The term naphthenic acid is used to explain all carboxylic acids present in crude oils, in addition including aromatic and acyclic acids. However, in petroleum engineering it is common to use this term to explain the whole range of organic acids presented within crude oils (Erstad, 2009). Borgund et al. (2009) reported that natural active components in the crude oils such as acids and bases attract with hydrate surfaces. Hoiland et al.(2005), developed a method based on phase inversion in crude oil/brine emulsions to investigate the effect of crude oil acids on hydrate

inhibiting properties. They extracted acids from crude oils with low tendencies to form hydrate plugs. Extracted acids were added in low doses to crude oils with high plugging tendencies. In some cases, they observed a conversion from plugging to dispersed systems that was attributed to the change in hydrate surface wettability due to interactions of hydrate surfaces with the acids. However, it has also been observed that not all crude oil acids can lead to this change. It can be concluded that the acid fractions that lead to a conversion from plugging to the dispersed systems hold likely certain compositional properties that the other acid fractions do not.

The influence of oil composition on the wettability of pipeline surfaces was investigated by Aspenes et al. (2010). They proposed that the oils that create oil-wet surfaces have higher acid content than bases, resulting in lower hydrate plugging tendency. Crude oil with low content of acid most likely tends to be hydrate plugging, whereas high acid content crude oil may either display plugging or non-plugging oil behaviour. Aspenes et al. (2010) indicated that the same natural surfactants in the crude oils that interact with pipeline surfaces also influence the hydrate surfaces.

Recently, micromechanical force measurements were used to identify the agglomeration properties of hydrate particles (Dieker et al., 2009; Sjöblom et al., 2010). Dieker et al. (2009) used three different crude oils and their modifications (deasphalted and pH-14 extracted) to investigate the effect of asphaltenes and acids on the adhesion forces between cyclopentane hydrate particles. When the surface active components were removed from the crude oil a significant increase was observed in the adhesive forces between hydrate particles. For instance, Figure 3.12 illustrates the adhesion force measured by Dieker et al. (2009) for the Caratinga crude oil, which is a crude oil with non-plugging hydrate tendency. It is clear that the adhesive forces between hydrate particles increases when the acidic components extracted from the crude oil (through a “pH-14 extraction” process), and a further increase in adhesion forces was observed when the asphaltenes components were removed.



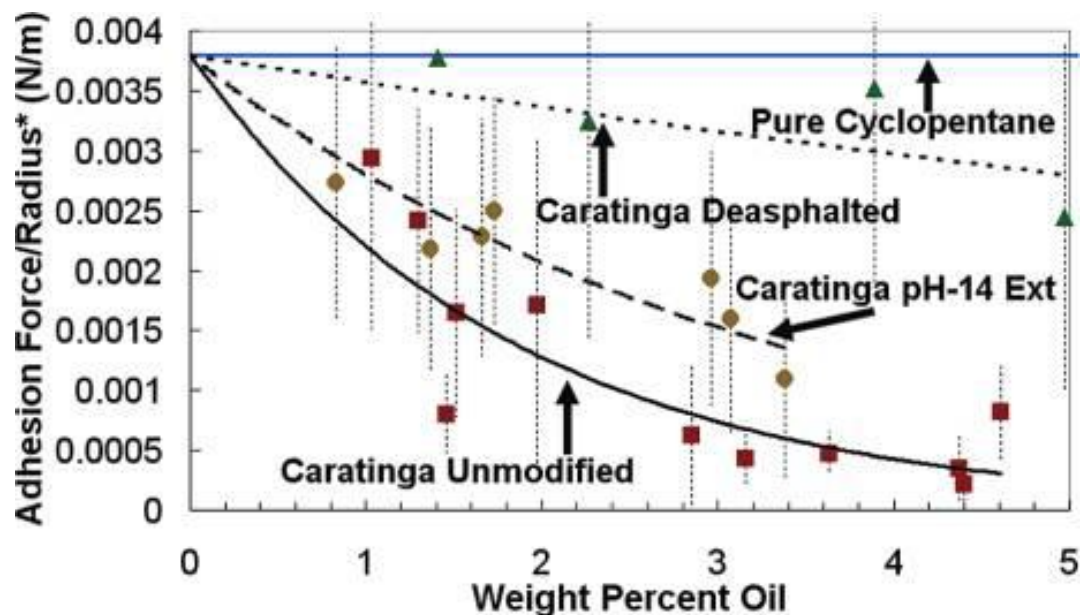


**Figure 3. 12 Summary of adhesion forces between cyclopentane hydrates particles for Caratinga crude oil in unmodified, deasphalted, and pH-14extracted conditions (Dieker et al., 2009)**

A recent study by Fotland et al. (2011) showed that different sub-fractions of petroleum acids presented different anti-agglomerant properties, even though all the acid fractions improved the agglomeration properties of the crude oil.

However, the debate is still opened about the exact nature of components in crude oil which are responsible for the anti-agglomerant like behaviour. Extracting and characterizing the true natural anti-agglomerant components of crude oil is to date a very complex and challenging objective. The specific chemical structures of these natural components are unknown, and the exact mechanisms that take place are not fully understood. The main problem of recognizing the natural anti-agglomerant components may be that they are present in very low amounts in the crude oil (Borgund, 2007). Therefore, it will be difficult to classify these natural anti-agglomerants without more successful methods.

### 3.7 REFERENCES

- Aichele, C.P., 2009. Characterizing water-in-oil emulsions with application to gas hydrate formation, PhD Thesis, Rice University, HOUSTON, TEXAS, 178 pages pp.
- Anklam, M.R., York, J.D., Helmerich, L. and Firoozabadi, A., 2008. Effects of antiagglomerants on the interactions between hydrate particles. *Aiche Journal*, 54(2): 565-574.
- Aske, N., 2002. Characterisation of crude oil components, asphaltene aggregation and emulsion stability by means of near infrared spectroscopy and multivariate analysis, PhD Thesis, Norwegian University of Science and Technology.
- Aske, N., Kallevik, H., Johnsen, E.E. and Sjöblom, J., 2002. Asphaltene aggregation from crude oils and model systems studied by high-pressure NIR spectroscopy. *Energy & Fuels*, 16(5): 1287-1295.
- Aske, N., Kallevik, H. and Sjöblom, J., 2001. Determination of saturate, aromatic, resin, and asphaltenic (SARA) components in crude oils by means of infrared and near-infrared spectroscopy. *Energy & Fuels*, 15(5): 1304-1312.
- Aspenes, G., 2009. The influence of pipeline wettability and crude oil composition on deposition of gas hydrates during petroleum production, PhD Thesis, University of Bergen.
- Aspenes, G., Høiland, S., Borgund, A.E. and Barth, T., 2010. Wettability of Petroleum Pipelines: Influence of Crude Oil and Pipeline Material in Relation to Hydrate Deposition. *Energy & Fuels*, 24(1): 483-491.
- Auflem, I.H., 2002. Influence of asphaltene aggregation and pressure on crude oil emulsion stability, Norwegian University of Science and Technology (NTNU), PhD Thesis.
- Austvik, T., LI, X. and Gjertsen, L.H., 2000. Hydrate plug properties: formation and removal of plugs. *Annals of the New York Academy of Sciences*, 912(1): 294-303.
- Balakin, B.V., 2010. Experimental and theoretical study of the flow, aggregation and deposition of gas hydrate particles, PhD Thesis, University of Bergen.
- Bancroft, W.D., 1915. The theory of emulsification, VI. *The Journal of Physical Chemistry*, 19(4): 275-309.
- Borgund, A.E., 2007. Crude oil components with affinity for gas hydrates in petroleum production, PhD Thesis, University of Bergen.
- Borgund, A.E., H iland, S., Barth, T., Fotland, P. and Askvik, K.M., 2009. Molecular analysis of petroleum derived compounds that adsorb onto gas hydrate surfaces. *Applied Geochemistry*, 24(5): 777-786.

Borgund, A.E., Hoiland, S., Barth, T., Fotland, P., Kini, R. A., Larsen, R., 2008. Critical descriptors for hydrate properties of oils: Compositional features, Proceedings of the 6th International Conference on Gas Hydrates (ICGH 2008), Vancouver, British Columbia, CANADA.

Burya, Y., Yudin, I., Dechabo, V. and Anisimov, M., 2001. Colloidal properties of crude oils studied by dynamic light-scattering. *International journal of thermophysics*, 22(5): 1397-1410.

Cairns, R.J.R., Grist, D.M. and Neustadter, E.L. (Editors), 1974. The Effect of Crude Oil-Water Interfacial Properties on Water-Crude Oil Emulsion Stability. In *Theory and Practice of Emulsion Technology*. Smith, A. L., pp 135-151 pp.

Campanelli, J.R. and Cooper, D.G., 1989. Interfacial viscosity and the stability of emulsions. *The Canadian Journal of Chemical Engineering*, 67(5): 851-855.

Colombel, E., Gateau, P., Barré, L., Gruy, F. and Palermo, T., 2009. Discussion of agglomeration mechanisms between hydrate particles in water in oil emulsions. *Oil & Gas Science and Technology-Revue de l'IFP*, 64(5): 629-636.

Davies, S.R., Boxall, J. A., Dieker, L.E., Sum, A. K., Koh, C.A., Sloan E. D., 2010. Predicting hydrate plug formation in oil-dominated flowlines. *Journal of Petroleum Science and Engineering*, 72(3-4): 302-309.

Dieker, L.E., Aman, Z. M., George, N. C., Sum, A. K., Sloan, E. D., 2009. Micromechanical adhesion force measurements between hydrate particles in hydrocarbon oils and their modifications. *Energy & Fuels*, 23(12): 5966-5971.

Ekott, E.J. and Akpabio, E.J., 2010. A review of water-in-crude oil emulsion stability, destabilization and interfacial rheology. *Journal of Engineering and Applied Sciences*, 5(6): 447-452

Eley, D., Hey, M. and Symonds, J., 1988. Emulsions of water in asphaltene-containing oils 1. Droplet size distribution and emulsification rates. *Colloids and surfaces*, 32: 87-101.

Erstad, K., 2009. The influence of crude oil acids on natural inhibition of hydrate plugs, PhD Thesis, University of Bergen, 85 pp.

Fadnes, F.H., 1996. Natural hydrate inhibiting components in crude oils. *Fluid Phase Equilibria*, 117(1-2): 186-192.

Fotland, P., Askvik, K.M. and Slamova, E., 2011. Natural anti-agglomerants in crude oil: Isolation, identification and verification of inhibiting effect, Proceedings of the 7th International Conference on Gas Hydrates (ICGH 2011), Edinburgh, Scotland, United Kingdom.

- Ganiev, R. Fomin, V. N., Belyaev, Yu. A., Malyukova, E. B., 2009. Stability of disperse systems. published in *Doklady Akademii Nauk*, Berlin, pp. 179-182.
- Head, I.M., Jones, D.M. and Larter, S.R., 2003. Biological activity in the deep subsurface and the origin of heavy oil. *Nature*, 426(6964): 344-352.
- Hoiland, S., Askvik, K.M., Fotland, P., Alagic, E., Barth, T., Fadnes, F., 2005. Wettability of freon hydrates in crude oil/brine emulsions. *Journal of Colloid and Interface Science*, 287(1): 217-225.
- Husebø, J., Ersland, G., Graue, A. and Kvamme, B., 2009. Effects of salinity on hydrate stability and implications for storage of CO<sub>2</sub> in natural gas hydrate reservoirs. *Energy Procedia*, 1(1): 3731-3738.
- Johansen, E.J., Skjærvø, I.M., Lund, T., Sjöblom, J., 1989. Water-in-crude oil emulsions from the norwegian continental shelf Part I. Formation, characterization and stability correlations. *Colloids and surfaces*, 34(4): 353-370.
- Jones, T., Neustadter, E. and Whittingham, K., 1978. Water-in-crude oil emulsion stability and emulsion destabilization by chemical demulsifiers. *Journal of Canadian Petroleum Technology*, 17(2).
- Kilpatrick, P.K. and Spiecker, M.P., 2001. Asphaltene Emulsions, in *Encyclopedic Handbook of Emulsion Technology* by Sjöblom J. Marcel Dekker, Inc.: New York, New York.
- Kokal, S., 2005. Crude-oil emulsions: A state-of-the-art review. *Spe Production & Facilities*, 20(1): 5-13.
- Kokal, S., 2008. Crude Oil Emulsions: Everything You Wanted to Know But Were Afraid to Ask, SPE-120500-DL.
- Kokal, S.L., 2006. Crude Oil Emulsions. *Petroleum Engineering Handbook*, 1.
- Koots, J.A. and Speight, J.G., 1975. Relation of petroleum resins to asphaltenes. *Fuel*, 54(3): 179-184.
- Langevin, D., Poteau, S., Henaut, I. and Argillier, I., 2004. Crude oil emulsion properties and their application to heavy oil transportation. *Oil & Gas Science and Technology*, 59(5): 511-521.
- Larsen, R., Lund, A., Andersson, V. and Hjarbo, K., 2001. Conversion of Water to Hydrate Particles, SPE 71550-MS, presented at the 2001 SPE Annual Technical Conference and Exhibition, New Orleans, Louisiana.
- Larter, S., Wilhelms, A., Head, I., Koopmans, M., 2003. The controls on the composition of biodegraded oils in the deep subsurface--part 1: biodegradation rates in petroleum reservoirs. *Organic Geochemistry*, 34(4): 601-613.

Le Ba, H., Cameirao, A., Herri, J.M., Darbouret, M., 2010. Chord length distributions measurements during crystallization and agglomeration of gas hydrate in a water-in-oil emulsion: Simulation and experimentation. *Chemical Engineering Science*, 65(3): 1185-1200.

Lee, R.F., 1999. Agents which promote and stabilize water-in-oil emulsions. *Spill Science & Technology Bulletin*, 5(2): 117-126.

Leontaritis, K. and Mansoori, G., 1987. Asphaltene flocculation during oil production and processing: A thermodynamic colloidal model. paper SPE, 16258.

Leporcher, E., Peytavy, J., Mollier, Y., Sjoblom, J. and Labes-Carrier, C., 1998. Multiphase transportation: hydrate plugging prevention through crude oil natural surfactants, SPE 49172, New Orleans, Louisiana.

Long, R.B., 1981. The concept of asphaltenes. *Chemistry of Asphaltenes*. American Chemical Society: Washington, DC. : 17-27.

Palermo, T., Fidel-Dufour, A., Maurel, P., Peytavy, J. and Hurtevent, C., 2005. Model of hydrates agglomeration-Application to hydrates formation in an acidic crude oil, Presented at the 12th International Conference on Multiphase Production Technology, Barcelona, Spain.

Palermo, T., Mussumeci, A. and Leporcher, E., 2004. Could hydrate plugging be avoided because of surfactant properties of the crude and appropriate flow conditions?, OTC 16681, Presented in the Offshore Technology Conference, Houston, Texas.

Ravey, J., Ducouret, G. and Espinat, D., 1988. Asphaltene macrostructure by small angle neutron scattering. *Fuel*, 67(11): 1560-1567.

Salager, J.L., 1994. *Interfacial Phenomena in Dispersed Systems*. FIRP Booklet, 120.

Schramm, L.L., 1992. Petroleum emulsions: basic principles. *Emulsions: fundamentals and applications in the petroleum industry*. American Chemical Society, Washington, DC: 1–51.

Shetty, C., Nikolov, A., Wasan, D. and Bhattacharyya, B., 1992. Demulsification of water in oil emulsions using water soluble demulsifiers. *Journal of dispersion science and technology*, 13(2): 121-133.

Siffert, B., Bourgeois, C. and Papirer, E., 1984. Structure and water--oil emulsifying properties of asphaltenes. *Fuel*, 63(6): 834-837.

Sjöblom, J., Aske, N., Auflem, I. H., Brandal, O., Havre, T. E., 2003. Our current understanding of water-in-crude oil emulsions. Recent characterization techniques and high pressure performance. *Advances in Colloid and Interface Science*, 100: 399-473.

Sjöblom, J., Ovreivoll, B., Jentoft, G.H., Lesaint, C., Palermo, T., 2010. Investigation of the Hydrate Plugging and Non-Plugging Properties of Oils. *Journal of dispersion science and technology*, 31(8): 1100-1119.

Sloan, E.D., 2005a. A changing hydrate paradigm--from apprehension to avoidance to risk management. *Fluid Phase Equilibria*, 228: 67-74.

Sloan, E.D., 2005b. Seven Industrial Hydrate Flow Assurance Lessons From 1993-2003, the Fifth International Conference on Gas Hydrates, Trondheim, Norway.

Sloan, E.D. and Koh, C.A., 2008. *Clathrate hydrates of natural gases*. 3<sup>th</sup> ed. CRC Press, New York.

Speight, J.G., 2007. *The chemistry and technology of petroleum*, 114. CRC.

Spiecker, P.M., 2001. The impact of asphaltene chemistry and solvation on emulsion and interfacial film formation, PhD Thesis, North Carolina State University: Raleigh p. 287 pp.

Strassner, J., 1968. Effect of pH on interfacial films and stability of crude oil-water emulsions. *Journal of Petroleum Technology*, 20(3): 303-312.

Tambe, D.E. and Sharma, M.M., 1994. Factors controlling the stability of colloid-stabilized emulsions. *Journal of Colloid and Interface Science*, 162: 1-10.

Thompson, D., Taylor, A. and Graham, D., 1985. Emulsification and demulsification related to crude oil production. *Colloids and surfaces*, 15: 175-189.

Vaessen, G.E.J., 1996. Predicting Catastrophic Phase Inversion in Emulsions, Ph. D. Dissertation, Eindhoven University of Technology, Netherlands.

Van der Waarden, M., 1958. Stability of emulsions of water in mineral oils containing asphaltenes. *Colloid & Polymer Science*, 156(2): 116-122.

Wasan, D., McNamara, J., Shah, S., Sampath, K. and Aderangi, N., 1979. The role of coalescence phenomena and interfacial rheological properties in enhanced oil recovery: an overview. *Journal of Rheology*, 23: 181.

Wasan, D. and Mohan, V., 1977. *Interfacial rheological properties of fluid interfaces containing surfactants*. Academic Press, New York.

Yan, N., Gray, M.R. and Masliyah, J.H., 2001. On water-in-oil emulsions stabilized by fine solids. *Colloids and Surfaces A: Physicochemical and Engineering Aspects*, 93(1-3): 97-107.

Yan, Y., Pal, R. and Masliyah, J., 1991. Viscosity correlations for emulsion--solids mixtures as bimodal systems. *Chemical Engineering Science*, 46(7): 1823-1828.

Yen, T.F., Erdman, J. and Pollack, S., 1961. Investigation of the structure of petroleum asphaltenes by X-ray diffraction. *Analytical Chemistry*, 33(11): 1587-1594.

Zerpa, L.E., Salager, J.L., Koh, C.A., Sloan, E.D. and Sum, A.K., 2011. Surface Chemistry and Gas Hydrates in Flow Assurance. *Industrial & engineering chemistry research*, 50: 188–197.

## **CHAPTER 4    EXPERIMENTAL APPARATUS**

### **4.1 INTRODUCTION**

This chapter focuses on the experimental set-ups that are used in this study to investigate the morphology of water-oil emulsions and rheological behaviour of hydrate slurries in the presence of salt and anti-agglomerants (AAs). This chapter splits into three parts. The first part describes the experimental setup and the technical observations that used for characterizing the type of emulsion and detection of the point of phase inversion from an oil-in-water emulsion into a water-in-oil emulsion or vice versa. The second part of this chapter describes a high pressure autoclave cell equipped with a Helical Tube Impeller (HTI). The cell has been calibrated to be used as a viscometer to measure apparent viscosity of hydrate slurries. Finally the third part of this chapter describes in detail the structure of a saturated flow loop that is used in this study to simulate the real hydrate slurry flow conditions encountered in production pipelines.

### **4.2 DETECTION OF EMULSION TYPE**

In order to detect the type of emulsions (water-in-oil or oil-in-water) during preparation of the emulsions or the samples taken during the experiments, a conductivity meter was used to measure the conductivity of the emulsion by means of a conductivity probe consisting of two 5 mm long platinised rods, vertical and parallel, with 8 mm spacing between the rods. Oil-in-water (O/W) emulsions have a high conductivity value (as water forms the continuous phase), whereas water-in-oil (W/O) emulsions have a very low conductivity due to nonconductive oil as the continuous phase. The conductivity suddenly changes when phase inversion takes places (Allouche et al., 2004; Song et al., 2008).

Occasionally, a dilution test (Omer, 2009) was carried out to detect emulsion type. This test is based on the fact that an emulsion is readily dispersed in the liquid that forms the continuous phase. A small amount of the emulsion was added to the two beakers containing pure oil and pure water, respectively. When the emulsion readily dispersed in



oil but did not disperse in water, it indicated that the emulsion was W/O type. If the emulsion is readily dispersed in water, the emulsion was O/W type.

### 4.3 PHASE INVERSION POINT MEASUREMENT SETUP

The experimental layout is shown in Figure 4.1. The core element is the mixing vessel, a 500 cm<sup>3</sup> glass beaker. The contents are stirred by a stainless steel impeller consisting of two parallel disks attached by vertical blades. An electrical motor is used to drive the mixer at the desired speed. The electrical current applied to the mixer as well as the RPM are continuously recorded during the experiments. The RPM is regularly adjusted to ensure a constant mixer speed throughout the experiment, as the viscosity increases approaching the phase inversion point. The dispersed phase is slowly added to the beaker using a HPLC (High Pressure Liquid Chromatography) pump with highly accurate constant flow rate. The pump is switched on at the start of the experiment to inject the dispersed phase to the beaker at a constant flow rate. The inversion of phases is detected by observing big changes in the viscosity of the emulsion which is directly followed by a big change in torque (current) applied on the electrical mixer to keep the RPM constant (Allouche et al., 2004; Song et al., 2008; Souvlis et al., 1998).

Visual observation can occasionally be used to detect phase inversion point during experiments.

Occasionally, phase inversion is easily found by direct visual observations. In a water-oil emulsion, the two continuities phases have different appearances because (Reeve et al., 2002):

- i) Oil-in-Water emulsions are looking brighter than water-in-oil emulsions
- ii) In continuous mixing, the water continuous emulsions are always looking more turbulent than oil continuous

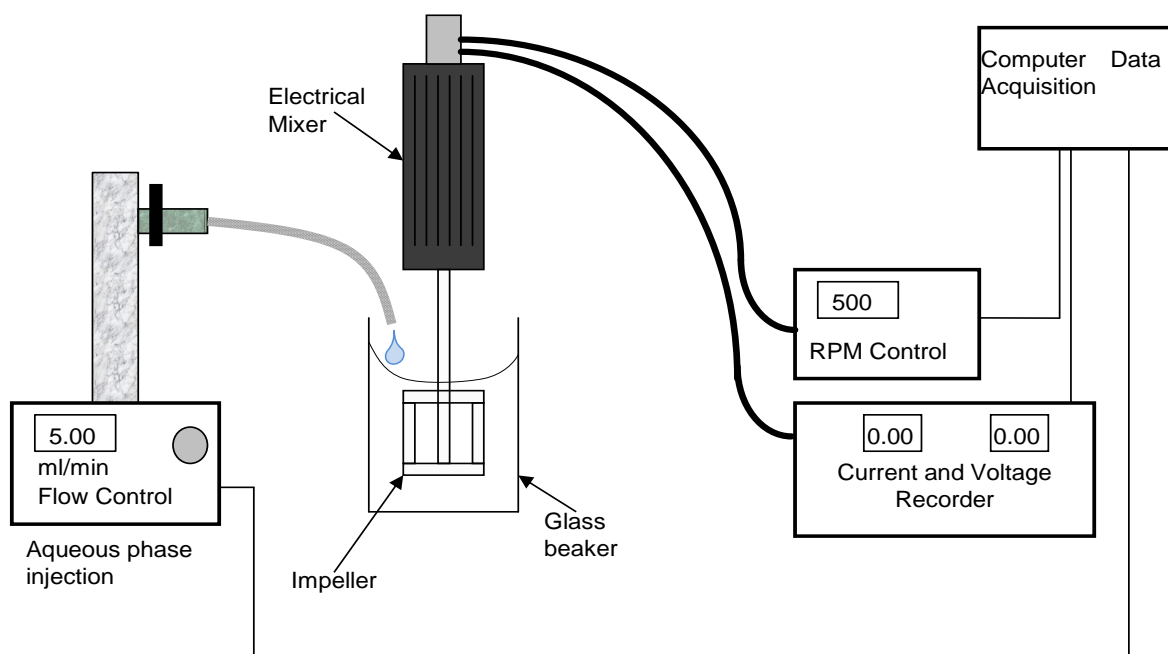


**Figure 4. 1 Setup for hydrate free phase inversion point measurement experiments.**

#### **4.4 RHEOLOGICAL STUDY OF HYDRATE SLURRIES USING HIGH PRESSURE AUTOCLAVE CELL EQUIPPED WITH HELICAL TUBE IMPELLER (HTI)**

Understanding the rheological prosperities of the fluid flow in the pipeline are the main issue, making it possible to design economically the process facilities to transport fluid flow through the pipelines. The effective viscosity measurement of fluid is one of the most important parameters that will aid in the assessment of rheological behaviour of fluid flow in the pipeline. The viscosities are generally measured in viscometers where the torque applied on the fluid is converted to the viscosity.

In the case of hydrate slurry flows, the slurries are suspensions containing macro-particles. Due to this property, hydrate slurry flow exhibits complex rheological properties and are typically characterized as non-Newtonian fluids. Existing instruments to measure viscosity of hydrate slurries are mostly custom-built (Azarinezhad, 2010; Sjöblom et al., 2010) and to the best of our knowledge there is no a standard device or methodology for measuring viscosity of hydrates suspensions to date.

Use of conventional viscometers (such as concentric cylinder or cone-and-plate) to measure viscosity of suspensions can cause large errors due to the nature of the

suspensions. Some problems that have been reported with conventional viscometers are (Metz et al., 1979):

- The suspensions tend to become inhomogeneous due to settling and particle interactions
- Because of centrifugal force, a less dense layer of liquid forms next to the surface of the measuring bodies
- Suspended particles are often of the same size of the annulus of the conventional viscometers, resulting in destruction of particles during the experiments

Therefore, an alternative method should be considered for measuring rheological behaviour of suspensions to avoid settling of particles during viscosity measurements.

An alternative method has been developed to measure viscosity of hydrate slurries by the Centre for Gas Hydrate Research at Heriot-Watt University (Azarinejad, 2010). In this technique like the conventional viscometers, limited sample amounts are required and the viscosity data are acquired using torque values. Instead of a concentric cylinder or cone-and-plate a Helical Tube Impeller (HTI) was used to provide a well mixing and promote fast dissolution of gas in the liquid phase. This could solve the problems mentioned for conventional viscometers, because the HTI achieves good mixing during the experiments. Similar experimental setup has been also employed by IFP (Institute of French Petroleum) group. They measured the apparent viscosities of hydrate slurries during hydrate formation at constant shear rate by an in-house high pressure rheometer equipped with a “helix-type” impeller (Sjöblom et al., 2010).

Investigations on the helical tube impeller have shown that they have many advantages compared with conventional impellers such as paddle type (Arjmandi, 2007; Azarinezhad, 2010): a) due to the passing fluid inside the tube during the rotation of the HTI, the fluid applies a shear force on the tube wall that can simulate the real fluid flow inside the pipeline b) the fluid movement direction inside the cell is mainly upward with minimum centrifugal force that prevent the hydrate particles to be pushed towards the inside wall of the cell as it was observed with paddle impellers c) due to generation of a large surface area between the impeller and the fluid, a large value of stable shear force can be produced on the HTI d) the HTI mainly applies a tangential force on the hydrate particles compared with conventional impellers, which strongly exerts vertical force on the particles, and

therefore the HTI has minimum impact on hydrate aggregates to simulate a more realistic hydrate slurry flow.

#### **4.4.1. High pressure Autoclave Cell- Small Scale Viscometer**

In this study, in order to investigation the rheological behaviour of water/oil/hydrate mixtures a high pressure autoclave cell equipped with a HTI was designed and constructed in-house. A schematic view of the cell is presented in Figure 4.2. The cell has been made from titanium and has a cylindrical shape uniform in diameter. The cell volume can be changed from 2,700 to 9,000 ml. The cell is held in a metallic jacket heated or cooled by a constant-temperature liquid bath. The temperature of the cell is controlled by circulating coolant from a cryostat within the jacket surrounding the cell. The temperature of the cell is measured using a platinum resistance probe placed inside the cell and monitored via computer. The calibrated probe has a reported accuracy of  $\pm 0.1$  °C. To achieve good temperature stability, the jacket is insulated with polystyrene board and the pipes, which connect it to the cryostat, are also insulated with plastic foam. The pressure is measured using pressure transducer mounted directly on the cell and connected to the computer for direct acquisition. To achieve a faster thermodynamic equilibrium and to provide a good mixing of the fluids, the cell is equipped with a HTI with adjustable rotational speed. The RPM, electrical current and voltage applied to the stirrer are recorded during run the experiments to allow calculation of torque apply on the fluid inside the cell. The sensor signals are transferred to a real time PC-based data acquisition system.

A gas make-up system is used to keep the test pressure constant during experiments. The gas make-up system injects gas into the cell to compensate the pressure reduction of the system during cooling and/or hydrate formation, using a high-pressure cylinder fitted with a piston. This cylinder is connected to the cell and water is used to displace the piston and inject the gas into the autoclave cell. Water is injected using a highly accurate HPLC (High Pressure Liquid Chromatography) pump.

During hydrate formation process the volume of water pumped to the cylinder corresponds to the volume of gas consumed for hydrate formation and can be related to the amount of hydrate formed in the system. Nitrogen is injected at the required operating pressure behind the piston in the cell (Figure 4.2) to maintain a constant pressure in the system. A

LabVIEW logging program is used to record the electrical voltage, current and RPM applied on the stirrer and also temperature and pressure inside the cell.

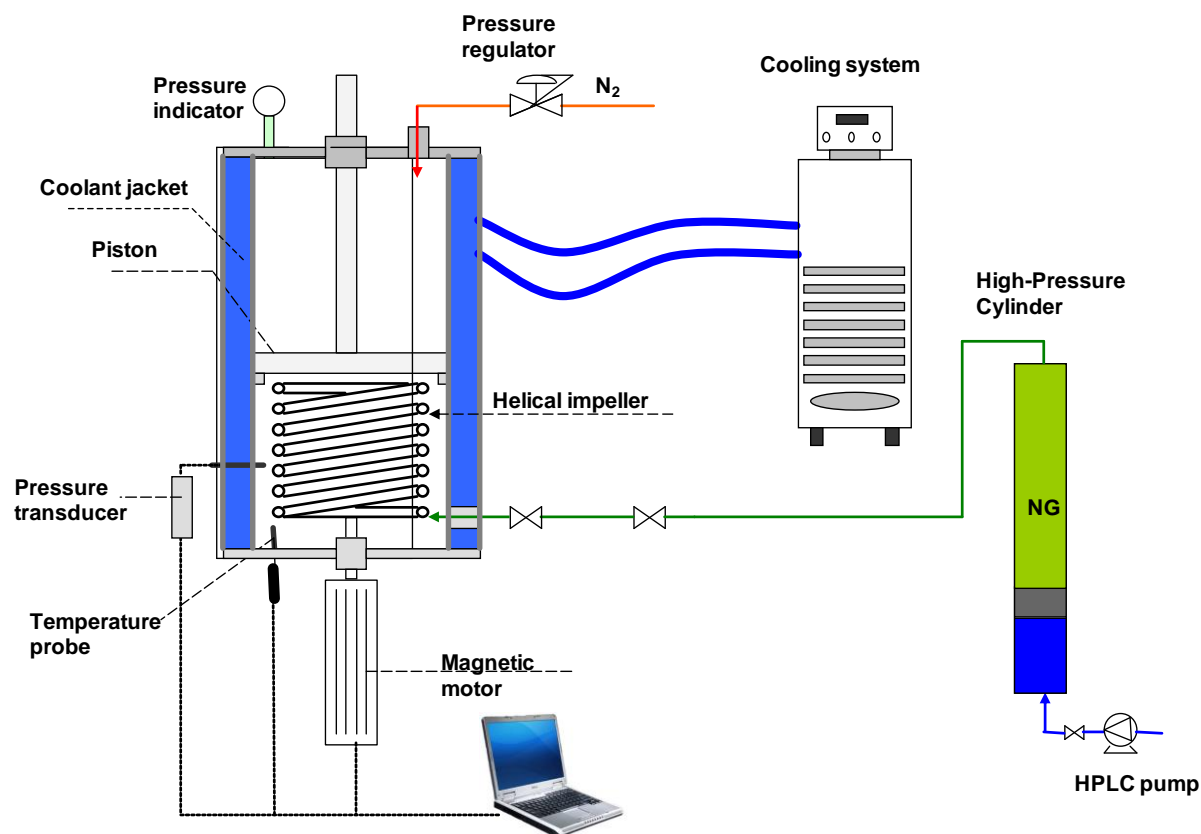


**Figure 4. 2 Flow diagram of the high pressure autoclave cell.**

The main part of the cell is the impeller which is a long tube coiled in helical shape. It is used for agitating the fluid inside the cell and also measuring the viscosity of hydrate suspensions. In this study the high pressure autoclave cell has been calibrated to measure the apparent viscosity of hydrate suspensions at constant shear rate. Calibration was performed using different Newtonian fluids with known viscosities. Detailed descriptions of the calibration of the autoclave cell equipped with HTI are given in Azarinezhad (2010). Chapters 5 and 6 show the results of viscosity measurements performed using the high pressure autoclave cell for the mixtures of water/oil/hydrate in high water cut systems. Then, Chapter 7 shows a validation on the data from Chapter 6 with similar tests conducted using a saturated flow loop system.

## 4.5 FLOW LOOP SYSTEM

A flow loop is an experimental facility where a certain amount of fluid is circulated in a closed loop. With a flow loop, thermodynamic and hydrodynamics conditions are close as possible to real field conditions and a large range of fluids can be used, particularly hydrocarbon fluids.

In order to qualify new technology under realistic conditions a test loop, which can handle sufficient flow rates, pressures and temperatures is required. On the other hand, in order to qualify the small scale data, it is essential to have valid data for real fluid systems. Since there is currently no or very few field data where gas hydrates have plugged a production pipeline, a flow loop is the best available option. Thus, it is possible to build a bridge between small-scale lab and field data with the selection of a suitable flow loop system.

Several types of flow loop exist, with each having their characteristics, advantages and disadvantages. This includes multiphase flow loop, saturated flow loop, gas lift flow loop, and wheel loop (Fidel-Dufour et al., 2006; Robole et al., 2006; Wolden et al., 2005). The type of flow loop required depends on what is the purpose of the loop, and cost limitations. The present study investigates the rheological behaviour of hydrate slurry in high water cut systems using a saturated flow loop where the liquid phase is saturated with natural gas and circulates up to a pressure of about 68 bars. Pressure is maintained at a constant value during experimental runs by means of natural gas make-up.

The saturated flow loop is a conventional gas-free loop consisting of a pipeline suitable to transport hydrate slurry during hydrate formation process. Due to the lack of free gas phase, the complexity of the system in regards to pumping of fluid significantly reduces. In the case of hydrate slurry flow in the pipelines the main reason for viscosity increases and pipeline blockage is related to the presence of hydrate aggregates which are suspended in the liquid phase. Therefore, saturated flow loops provide simple systems that can be used to accurately manipulate and investigate the rheological properties of hydrate slurries in a real pipeline without troubles due to presence of free gas in the system.

In the following section, the principles of the saturated flow loop are outlined. Further the main layout of the loop is described, as well as its auxiliary equipment and accessories.

#### **4.5.1 Design**

Figures 4.3 and 4.4 display an overall view and a flow diagram of the saturation flow loop. The main constituents are the main pump, storage tank, gas make-up system, differential pressure transducer and liquid and gas flow meters. The components are interconnected with 1 inch pipe. The shape of the loop is a double horizontal ring with a total length of 40 meter from the outlet to the inlet of the main pump. The flow loop will be used with water and petroleum fluids. Salts and AAs can be added in some experiments. Thus it was decided to go for stainless steel in all units as well as in tubing and fittings designed for maximum working pressure of 200 bars.

The saturated flow loop is housed inside an environmentally controlled room which can be operated from -15 to +25 °C. The fluids can be set in motion by a Moineau type pump. A data acquisition system monitors temperatures and pressures in different locations of the flow loop. The volume flow rate of liquid phase flows inside the pipe and the total volume of gas phase injects into the flow loop are monitored by a Coriolis flow meter and a gas flow meter, respectively.

For safety reasons it was decided that the main electric motor of the pump and all electronic devices in the controlled room to be certified to the ATEX (The ATEX directive consists of two EU directives describing what equipment and work environment is allowed in an environment with an explosive atmosphere).

#### **4.5.2 Main Pump**

The main pump is used to circulate fluid inside the flow loop. It is Moineau type designed and constructed by PCM. This type of pump has low shearing power and conveys a slurry flow with large particles (Peytavy et al., 2008). The pump will circulate liquid to a maximum discharge pressure of 200 bars and operates at temperature range from -15 to +25 °C. A maximum differential pressure of 20 bars is allowed across the pump. The pump is equipped with a frequency controller which controls the rotation frequency of electro motor up to 50 Hz to produce a variable pump speed. It can provide maximum volume flow rate of 5000 L/hr resulting in liquid velocities up to 3 m/s.



**Figure 4. 3** The overall view of the saturated flow loop



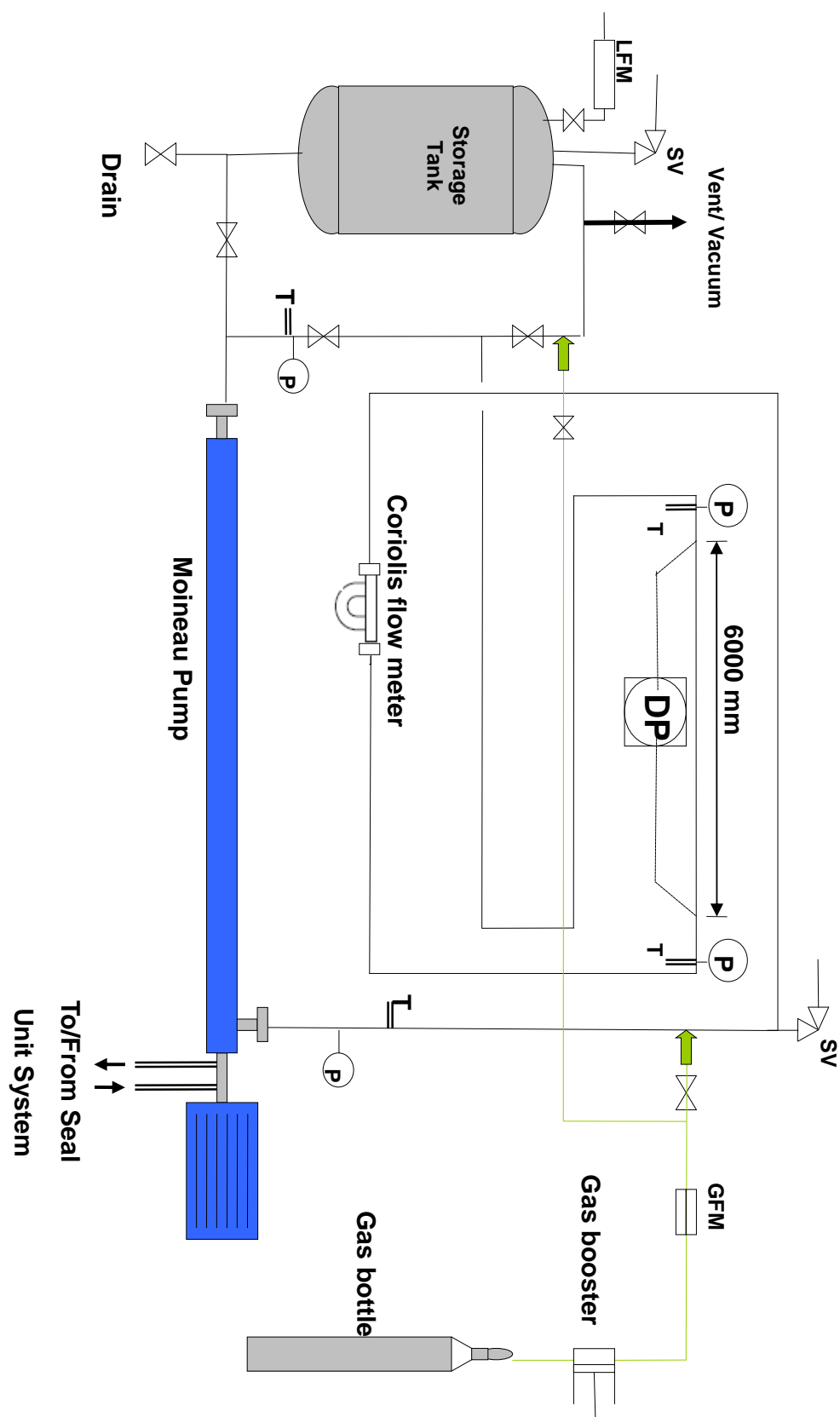


Figure 4. 4 Flow diagram of the saturated flow loop.

### 4.5.3 Storage Tank

The storage tank is made of stainless steel with a volume of 60 litres. This tank has several purposes;

- The required liquid is first pumped into the storage tank as it facilitates liquid loading into the flow loop
- It allows adding water, oil or other additives to the loop without the need to drain the system after each single test.
- It is used for saturating the liquid with gas, by providing a large liquid/gas contact area
- It has been located at the suction side of main pump, resulting in prevention of the gas phase to enter the main pump (preventing the risk of gas cavitation)
- Provides a large volume buffer to prevent the unwanted pressure increases during hydrate dissociations.
- Operate as a flash vessel to remove any liquid from the vent system in the event of overpressures

### 4.5.4 Seal Unit System

The pump is sealed with a mechanical seal which is a dual pressurized seal type. It is equipped with a John Crane seal oil system (plan 53B) to maintain back pressure on the mechanical seal as well as provide cooling and lubrication of the seal (Figure 4.5). This seal oil system constantly adjusts the back pressure on mechanical seal to track the flow loop pressure. Seal unit system comprises an inner and outer seal between which a barrier liquid is provided at a pressure higher than the process condition on the inner seal. It ensures a zero process leakage to the atmosphere. The minimum barrier pressure should be set at least 10% or 5 bars above the maximum loop pressure, whichever is the greater value. The system manages the barrier liquid and includes an accumulator for the barrier liquid which its pressure is maintained constant through the energy retained in the gas bladder in the accumulator. The bladder is initially charged to a pressure near to experimental test with an inert gas (Nitrogen). Moreover, it contains an air cooler installed in the pipe work connecting the inlet and outlet of seal to remove heat from barrier liquid.

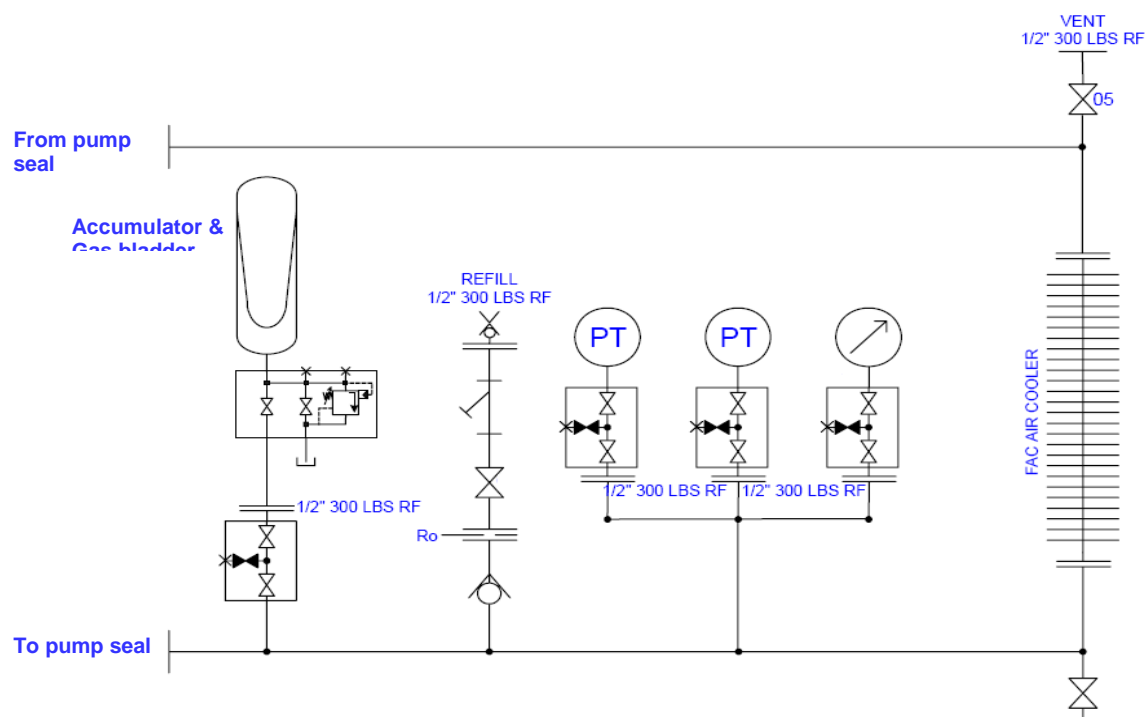


**Figure 4. 5 Flow diagram of the main pump seal unit**

#### 4.5.5 Gas Make-Up System

A gas make-up system is provided to keep the test pressure constant during experiment. Gas is introduced into the flow loop to compensate the pressure reduction of system during cooling and hydrate formation. The gas is supplied through a pipeline connected to normal laboratory-size bottles (50 litres with a maximum pressure of 200 bar), which are located outside the laboratory in a well-ventilated space. Inside the laboratory is a reciprocating gas booster to provide gas make-up at the desired pressure. The booster works rapidly at first, then slower and stops at a pressure balance. When a pressure imbalance occurs between the flow loop and the desired booster pressure due to cooling and or hydrate formation processes, the booster will automatically restart to restore the pressure balance. The total volume of the gas phase make-up is measured using a gas flow meter located upstream of the gas booster. For constant pressure tests, the measured amounts of gas phase injected into the flow loop is a measurement of hydrate formation.

#### **4.5.6 Cooling System**

Several heat sources are in the system which causes temperature to be increased. As the system is a closed loop, the main source of heat is fluid friction which increases with fluid velocity. Heat is also added from the mechanical equipment. Moreover, being an exothermic reaction, the hydrate formation releases heat. To remove all these heats from the flow loop and to reach the fluid temperature to the required temperature, the flow loop system is housed in a Low Temperature Lab (LTL). A series of air handling units is mounted behind the LTL to keep the room temperature between -15 to +20 °C. The air handling units contain all components necessary for correct close tolerance temperature control of the room. Mounted in the handling units are the circulation fans, refrigeration coil and all sensing probes. The cooling system is fully automatic with the control system deciding which units should be running in order to achieve the temperature set for experimental test from the front panel. The cooling system is dual unit with fully automatic changeover in the event of a unit failure. They will also automatically changeover on a 24 hour cycle to prevent uneven wear and to ensure that both systems are ready for use.

#### **4.5.7 Instrumentation and Data Acquisition**

The instrumentation of the flow loop includes measurements of temperature, pressure, differential pressure, liquid flow rate, and total gas injected. The operation of the flow loop is regulated using these variables and instrument signals are recorded to file on a continuous basis.

Several temperature and pressure sensors are located throughout the flow loop, as shown in Figure 4.4. During the whole period of an experiment, the volume-flow rate of the fluid inside the pipe is controlled by means of a Micro-Motion flow meter from Rosemont. It works based on Coriolis-force measuring principle. The volumetric flow rate range is 0-5000 litre/hr. The output data are 4 to 20 mA and are converted into voltage signals of 2 to 10 volt before sending to the PC-based data acquisition system. The pre-calibration from the manufacturer was used for calibrating of the output data.

Differential pressure measurement is carried out with a Fuji differential pressure transmitter. It is used to measure the differential pressure between the inlet and outlet of a 6 meter straight horizontal pipe which is used for viscosity measurements. It is able to measure differential pressure between 0-20 bars. The output signals are 4 to 20 mA DC

which are converted into voltage signals (2 to 10v) before transferred to the PC-based data acquisition system. It was calibrated according with the per-calibration performed by supplier.

The gas injection point is as close as possible to the output of the main pump to prevent any free gas from entering the pump. A Brooks gas flow meter (Model 5860S) is used to measure the gas injection rate during the test period. The gas flow meter is installed to measure the gas flow rates in terms of normal litre per minute (nl/min). The heart of this system is the thermal mass flow sensor, which produces an electrical output signal as a function of flow rate. The measurement range is between 0.003 and 30 nl/min. A Brooks Model 0254 secondary electronics is used to record the total volume of gas injected at the time of experiments.

Differential pressure, total gas flow, fluid flow rate, pressures and temperatures are shown in real time in the flow loop. Voltage signals from these instruments are transferred to a separate control room for data acquisition on a personal computer (PC). The signals are digitalized, imported and processed in the PC-based on a program implemented in LabVIEW. The statues of the flow loop experiments can be monitored from the PC, and the logged data are saved to file at an optional frequency for later analysis.

## 4.6 REFERENCES

- Allouche, J., Tyrode, E., Sadtler, V., Choplin, L. and Salager, J.L., 2004. Simultaneous conductivity and viscosity measurements as a technique to track emulsion inversion by the phase-inversion-temperature method. *Langmuir*, 20(6): 2134-2140.
- Arjmandi, M., 2007. Gas hydrate control by low dosage hydrate inhibitors, Ph.D. Thesis, Petroleum Engineering, Heriot-Watt University, Edinburgh.
- Azarinezhad, R., 2010. A chemical based wet cold flow approach for addressing hydrate flow assurance problems, PhD Thesis, Heriot-Watt University, Edinburgh
- Fidel-Dufour, A., Gruy, F. and Herri, J.M., 2006. Rheology of methane hydrate slurries during their crystallization in a water in dodecane emulsion under flowing. *Chemical Engineering Science*, 61(2): 505-515.
- Metz, B., Kossen, N. and van Suijdam, J., 1979. The rheology of mould suspensions. *Advances in Biochemical Engineering*, Volume 11: 103-156.
- Omer, A., 2009. Pipeline Flow Behavior of Water-In-Oil Emulsions, PhD Thesis, University of Waterloo, Waterloo.
- Peytavy, J.L., Glénat, P. and Bourg, P., 2008. Qualification of Low Dose Hydrate Inhibitors (LDHIs): field cases studies demonstrate the good reproducibility of the results obtained from flow loops, *Proceedings of the 6th International Conference on Gas Hydrates (ICGH 2008)*, July 6-10, 2008, Vancouver, British Columbia, CANADA.
- Reeve, R., Godfrey, J. and Bradford, S., 2002. Phase inversion during liquid-liquid mixing in continuous flow, pump-mix, agitated tanks. *Chemical Engineering Research and Design*, 80(8): 864-871.
- Robole, B., Kvandal, H.K. and Schuller, R.B., 2006. The Norsk Hydro Multi Phase Flow Loop. A high pressure flow loop for real three-phase hydrocarbon systems. *Flow Measurement and Instrumentation*, 17(3): 163-170.
- Sjöblom, J., Ovreivoll, B., Jentoft, G.H., Lesaint, C., Palermo, T., 2010. Investigation of the Hydrate Plugging and Non-Plugging Properties of Oils. *Journal of dispersion science and technology*, 31(8): 1100-1119.
- Song, D., Zhang, W., Melby, E.G. and Gupta, R.K., 2008. An instrumented mixer setup for making tackifier dispersions used to make pressure-sensitive adhesives. *Measurement Science and Technology*, 19: 045801.
- Souvlis, E., Doulia, D. and Angeli, P., 1998. Power requirements and phase inversion during oil-water mixing. *ICHEME Research Event* (Rugby, UK: Institution of Chemical Engineers): pp816-22.

Wolden, M., Lund, A., Oza, N., Makogon, T., Argo, C.B., Larsen, R., 2005. Cold flow black oil slurry transport of suspended hydrate and wax solids, *Proceedings of the Fifth International Conference on Gas Hydrates*, Trondheim, Norway.

## **CHAPTER 5 MORPHOLOGY OF WATER-OIL EMULSIONS WITH AND WITHOUT HYDRATES**

### **5.1 INTRODUCTION**

In deepwater exploration and production, where long tieback multiphase pipelines are a preferred economic option, gas hydrate blockages pose serious problems for flow assurance to produce hydrocarbon with high water cuts because the traditional techniques, such as insulation, heating or injection of thermodynamic inhibitors, often become economically and logistically unpractical. For this reason, the potential for transporting hydrate particles as a transportable water/oil/hydrate mixture is an attractive scenario to the oil and gas industry.

One of the new technologies to create transportable hydrate slurry is the injection of anti-agglomerants (AAs) which has received considerable attention. In low water cut systems, stable water-in-oil emulsions are usually formed, and by converting water droplets into the hydrate particles, transportable hydrate-in-oil slurry can be formed (Groeneweg et al., 1998). However, for high water cut systems, by converting some of the water phase into the hydrate, the behaviour of the hydrate slurry will be strongly dependent on the water-oil emulsion which acts as a carrier fluid to transport the hydrate particles. In this case, water-oil emulsions present far more complex behaviour, in which many parameters, such as the presence of natural surfactants, AAs, salt and even hydrate particles, might affect the morphology of the emulsion (Binks and Lumsdon, 2000; Groeneweg et al., 1998; Hoiland et al., 2005; Leporcher et al., 1998). AAs are a type of surfactant and they have been used to produce transportable gas hydrate slurries in low water cut systems, which often form a water-in-oil emulsion (Kelland, 2006; Sloan and Koh, 2008). However, in the case of high water cut systems, both water-in-oil (W/O) or oil-in-water (O/W) emulsions may occur, depending on the system conditions. Therefore, a better understanding of the characteristics of water-oil emulsions in the presence of AA is a prerequisite to understanding the behaviour of hydrate slurry in high water cut systems.

A considerable amount of literature has been published on the various aspects of water-oil emulsions; however, there is a lack of published study on the effect of AAs on the characteristics of emulsions. Hence, one of the objectives of this chapter is to study the effect of AAs on stability and phase inversion of water-oil emulsions. Another goal of



this chapter is to investigate the effect of hydrate particles that are formed in the presence of different AA concentrations on the morphology of these emulsions.

## **5.2 MORPHOLOGY OF WATER-OIL EMULSIONS WITHOUT HYDRATES**

Surfactants are usually used as emulsifiers and their selection will depend on the produced oil and the properties desired in the end product. Selection of surfactant plays an important role in determining the class of emulsion. For example adding water soluble surfactants to increase the productivity of viscous crude oil reservoirs, with the aim of reducing the viscosity of water-oil emulsions, causes the usual W/O emulsion stabilised by natural surfactants to convert to O/W emulsions (Zaki et al., 2000). In contrast, W/O emulsion drilling muds are preferred in the drilling industry (Schramm, 1992).

In order to produce transportable hydrate slurries, AAs are usually injected in oil and gas production pipelines. With reducing interfacial tension between water and oil phases, AAs lead to produce W/O emulsions in low water cut systems (Kelland, 2006; Sloan and Koh, 2008). With increasing water content in the system, however, both W/O or O/W emulsions may occur, depending on the system conditions. It is therefore necessary to understand, as fully as possible, the effect of AAs on the characteristics of emulsions. So far, although a large number of studies have been performed indicating the effect of AAs on hydrate slurry transportability (Anklam et al., 2008; Frostman, 2000b; Huo et al., 2001; Zanota et al., 2005), very little attention has been paid to investigating the effect of AAs on water-oil emulsion morphology. Some preliminary experiments were conducted in this study to investigate the stability and phase inversion of water-oil emulsions in the presence of different AA concentrations.

### **5.2.1 Emulsion Stability Measurements**

Recent evidence suggests that some stable W/O emulsions produce transportable hydrate slurries in low water cut systems (Boxall et al., 2008; Hemmingsen et al., 2007). Therefore knowledge of the morphology of water-oil emulsions before hydrate formation can provide insights on the hydrate slurry transportability.

The stability of an emulsion is described as the resistance of the dispersed phase droplet against coalescence. Phase separation in emulsions is imposed by thermodynamics, because there is a natural tendency for oil and water to form two separated and continuous phases as the interfacial area and consequently the interfacial energy of the

dispersion are reduced. Therefore, the characteristics of the emulsion cannot remain unchanged with time. According to the degree of kinetic stability of emulsions, Kokal (2005) classified emulsions into loose, medium, and tight emulsions depending on whether their stability of them limits to a few minutes, ten minutes or more and an hour to days, respectively. To form a liquid-liquid emulsion, an interfacial film has to exist between the liquid phases. The material of this film has the property of accumulating at the interface of liquids. It is well-known that emulsion stability is closely associated with the physical properties of the interfacial film around the dispersed droplets, which resists droplet coalescence (Campanelli and Cooper, 1998; Ekott and Akpabio, 2010; Kokal, 2005). The strength of this film not only depends on temperature, pH, and oil and brine compositions, but also mainly depends on the structure of the surfactant molecules and heavy polar fractions in water-oil interface (Ekott and Akpabio, 2010; Kokal, 2008). Adding surfactants into the emulsion may be performed with the purpose of emulsifying or demulsifying the emulsions; therefore, they should have different effects on interfacial film depending on the physico-chemical characteristics of the surfactants. However in the case of adding AAs to the emulsions (which can be W/O or O/W), the main aim is to prevent hydrate agglomeration and its effect on the emulsion is not taken into consideration directly.

#### **5.2.1.1 Experimental Set-Up and Material**

The stability measurements were carried out via bottle tests. Two different crude oils were used in this study, named as oil (A) and oil (B). The compositions of oil (A) and oil (B) are shown in Tables A.1 and A.2, respectively. The main physico-chemical properties of the crude oils are presented in Table 5.1. The total acid number (TAN), which corresponds to the mass of KOH in milligrams necessary to neutralize the acid contained in 1 g of oil, are relatively low for both crude oils and their values are almost equal. However, there is a significant difference between their resin and asphaltene contents (the asphaltene content for crude oil (A) is more than 10 times higher than that for crude oil (B)). The aqueous phase consists of deionised water, a commercial water-soluble AA type quaternary ammonium salt (labelled as AA1) and salt ( $\geq 99\%$  anhydrous NaCl (Aldrich)).

**Table 5. 1 Properties of crude oils**

	Crude oil (A)	Crude oil (B)
Density (kg/m <sup>3</sup> ) at 21 °C	883	869
Viscosity(mPa.s) at 21 °C	36	24
TAN (mg KOH/g) <sup>1</sup>	0.20	0.30
Resins (% wt/wt) <sup>2</sup>	10.8	9.4
Asphaltenes (% mass) <sup>3</sup>	2.5	0.25

1. Total Acidity Number by IP408

2. Resins by MT/LCH/05 (prep HPLC)

3. IP143. Determination of Asphaltenes (heptane insoluble) in crude petroleum and petroleum products

### 5.2.1.2 Measurements of the Stability of the Prepared Emulsions

The main purpose of the stability measurements is to investigate the effect of the type of emulsion, AA and salt on the stability of emulsions. The samples of W/O or O/W emulsions were prepared by agitating the continuous phase vigorously at 600 RPM using a standard three blade impeller at ambient pressure and temperature. All the experiments were carried out for the oil to water ratio of 1:1 by volume and a mixing time of 10 minutes. Depending on the test conditions, the aqueous phase was pure deionised water, deionised water containing the desired concentration of AA with or without 5 wt % NaCl. In order to prepare the emulsions, the dispersed phase was added gradually into the continuous phase while agitating the mixture with the impeller. During mixing, the electrical resistance of the emulsion was monitored using a digital resistance meter, to ensure that there was no phase inversion between the continuous and dispersed phases. Because the electrical resistance of W/O and O/W emulsions differs by several orders of magnitude, the phase inversion of the emulsions is readily recognizable. The prepared emulsion was poured into bottles immediately and the amount of water separated from the emulsions was monitored for 24 hours. The water separation is calculated as separation efficiency, “e”, from the volume of water observed in the clear measurement tube as follows:

$$\% \text{ separated water, } e = \frac{V}{V_0} \times 100$$

where,  $V$  is the volume of water separated  $V_0$  is the original volume of water content.

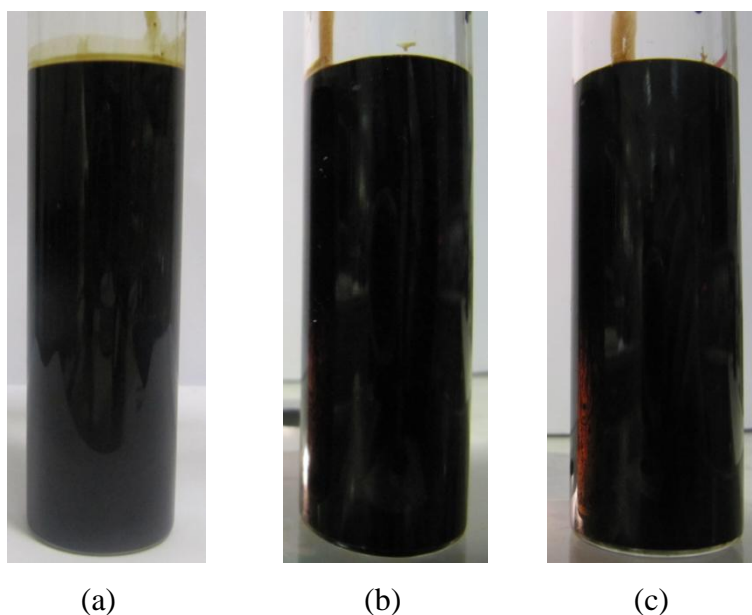
### 5.2.1.3 Results and discussion

The purpose of the current study is to investigate the effect of AA and salt on the stability of W/O and O/W emulsions for two different crude oils (oil (A) and oil (B)). Emulsion stability data presented in Table 5.2 indicate the effect of AA and salt on the stability of the W/O and O/W emulsions of Oil A. In the case of W/O emulsions, no water separation was observed within 24 hours, as the emulsion was very stable (Figure 5.1). This emulsion can be classified as a “*tight emulsion*”(Kokal, 2005). Adding AA and salt did not affect the stability of the W/O emulsion and they also presented highly stable emulsion characteristics after one day (Figure 5.1). Bottle tests were performed on the O/W emulsions, as listed in the Table 5.2. It is seen that the untreated O/W emulsion (with no AA and salt) was highly unstable, since a clear layer of decanted water had collected at the bottom of the container immediately after starting the test. A large amount of water (60%) separated within the first 1.3 minutes of the test. It is apparent from Table 5.2 that AA improved O/W emulsion stability, as it decreased the rate of water separation. The test was also carried on with addition of 5 wt. % NaCl into the aqueous phase, in the presence of AA. It was observed that salt promoted the water separation, as 60% of the water separated from the emulsion within the first 3.5 minutes of the test. The above bottle tests were repeated for another crude oil (oil B) and the results are presented in Table 5.3. For W/O emulsions, the emulsion was not as stable as oil (A). It can be seen that within the first 72 minutes of the test, 60% of the water separated from the emulsion (Figure 5.2). This emulsion can be classified as “*medium emulsion*”(Kokal, 2005). Figure 5.3 shows that a clear layer of water had collected at the bottom of the container after 135 minutes, which is about 87.5% of the water content. The results also indicate that adding AA promoted the water separation from the emulsion, as 60% of water separated within the first 47 and 38 minutes of the test with addition of 0.3 and 1.0 wt. % AA, respectively. Adding salt to the emulsion in the presence of AA increased the instability of the emulsion, as the time for separation of 60% of water decreased to 29 minutes. Similarly to oil (A), the presence of AA improved the stability of oil (B)-in-water emulsion, and adding 5 wt. % NaCl significantly reduced the emulsion stability.

**Table 5. 2 Emulsion stability results for oil (A)**

Type of emulsion	AA wt. %	NaCl wt. %	Time for separation of 60 vol. % of the initial aqueous phase / minutes	Comments
Water in oil	0	0	highly stable emulsion	no water separation <sup>1</sup>
Water in oil	1	0	highly stable emulsion	no water separation <sup>1</sup>
Water in oil	1	5	highly stable emulsion	no water separation <sup>1</sup>
Oil in water	0	0	1.3±0.1	
Oil in water	1	0	54±3	
Oil in water	1	5	3.5±0.2	

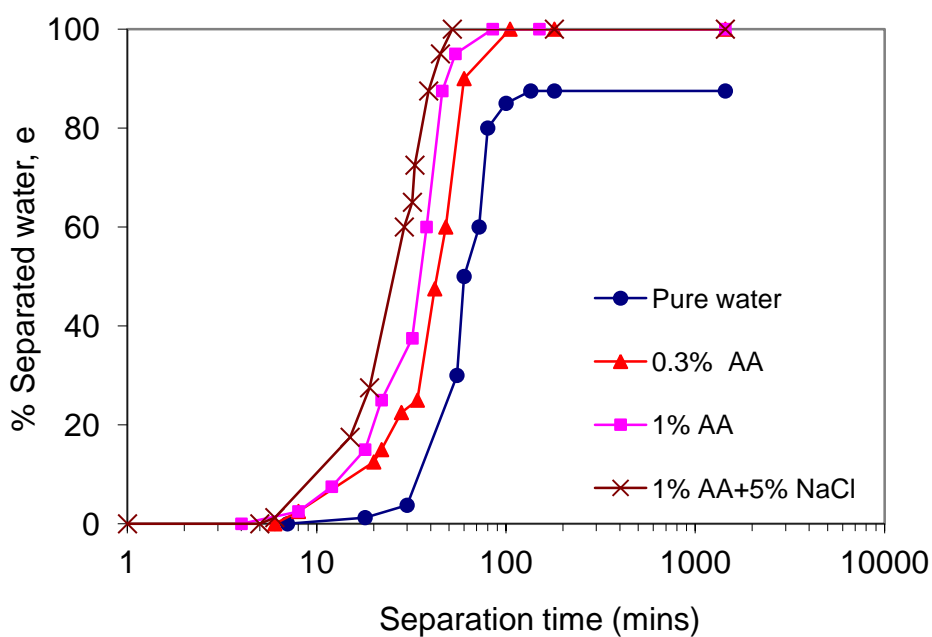
1: No water separation was observed after the 24 hours period



**Figure 5. 1 Appearance of the samples used in the bottle tests for W/O emulsion of oil (A) after 24 hrs when the aqueous phase is; a) pure deionised water, b) deionised water with 1.0 wt. % AA, c) deionised water with 1.0 wt. % AA and 5 wt. % NaCl.**

**Table 5. 3 Emulsion stability results for oil (B)**

Type of emulsion	AA wt. %	NaCl wt. %	Time for separation of 60 vol. % of the initial aqueous phase / minutes
Water in oil	0	0	72±3
Water in oil	0.3	0	47±3
Water in oil	1	0	38±3
Water in oil	1	5	29±2
Oil in water	0	0	0.55±0.0
Oil in water	1	0	89±3
Oil in water	1	5	4.1±0.2

**Figure 5. 2 Bottle test results for W/O emulsions of oil (B) for different AA and salt concentrations.**

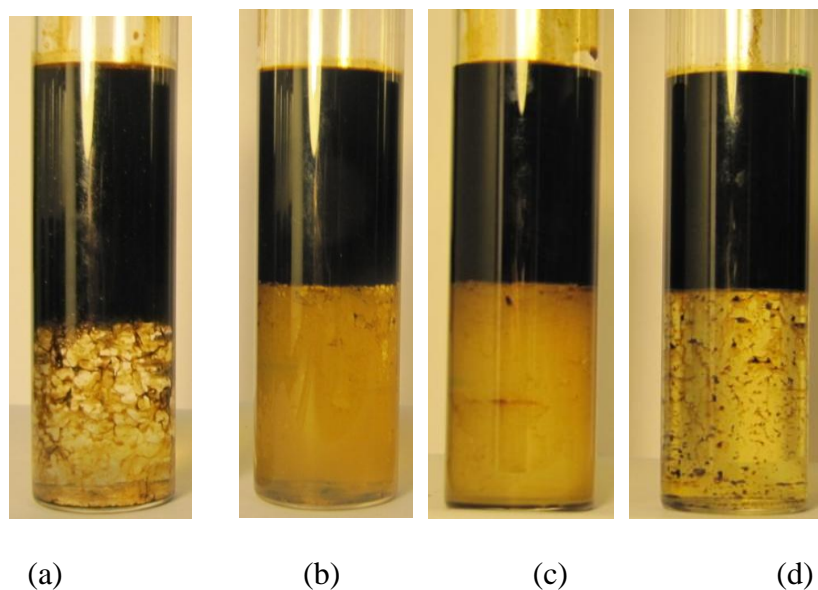


**Figure 5. 3 Appearance of the samples used in the bottle tests for W/O emulsions of oil (B) a) untreated water after 135 minutes, b) treated with 0.3 wt. % AA after 105 minutes, c) treated with 1 wt. % AA after 85 minutes, d) treated with 1 wt. % AA and 5 wt. % NaCl after 52 minutes.**

The results of emulsion stability measurements show that the emulsion stability strongly depends on the type of emulsion. For example for oil (A) the formation of W/O emulsions caused a highly stable emulsion: however, it was completely unstable when the emulsions were O/W. Similar trends were observed for oil (B). The reason for this behaviour can be attributed to the formation of rigid interfacial films in the crude oil-water interface that form a layer around the water droplets dispersed in the emulsions and prevent the droplets from coalescing (Kokal, 2005). It can be concluded that oil (A) produced a stronger interfacial film than oil (B), which can be attributed to the presence of more natural surfactants (asphaltenes, resins, etc) in oil (A). In the case of W/O emulsions, natural surfactants absorbed on the outer surface of water droplets and result in the formation of a rigid film preventing the water droplets from rapid coalescence (Kokal, 2005). However, for O/W emulsions this rigid layer is absorbed on the internal surface of oil droplets and there will be a very high tendency for oil droplets to coalesce and form separated oil and water phases.

The results also showed that for oil (B) emulsions, adding AA promoted the coalescence of the water droplets in the W/O emulsions. It has been reported that AAs have helped in demulsifying several black oil emulsions (Frostman, 2000a). This trend is consistent with the Bancroft's rule (1913) which says when oil, water and surfactant are mixed, the continuous phase is the phase where the surfactant is more soluble. The

findings are also consistent with those of Lin (1968) who found that to produce an O/W emulsion, it is better to put all the surfactants in the aqueous phase. It can be therefore assumed that AAs find a place between the existing natural surfactants or displace them in the interfacial film around the water droplets (Figure 5.4). High interfacial viscosities (the fluid viscosity at the water-oil interface) significantly slow the liquid drainage rate and thus have a stabilizing effect on the emulsion. Wasan et al., 1979; Wasan and Mohan, 1977 have shown that surfactants which lower the interfacial viscosity also destabilize crude oil-water emulsions. In contrast, surfactants which maximize interfacial viscosity maximize emulsion stability. Therefore, it can be suggested that the interfacial viscosity may be reduced with the type of AA used in this study, resulting in reduction of stability of W/O emulsions.

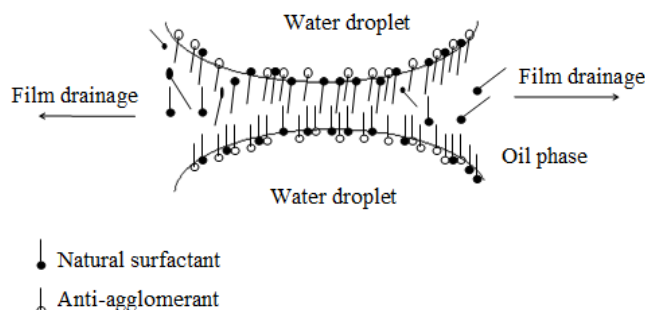


**Figure 5. 4 Anti-agglomerants displace the natural surfactants in the interface film.**

It is interesting to note that adding AA significantly increased the stability of O/W emulsion. In the case of O/W emulsions the hydrophobic tails of AA molecules are placed inside the oil droplets and the hydrophobic heads are placed in the oil-water interfaces (Figure 3.13). For the O/W emulsions in which water is continuous phase, because of water is a polar liquid the effect of electrical repulsive force is more pronounce. Therefore, a possible explanation for this might be that for O/W emulsions addition of AA improves the electrical double layer effect around oil droplets and prevent droplets coalescence.

Effect of salt on the emulsion stability was examined in the presence of AA. The results indicated that adding salt significantly reduced the stability of both W/O and O/W emulsions (except oil (A) which formed a tight W/O emulsion). These results are consistent with those of other studies (Binks, 1993; Binks et al., 2000; Moradi et al., 2011; York and Firoozabadi, 2009). York and Firoozabadi (2009) observed that salt significantly reduced the stability of water-oil emulsions in the presence of two types of AAs (quaternary ammonium salt and rhamnolipid biosurfactant).



### 5.2.2 Phase Inversion in Liquid-Liquid Dispersions

The phenomenon of phase inversion refers to the process whereby the dispersed and continuous phases of an emulsion are inverted or suddenly change form, i.e., from O/W emulsion to W/O emulsion or vice versa. The dispersed phase droplets continuously coalesce and break-up in the turbulent flow field generated by the stirrer. For the dispersed phase with low droplet hold-ups, coalescence and breakage events are always in a dynamic equilibrium; however, at large hold-ups, the coalescence events overcome the breakage events and result in phase inversion. Catastrophic inversion takes place by the gradual increase in the volume fraction of the dispersed phase that follows a sudden change in the behaviour of the emulsion.

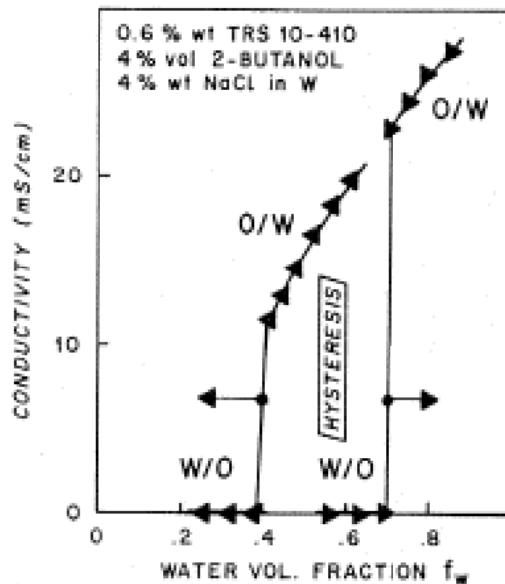


**Figure 5.5 Variation of the emulsion conductivity through a dynamic inversion produced by an increase in internal phase ratio, Arrows indicate the direction of change (Becher, 1988).**

When the amount of dispersed phase in the emulsion reaches a critical value, phase inversion occurs and finally a stable emulsion is formed (Jahanzad et al., 2009; Zambrano et al., 2003). Phase inversion is a very complex occurrence. Several factors can affect the critical dispersed phase hold-up such as the viscosity, density, interfacial tension, type of impeller, input energy (impeller speed), temperature, type and concentration of surfactants, etc. (Norato et al., 1998).

The actual mechanism of phase inversion in the emulsion still remains unclear, although apparently some processes of coalescence and break-up of the dispersed drops

are involved. The phase inversion is not always precisely reversible. Hysteresis can take place if the inversion point is approached from both directions, i.e. adding aqueous phase to organic phase and vice versa. Figure 5.5 shows the variation of conductivity of the W/O emulsion when the water phase content is increased (arrows pointing to the right), and the same data for the O/W emulsion when the oil phase content is increased (arrows pointing to the left). Obviously, the emulsion inversion does not occur at the same water volume fraction. It is clear that dynamic inversion shows a hysteresis zone, i.e., a region in which the emulsion may be either O/W or W/O, depending on emulsion conditions.

It is well known that the viscosity of an emulsion increased with an increase in the amount of dispersed phase, up to a maximum value near to the inversion point, due to a change in the emulsion morphology. In order to determine the phase inversion point, several techniques can be utilized. Measuring electrical conductivity is the easiest method (Norato et al., 1998). Apart from this method, viscosity/torque (Allouche et al., 2004) or power measurement (Souvlis et al., 1998) are also often applied.

#### **5.2.2.1 Experimental setup and materials**

Phase inversion experiments were carried out in a stirred beaker, in which the morphology of the emulsion is measured by means of the torque applied on the stirrer at constant RPM. The experimental setup is explained in details in Chapter 4.

Two crude oils (A) and (B) (properties listed in Table 5.1) were used in this study. The aqueous phase consists of deionised water, a commercial water-soluble AA (labelled as AA1) and salt ( $\geq 99\%$  anhydrous NaCl (Aldrich)).

#### **5.2.2.2 Phase inversion point determination**

All the experiments were carried out in a 500 ml cylindrical glass beaker at room temperature. The contents are agitated by a stainless steel impeller comprising two parallel disks attached by vertical blades. Since insertion of probes for measuring the electrical conductivity/ resistivity may cause variations of the flow pattern of the dispersion (Kinugasa et al., 1998), in this work inversion points were determined by monitoring the electrical torque/current measurements of the stirrer motor. An electrical motor (Maxon DC motor Model 6180300 C) is used to drive the stirrer at constant operating speed of 500 RPM. The RPM of the impeller and the electrical current, which is proportional to the torque acting on the motor, are continuously monitored. Before starting the experiments, the beaker was filled with 50 ml of the continuous phase and it

was agitated for 10 min at 500 RPM to reach stable conditions. The dispersed phase (aqueous phase, in the case of W/O emulsions, and oil phase, in the case of O/W emulsions) at the operating temperature was added into the beaker at a constant flow rate using a highly accurate constant flow rate pump. The pump is switched on from the start of the experiment to inject the dispersed phase into the beaker at a constant flow rate of 5 ml/min.

### 5.2.2.3 Results and discussion

#### *Inversion point from W/O to O/W for untreated emulsions*

At the start of the experiment, the beaker was filled with 50 ml of oil (A) and it was stirred for 10 min at 500 RPM. The test started with injecting pure deionised water (no AA and no salt) into the beaker. Visual observations showed that below 60% water cut the emulsion seemed homogeneous and transportable (emulsion can be moved easily by the stirrer). As more and more water was added (up to 70% water cut), the emulsion became visibly more viscous and the electrical mixer current gradually increased, although the emulsion still seemed transportable. When the water content reached around 76% the emulsion turned into a thick paste, although still accepting more water. However, the emulsion did not seem transportable and the motor current increased significantly.

With addition of more water, up to about 85% water cut, the emulsion looked saturated and the additional water formed a separated phase, i.e., it was not possible to incorporate all the additional water into the emulsion (see Figure 5.6). At this point, the fluid emulsion turned into a hard gel and almost all the emulsion was attached either to the inside wall of the beaker or the impeller. As further water was added, a water film was formed on the top of the emulsion and the mixture seemed to consist of two separated phases, a thick paste emulsion and a free water phase. A similar test was conducted with oil (B) with injection of pure deionised water as a dispersed phase. Visual observations showed that, at about 83% water cut, the emulsion reached a saturated state, in which water could not dissolve in the emulsion and remained as a separated phase. The appearance of the emulsion looked like a soft gel and Figure 5.7b shows the resulting fluid at the bottom of beaker. The above experiments showed that for the test with untreated water, phase inversion could not occur for both crude oil emulsions and after certain water cut the emulsions became water saturated and the added water could not be incorporated in the emulsion. It was also observed that, at very

high water cuts, oil (A)-emulsion exhibited very hard gel behaviour while oil (B)-emulsion exhibited soft gel behaviour. The reason can be attributed to the formation of a very rigid interfacial film around the water droplets in oil (A)-emulsion, compared to a soft film around the water droplets in oil (B)-emulsion.

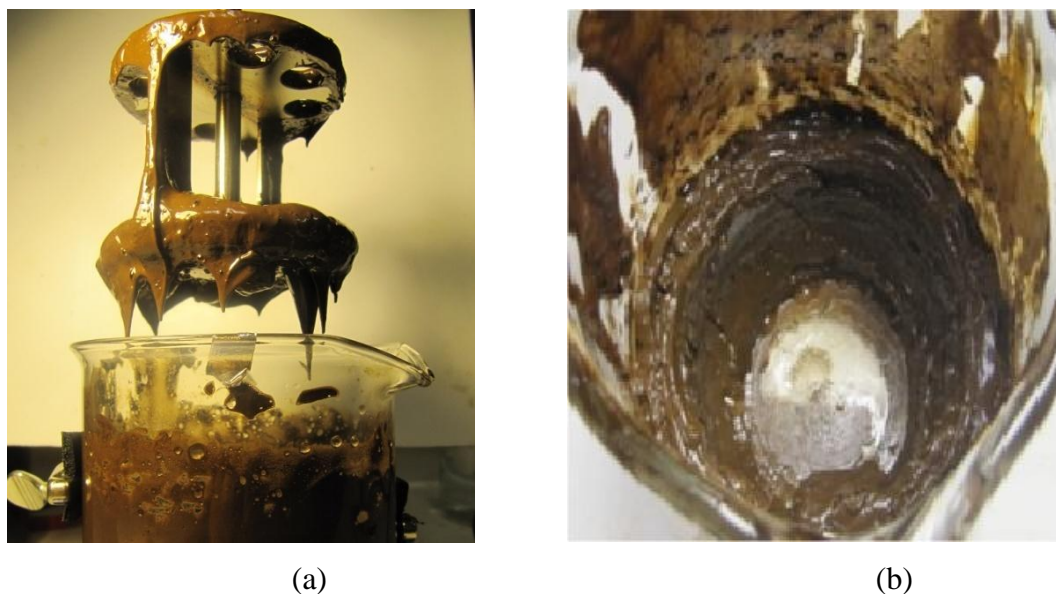


**Figure 5.6 Oil (A) emulsion with about 85% water cut turned into a thick paste. Aqueous phase is deionised water. Figure (b) shows the water cannot be dissolved into the emulsion and it remained as a separate phase.**



**Figure 5. 7 Oil (B) emulsion with about 83% water cut turned into a soft gel. Aqueous phase is pure deionised water. Figure (b) shows the water cannot be dissolved in the emulsion and it remained as a separate phase.**

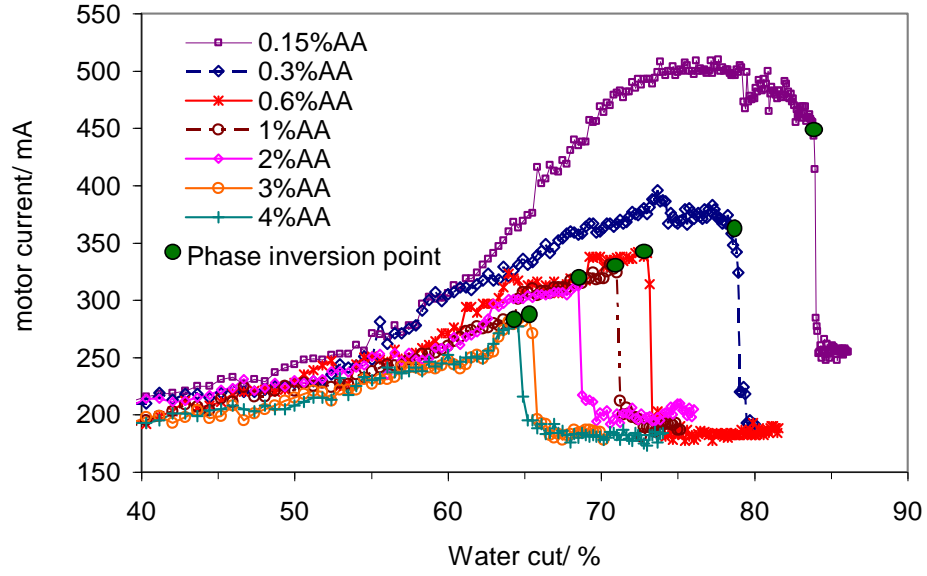
***Effect of anti-agglomerant concentration on phase inversion from W/O to O/W***

The experiments were continued by adding different concentrations of AA to the aqueous phase. The presence of AA significantly reduced the electrical current applied to the mixer and a homogeneous and transportable emulsion was observed even close to the inversion point. The experiments were performed for different AA concentrations to study the effect of AA dosage on the phase inversion point. Visual observations showed that addition of 0.15 wt. % AA significantly affected the transportability of emulsion at very high water concentrations, even close to inversion point. The formation of pasty emulsions, which was produced in high water cut, was completely rectified by adding small dosage of AA and the emulsion could easily pass the inversion point.

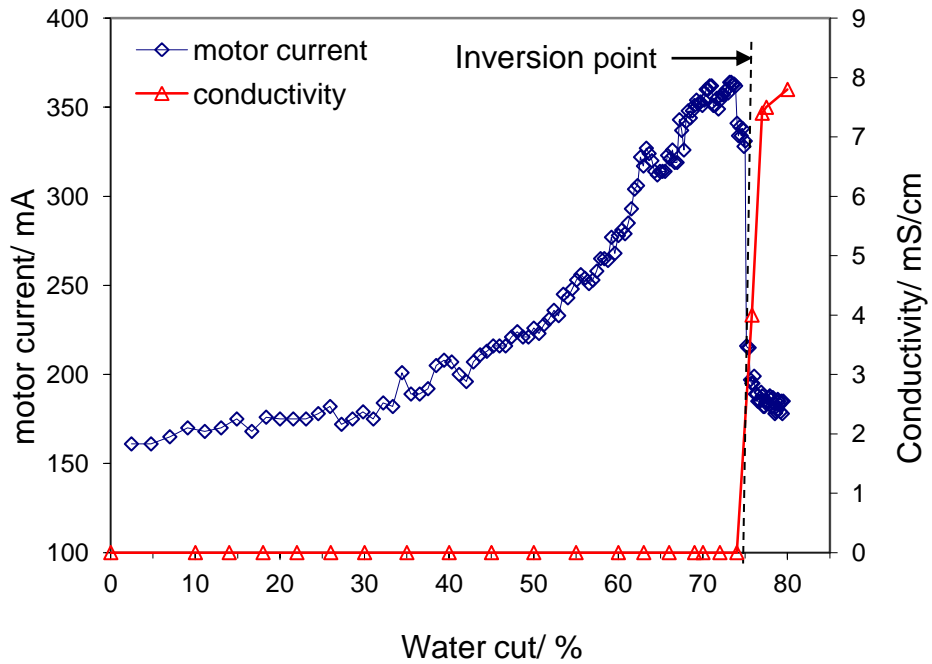
Figure 5.8 shows the motor current as a function of the volume percent of water for the experiments carried out with different AA concentrations. For all experiments the motor current increases continuously until it reaches a maximum, and then it rapidly decreases and finally levels off. In these tests, the same aqueous-feeding rate and mixer speed were used, i.e., 5 ml/min and 500 RPM, respectively. The curves show a pronounced peak which is believed to correspond to the phase inversion points. The point of phase inversion is regarded as the volume percent of water at which the emulsion converts from being oil continuous to being water continuous. The increase in the volume fraction of the aqueous phase resulted in a consequent increase in the viscosity of the emulsion until phase inversion point. After phase inversion point, the emulsion morphology was changed and the aqueous phase became the continuous phase. Phase inversion was also easily detectable through visual observation. The two continuous phases had different appearances, i.e., the aqueous continuous phase always looking more turbulent than the organic continuous phase (Reeve et al., 2002).

Figure 5.8 also indicates that with increasing AA concentration the electrical current applies on the magnetic motor significantly decreased. This means that emulsion viscosity decreases with the amount of AA in the aqueous phase.

To verify the above results, a separate experiment was conducted, using electrical conductivity measurements of the emulsion and motor current simultaneously. The electrical conductivity of the emulsion was measured by means of a conductivity probe. In this test, the aqueous phase consisted of distilled water with 0.3 wt. % AA and 0.5 wt. % NaCl. Salt was necessary to improve the conductivity of the aqueous phase. From Figure 5.9, it can be seen that the electrical conductivity suddenly increases due to phase inversion from oil continuous to water continuous phase, and it validates the motor current measurements.



**Figure 5.8** Motor current as a function of water cut for different AA concentrations (W/O to O/W emulsion). The phase inversion occurs when the motor current approach a maximum value and suddenly drops off.



**Figure 5.9** Motor current and conductivity as a function of water cut. Phase inversion point occurs when conductivity/mixer power change abruptly.

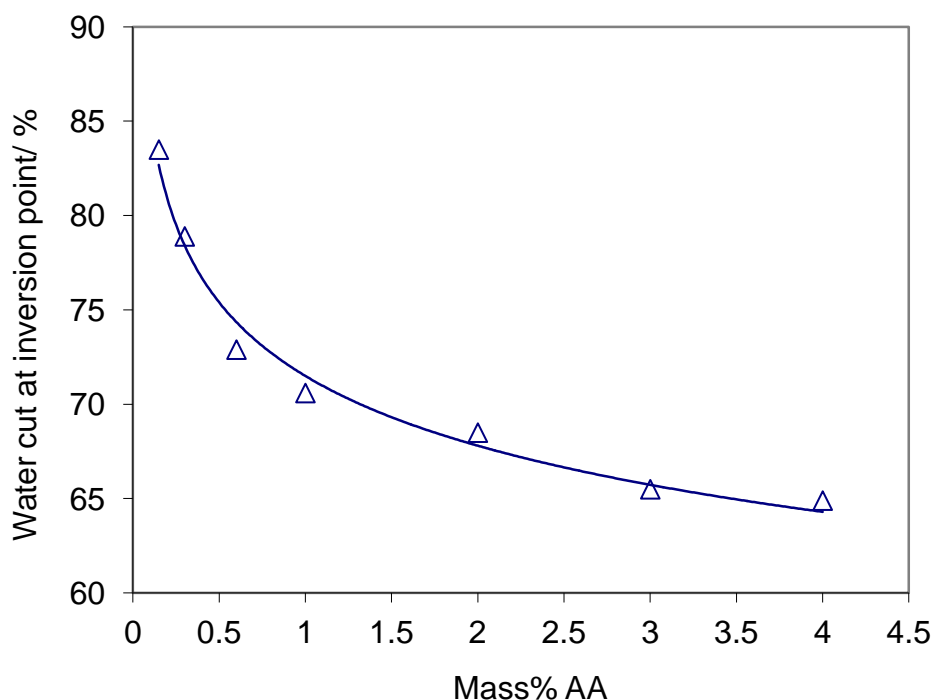


**Figure 5.10** Phase inversion point as a function of AA concentration in the aqueous phase (oil (A)).

Figure 5.10 shows the influence of the AA concentration in the aqueous phase on the inversion point for oil (A) emulsions. As the figure indicates, the phase inversion point shifts to lower water cuts with increasing AA concentration. It is apparent that adding AA to the aqueous phase encourages phase inversion to occur at lower water contents. However, as shown in Figure 5.10, the water-cut levels off as the concentration of AA increases. The water volume at the phase inversion point has reached a limit of around 65%, which seems to be independent of the AA dosage.

Figure 5.11 presents the influence of AA concentration on the water volume fraction at inversion point for oil (B). It is also clear that with increasing AA concentration the inversion point moves to lower water cuts at inversion point. The most striking result to emerge from the data is that for both crude oils an increase in AA concentration reduces aqueous phase hold-up at the inversion point and this effect is more pronounced at lower AA concentrations. This is in agreement with our earlier observations, which showed that stability of W/O emulsions decreases with adding AA to the aqueous phase. The rate of droplet coalescence overwhelms the rate of droplet breakage and leads to phase inversion at lower water volume fractions, due to a reduction of the strength of the interfacial film around the water droplets with addition of AA. For the same AA concentrations the aqueous phase hold-up at the inversion point for oil (A) is

higher than that for oil (B). The reason can be attributed to the lower stability and lower interfacial viscosity of oil (B) compared to oil (A).

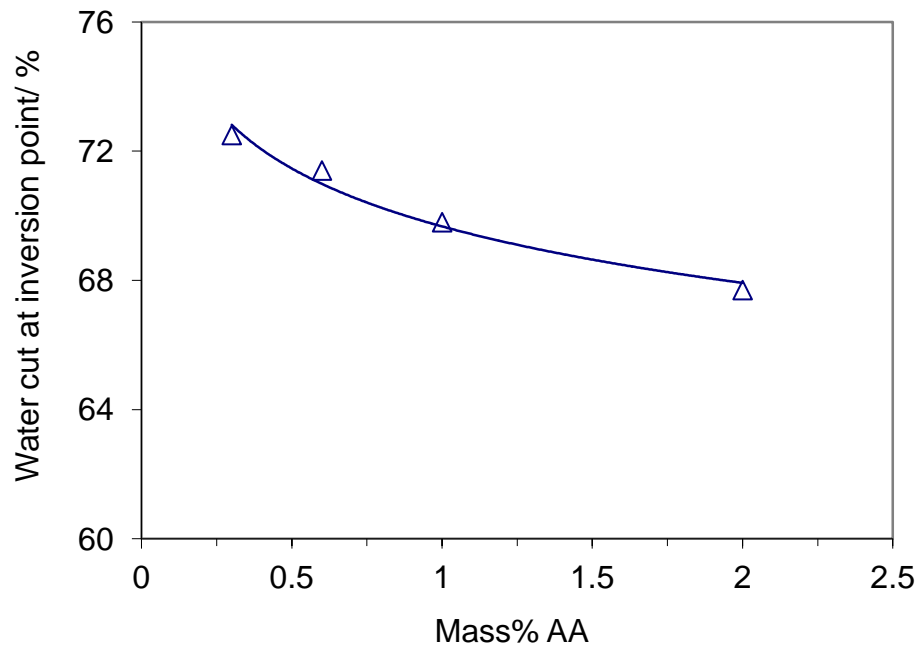


**Figure 5. 11 The phase inversion point as a function of AA concentration in the aqueous phase (oil (B)).**

***Effect of salt on phase inversion from water-in-oil to oil-in-water in the presence of different anti-agglomerent concentrations***

The experiments with addition of 5 wt. % NaCl in aqueous phase were performed for different AA concentrations to study the effect of both salt and AA on the phase inversion point. Figures 5.12 and 5.13 also show the results of inversion point measurements for emulsions with and without salt as a function of AA concentration for two different crude Oils, A and B. As the figures indicate, adding salt did not change the trend of phase inversion points against AA concentration. However, salt slightly decreased water volume fraction at the inversion points for the same AA concentrations. This can probably be explained by considering the fact that inter-droplet attraction increases in presence of salt, leading to an increase in the rate of dispersed phase coalescence (Binks et al., 2000; Moradi et al., 2011; Wang et al., 2011). The most important result of these experiments is that in the presence of AA, the formation of O/W emulsions is more favoured in the systems with salt than without salt.



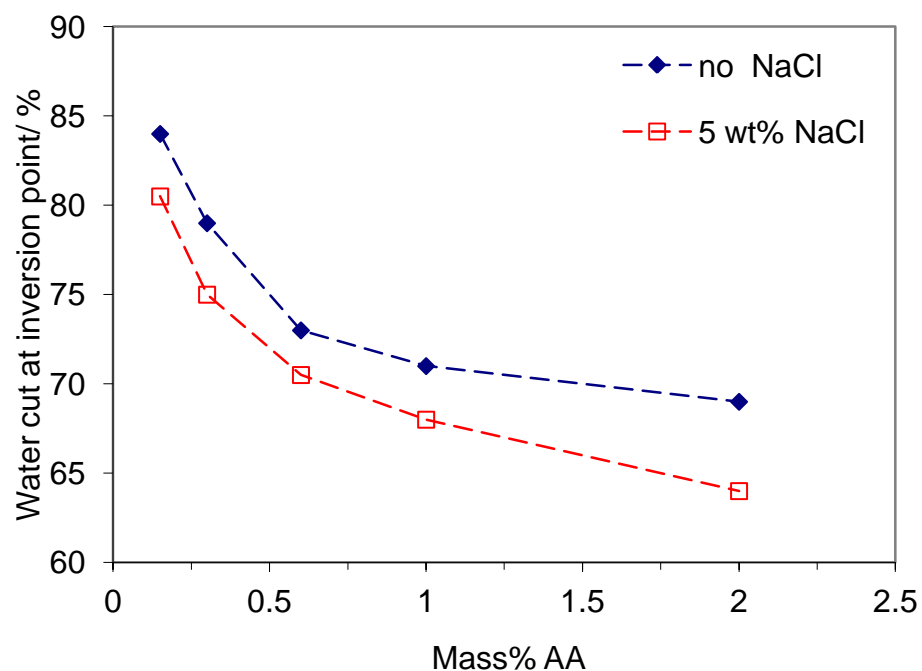


**Figure 5. 12** Water cut at phase inversion point from W/O to O/W emulsion as a function of AA concentration in the presence or absence of 5 wt. % NaCl (oil (A)).

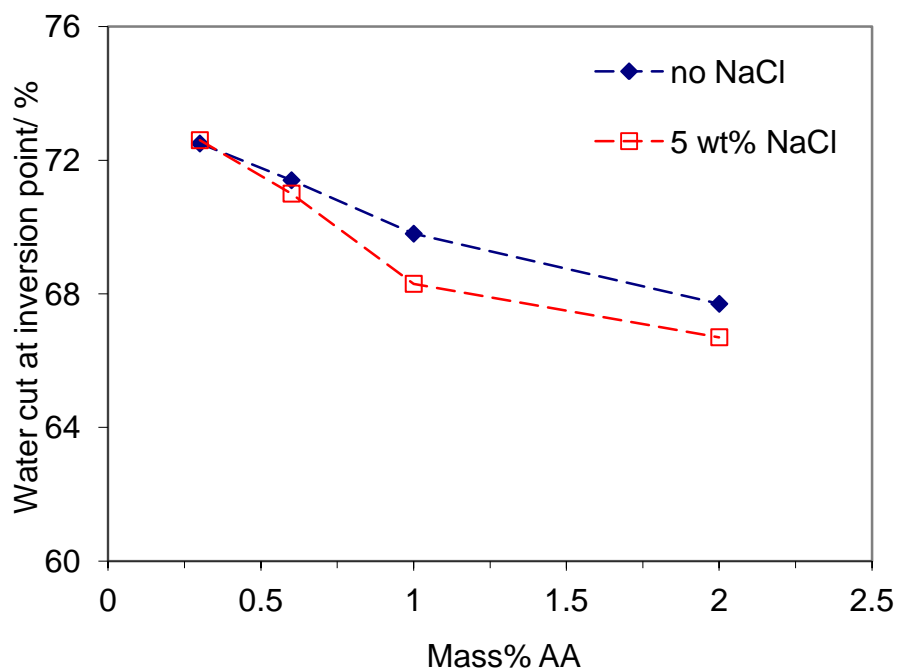


**Figure 5. 13** Water cut at phase inversion point from W/O to oil-in water emulsion as a function of AA concentration in the presence or absence of 5 wt. % NaCl (oil (B)).

***Effect of anti-agglomerant concentration and salt on phase inversion from oil-in-water to water-in-oil emulsion***

In this section, the effect of AA and salt on phase inversion from O/W to W/O emulsions is investigated. The beaker was filled with 50 cm<sup>3</sup> aqueous phase containing the desired value of AA and salt. The oil phase (oil (A)) was then added gradually to the continuous aqueous phase at a constant feed rate 5 ml/min, while the shaft of the stirrer was rotating at constant speed (500 RPM). The point of phase inversion was determined by a step change in the motor current due to the switch of the continuous phase from aqueous phase to oil phase.

To verify the test procedure, a separate experiment was conducted, by measuring the electrical resistance of the emulsion using a probe held in the beaker. Electrical resistance and motor current were recorded simultaneously during the test. The results are shown in Figure 5.14. The electrical resistance curve in the figure reflects the changes in the electrical resistance of the emulsion in the process. Initially, the electrical resistance of the system was very low, at low oil fractions that show electrical resistance of saline water. It increased sharply at around 41 vol%, indicating the phase inversion from O/W to W/O. It is obvious that the results of the electrical resistance measurements agree with the motor current measurements as shown in Figure 5.14. Systematic experiments were carried out to investigate the effect of AA and salt on phase inversion points from O/W to W/O emulsion for oil (A). The point of phase inversion is regarded as the volume percent of oil at which the emulsion converts from being water continuous to being oil continuous. Figure 5.15 shows the phase inversion point as a function of AA concentration for emulsions with and without salt. As the figure indicates, the phase inversion points shift to higher oil fractions with increasing AA concentration. This trend shows that adding AA (which is in this case a water soluble surfactant) into the aqueous phase increases the ability of water continuous emulsion to hold more oil droplets as a dispersed phase. These results are consistent with our previous findings on the effect of AA on O/W emulsion stability. As observed from the stability measurements (Section 5.2), the presence of AA improved the stability of O/W emulsions. From the data in Figure 5.15, it is also apparent that crude oil droplets in the aqueous phase slightly increase with adding 5 wt% NaCl, which can be attributed to an increase in the ionic strength of the aqueous phase (Moradi et al., 2011).

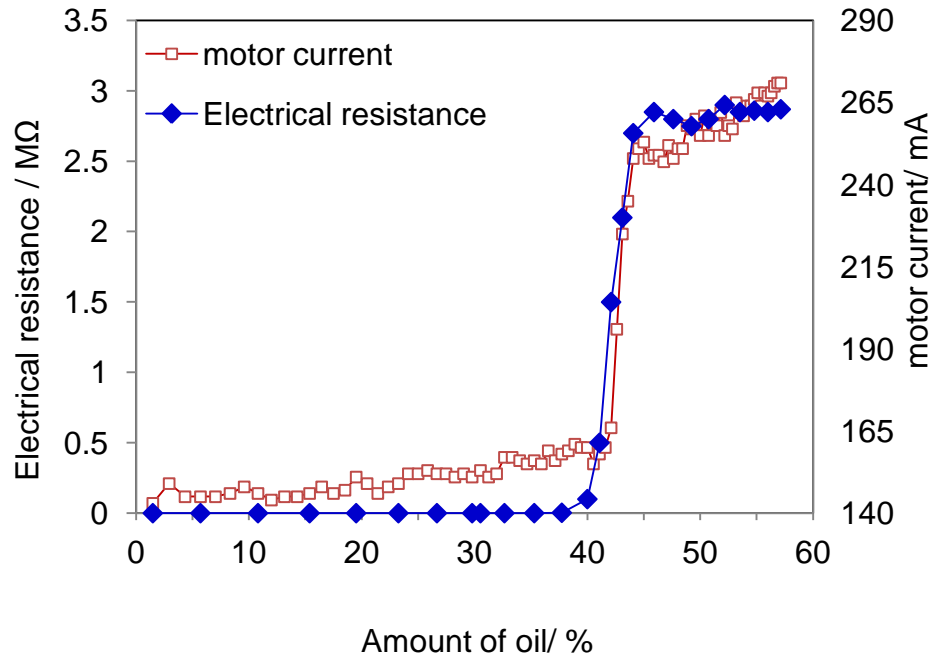


**Figure 5. 14** Motor current and electrical resistance of emulsion as a function of oil volume fraction (O/W to W/O emulsion). Phase inversion results in a sharp increase in motor current and electrical resistance.

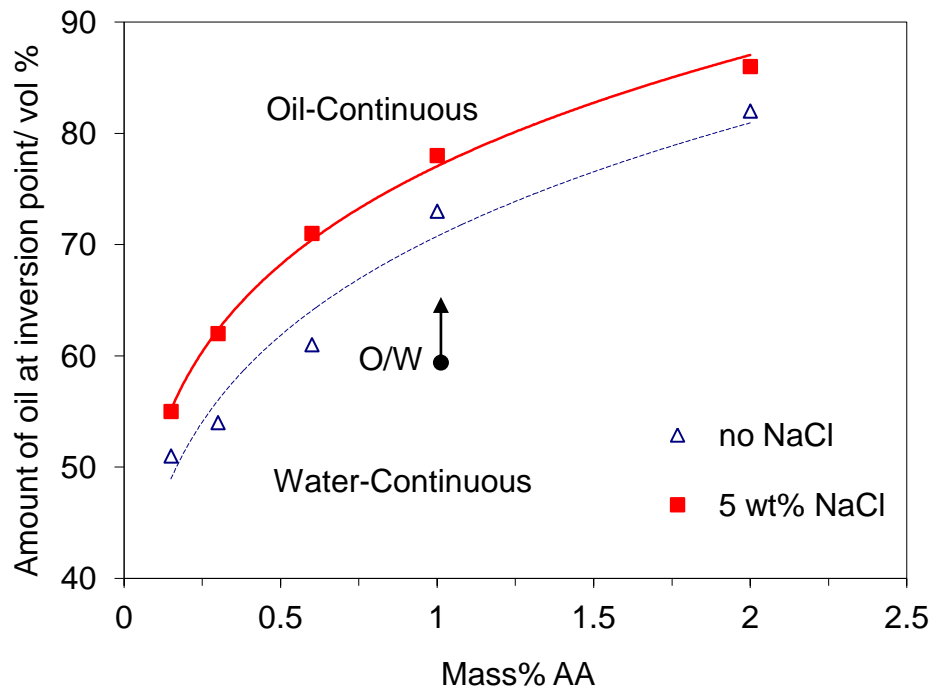


**Figure 5. 15** Phase inversion point as a function of AA concentration for O/W to W/O emulsion (in the presence and absence of salt).

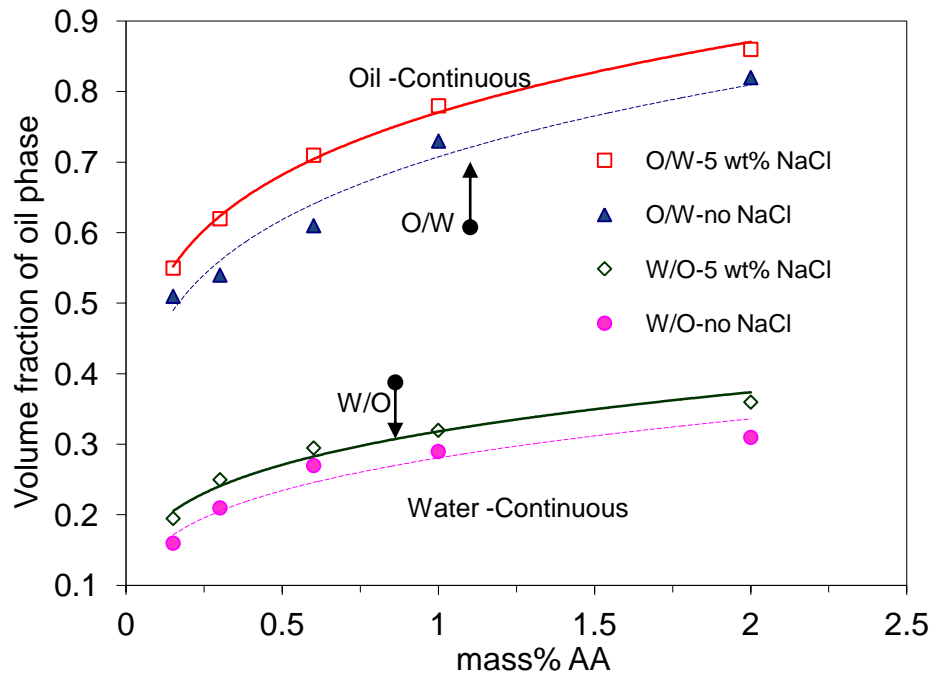


**Figure 5. 16 Comparison of phase inversion point for two types of W/O and O/W emulsions as a function of AA concentration in the presence and absence of salt.**

#### *Comparison of Phase Inversion Point of Oil-in-Water and Water-in-Oil Emulsions*

As mentioned above, the phase inversion point depends mainly on the type of initial emulsion, amount of AA and salt in the aqueous phase. Figure 5.16 displays the volume fraction of oil phase in the system at the phase inversion point for oil (A) in experiments for two types of emulsion systems. The upper curves represent the oil volume fraction at the phase inversion point, as measured during water-to-oil continuous phase experiments; the lower curves give the oil volume fraction at inversion point measured during oil-to-water continuous experiments. From the figure, three distinct regions of operation are observed: i) at large volume fractions of oil, the oil is always the continuous phase ii) at small volume fractions of oil, the oil is always the dispersed phase iii) in between, there is an ambivalent region where both types of emulsions can exist, as long as stirring is maintained. As seen from the figure, the ambivalent region is a function of AA and salt concentrations. In W/O emulsions (lower curves) the droplet holdup (aqueous droplets) decreases while increasing AA. However, for the O/W emulsions (upper curves) the droplet holdup (oil droplets) have an increasing trend. Moreover, the figure indicates that adding salt in the presence of AA has changed the droplet holdups for both O/W and W/O emulsions. With addition of salt the location of the inversion curves has shifted slightly upwards; however, the general form of the ambivalent region has remained almost unchanged.

### **5.3 EFFECT OF HYDRATE FORMATION ON PHASE INVERSION IN HIGH WATER CUT SYSTEMS**

Gas hydrate formation is a significant problem in the oil and gas production industry. In high water cut systems when a part of the water phase converts into hydrate particles, the water-oil emulsion, which carries the hydrate particles, plays an important role in the transportability of the hydrate slurry. Hence, knowledge about the morphology of the emulsion during hydrate formation will lead to improved mitigations for hydrate related flow assurance problems.

Our previous study on the phase inversion of emulsions without hydrate (Section 5.2.2) has shown that W/O or O/W emulsions during the mixing process can be stable for oil dominating or water dominating systems, respectively. However, there is an unstable emulsion region where both types of emulsions can exist as long as stirring is maintained. It was mentioned that AA and salt in the aqueous phase affect the phase inversion point. A number of studies have investigated the phase inversion of emulsions during the initial stage of hydrate formation (Azarinezhad, 2010; Fotland and Askvik, 2008; Hoiland et al., 2005; Klomp, 2008). For example, Hoiland et al. (2005) have demonstrated that the inversion of emulsions can also be influenced by adding hydrate particles into the emulsion. They conducted simple tests to determine the wettability of hydrate particles formed in different crude oil emulsions. Hoiland and co-workers (2005) added Freon 11 into the oil phase at atmospheric pressure. Brine and additional water (to form the appropriate amount of Freon 11 hydrate) were then added to the oil phase. They claimed that depending on the oil composition, the phase inversion point differs in the presence of hydrate particles. They attributed this phenomenon to the wettability of hydrate particles. Hoiland and co-workers (2005) concluded that the point of phase inversion from W/O to O/W was reduced with water-wet hydrates, whereas it was increased with oil-wet hydrates.

The objective of this work is to investigate the effect of hydrate particles on phase inversion when the initial emulsion is O/W or W/O, in the presence of different AA concentrations for various oil compositions. This study differs in several key aspects from that of Hoiland et al. (2005). Firstly, natural gas, not Freon 11 was used as the hydrate former, which was used for achieving the desired pressure in the system containing emulsion (i.e., simulating real pipeline conditions).

Secondly, this work investigates how an existing emulsion with a high water fraction destabilizes and potentially inverts during hydrate formation when the water phase is

converted to hydrate, as opposed to the situation where water is added in the presence of hydrates to achieve phase inversion.

Since the focus of this study was on high water cut systems and O/W emulsions are more favourable in these systems, most of our experiments were conducted starting with an O/W emulsion, and for comparison purposes some tests were initiated with W/O emulsion. In high water cut systems, formation of hydrate particles may change the stability of the emulsion during hydrate formation, which can influence the rheology of the hydrate slurry.

### **5.3.1 Experimental Set-Up and Materials**

All the experiments were conducted in a high pressure autoclave cell. The experimental setup has been explained in detail in Chapter 4. Three different oils were used in this study as the liquid hydrocarbon phase; two crude oils (A) and (B) and one refined diesel oil, which is named as oil (C). Characteristics of oil (A) and oil (B) were described in Table 5.1. The asphaltene contents for crude oil (A) is more than 10 times higher than crude oil (B) and W/O emulsion stability measurements showed that oil (A) and oil (B) present tight and medium emulsion behaviours (Kokal, 2005), respectively (Figure 5.17). Oil (C) has a clear and bright appearance with a density of  $831 \text{ kg/m}^3$  (at  $15^\circ\text{C}$ ). Water-in-oil (C) emulsion exhibits loose emulsion behaviour that can be due to lack of natural surfactants (Figure 5.17). The composition of oil (C) has been shown in Table A.3. Experiments were conducted at various high water cuts, normally from 60 to 80 vol %. The aqueous phase consisted of deionised water with desired concentrations of water-soluble AA (AA1) and 5 wt. % NaCl ( $\geq 99\%$  anhydrous NaCl (Aldrich)). A standard natural gas supplied by Air Product was used as the hydrate-forming gas (composition given in Table A.4).

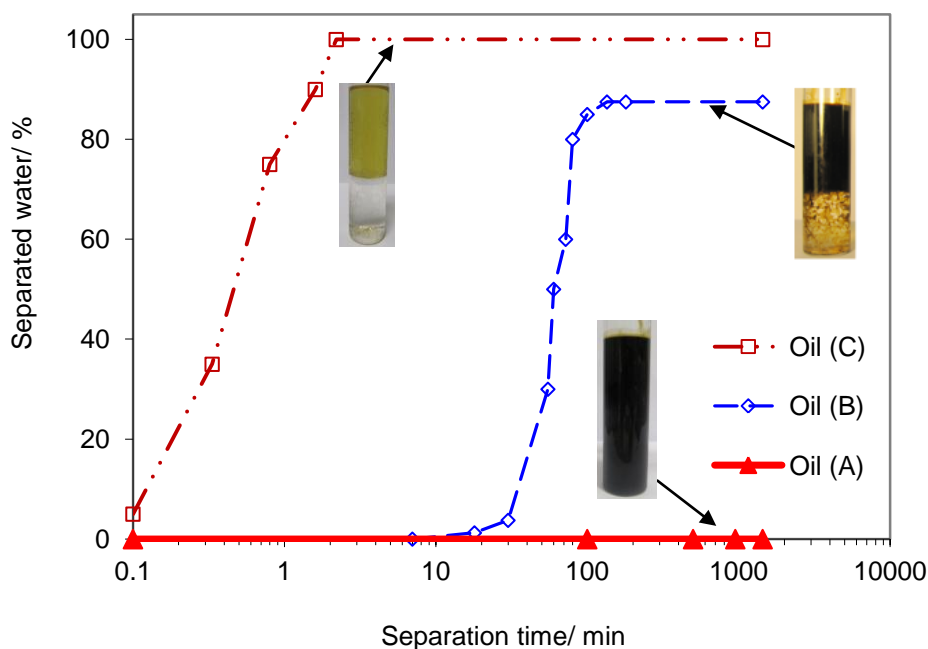


**Figure 5. 17 W/O emulsion stability characterised based on separated water as a function of time.**

### 5.3.2 Experimental Procedure

The experiments were carried out with the saturated oil-water emulsion. For each test, the cell was evacuated and then loaded with appropriate sample liquids (aqueous and hydrocarbon liquids) at atmospheric pressure and ambient temperature. Depending on the experimental conditions, AA concentrations with respect to the total mass of the aqueous phase were varied from 0.3 to 2.0 wt.% dissolved in the initial deionised water. The opposite side of the piston in the high pressure autoclave cell was pressurised with nitrogen, to the desired pressure, then the mixer speed was set at the required RPM. All tests were carried out at constant pressure and constant mixer speed. Natural gas was gradually charged into the cell to increase pressure up to operating pressure (about 68 bars) at 20 °C. To ensure the saturation of the liquid phases with the gas and to check for leaks, the system was allowed stabilizing for at least 3 hours. The cooling cycle was initiated by setting the cooling system temperature at 2 °C. The mixer speed was adjusted manually to keep a constant speed of 200 RPM during the experiments. Natural gas was also injected to ensure isobaric conditions during the cooling process and hydrate formation. Natural gas was injected at the test pressure to compensate the pressure reduction in the system due to consumption of dissolved gas by hydrates. Hydrate onset was indicated by; i) an increase in the temperature, because hydrate formation is an exothermic reaction, ii) a temporary reduction of the cell pressure (the

pressure drop was offset by injecting gas), iii) an increase in the rate of gas injection into the system. During the experiment the viscosity of the mixture was measured for different hydrate contents (volume fraction of hydrate based on the total volume) at constant RPM.

### 5.3.3 Results and Discussion

Experimentally, the phase inversion point during hydrate formation can be easily determined by an abrupt change in the apparent viscosity of the water/oil/hydrate mixture. The point of phase inversion,  $\phi_h^{inv}$ , is regarded as the volume fraction of hydrate at which W/O emulsion converts to O/W emulsion or vice versa.

Figures 5.18 and 5.19 indicate the rheological behaviour of emulsions for crude oils (A) and (B) during hydrate formation for 60% water cut. For each crude oil, the experiments were initiated with both W/O and O/W emulsions. From these figures, it is clear that, depending on the type of the initial emulsion, a phase inversion during the experiments might occur. In the case of W/O emulsions, the apparent viscosity increases very slowly with increasing hydrate volume fraction, until reaching the critical point (at which the apparent viscosity increases relatively faster as the hydrate volume fraction is increased). No abrupt change in the mixture viscosity has been observed during the hydrate formation before the critical point. However, in the case of O/W emulsions, at the beginning, the apparent viscosities were very low (since water is the continuous phase) but soon after the onset of hydrate formation, it rapidly increased up to the viscosity of the systems that their initial emulsions were W/O. This phenomenon was attributed to the phase inversion of initial emulsion that acts as carrier fluid to transport hydrate particles. After phase inversion the trend of apparent viscosity increments is very much similar to that presented for the experiments with the W/O emulsions. It can be concluded that for the systems used in this study the ratio of water to oil in the emulsion decreases during hydrate formation. These results suggest that when water phase converts to hydrate, it comes out of the water-oil emulsion and forms a separate solid phase in the system. Therefore when the initial emulsion is W/O, as the water phase is converted into the hydrate particles, the stability of the emulsion increases, due to reduction of water phase in the emulsion. In contrast, in the case of O/W emulsions, as the water phase is converted into the hydrate particles, the emulsion will be unstable, due to decrease of the continuous (aqueous) phase in the emulsion.



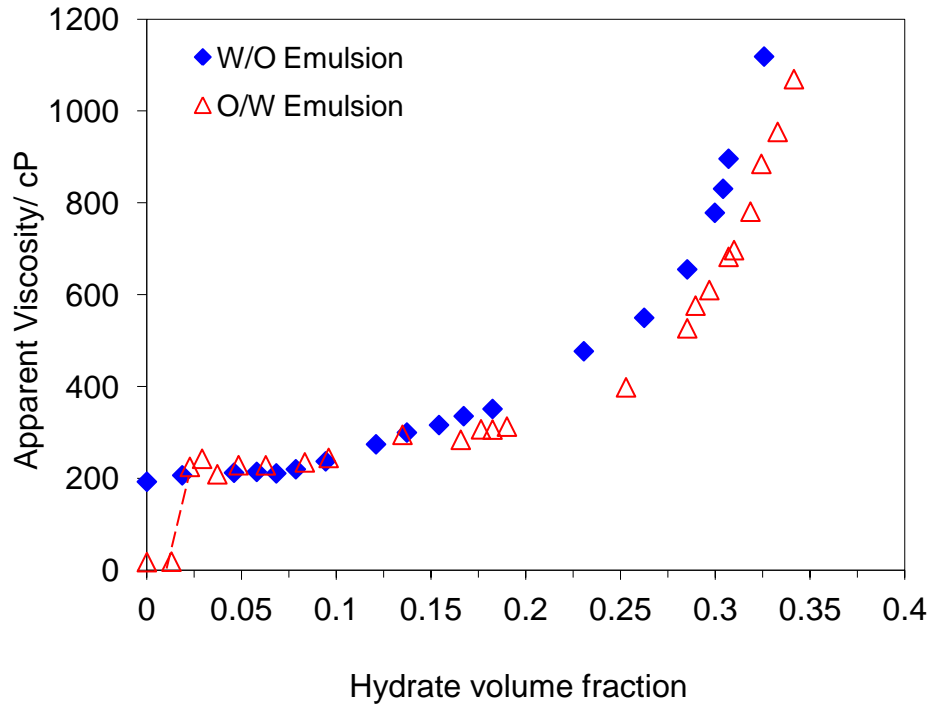


**Figure 5. 18** Effect of emulsion type on the mixture viscosity as a function of hydrate volume fraction (60% water cut, 5.0 wt% NaCl, 1.0 wt% AA), oil (A).

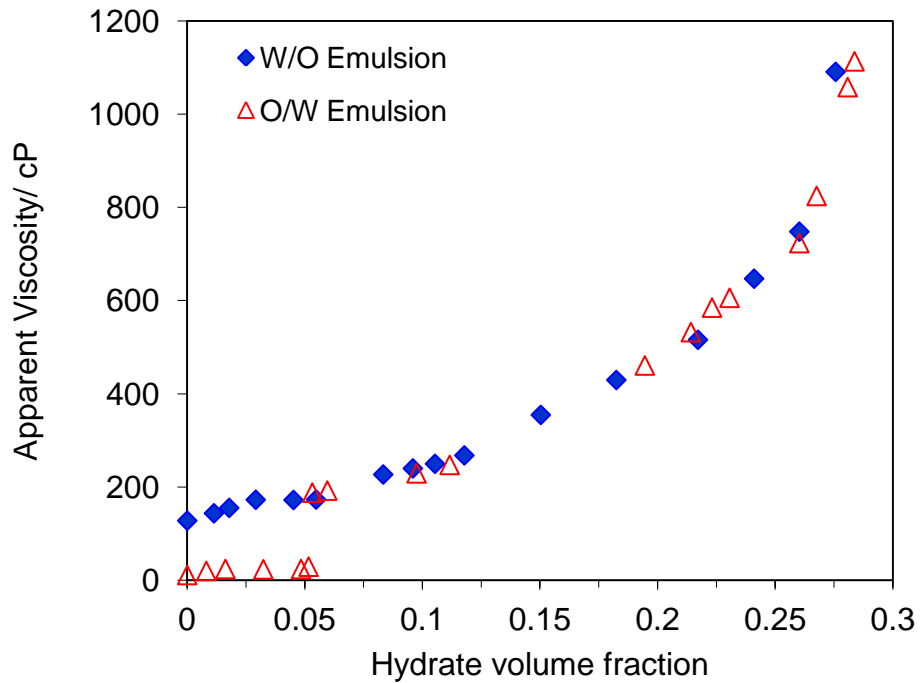


**Figure 5. 19** Effect of emulsion type on the mixture viscosity as a function of hydrate volume fraction (60% water cut, 5.0 wt% NaCl, 1.0 wt% AA), oil (B).

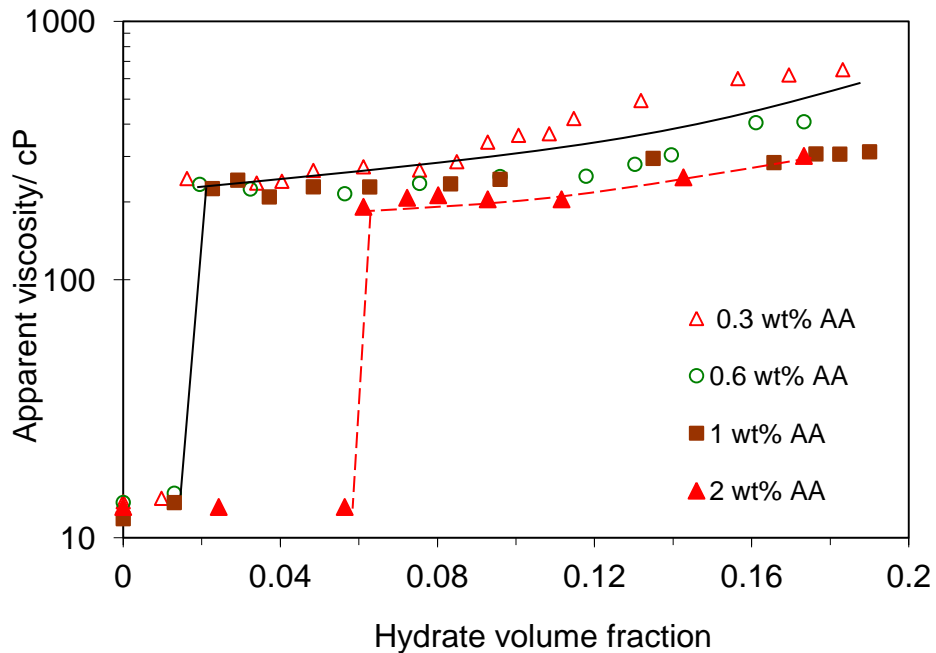
In order to determine the effect of AA concentration on the phase inversion point during hydrate formation, the AA concentration was varied from 0.3% to 2.0 wt. %. Figures 5.20 and 5.21 show that when the initial type of the emulsion is O/W, depending on AA concentration, phase inversion occurs at the initial stage of hydrate formation. It is apparent from the figures that for the tight crude oil (A) phase inversion points are almost identical for the tests with AA concentrations below 2.0 wt. % and it shifts to the higher hydrate volume fraction with increasing AA to 2.0 wt. %. For the tests with crude oil (B) a gradual increase is observed in hydrate volume fraction at inversion point,  $\varphi_h^{inv}$ , with increasing AA concentration.

Figure 5.22 shows the results of the experiments for three different oils as a function of AA concentrations at 60% water cut. This Figure indicates that for all experiments conducted at 60% water cut, water continuous emulsions changed to oil continuous emulsions during hydrate formation. It would be reasonable if we consider the water/oil/hydrate mixture as two separate systems: water-oil emulsion and solid hydrate particles. Therefore, during hydrate formation, water from the emulsion comes out from the emulsion to convert into the hydrate particles as a separated phase. The reduction of the water phase in the emulsions due to hydrate formation can also be the main cause of W/O emulsions remaining at the end of the experiments, for the cases that the initial emulsions are W/O before hydrate formation (Figures 5.18 and 5.19). A possible explanation for these trends is that for water continuous emulsions, the AA used in this study increases the electrical repulsive force between oil droplets, resulting delay in droplets coalescence.

From Figure 5.22, it can be seen that there is a significant difference between hydrate volume fractions at the inversion point,  $\varphi_h^{inv}$  for the three different oils at the same AA concentrations. For tight oil emulsion (oil (A)), the oil continuous emulsion breaks at lower  $\varphi_h^{inv}$  than the medium and loose oil emulsions (oil (B) and oil (C)). This means that formation of W/O emulsion during hydrate formation is more favoured in the systems which have higher W/O emulsion stability (i.e. higher natural surfactants). Moreover, it is observed that with increasing AA concentration, the value of  $\varphi_h^{inv}$  increases. This is consistent with our previous results in Section 5.2.2, in which the phase inversion from water continuous to oil continuous phases shifted to higher oil droplet holdups with increasing AA concentration.

To investigate the effect of water cut on the phase inversion point during hydrate formation, similar experiments were conducted for 70 and 80% water cuts with water-

oil (A) emulsion, in the presence of different AA concentrations from 0.3 to 2.0 wt. %. The results are shown in Table 5.4. Similarly to the 60% water cut experiments, for 70% water cut experiments, phase inversion occurred from O/W to W/O during hydrate formation below 2.0 wt. % AA.



**Figure 5. 20** Effect of emulsion type on the mixture viscosity as a function of hydrate volume fraction for oil (A) (60% water cut, 5.0 wt% NaCl, 0.3-2.0 wt% AA).

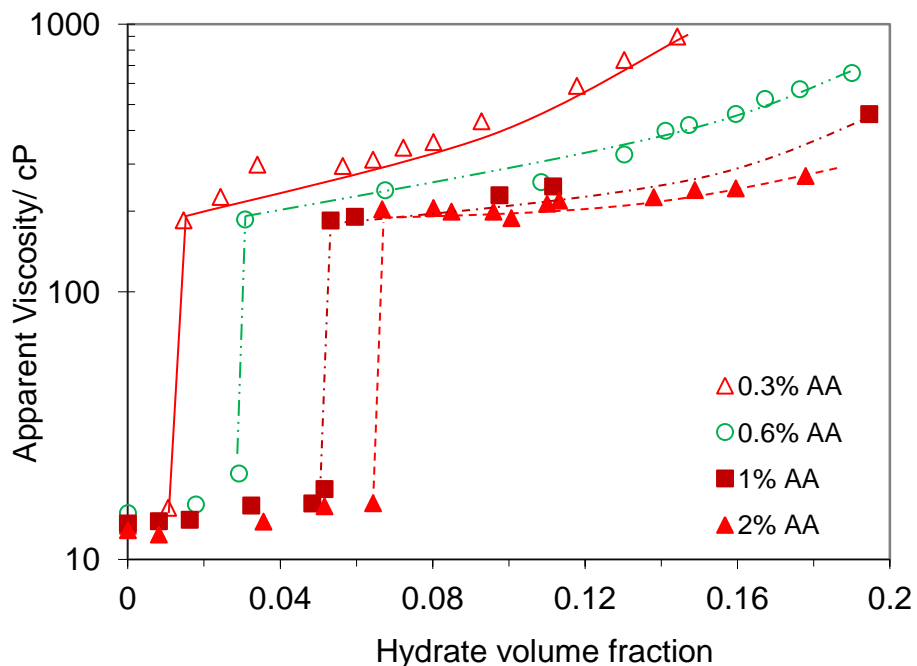


**Figure 5. 21** Effect of emulsion type on the mixture viscosity as a function of hydrate volume fraction for oil (B) (60% water cut, 5.0 wt% NaCl, 0.3-2.0 wt% AA).

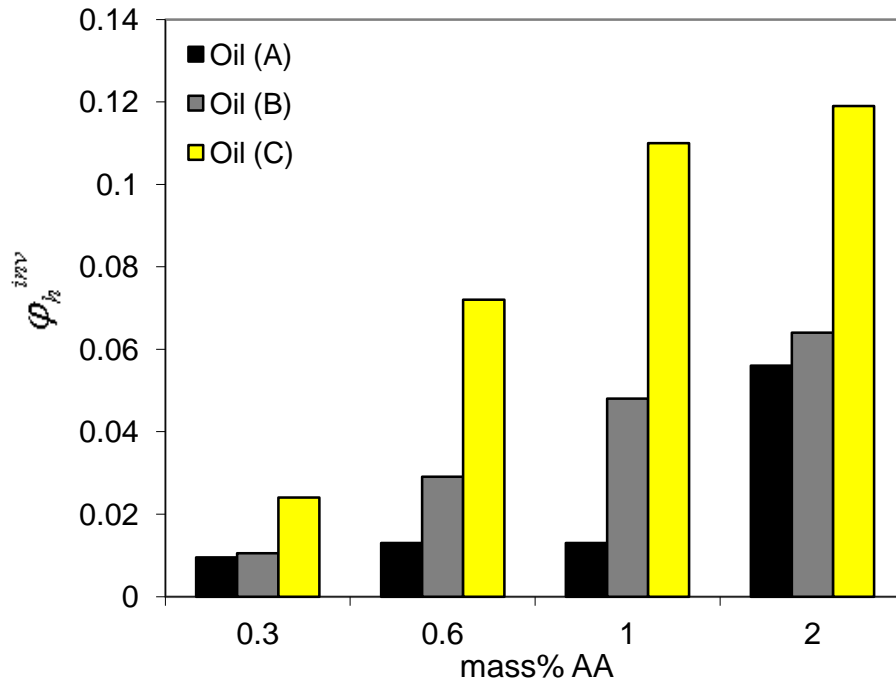


**Figure 5. 22 Hydrate volume fractions at phase inversion point  $\phi_h^{inv}$  from water continuous to oil continuous emulsions as a function of AA concentration, 60% water cut.**

However, phase inversion was not observed during the test for 70% water cut with 2.0 wt. % AA and also for all experiments with 80% water cut. For very high water cut systems, the presence of high volume fractions of free water in the system can be the main reason for the water phase persisting as a continuous phase by the end of experiments. The most striking results to emerge from the above study are that phase inversion during the hydrate formation process strongly depends on initial morphology of the emulsion, AA concentration, initial water cut and the nature of the liquid hydrocarbon phase.

**Table 5. 4 Determination of phase inversion point from water continuous to oil continuous emulsion as a function of vol. % of hydrate (total volume of the cell) for oil (A)**

AA (wt. %)	Water cut %		
	60	70	80
0.3	1.0	1.3	no inversion
0.6	1.3	8.0	no inversion
1	1.3	9.0	no inversion
2	6.0	no inversion	no inversion

## **5.4 CONCLUSIONS**

The objective of this chapter was to examine the effect of AA concentration and salt on the stability, and morphology of water-oil emulsions. The experiments were conducted under two different scenarios: atmospheric conditions (hydrate free) and during hydrate formation. Three different types of oils were used as the organic phase and deionised water as the aqueous phase. A commercial water soluble AA (which is believed to be frequently used to produce transportable hydrate slurry) was used as a surface active agent. Since saline water is naturally present in oil production pipelines, the effect of AA in saline water containing 5 wt. % NaCl was studied. The most important findings having emerged from this study are as follows:

1. Stability of crude oil emulsion strongly depends on the morphology of the emulsion, as W/O emulsions exhibit much higher stability compared to O/W emulsions
2. In the case of W/O emulsions, the presence of natural surfactants (asphaltenes and resins) in the liquid hydrocarbon phase plays an important role in the stability of the emulsions.
3. In case of W/O emulsions, adding AA in the aqueous phase did not influence the stability of the tight emulsion (oil (A)), however, it reduced the stability of the medium emulsion (oil (B))
4. Adding salt (NaCl) did not affect the stability of the tight emulsion (oil (A)), however, it reduced the stability of the medium emulsion (oil (B))
5. In the case of O/W emulsions, adding water soluble AA significantly improved the stability of the emulsions, for both medium and tight emulsions. It can be attributed to improvement in electrical repulsive forces between oil droplets.
6. Untreated W/O emulsions behaved as a thick paste at very high water cuts and no phase inversion was observed, as the extra water formed a separated phase. However, adding a small concentration of AA (0.15-0.3 wt. %) completely changed the emulsion behaviour and resulted in phase inversion.
7. Tight emulsions (oil (A)) were more favourable to forming W/O emulsions than medium emulsions (oil (B)). This can be attributed to the presence of natural surfactants (asphaltenes and resins) in oil (A) that formed a more rigid film around water droplets to prevent water coalescence.

8. Increasing AA concentration in the aqueous phase increased droplet hold-up (oil droplets) at the inversion point for O/W emulsions but decreased droplet hold-up (water droplets) for W/O emulsions.
9. The morphology of emulsions may change during the hydrate formation process, which strongly depends on the type of the initial emulsion, AA concentration, initial water cut and the nature of the liquid hydrocarbon phase.
10. The results suggest that when the water phase is converted into hydrate, it comes out from the water-oil emulsion and forms a separate solid phase in the system. Therefore, during hydrate formation, where a part of the water phase is converted into hydrate, the initial binary water-oil emulsion changes to a ternary water/oil/hydrate mixture
11. Crude oil (A) (a natural surfactant-rich crude oil) with O/W emulsion morphology converted to W/O emulsion at lower hydrate volume fractions than oil (C) (an oil poor in natural surfactants) during the hydrate formation process.

## 5.5 REFERENCES

- Allouche, J., Tyrode, E., Sadtler, V., Choplin, L. and Salager, J.L., 2004. Simultaneous conductivity and viscosity measurements as a technique to track emulsion inversion by the phase-inversion-temperature method. *Langmuir*, 20(6): 2134-2140.
- Anklam, M.R., York, J.D., Helmerich, L. and Firoozabadi, A., 2008. Effects of antiagglomerants on the interactions between hydrate particles. *Aiche Journal*, 54(2): 565-574.
- Azarinezhad, R., 2010. A chemical based wet cold flow approach for addressing hydrate flow assurance problems, PhD Thesis, Heriot-Watt University, Edinburgh
- Bancroft, W.D., 1913. *J. Phys. Chem*, 17: 501-19.
- Becher, P., 1988. *Encyclopedia of Emulsion Technology: Basic theory*, 3. CRC.
- Binks, B.P., 1993. Surfactant monolayers at oil-water interfaces. *Chemistry and Industry*(14): 537-41.
- Binks, B.P., Cho, W.-G., Fletcher, P.D.I. and Petsev, D.N., 2000. Stability of oil-in-water emulsions in a low interfacial tension system. *Langmuir*, 16: 1025-1034.
- Binks, B.P. and Lumsdon, S.O., 2000. Transitional phase inversion of solid-stabilized emulsions using particle mixtures. *Langmuir*, 16(8): 3748-3756.
- Boxall, J.A., Davies, S.R., Nicholas, J.W., Nicholas, J., Koh, C. Sloan, E. D., 2008. Hydrate Blockage Potential in an Oil-Dominated System studied using a Four Inch Flow Loop, 6th International Conference on Gas Hydrates, Vancouver, British Columbia, CANADA.
- Campanelli, J.R. and Cooper, D.G., 1998. Interfacial viscosity and the stability of emulsions. *The Canadian Journal of Chemical Engineering*, 67: 851-855.
- Ekott, E.J. and Akpabio, E.J., 2010. A review of water-in-crude oil emulsion stability, destabilization and interfacial rheology. *Journal of Engineering and Applied Sciences*, 5(6): 447-452
- Fotland, P. and Askvik, K., 2008. Some aspects of hydrate formation and wetting. *Journal of Colloid and Interface Science*, 321(1): 130-141.
- Frostman, L., 2000a. Anti-Agglomerant Hydrate Inhibitors for Prevention of Hydrate Plugs in Deepwater Systems, SPE 63122, Society of Petroleum Engineers, Houston, Texas.
- Frostman, L.M., 2000b. Anti-Agglomerant Hydrate Inhibitors for Prevention of Hydrate Plugs in Deepwater Systems. SPE 63122.
- Groeneweg, Agterof, W.G.M., Jaeger, P., Janssen, J.J.M., Wieringa, J.A., Klahn, J.K., 1998. On the mechanism of the inversion of emulsions. *Chemical Engineering Research & Design*, 76(A1): 55-63.

- Hemmingsen, P.V., Li, X., Peytavy, J.L. and Sjöblom, J., 2007. Hydrate plugging potential of original and modified crude oils. *Journal of dispersion science and technology*, 28(3): 371-382.
- Hoiland, S., Askvik, K.M., Fotland, P., Alagic, E., Barth, T., Fadnes, F., 2005. Wettability of freon hydrates in crude oil/brine emulsions. *Journal of Colloid and Interface Science*, 287(1): 217-225.
- Huo, Z., Freer E., Lamar M., Sannigrahi B., Knauss D. M., E. D. Sloan Jr., 2001. Hydrate plug prevention by anti-agglomeration. *Chemical Engineering Science*, 56: 4979–4991.
- Jahanzad, F., Crombie, G., Innes, R. and Sajjadi, S., 2009. Catastrophic phase inversion via formation of multiple emulsions: A prerequisite for formation of fine emulsions. *Chemical Engineering Research and Design*, 87(4): 492-498.
- Kelland, M.A., 2006. History of the development of low dosage hydrate inhibitors. *Energy & Fuels*, 20(3): 825-847.
- Kinugasa, T., Watanabe, K., Sonobe, T. and Takeuchi, H., 1998. Phase inversion of stirred liquid-liquid dispersions. *International Symposium on Liquid-Liquid Two Phase Flow and Transport Phenomena*, 575-582 pp.
- Klomp, U., 2008. The World of LDHI: From Conception to Development to Implementation, 6th International Conference on Gas Hydrates, Vancouver, British Columbia, CANADA.
- Kokal, S., 2005. Crude-oil emulsions: A state-of-the-art review. *Spe Production & Facilities*, 20(1): 5-13.
- Kokal, S., 2008. Crude oil emulsions: everything you wanted to know but were afraid to ask, SPE 120500-DL.
- Kokal, S.L., 2006. Crude Oil Emulsions. *Petroleum Engineering Handbook*, 1.
- Leporcher, E., Peytavy, J., Mollier, Y., Sjöblom, J. and Labes-Carrier, C., 1998. Multiphase transportation: hydrate plugging prevention through crude oil natural surfactants, SPE 49172, New Orleans, Louisiana.
- Lin, T.J., 1968. Effect of initial surfactant location on the viscosity of emulsions. *J. Soc. Cosmetic Chemists*, 19: 683–697.
- Moradi, M., Alvarado, V. and Huzurbazar, S., 2011. Effect of Salinity on Water-in-Crude Oil Emulsion: Evaluation through Drop-Size Distribution Proxy. *Energy & Fuels*, 25: 260–268.
- Norato, M.A., Tsouris, C. and Tavlarides, L.L., 1998. Phase inversion studies in liquid-liquid dispersions. *Canadian Journal of Chemical Engineering*, 76: 486-494.
- Reeve, R., Godfrey, J. and Bradford, S., 2002. Phase inversion during liquid-liquid mixing in continuous flow, pump-mix, agitated tanks. *Chemical Engineering Research and Design*, 80(8): 864-871.



Schramm, L.L., 1992. Petroleum Emulsions - Basic Principles. Advances in Chemistry Series(231): 1-49.

Sloan, E.D. and Koh, C.A. (Editors), 2008. Clathrate Hydrates of Natural Gases. CRC Press, New York.

Souvlis, E., Doulia, D. and Angeli, P., 1998. Power requirements and phase inversion during oil-water mixing. IChemE Research Event (Rugby, UK: Institution of Chemical Engineers): pp816–22.

Wasan, D., McNamara, J., Shah, S., Sampath, K. and Aderangi, N., 1979. The role of coalescence phenomena and interfacial rheological properties in enhanced oil recovery: an overview. Journal of Rheology, 23: 181.

Wasan, D. and Mohan, V., 1977. Interfacial rheological properties of fluid interfaces containing surfactants. Academic Press, New York.

York, D. and Firoozabadi, A., 2009. Effect of Brine on Hydrate Antiagglomeration. Energy & Fuels 23: 2937–2946.

Zaki, N.N., Ahmed, N.S. and Nassar, A.M., 2000. Sodium lignin sulfonate to stabilize heavy crude oil-in-water emulsions for pipeline transportation. Petroleum Science and Technology, 18(9-10): 1175-1193.

Zambrano, N. et al., 2003. Emulsion catastrophic inversion from abnormal to normal morphology. 1. Effect of the water-to-oil ratio rate of change on the dynamic inversion frontier. Industrial & engineering chemistry research, 42(1): 50-56.

Zanota, M.L., Dicharry, C. and Graciaa, A., 2005. Hydrate Plug Prevention by Quaternary Ammonium Salts. Energy & Fuels 19: 584-590.

## **CHAPTER 6    EXPERIMENTAL INVESTIGATION ON RHEOLOGICAL BEHAVIOUR OF HYDRATE SLURRIES IN HIGH WATER CUT SYSTEMS**

### **6.1 INTRODUCTION**

The move of the oil and gas industry into increasingly deeper and colder locations and/or production from mature reservoirs, in which water cuts can be relatively high, have made the industry to face a major challenge. The challenge is flow assurance and avoiding gas hydrate problems, as the traditional hydrate prevention methods are very expensive (i.e., high CAPEX and/or OPEX) and even, in some cases, unfeasible. Forming dispersed hydrate particles, using surface active additives, is currently an attractive option for overcoming hydrate blockage problems, especially for long tieback and high subcooling systems. Anti-agglomerants (AAs) have long been considered for improving transportability of hydrate slurry flow in pipelines in low and high water cut systems (Alapati et al., 2008; Gao, 2009). Although many pilot tests and a few field tests have been conducted, the economics of AA injection have rarely been favourable. From an economical point of view, it would be more profitable to decrease the AA concentration as much as possible, in particular in high water cut systems.

The presence of natural surfactants in some crude oils with low water cut has produced transportable hydrate slurry with low or no risk of plugging (Erstad, 2009; Fadnes, 1996; Leporcher et al., 1998; Palermo et al., 2004). Asphaltenes, resins and acidic fractions in the crude oils are the main components to which this phenomenon has been attributed (Dieker et al., 2009; Fadnes, 1996; Leporcher et al., 1998, Fotland et al. 2011). The effect of natural surfactants in the crude oils on hydrate transportability has been investigated by many researchers; however, to the best of our knowledge, there has been no experimental examination of the effect of natural surfactants on the performance of commercial AAs.

Gas hydrate formation is an interfacial phenomenon which occurs at the interface between water and liquid hydrocarbon phase saturated with gas. Hydrate shells cover the water droplets and form a diffusion barrier between hydrate forming components and the water trapped inside the hydrate particles. In this stage, the presence of free water in the system leads to capillary forces, formed by a liquid bridge, holding the particles together (Austvik et al., 2000). Flowing hydrate

particles may aggregate, leading to a further increase of the slurry viscosity. The formation of hydrate aggregates can trap a volume of the liquid phase (including oil and water) that presents an effective volume fraction higher than the real volume fraction of the particles (Colombel et al., 2009; Leba et al., 2010). The apparent viscosity significantly increases at a certain hydrate volume fraction, depending on the experimental conditions and agglomeration of hydrate particles. This fraction of hydrate is called the “*critical hydrate value fraction*” at which the mixture viscosity increases sharply.

In this chapter, the rheological behaviour of hydrate slurry during hydrate formation has been investigated in high water-cut systems (from 60 to 80%), as these are probably the most difficult conditions for managing flow assurance issues using conventional techniques. In this experimental work, gas is the limiting reactant and there is always excess water in the system. All experiments were conducted in a high pressure autoclave cell under isobaric conditions during the test periods. Specific objectives are:

- Evaluation of the performance of AAs using viscosity measurements as a function of hydrate volume fraction in high water cut systems
- Investigation of the effect of AA concentration and water cut on rheological behaviour of hydrate slurry in high water cut systems
- Studying the effect of natural surfactants on the performance of AAs in high water cut systems
- Studying the effect of mixer speed/shear rate on rheological behaviour of hydrate slurry in the presence of various AA concentrations
- Investigating the effect of oil blending on rheological behaviour of hydrate slurry in high water cut systems
- Studying the effect of hydrate formation and dissociation on water-in-oil (W/O) emulsion stability in high water cut systems
- Examination of the effect of salt (NaCl) concentration on the performance of AAs in high water cut systems
- Investigation of shut-in conditions for two different scenarios
  - With no hydrate before shut in
  - With different amounts of hydrate formed before shut-in

## **6.2 EXPERIMENTAL EQUIPMENT**

All the experiments in this study were conducted in a high pressure autoclave cell to facilitate experiments at constant pressure conditions. The experimental setup has been explained in detail in Chapter 4.

## **6.3 MATERIALS**

Three different oils are used in this study as liquid hydrocarbon phase: two crude oils and one refined diesel oil, which are named as oil (A), oil (B) and oil (C), respectively. The main physico-chemical properties of the crude oils are presented in Table 5.1 and the oil compositions are given in Tables A.1, A.2 and A.3. Figure 5.17 showed the results of untreated W/O emulsion stability measurements for three oils A, B and C. The stability of emulsions was tested in the so-called “bottle tests”, explained in Chapter 5. Oil (A), oil (B) and oil (C) exhibited tight, medium and loose emulsion behaviours, respectively.

The aqueous phase consists of deionised water, a commercial water-soluble AA and salt ( $\geq 99\%$  anhydrous NaCl (Aldrich)). Three different AAs labelled as AA1, AA2 and AA3 are used. A typical natural gas is used in all experiments (composition given in Table A.4).

## **6.4 RHEOLOGICAL STUDY OF HYDRATE SLURRIES IN HIGH WATER CUT SYSTEMS**

The experiments were carried out at saturated liquid (aqueous and hydrocarbon phases) condition using high pressure autoclave cell as per following procedure::

- Evacuate the high pressure autoclave cell (0.05-0.1 bars)
- Load the required mass of the prepared water-oil emulsion into the cell at atmospheric pressure and room temperature
- Set Nitrogen pressure (the opposite side of the piston inside the cell, Figure 4.2) on the required operating pressure
- Mix the emulsion with magnetic stirrer and charge gradually the required amount of gas into the cell at ambient temperature and bring the system to operating pressure.
- Set the mixer speed on the required RPM

- Stabilize the system for at least three hours to verify saturation of liquid phase with gas and to check for leaks
- Start the experiment by setting the cooling system at 2 °C
- Charge gas to the cell to keep the pressure constant during cooling and hydrate formation processes
- Set mixer speed manually on the required RPM during the experiment
- Once hydrate starts to form, continue the gas injection until the desired hydrate volume fraction in the system or the equipment limit (i.e. when the mixer power is maximum and it cannot keep the mixer speed on the required RPM).

### **6.4.1 Results and Discussion**

As mentioned above, there is significant interest in using surface active additives to overcome hydrate blockage problem, especially for long tieback and high subcooling systems. The method has been proven to be quite successful for low water cut systems because of low viscosity of the resulting hydrate slurry (Frostman, 2000; Palermo and Maurel, 1999). In low water cut systems, however, hydrate volume fraction is limited to the amount of water present in the system, as there is normally excess gas. Therefore, a transportable hydrate slurry is achievable, in particular in the presence of a suitable AA. However, for high water cut systems, the limiting factor is the amount of gas, as there is normally enough water to convert the gas present into hydrates.

The following experimental results show the rheological behaviour of hydrate slurry for three different oils (A), (B) and (C). The apparent viscosity significantly increases at a certain hydrate volume fraction (critical hydrate value fraction), depending on the experimental conditions and agglomeration of hydrate particles.

#### **6.4.1.1 Evaluation of the performance of AAs in high water cut systems**

AAs provide an additional tool for controlling hydrates in oil and gas pipelines. Several commercial AAs are available in the market from various suppliers. Current AAs are limited to use in a 50 % water-cut system or less. Although a newly developed AA has been successfully applied for water cuts up to 80% (Alapati et al., 2008), this may be the only known exception. Moreover, the amount of hydrate and blockage prevention is not well-understood in such a high water cut system. Therefore, using AAs in the high water cut systems still require further

investigation. Several techniques are used to evaluate the performance of AAs. Hydrate visualisation and monitoring the current/torque applied on the mixer are the common methods used for AA evaluation (Arjmandi, 2007; Herri et al., 1999; Huo et al., 2001; Zanota et al., 2005). In addition, rocking cells with a rolling ball, with and without optical windows, are the most popular laboratory devices used for evaluating AA performance (Gao, 2009; Huo et al., 2001). However, none of these techniques can evaluate the effectiveness of AAs based on the rheological behaviour of hydrate slurry during hydrate formation. This means that it is not possible to understand how much hydrate has been formed in the system before plugging occurs. In this study hydrate are slowly formed in the system (as there is no free gas in the system, i.e., the system is kept at pressures above bubble point) and the viscosity of the water/oil/hydrate mixture is measured as a function of hydrate volume fraction (volume fraction of hydrate to total volume) in the system. Three different AAs (AA1, AA2, and AA3) have been tested and the results compared with the untreated system (without AA). All the experiments were conducted using Oil (A) with 60% water cut. The aqueous phase includes 5 wt% NaCl and all treated systems includes 1% AA as well. Figure 6.1 shows the results of the evaluation of the AAs performance.

Comparison of the apparent viscosity of W/O emulsions before hydrate onset indicates that adding AA significantly reduced the apparent viscosity of the W/O emulsion for all treated systems. The effect of reduction of apparent viscosity of emulsions with addition of surfactants has been also reported by many researchers (Azarinezhad, 2010; Pleguea T. H. , 1986; Pleguea T. H. , 1989; Zaki et al., 2000). It is believed that droplet deformation has an important effect on the viscosity of an emulsion, as the rigid particles show higher viscosity than deformable droplets at the same dispersed phase concentrations (Plegue et al., 1986; Plegue et al., 1989; Sinclair, 1970; Steinborn and Flock, 1983b; Zaki et al., 2000). It can therefore be assumed that adding AAs to the emulsions enhances the droplet deformability, due to its effect on the interfacial film around the water droplets. Two different reasons have been reported in the literature as to why droplet deformability reduces the emulsion viscosity. Firstly, the maximum packing fraction is higher for deformable droplets (Yana et al., 1991); thus, theoretically the apparent viscosity would be lower. Secondly, the surface deformation may lead to droplets sliding on each other, resulting in an emulsion less resistant to the applied shear, hence a reduced emulsion viscosity (Abivin P., 2009; Sinclair, 1970; Steinborn and Flock, 1983b).

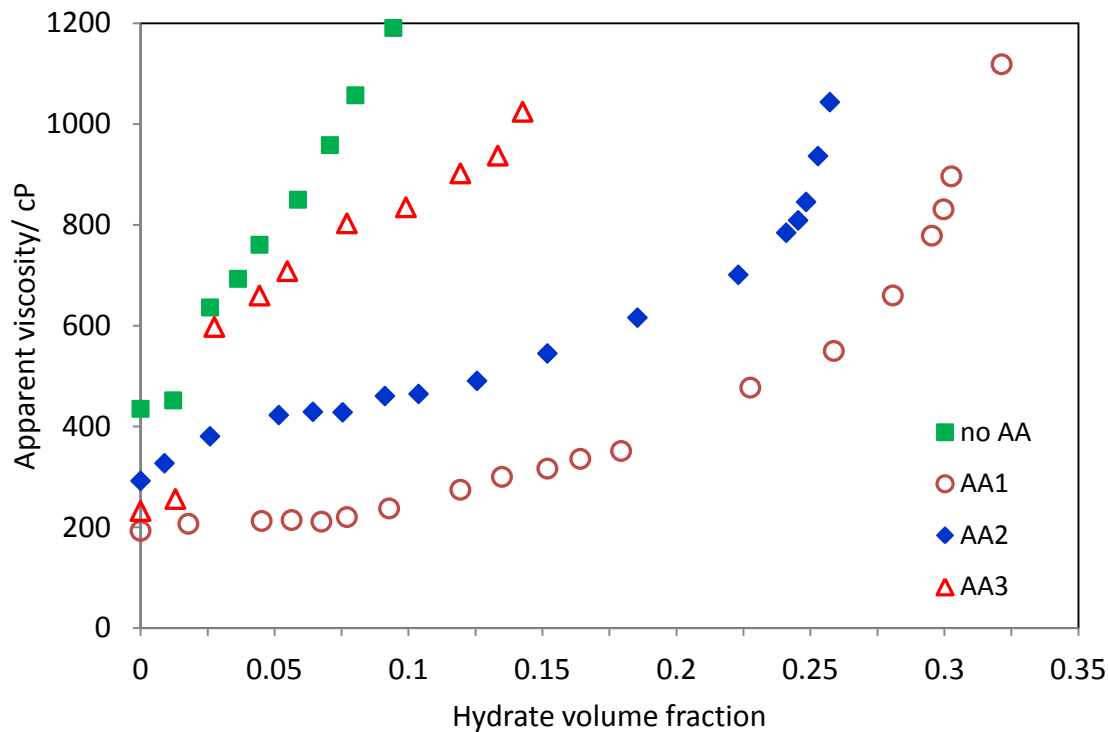


**Figure 6. 1 Apparent viscosity of water/oil/hydrate mixture as a function of hydrate volume fraction to evaluate performance of different AAs (1.0 wt% AA) in 60% water cut.**

From Figure 6.1, it is clear that different AAs present different rheological behaviour during hydrate formation. The apparent viscosity of the mixture suddenly increases at the onset of hydrate formation for the experiment with AA3. It shows that AA3 is not suitable for W/O emulsion in high water cut systems, as it could not prevent formation of large lumps of hydrate aggregates in the systems. However, AA1 prevented formation of large hydrate lumps and kept the apparent viscosity almost near to the pure emulsion viscosity (without hydrates) during hydrate formation, for a wide range of hydrate volume fractions. Although AA2 did prevent large apparent viscosity increases during the hydrate formation process, the rate of viscosity increase is significantly higher than in the experiment with AA1. The results suggest that it is possible to produce transportable hydrate slurry in high water cut systems within a certain range of hydrate volume fraction using a suitable and efficient AA.

#### 6.4.1.2 High water cut experiments with oil (A)

Restricting the use of AAs to low AA concentrations is expected to benefit not only the economic viability of the oil and gas production industry but also minimize the potential environmental impact of the AA itself.

Systematic experiments have been conducted to determine the effect of AA concentration on rheological behaviour of water/oil/hydrate mixtures for crude oil (A) at AA (AA1) concentrations ranging from 0.15% to 2.0 wt. % of aqueous phase. The water cut in the initial emulsion is varied from 60% to 80%. The experimental matrix is given in Table 6-1.

**Table 6. 1 Experimental matrix for Oil (A)**

Test #	AA (wt. %)	NaCl (wt. %)	Water cut (vol. %)	Mixer speed (RPM)	Pressure (bars)	Emulsion type <sup>a</sup>
1	0	5	60	200	68	W/O
2	0.15	5	60	200	68	W/O
3	0.3	5	60	200	68	O/W
4	0.6	5	60	200	68	O/W
5	1	5	60	200	68	O/W
6	2	5	60	200	68	O/W
7	0.3	5	70	200	68	O/W
8	0.6	5	70	200	68	O/W
9	1	5	70	200	68	O/W
10	2	5	70	200	68	O/W
11	0.3	5	80	200	68	O/W
12	0.6	5	80	200	68	O/W
13	1	5	80	200	68	O/W
14	2	5	80	200	68	O/W

a: Type of emulsion before hydrate onset

The effect of AA concentration and hydrate volume fraction on the apparent viscosity of water/oil/hydrate mixture for 60% water cut experiments is demonstrated in Figure 6.2. The hydrate values represented by arrows in the figures indicate the hydrate volume fractions at



which the apparent viscosity is about 600 cP. Tests conducted without AA or at very low AA concentration (0.15 wt. % AA) show that water/oil/hydrate mixture with viscosity values below 600 cP could only be prepared at hydrate volume fractions less than 0.026 and 0.061, respectively. Comparison of apparent viscosity of these two emulsions before hydrate onset indicates that the presence of 0.15 wt. % AA significantly reduced the apparent viscosity of the W/O emulsion. In this case it is also clear that 0.15 wt. % AA was not enough to produce transportable hydrate slurry. It means that this amount of AA cannot reduce the strength of capillary forces between hydrate particles, which leads to hydrate agglomeration. From Figure 6.2, it is obvious that for the untreated systems (without AA or very low AA concentration) with converting the water droplets into the hydrate particles the flow regime does not follow a regular pattern. This could be due to the agglomeration tendency of hydrate particles, resulting in forming big lumps in the bulk fluid. These hydrate lumps normally trap large amounts of liquid phase in their internal pores, among the hydrate particles. This leads to an increase in the effective hydrate volume fraction compared to the volume fraction of individual hydrate particles (Austvik et al., 2000; Fidel-Dufour et al., 2006; Leba et al., 2010). Large hydrate lumps might be broken randomly during hydrate formation/mixing and form aggregates of different shapes and sizes inside the cell. Therefore, the increasing rate of effective hydrate volume fraction may not be constant during hydrate formation, resulting in the irregular trend of the apparent viscosity.

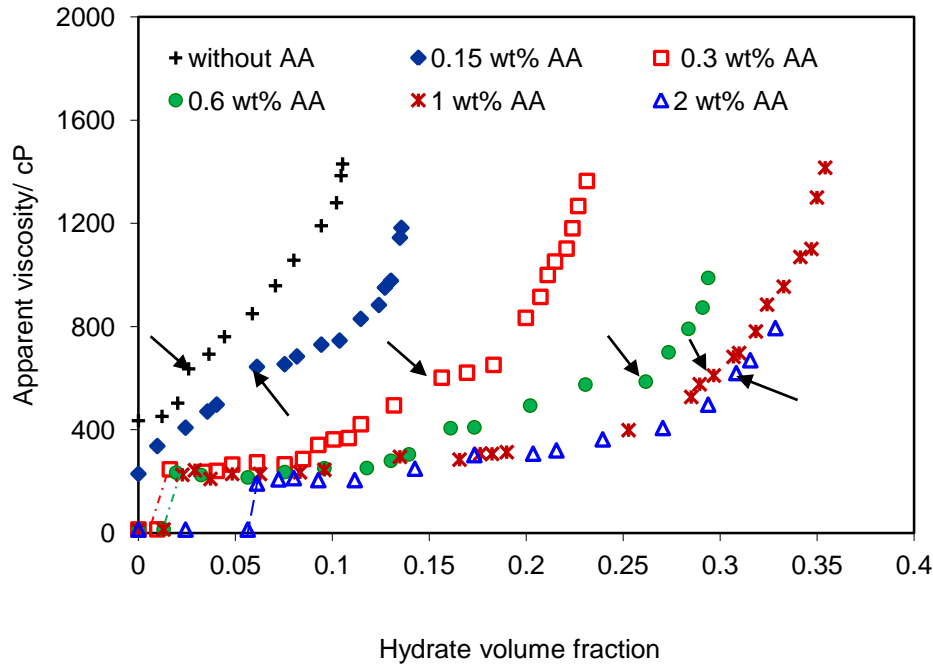


**Figure 6. 2 Hydrates in crude oil (A) with 60% water cut. The hydrate value represented by arrows in the figure indicates the hydrate volume fractions at which the apparent viscosity is about 600 cP. Experiments without AA and with 0.15 wt% AA initiated with W/O emulsions, while other experiments started with O/W emulsions.**

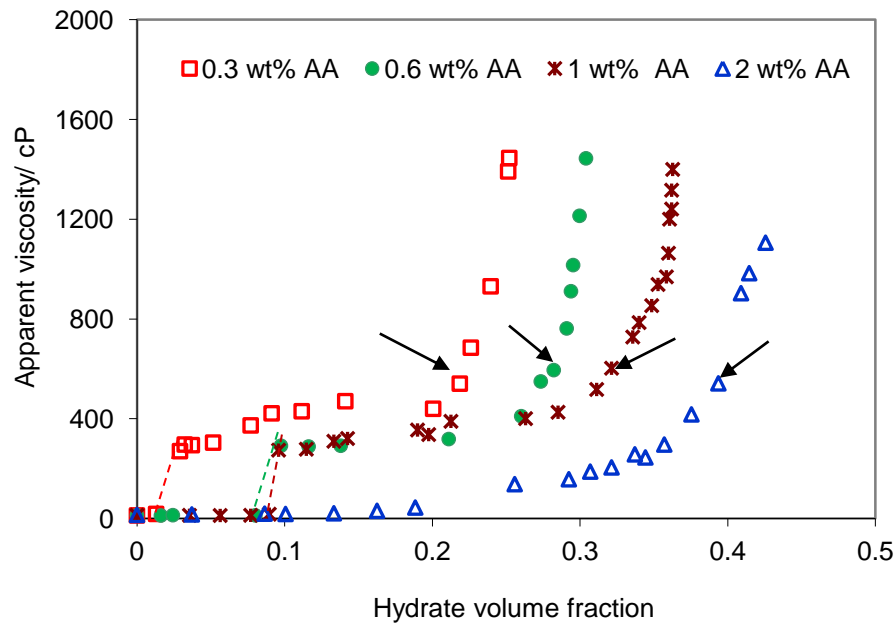


**Figure 6. 3 Hydrates in crude oil (A) with 70% water cut. The hydrate value represented by arrows in the figure indicates the hydrate volume fractions at which the apparent viscosity is about 600 cP. All experiments started with O/W emulsions.**

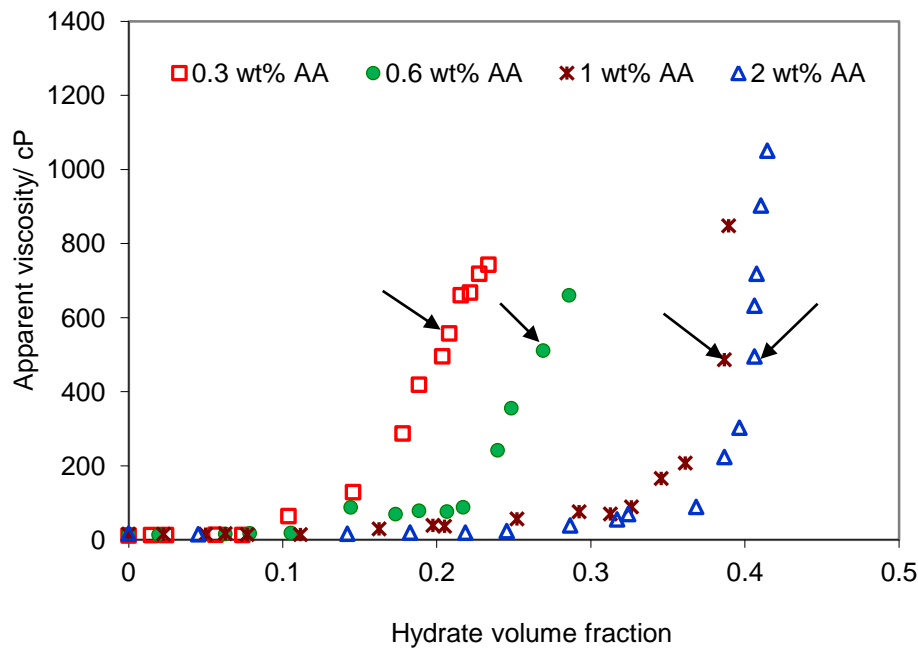


**Figure 6. 4 Hydrates in crude oil (A) with 80% water cut. The hydrate value represented by arrows in the figure indicates the hydrate volume fractions at which the apparent viscosity is about 600 cP. All experiments started with O/W emulsions.**

Figure 6.2 also shows the results of experiments with 0.3% to 2.0 wt. % AA in 60% water cut. Initially, the type of emulsion was oil-in-water (O/W). However, shortly after hydrate formation, the apparent viscosity suddenly jumped to a value around W/O emulsion due to phase inversion. The occurrence of a phase inversion step during hydrate formation process is consistent with the findings of other studies in high water cut systems (Klomp, 2008; Azarinezhad, 2010). From this figure, hydrate volume fractions for which the apparent viscosity of 600 cP is attained are seen for different AA concentrations. Although adding 0.3% and 0.6 wt. % AA improved hydrate transportability, an irregular trend on the apparent viscosity data is still observed.

For AA concentrations of 1.0% and 2.0 wt. %, the apparent viscosity is less sensitive to changes in the hydrate volume fractions, such that it remains almost constant during hydrate formation, up to critical hydrate volume fraction. It can be concluded that increasing AA concentration leads to a reduction of the immobilized liquid phase trapped in the internal porosity of aggregates and consequently reduces hydrate aggregate size. Therefore, the reduction of the apparent

viscosity with increasing AA concentration can be attributed to the considerable reduction of the effective hydrate volume fraction.

Although the occurrence of big hydrate aggregates can be the main reason of viscosity increases, these findings indicated that AA concentration is the predominant factor in the reduction of hydrate aggregate size. Figure 6.3 shows the relationship between mixture viscosity and hydrate volume fraction at 70% water cut for different AA concentrations, ranging from 0.3% to 2.0 wt. % of aqueous phase. Similar to the 60% water cut experiments, the apparent viscosity of the mixtures sharply increased due to the emulsion phase inversion from O/W to W/O for the experiments containing 0.3% to 1.0 wt. % AA. It is clear that, with increasing AA concentration, the inversion points have been shifted to higher hydrate volume fractions. However, for 2.0 wt. % AA concentration test, a sudden increase was not observed in the apparent viscosity during the hydrate formation process. It seems that the type of emulsion remained as O/W until the end of the experiment. This trend could be due to the presence of the high AA concentration and high initial water in the system. It is also clear that the hydrate volume fraction before the apparent viscosities reaches 600 cP significantly increased with the AA concentration and it is more pronounced for the test with 2.0 wt. % AA in which the continuous phase was the aqueous phase during the test.

In order to determine the effect of AA concentration on the rheological behaviour of O/W emulsions, systematic experiments were conducted at very higher water cut, i.e. 80% (Figure 6.4). The concentration of AA was varied from 0.3% to 2.0 wt. %. The arrows in Figure 6.4 indicate the hydrate volume fractions at which the apparent viscosity of the mixture is near 600 cp. It is clear that due to presence of a high volume fraction of water in the system, no phase inversion in the 80% water cut experiments was observed. As water was the continuous phase, the experiments resulted in a very low apparent viscosity. In O/W emulsions, similarly to W/O emulsions, hydrate transportability improved with increasing AA concentration.

For the tests with 60 and 70% water cut with AA concentration up to 1.0 wt. % , where the type of emulsions after phase inversion is W/O, the difference between hydrate volume fractions at apparent viscosities of about 600 cP are not considerable (Figure 6.5). However, in the case of 2.0 wt. % AA tests a significant difference is observed between 60% and 70% water cut experiments, which can be attributed to the effect of emulsion type on hydrate transportability. Similar differences are also observed between the 60% and 80% water cut tests with 1.0% and

2.0 % wt. % AA. One explanation for this trend is that for water continuous emulsions, a massive amount of aqueous phase exists in the system, in which hydrate particles can be well dispersed, resulting in a reduction of the inter-particle interaction between hydrate particles. Another explanation could be that the very low emulsion viscosity (water continuous phase) can also improve the case of hydrate transportation. In case of 60% and 80% water cut tests, it is clear that 1.0 wt. % AA can be an optimum effective dosage for the systems tested in this study, because the hydrate volume fraction rapidly increases between 0.3 and 1.0 wt. % AA and then levels off.

#### 6.4.1.3 High water cut experiments with oil (B) and oil (C)

For further investigation of the above results on the rheological properties of hydrate slurry and the effect of AA concentration on hydrate transportability in high water cut systems, a series of experiments were carried out with two other oils (B) and (C). These experiments also investigate the effect of oil composition on performance of AA and hydrate transportability in high water cut systems. Four experiments were carried out for each oil-water emulsion at water cut 60% with different AA (AA1) concentrations, ranging from 0.3% to 2.0 wt. %. The experimental matrix is given in Table 6-2.

**Table 6. 2 Experimental matrix for Oil (B) and Oil (C)**

Type of Oil	AA (wt %)	NaCl (wt %)	Water cut (vol. %)	Mixer speed (RPM)	Pressure (bars)	Emulsion <sup>a</sup> type
Oil (B)	0.3	5	60	200	68	O/W
Oil (B)	2	5	60	200	68	O/W
Oil (B)	0.3	5	60	200	68	O/W
Oil (B)	2	5	60	200	68	O/W
Oil (C)	0.3	5	60	200	68	O/W
Oil (C)	2	5	60	200	68	O/W
Oil (C)	0.3	5	60	200	68	O/W
Oil (C)	2	5	60	200	68	O/W

a: Type of emulsion before hydrate formation

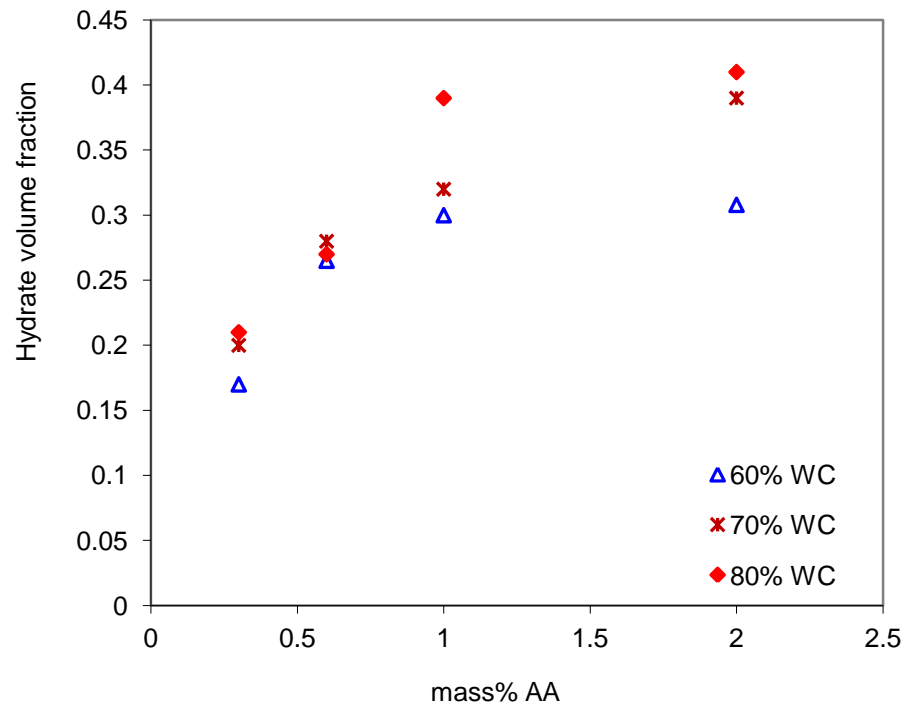


**Figure 6. 5 Hydrate volume fractions at about 600 cP as a function of AA concentration for different water cuts.**

The apparent viscosity of the water/oil/hydrate mixture during hydrate formation is shown in Figures 6.6 and 6.7 as a function of AA concentration. The type of emulsion for all experiments before the onset of hydrate formation was O/W and the emulsion inverted into W/O after hydrate formation, as is obvious from the sudden increase in the apparent viscosities. The point of phase inversion shifts to high hydrate volume fractions with increasing AA concentration. From the figures, it is also obvious that after the phase inversion of emulsion, the increase in apparent viscosity is small but it rapidly increases from a critical hydrate volume fraction as it can be assumed that water/oil/hydrate mixtures behave as highly viscous gels. Similarly to the experiments conducted with crude oil (A), transportability of water/oil/hydrate mixture improved with increasing AA concentration in the aqueous phase. A comparison of the data from the figures shows that the effect of AA concentration on hydrate slurry transportability considerably depends on the nature of liquid hydrocarbon phase.

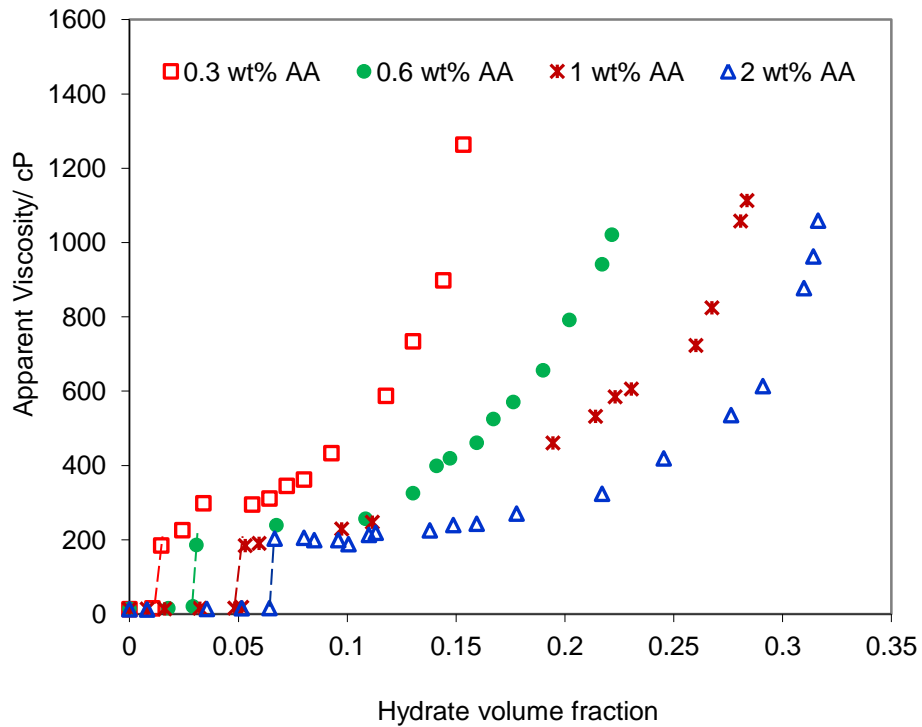


**Figure 6.6 Hydrates in crude oil (B) with 60% water cut at different AA concentrations. All experiments started with O/W emulsions.**

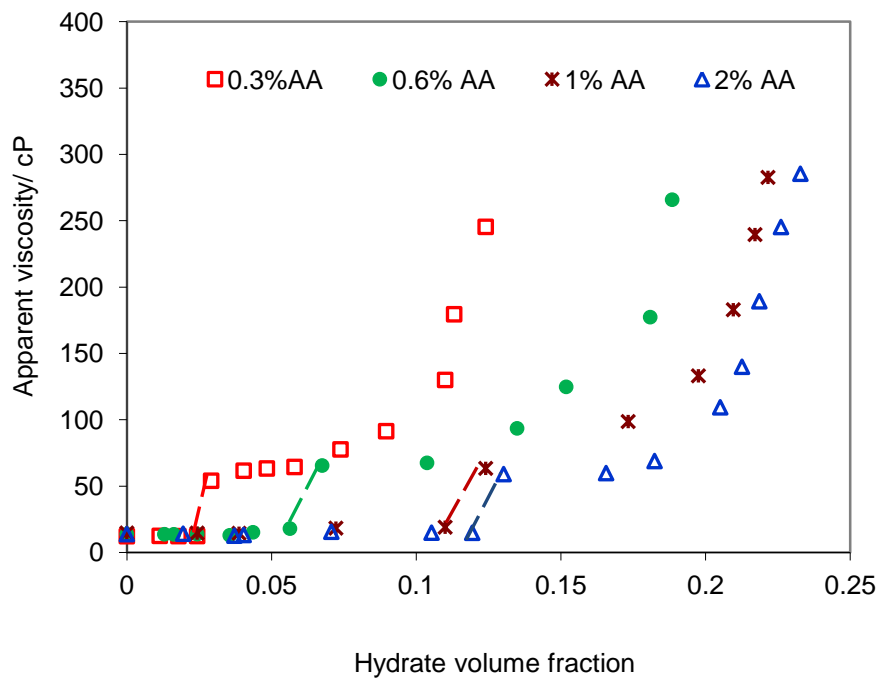


**Figure 6.7 Hydrates in crude oil (C) with 60% water cut at different AA concentrations. All experiments started with O/W emulsions.**

#### **6.4.1.4 Comparison of hydrate transportability of high water cut systems with different oil compositions**

It is well documented that the presence of asphaltenes and resins, called natural surfactants, in some crudes is responsible for stability of W/O emulsions (Leporcher et al., 1998; Siquin et al., 2004). Comparison of the rheological behaviour of different water-oil emulsion systems shows the benefit of the presence of natural surfactants on transportability of hydrate slurry in high water cut systems for different AA concentrations. As mentioned earlier, in the high water cut systems tested in this study, the presence of natural surfactants alone could not prevent the viscosity rise at low hydrate volume fractions, as the system was plugged immediately after the onset of hydrate formation (Figure 6.3). However, adding 0.3 wt. % AA could slow down the viscosity increase of the mixtures for a certain range of hydrate volume fraction. The rheological behaviour of water/oil/hydrate mixture for the oils in high water cut of 60% in the presence of different concentration of AA is shown in Figures 6.8- 6.11.

In the case of mixture transportability at low AA concentrations, significant gap is observed between low emulsion stable oils (B) and (C) and high emulsion stable oil (A) (Figures 6.8 and 6.9). With increasing AA concentration, the difference between crude oils (A) and (B) significantly decreases, but there is still a large difference between crude oils (A) and (B) with loose emulsion oil (C) (Figure 6.11 ). It can be concluded that when the concentration of AA is insufficient, the systems containing higher amounts of natural surfactants have higher potential for transporting hydrate particles than systems with lower natural surfactant concentration.

In order to further elucidate the effect of AA concentration on hydrate transportability, final water conversion into hydrates before hydrate blockage, as a function of AA concentration is shown in Figure 6.12 for each system. It is obvious that the final water conversion increases with AA concentration.

It is clear that with increasing AA concentration, even up to 2.0 wt. %; oil (C) was not able to convert more than around 33% of the water phase before hydrate blockage, while oil (A) was able to convert almost 47% water with 1.0 wt. % AA.

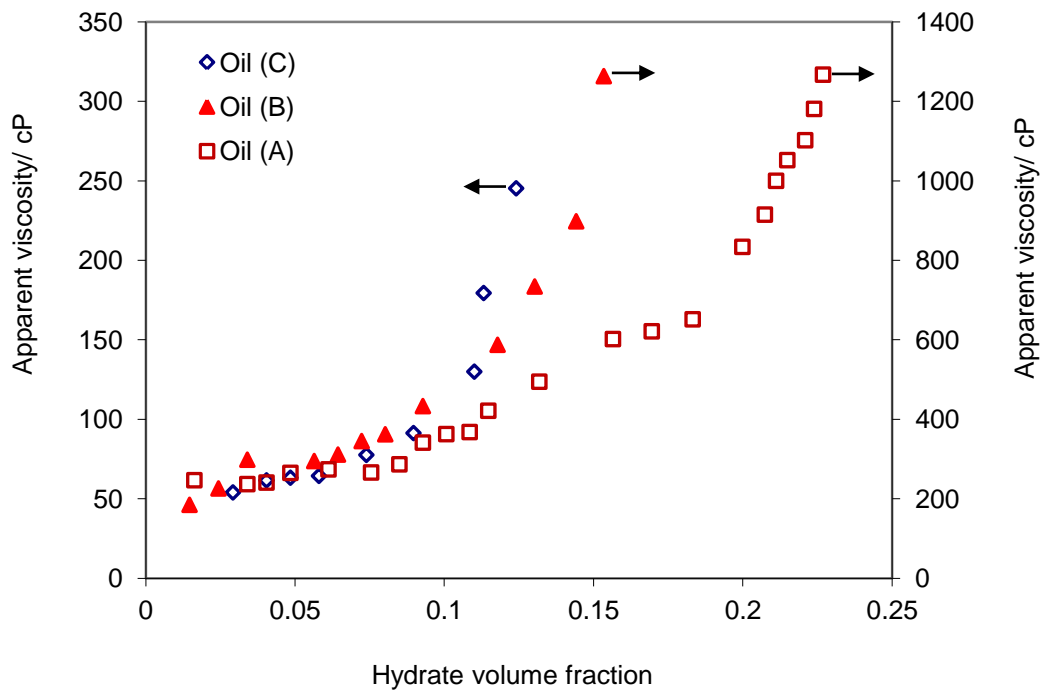
The reason for this trend can be related to the size of hydrate aggregates. For oils that produce a stable W/O emulsion, the capillary force between hydrate particles, which is responsible for agglomeration of hydrate particles, significantly decreases with addition of AA, resulting in a decrease in the size of hydrate aggregates. However, in loose emulsion systems (oil (C)), due to



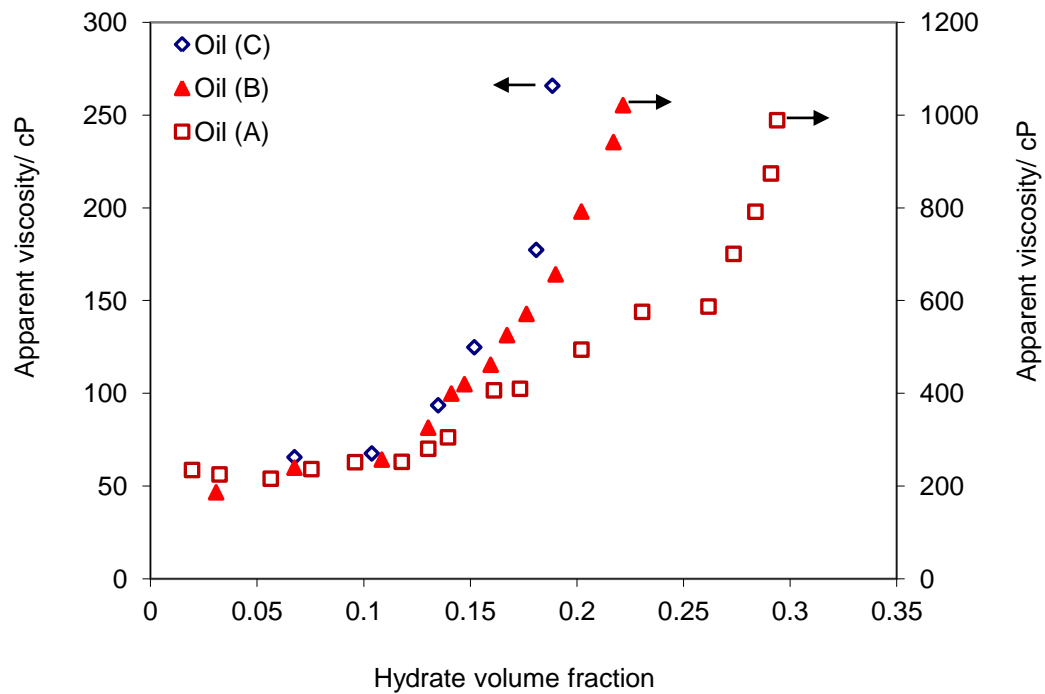
lack of natural surfactants, adding AA alone is not enough to reduce capillary forces properly, resulting in formation of large hydrate aggregates, trapping a large amount of unconverted water inside the hydrate aggregates.

Figure 6.12 also reveals that a large amount of free water always exist in the high water cut systems. These findings provide a new understanding of the rheological behaviour of hydrate slurry in high water cut systems. It is concluded that during hydrate formation, with conversion of a part of the water phase into hydrate aggregates, the initial binary water-oil emulsion alters to a ternary water/oil/hydrate mixture. The most striking result which emerges from the above data is that the required concentration of AA to manage hydrate transportability is strongly dependent on the nature of the liquid hydrocarbon phase (i.e. the presence of natural surfactants). To illustrate this fact, Figure 6.13 shows the apparent viscosity of the mixture as a function of hydrate volume fraction for different oils. It can be seen from the figure that loose emulsion (oil (C)) needs 1.0 wt. % AA to transport around 0.22 of hydrate volume fraction, while for the medium (oil (B)) and tight (oil (A)) emulsions, only 0.6% and 0.3 wt. % AA are required to transport the same hydrate volume fraction.

From these results, it can be suggested that the presence of natural surfactants (asphaltenes and resins) in the crude oil significantly reduce adhesive force between hydrate particles and supports the application of AAs to reduce the hydrate aggregate sizes. It means that the natural surfactants act as co-surfactants to improve the effectiveness of commercial AAs.



**Figure 6. 8 Apparent viscosity of water/oil/hydrate mixture as a function of hydrate volume fraction for 60% water cut and 0.3 wt. % AA.**



**Figure 6. 9 Apparent viscosity of water/oil/hydrate mixture as a function of hydrate volume fraction for 60% water cut and 0.6 wt. % AA.**

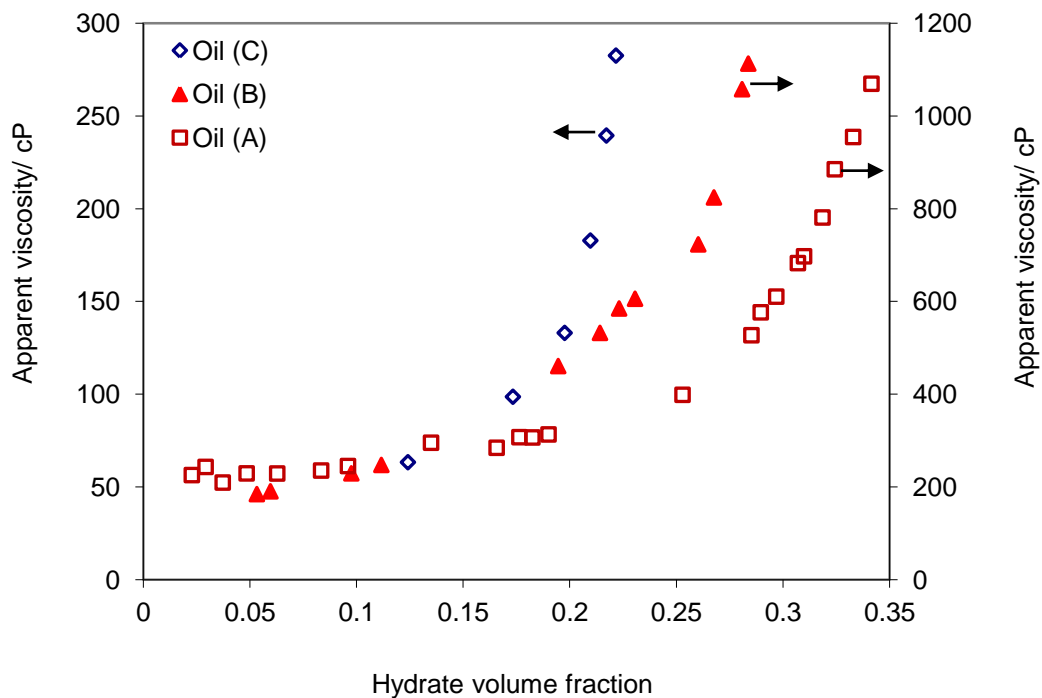


**Figure 6. 10 Apparent viscosity of water/oil/hydrate mixture as a function of hydrate volume fraction for 60% water cut and 1.0 wt. % AA.**

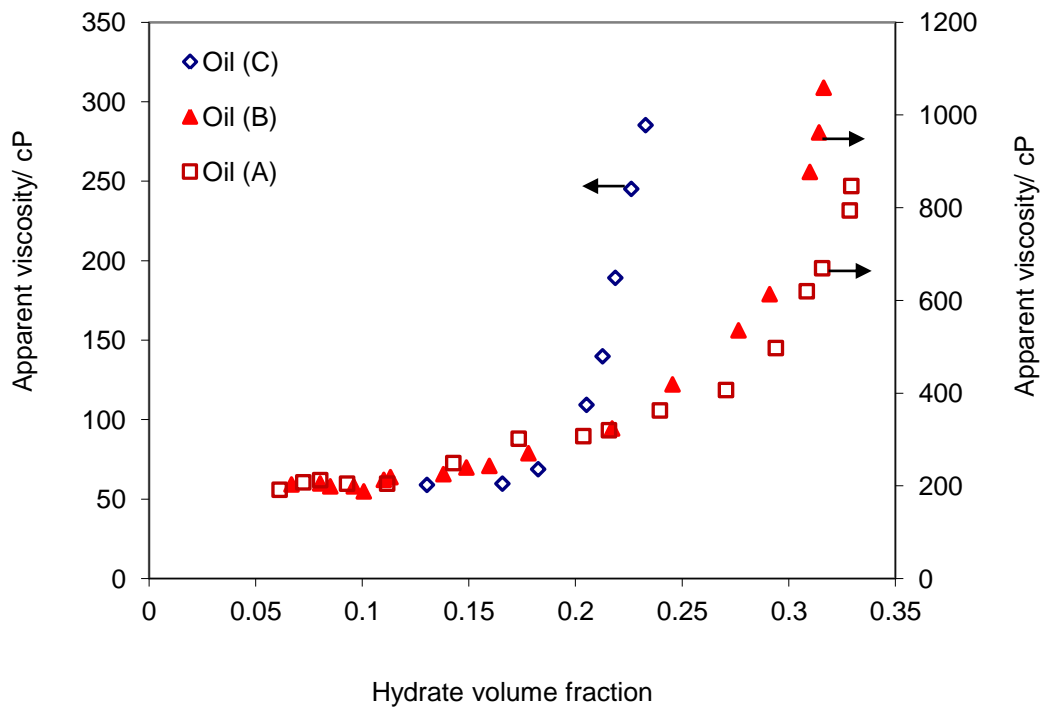


**Figure 6. 11 Apparent viscosity of water/oil/hydrate mixture as a function of hydrate volume fraction for 60% water cut and 2.0 wt. % AA.**

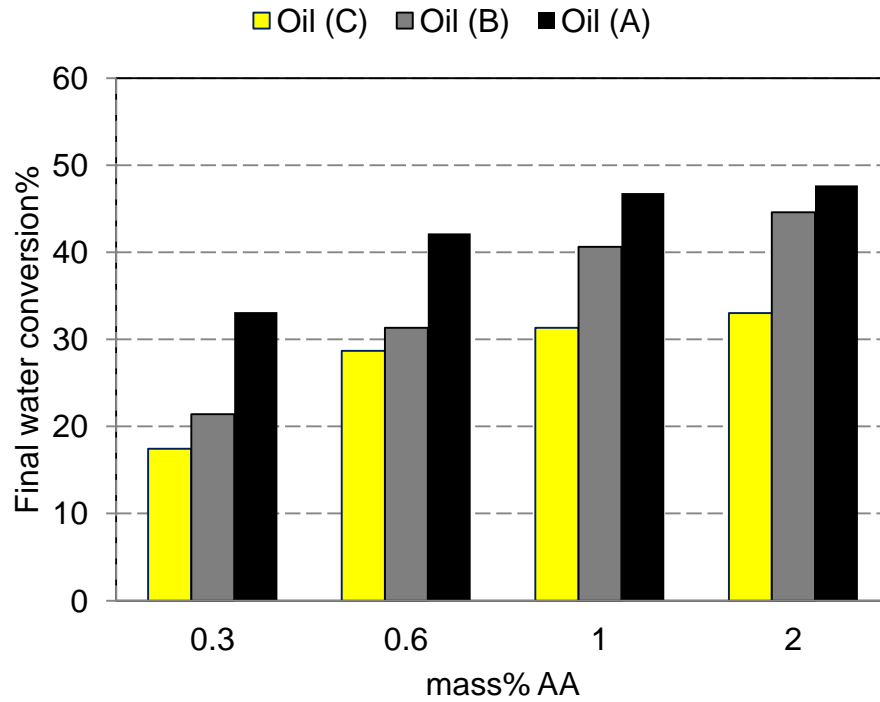


Figure 6. 12 Final water conversions versus AA concentration for different water-oil emulsions with 60% WC.

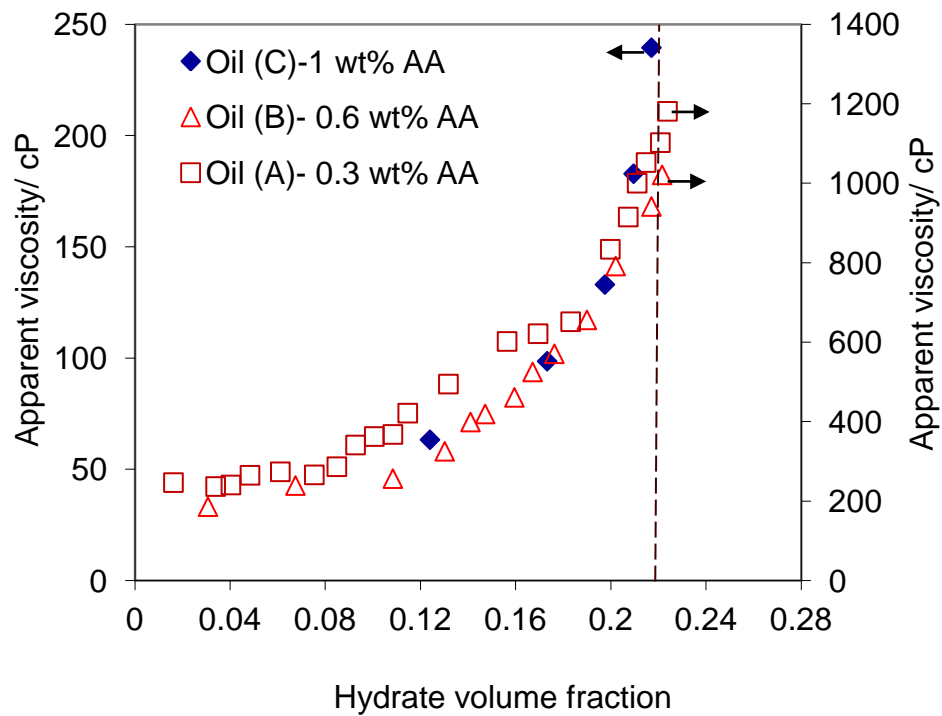


Figure 6. 13 Comparison of required AA concentration to transport a certain hydrate volume fraction for different oil-water emulsion systems, 60% water cut.

#### **6.4.1.5 Effect of mixer speed/shear rate on rheological behaviour of water/oil/hydrate mixtures in high water cut systems**

One of the main factors that may affect transportability of hydrate slurries are shear rate to which the slurry will be subjected. It has been reported that for some low water cut systems suitable shear can enable plug-free operation in the hydrate region (Sjöblom et al., 2010). In this study the effect of mixer speed/shear rate is examined on the hydrate slurry transportability for different AA concentrations in high water cut systems.

Four experiments were carried out at 200 and 400 RPM, for two different AA concentrations with oil (C) (Table 6.3).

Figures 6.14 and 6.15 show the apparent viscosity of the mixture for the tests with 0.3% and 2.0 wt. % AA as a function of hydrate volume fraction. From the figures, it can be seen that, after phase inversion, the apparent viscosity increase is significant for lower mixing speed cases and it is more pronounced for the tests with low AA concentrations (Tests 1 and 3). It can be also observed that apparent viscosities at the same hydrate volume fraction are lower for the tests with higher mixing speed and this is more pronounced at low AA concentrations. This trend can be attributed to the effect of shear rate on the W/O emulsion viscosity: the higher the shear rate (mixing speed), the lower the emulsion viscosity in high water cuts (Steinborn and Flock, 1983a). The water conversion rates for the tests with higher mixing speed were significantly higher, as shown in Figures 6.16 and 6.17. One explanation for this trend is that for higher mixing speeds, there is more agitation between the phases, which facilitates gas diffusion into the oil and water phases to form hydrate particles. Another explanation is that higher mixing can also result in smaller water droplets in W/O emulsions; thus, the surface area for hydrate formation is increased as the gas consumption increases compared with that at low mixing speed. From the figures, it is clear that higher water conversion is achieved for the higher mixing speed experiments.

**Table 6. 3 Experimental matrix for studying the effect of mixer speed, oil (C).**

Test #	AA (wt %)	NaCl (wt %)	Water cut (vol. %)	Mixer speed (RPM)	Pressure (bars)	Emulsion <sup>a</sup> type
1	0.3	5	60	200	68	O/W
2	2	5	60	200	68	O/W
3	0.3	5	60	400	68	O/W
4	2	5	60	400	68	O/W

a: Type of emulsion before hydrate formation

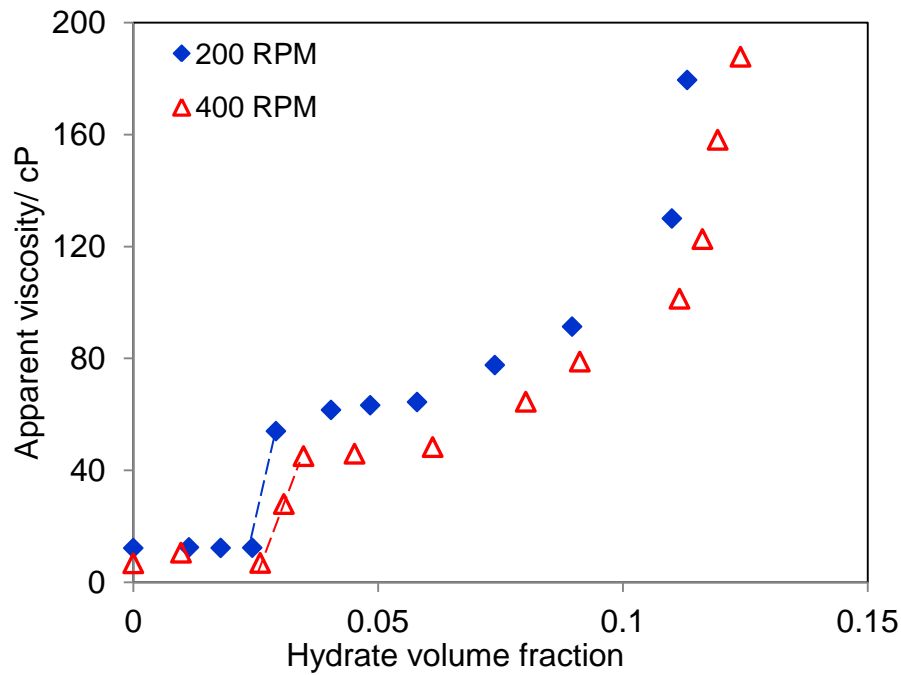


**Figure 6. 14 Apparent viscosity of water/oil/hydrate mixture as a function of hydrate volume fraction for two different mixer speeds of 200 and 400 RPM. Water cut is 60% with 0.3 wt. % AA. Experiments started with O/W emulsions.**

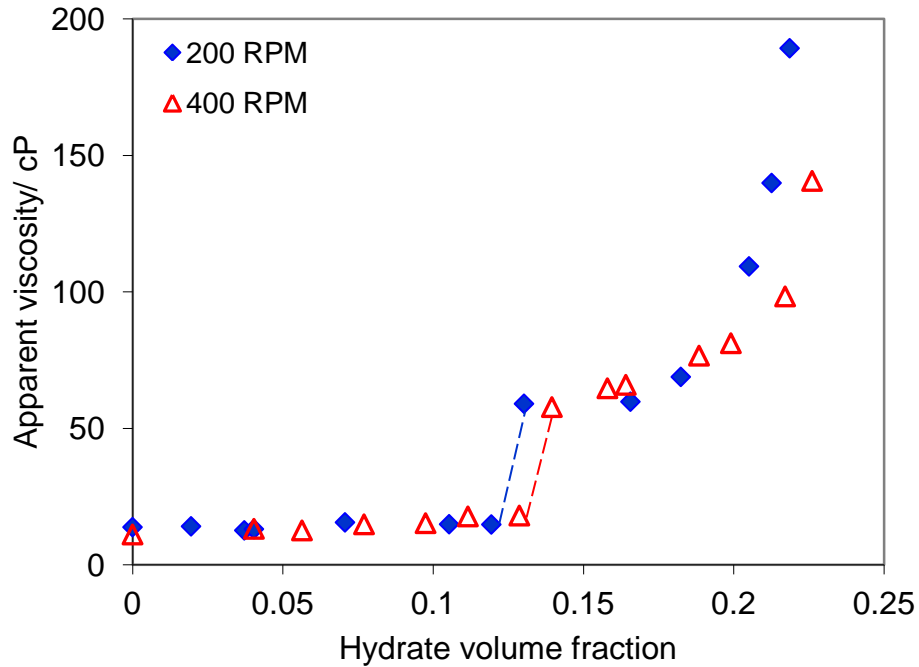


**Figure 6. 15 Apparent viscosity of water/oil/hydrate mixture as a function of hydrate volume fraction for two different mixer speeds of 200 and 400 RPM. Water cut is 60% with 2.0 wt. % AA. Experiments started with O/W emulsions**

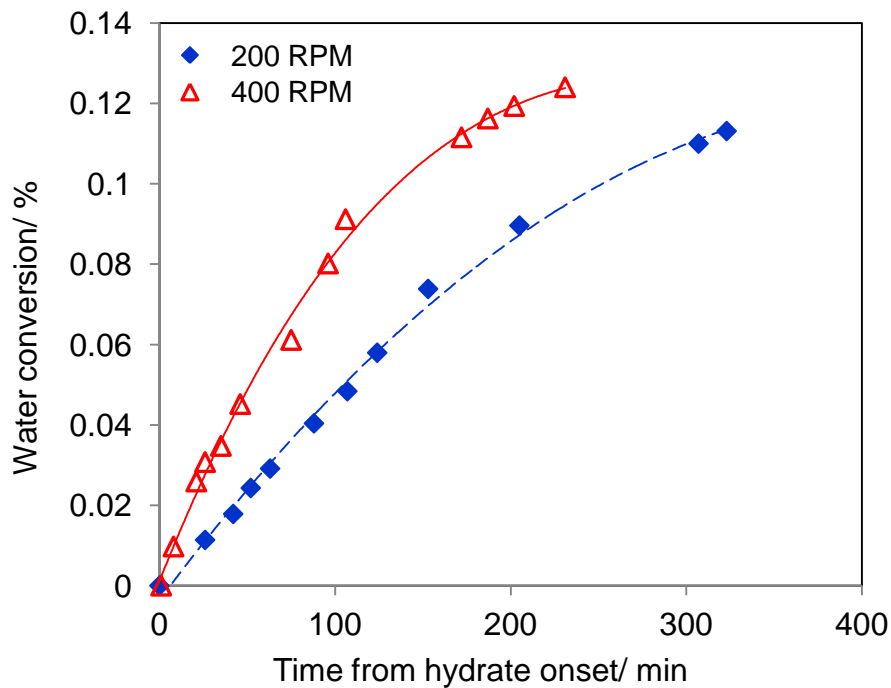


**Figure 6. 16 Water conversion rates for tests with 60% water cut and 0.3 wt. % AA at different mixer speeds.**

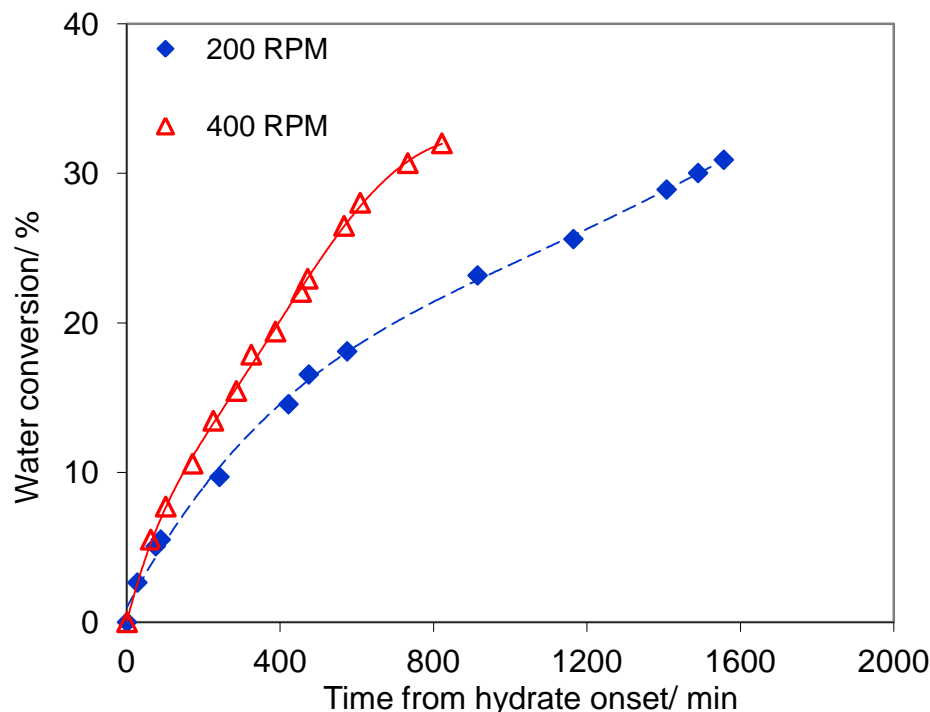


**Figure 6.17** Water conversion rates for tests with 60% water cut and 2.0 wt. % AA at different mixer speeds.

### 6.5 EFFECT OF OIL BLENDING ON RHEOLOGICAL BEHAVIOUR OF HYDRATE SLURRIES

In oil and gas systems using subsea tieback technology, which have a tendency to form hydrate plugs, the conventional thermodynamic hydrate inhibition approaches (e.g., methanol, glycols) are being superseded by more cost-effective emerging technologies such as Hydraflow technology (Haghighi et al., 2007). In these technologies, which may use a loop pipeline concept, gas hydrate is encouraged to form in the pipeline as a transportable hydrate slurry flow (using AAs if necessary) and collected from different wells towards onshore facilities. In field applications, the oils produced from various wells have different compositions and thus blending these oils in the loop not only influences the composition but also the natural surfactant content of the downstream fluid in the loop pipeline. Natural surfactants have different compositions and properties from one crude oil to another (Leporcher et al., 1998). In order to investigate the effect of blending different oils on hydrate transportability and the economics of AAs, two tests were conducted at different AA concentrations by blending crude oil (A) (a natural surfactant-rich crude oil) and diesel oil (C) (an oil poor in natural surfactants) with volume ratios of 20/80. All



the experiments were carried out in the high pressure autoclave cell following the procedure explained previously (Section 6.4). The experimental matrix is given in Table 6.4.

**Table 6. 4 Experimental matrix for blended oils.**

Test #	Oil (C) vol. %	Oil (A) vol. %	AA (wt. %)	NaCl (wt. %)	Water cut (vol. %)	Mixer speed (RPM)
1	80	20	0.6	5	60	200
2	80	20	2	5	60	200

Figures 6.18 and 6.19 compare the results obtained from viscosity measurements during hydrate formation for water-oil emulsions with pure oil (C) and with blends of oil (A) and oil (C) for different AA concentrations. From the figures, it can be seen that adding 20% crude oil (A) to diesel oil (C) has significantly improved the hydrate transportability in the system. It is clear that mixing 20 vol.% of crude oil (A) leads to an increase in natural surfactants (asphaltenes and resins) in the oil (C) thereby improving its hydrate transportability properties. These findings enhance our understanding of managing AA consumption by mixing sufficient volumes of different oils together in order to control hydrate agglomeration. This method could reduce or eliminate the need to add AA in the pipeline loop systems of various oil and gas wells (subsea tiebacks), thus, resulting in large savings.

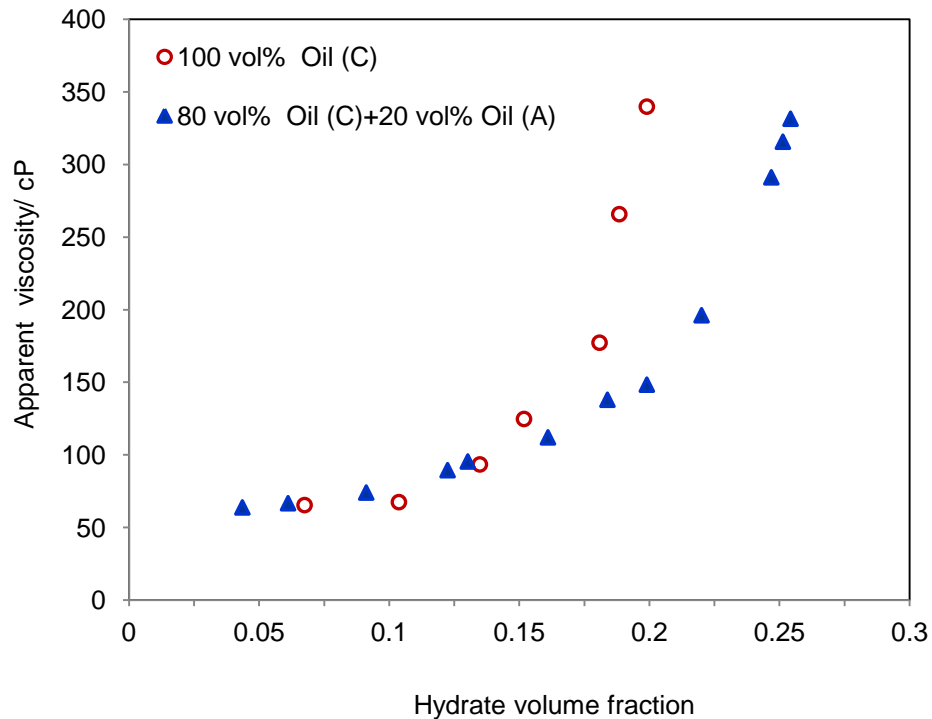


**Figure 6. 18 Hydrate transport for blends of crude oil (A) and diesel oil (C) with ratio of 20/80. Water cut is 60% and AA concentrations are 0.6 wt. % of aqueous phase.**

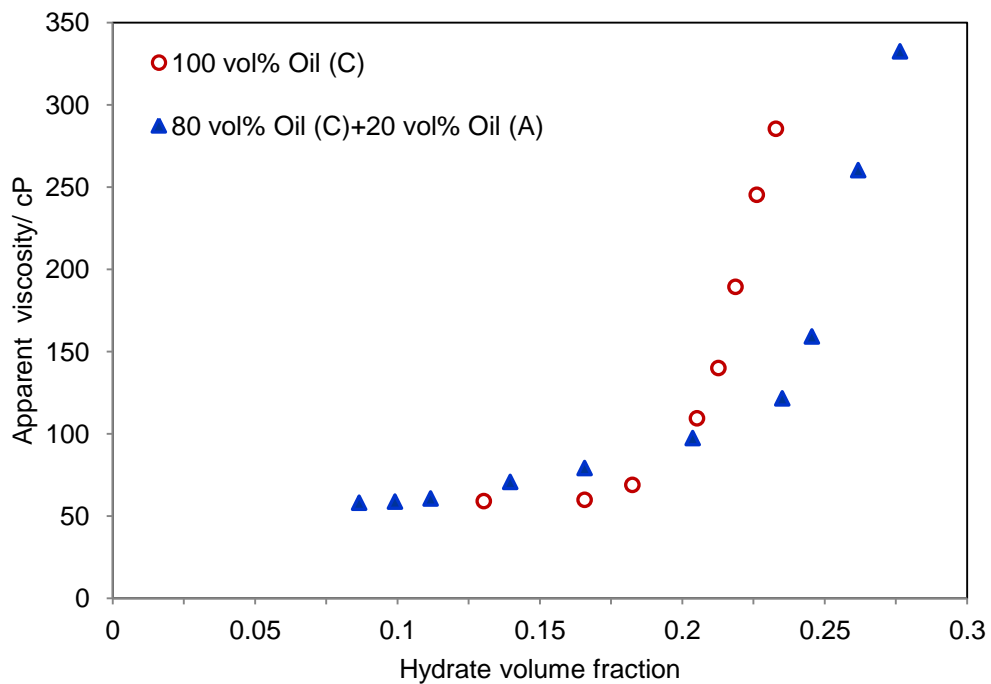


**Figure 6.19 Hydrate transport for blends of crude oil (A) and diesel oil (C) with ratio of 20/80. Water cut is 60% and AA concentrations are 2.0 wt. % of aqueous phase.**

## 6.6 EFFECT OF HYDRATE FORMATION AND DISSOCIATION ON EMULSION STABILITY IN HIGH WATER CUT SYSTEMS

Large quantities of water are produced along with hydrocarbons in petroleum reservoirs all over the world. The water produced continues to increase as the oil and gas reservoirs reach maturity. Formation water comes as a bi-product of oil and gas production and needs to be controlled efficiently. In addition to hydrate plugging problems in subsea oil and gas production pipelines, there are many potential challenges in the oil and water separation processes. A typical problem is to separate stable oil-water emulsions. Increased chemical consumption (demulsifier) and energy consumption (in the heat exchangers) are two well-known methods to attempt to overcome the separation problems; however, the above techniques have a massive impact on the operational costs.

Recent evidence suggests that gas hydrate formation and dissociation may destabilise some water-in-crude oil emulsions (Greaves et al., 2008; Lachance et al., 2008; Palermo et al., 2005).

**Table 6. 5 Viscosity changes during hydrate formation and dissociation processes.**

Step no.	Temperature/ °C	Apparent viscosity/ cP	Comments
1	20	148	W/O Emulsion
2	2.4	251	W/O Emulsion, before hydrate onset
3	3.9	1078	Hydrate volume fraction=0.32
4	20	12.6	After hydrate dissociation, O/W Emulsion

This study investigates the effect of hydrate formation and dissociation on emulsion stability for high water cut systems with the measurement of the viscosity during the hydrate formation and dissociation processes. The asphaltene fraction in crude oils has been reported as an agent resisting the destabilization of W/O emulsions caused by the hydrate formation (Lachance et al., 2008).

Crude oil (A), which contains high amounts of asphaltene and resin, was used as liquid hydrocarbon phase. The high pressure autoclave cell was loaded with the W/O emulsion. The emulsion was 70% water cut with 1 wt% AA1 and 5 wt% NaCl. All the experiments have been conducted in the high pressure autoclave cell and the test procedure was similar to the experiments conducted in Section 6.4. When the amount of hydrate volume fraction reached about 0.32, the cooling system temperature was set on 20 °C to dissociate the hydrates. The viscosities of the water/oil emulsion and water/oil/hydrate mixture were measured during the experiment and the results are listed in Table 6.5. The experiment was begun with W/O emulsion and the large difference between the viscosity of the emulsion at the beginning (Step 1) and after hydrate dissociation (Step 4) can be attributed to the changing emulsion morphology from W/O to O/W. In order to confirm this trend, emulsion samples were taken at Steps 1 and 4. From Figure 6.20 (b), the separation of the aqueous and oil phases is clearly visible and the emulsion observed to break up immediately. The results for emulsion stability in Chapter 5 revealed that a W/O emulsion of oil (A) in the presence of 5 wt.% NaCl and 1 wt.% AA1 exhibited very high emulsion stability, even after 24 hours. However, it was very unstable when the emulsion type was O/W. This confirms that hydrate dissociation broke up the initial W/O emulsion which reformed as an O/W emulsion.

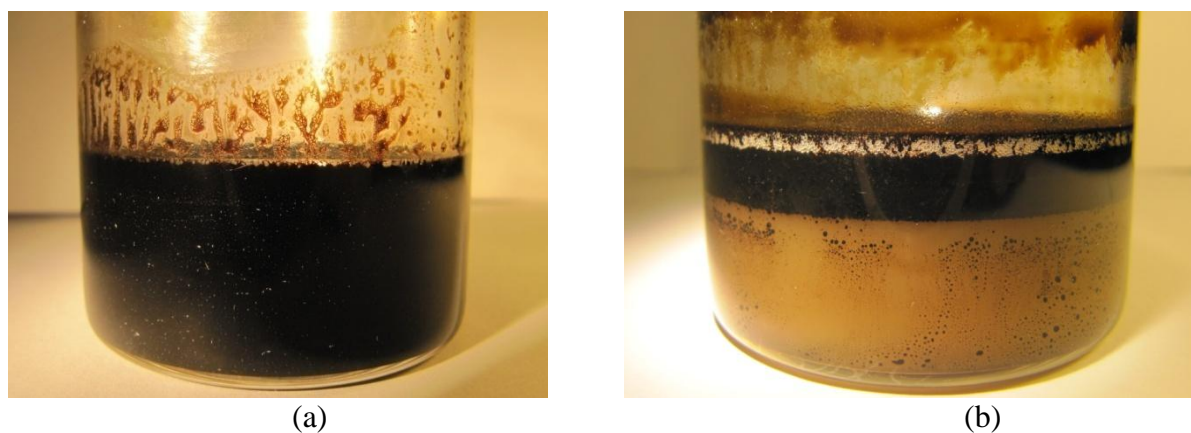


**Figure 6. 20 Emulsion samples taken from a) Step1, before hydrate formation (2 hours after sampling) b) Step 4, after hydrate dissociation (3.5 minutes after sampling).**

Conceptual illustrations of these W/O emulsion destabilizations have been suggested, to explain the agglomeration tendencies of hydrate particles or phase inversion of emulsion during hydrate formation process (Greaves et al., 2008; Palermo et al., 2005). Figure 6.21 shows that once

hydrates agglomerate, upon dissociation, the water droplets will come together and form new larger water droplets, which are much bigger than the original droplets. Therefore, the contact surface area between water and oil phases significantly decreases, resulting in a phase inversion from W/O to O/W in high water cut systems.

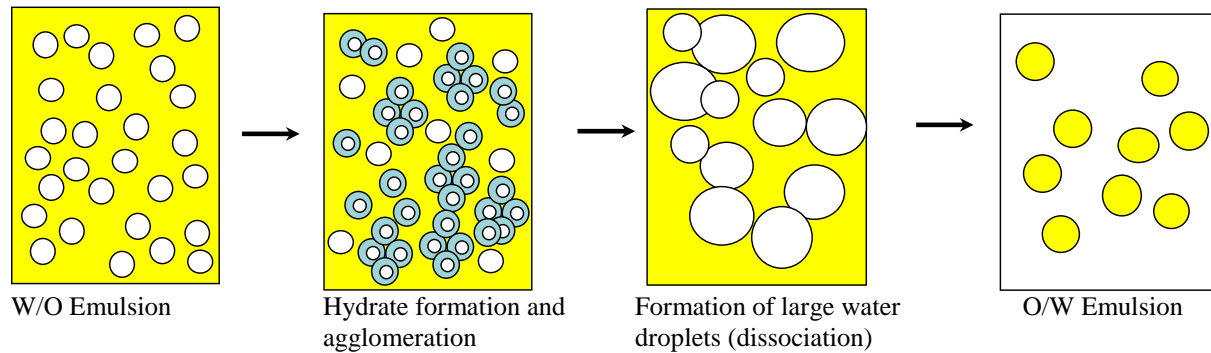


**Figure 6. 21 Schematic representation of phase inversion from W/O to O/W emulsion for 70% water cut system tested in this study during the hydrate formation and dissociation process. Adapted from Greaves et al. (2008).**

## **6.7 EXAMINATION OF THE EFFECT OF SALT (NaCl) CONCENTRATION ON THE PERFORMANCE OF AAS IN HIGH WATER CUT SYSTEMS**

The produced water from oil and gas wells usually contains a high level of dissolved salts. Presence of salt influences the hydrate stability zone and thus the gas hydrate formation process. Dissolved salts may also affect the performance of AAs, but there is still much discussion in the available literature about the effect of different salt concentrations on the effectiveness of commercial AAs. Several studies have revealed that some commercial AAs do not work in fresh water or low salinity systems (Cowie et al., 2005; Kelland, 2006; Kelland et al., 2006). Mehta et al. (2002) highlighted the need for a minimum salinity of 1.5 wt % for a particular AA employed to be effective. In other studies, the authors have stated that hydrate slurry transportability significantly improves with increasing NaCl concentration in aqueous phase (Azarinezhad et al., 2010; Gao, 2009). In a more recent work, the effect of adding salt (NaCl and  $MgCl_2$ ) on the performance of two different types of AA (an anionic quaternary ammonium salt and a nonionic rhamnolipid surfactant) was investigated by York and Firoozabadi (2009). Their results revealed that there were no observable indications of hydrate agglomeration for the experiments with AA and without salt. However, in some cases, addition of salt could result in hydrate agglomeration, depending on the nature and concentration of AAs and salts in the aqueous phase. They concluded that there was a range of salt concentrations at which AAs may work properly.

The above reported results give good information about the salinity effects upon AA performance. But they are not clear, and generally, do not present systematic data. It seems that the salinity effects upon AA performance not only depend on the salt concentration in the aqueous phase, but also strongly on the type of AA, liquid hydrocarbon phase and thermodynamic conditions of the system.

Therefore, for each particular system, separate experimental investigations are needed to determine the effect of salt concentration on the rheological behaviour of the hydrate slurry and the performance of commercial hydrate AAs.

In this study several experiments were carried out using the high pressure autoclave cell to investigate the effect of salt concentration on AA performance and, consequently, on rheological behaviour of water/oil/hydrate mixers in high water cut systems.

### **6.7.1 Materials and Experimental Procedure**

Crude oil (A) was selected as the liquid hydrocarbon phase for these experiments. The aqueous phase consisted of deionised water, commercial water-soluble AA (AA1) (1 mass%

of aqueous phase) and different concentrations of NaCl (1.5, 3, 5 and 10 wt. % of aqueous phase). The experimental matrix is given in Table 6.6. The experimental procedures were similar to Section 6.4.

**Table 6.6 Experimental matrix for studying the effect of salt on AA performance.**

Test #	AA (wt. %)	NaCl (wt. %)	Water cut (vol. %)	Mixer speed (RPM)	Emulsion <sup>a</sup> type
1	1	1.5	70	200	O/W
2	1	3	70	200	O/W
3	1	5	70	200	O/W
4	1	10	70	200	O/W

a: Type of emulsion before hydrate formation

## 6.7.2 Results and Discussion

The experiments were conducted at almost constant subcooling (about 6.1 °C). The results are shown in Figure 6.22. The hydrate values represented by arrows in the figures indicate the hydrate volume fractions at which the apparent viscosity is about 600 cP. It is clear that the hydrate volume fraction for apparent viscosities below 600 cP significantly increases with the salt concentration.

Salts acts as a hydrate inhibitor and can alter the thermodynamic stability of the gas hydrate . Salts do not participate in the hydrate structure and this results in a salinity gradient at the hydrate forming front (Nagashima et al., 2005). During hydrate formation, the salinity of the remaining water in the surroundings of the hydrate increases so that the potential of unconverted water to form further hydrate significantly drops. For relatively high concentration of salt (or ions) in the aqueous phase, the aqueous phase will be more thermodynamically stable than the hydrate. Therefore, this could be the reason why hydrate formation almost ceased for the experiment with 10 wt. % NaCl, before system blockage occurred (at about 0.34 of hydrate volume fraction). That is, as the water was converted into hydrates, the salinity of the aqueous phase increased, eventually leading to self-inhibition.

The results of this investigation show that NaCl has a positive effect on the AA performance. At the same AA concentrations, the ability of the systems to transport hydrate particles increases with NaCl concentration. Figure 6.23 indicates the hydrate volume fraction at 600 cP as a function of NaCl concentration in the aqueous phase. It is clear that the hydrate volume fraction in the system increases with increasing NaCl concentration and it is more

pronounced at lower NaCl concentrations. From this figure it can be seen that the effect of NaCl on AA performance levelled off after 5 wt. % NaCl, for the systems tested in this study.

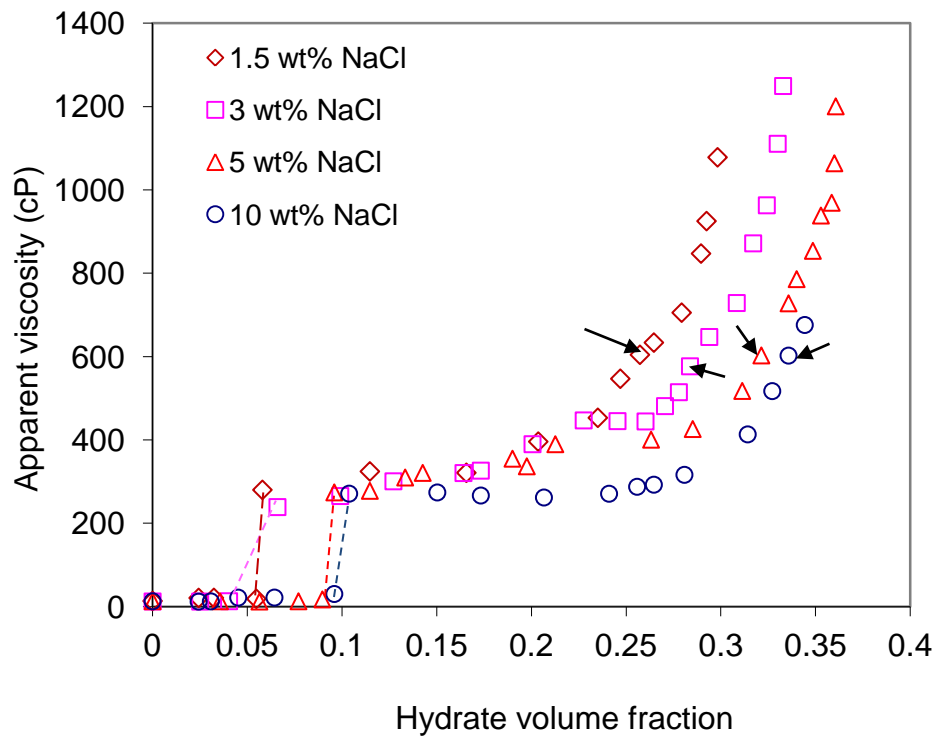


**Figure 6.22 Effect of salt concentration on the mixture viscosity as a function of hydrate volume fraction.**



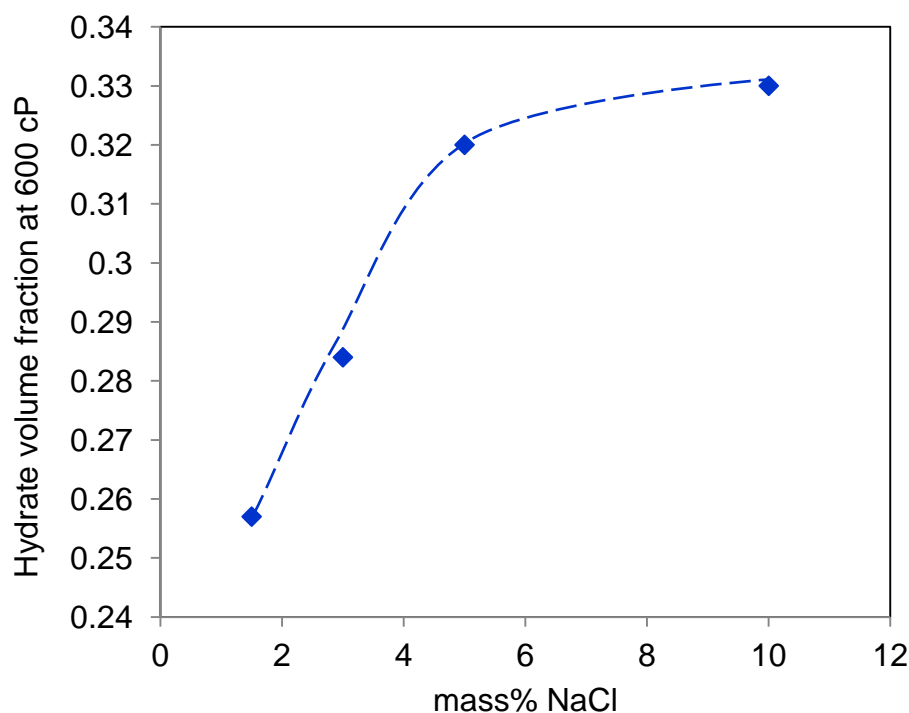


**Figure 6. 23 Hydrate volume fractions for the mixture viscosity at 600 cP as a function of NaCl concentration.**

## 6.8 SHUT-IN AND START-UP

The successful use of AAs is not limited to forming transportable hydrate slurry only when it is flowing, but the slurry must also be easily transportable and remain stable during extended shut-ins and be easily re-mobilized on restart. There are several studies in the literature on the applicability of AAs at shut-in and restart conditions for low water cut systems, from the laboratory and pilot-plant stage up to field deployment (Behar et al., 1994; Palermo and Maurel, 1999) but few data have been reported for high water cut systems.

As our results have shown, in high water cut, the plugging of the system occurred at a critical hydrate volume fraction (where viscosity increases sharply with further increase of hydrate concentration). Therefore, operations can be managed by controlling the amount of hydrate in the system. The aim of the present work is to investigate the transportability of hydrate slurry for a high water cut system operating below the critical hydrate volume fraction after a period of shut-in.

Two different shut-in and restart scenarios were carried out i) no hydrate before shut-in (hydrate forms during shut-in) ii) different amount of hydrates present before shut-in (below the critical hydrate volume fraction).

### 6.8.1 Experimental Procedure

All experiments were conducted with a 70% water cut of oil (A)-in-water emulsion. The aqueous phase contained 1 wt. % AA1 and 5 wt. % NaCl. For the first scenario, the system was pressurized up to test pressure of about 68 bars at room temperature, while the mixer was in operation, to produce a saturated O/W emulsion. The system was stabilized when there was not any gas observed consumption for at least 3 hours. The gas injection was then stopped. Shut-in testing was started, setting the cooling system at 2°C and the emulsion was left unmixed during the shut-in period. Then the mixer was restarted, to study the effect of shut-in condition on hydrate slurry transportability.

The objective of the second scenario was to investigate the transportability of hydrate slurry after 48 hours of shut-in when two different amounts of hydrate had been formed before shut-in. After loading and pressurizing of the O/W emulsion at up to about 68 bars at room temperature, the experiment was started, setting temperature on 2°C. The experiments were continued at constant pressure by injecting gas to form a certain amount of hydrate in the system. Then the mixer and gas injection system were stopped simultaneously for 48 hours. Finally, the mixer was restarted to study the effect of shut-in condition on hydrate slurry transportability.

### 6.8.2 Results and Discussion

#### 6.8.2.1 No hydrate before shut-in

Figure 6.24 shows pressure and temperature of the system along with the mixer speed and current applied on the mixer, as a function of time. The first pressure reduction is due to a reduction in the emulsion temperature. At about 15 hours, the second rapid pressure drop was followed by a temperature increase, showing hydrate onset. Hydrate firstly formed very rapidly but it ceased after a few hours, with decreasing system pressure resulting in reduction of driving force for hydrate formation. Hydrate formation also stopped because of the limited mass transfer (no mixing) and limited amount of hydrate formers (no free gas). The mixer was then started after 29 hours of hydrate formation and started moving immediately. A small pressure drop after start-up was evidence of an increase in the rate of hydrate formation, due to the mixing process. The current applied on the mixer to keep the mixer speed constant increased slightly after restart, due to initial friction, but it approached a constant value about 250 mA. Viscosity measurement shows that the apparent viscosity was 15 cP at 2°C, which is similar to that of an O/W emulsion.

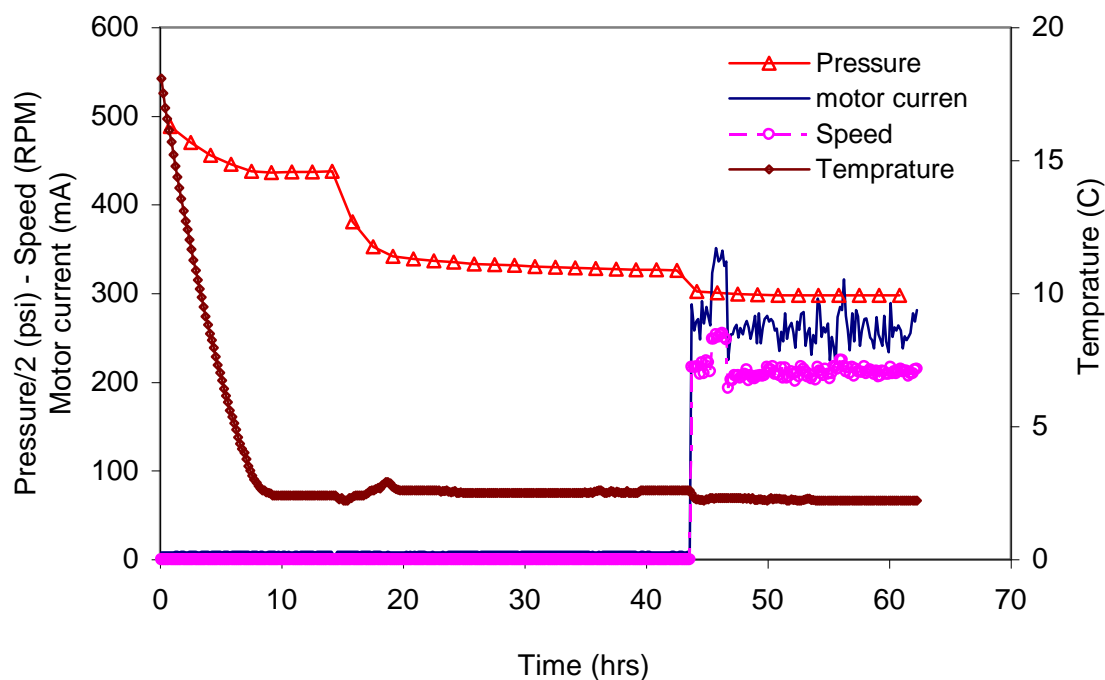


**Figure 6.24 Shut-in and restart test when no hydrate present before shut-in.**

The results show that the type of emulsion didn't change during the shut-in conditions. The water/oil/hydrate mixture was easily transportable and stable during extended shut-in and easily re-mobilised after restarting.

### 6.8.2.2 Hydrates present before shut-in

At the start of the experiments the types of emulsions were O/W, as the motor currents were very low about 250 mA (apparent viscosity was near 15 cP). However, shortly after hydrate formation, the motor currents increased suddenly up to about 1150 mA, due to changes in the type of emulsions (from O/W to W/O). Figures 6.25 and 6.26 show the test conditions for the second scenario, for two different hydrate contents before shut-in. Hydrates were allowed to form until reaching the desired hydrate volume fraction and then the shut-in testing was started, by stopping the mixer and gas injection simultaneously. The systems were restarted after 48 hours of shut-in. Both mixtures in the cell started moving immediately. Table 6.7 summarises the apparent viscosity of the mixtures and current applied on the mixer before shut-in and after restart. It is observed that apparent viscosity and mixer current slightly increased that can be attributed to a very small amount of hydrate, possibly formed using the dissolved gas. The apparent viscosities almost regained their values prior to shut-in, indicating that no gross hydrate aggregation and/or hydrate deposition has taken place during shut-in. It is clear that the tested water soluble AA1 was efficient during shut-in conditions.

**Table 6. 7 Results of second scenario before shut-in and after restart.**

$\varphi_h$ <sup>1</sup>	Apparent Viscosity <sup>2</sup> (cP)	Apparent Viscosity <sup>3</sup> (cP)	Mixer speed (RPM)	Mixer Current <sup>2</sup> (mA)	Mixer Current <sup>3</sup> (mA)
0.11	294	322	200	1140	1210
0.24	465	481	200	1470	1504

1: Hydrate volume fraction in the system

2: Apparent viscosity/ mixer current before shut in of the system

3: Apparent viscosity/ mixer current after restart, once system conditions were stabilised

The results indicate that during the 48 hours shut-in, the W/O emulsion was still stable. This can be attributed to a reduction in the water phase from the W/O emulsion. This reduction occurred because water droplets were taken from the emulsion and converted into the separated hydrate phase. The results of this study show that by managing the amount of hydrate in the presence of AA in high water cut systems, it is possible to prevent hydrate blockage during shut-in conditions.

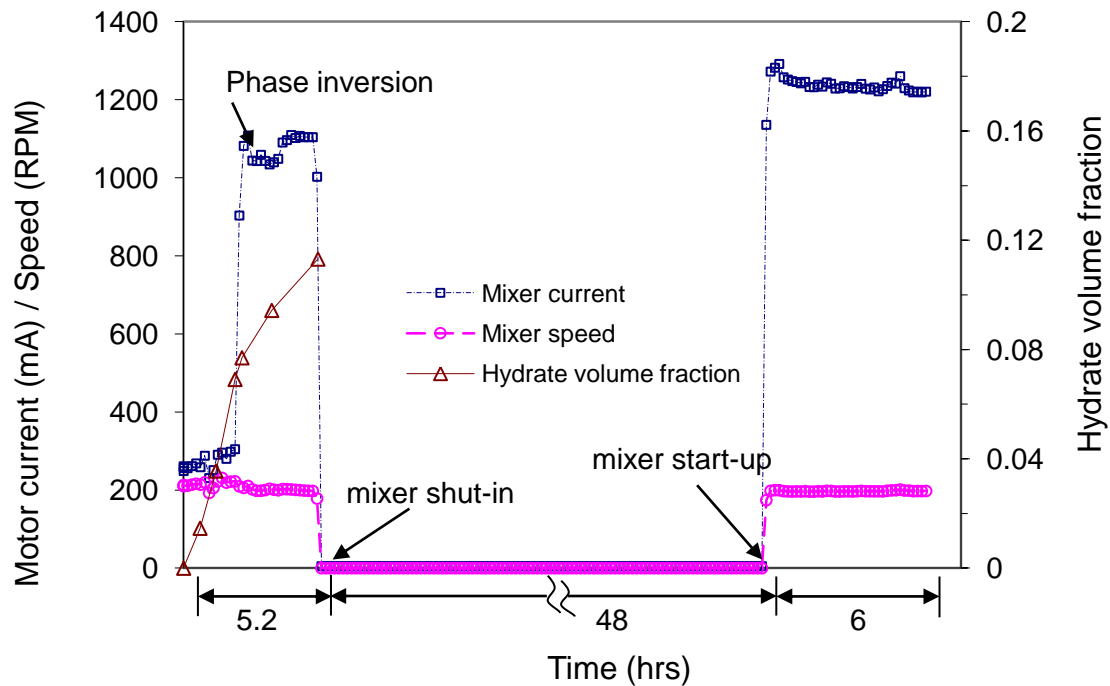


**Figure 6.25 Shut-in and restart test when the hydrate volume fraction is 0.11 before shut-in.**

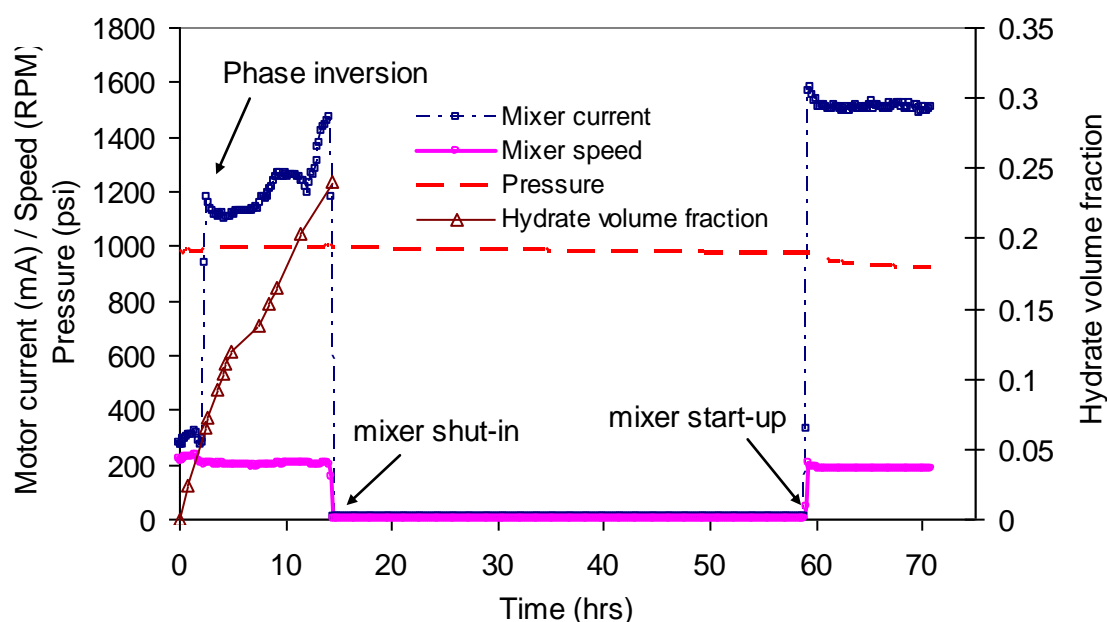


**Figure 6.26 Shut-in and restart test when the hydrate volume fraction is 0.24 before shut-in.**

## 6.9 CONCLUSIONS

The experimental results from this study led to a better understanding of the rheological behaviour of water/oil/hydrate mixtures in high water cut systems. It was found that the morphology of a water-oil emulsion has a significant effect on hydrate transportability in high water cut systems, as water continuous emulsions can transport more hydrates compared to oil continuous emulsions at sufficient AA concentration. It has been noticed that the type of emulsion during hydrate formation strongly depends on AA concentration and initial water cut. In order to transport a certain hydrate volume fraction, different AA concentrations are required, that depend on liquid hydrocarbon chemistry. A higher AA performance was achieved in the crude oil which exhibited higher W/O emulsion stability. The results show that loose emulsion (oil (C)) needed 1.0 wt. % AA to transport around 0.22 of the hydrate volume fraction while for the medium (oil (B)) and tight (oil (A)) emulsions only 0.6% and 0.3 wt. % AA were required to transport the same hydrate volume fraction. This behaviour can be attributed to the presence of natural surfactants (asphaltenes and resins) in the crude oil. It indicates that natural surfactants can act as co-surfactants to improve the effectiveness of commercial AAs. The results of this investigation also show that:

- Different AAs may cause different rheological behaviour of hydrate slurries, which depends on the structure and nature of AA. The results suggest that it is possible to

produce transportable hydrate slurry in high water cut systems, within a certain range of hydrate volume fraction, using a suitable and efficient AA.

- From the tests with diesel oil (C) (loose emulsion) mixed with crude oil (A) (presented as a tight emulsion), it was shown that the performance of AA significantly improved, as the system was able to transport more hydrates. This result is very important because it indicates that an appropriate blend of a loose and tight emulsion oil can behave similarly to a medium or tight emulsion and result in large savings in AA consumption.
- Hydrate formation and dissociation effectively destabilize highly stable W/O emulsion (oil (A)). Hydrate formation and dissociation of a W/O emulsion system with 70% water cut broke up the W/O emulsion, forming an O/W emulsion.
- NaCl has a positive effect on the performance of the AA (AA1) used in this study, as the ability of the systems to transport hydrate particles increased with NaCl concentration. It was observed that the effect of NaCl on the AA performance levelled off after 5 wt. % NaCl.
- In the presence of an efficient AA for hydrate volume fractions below the critical point, after shut in, high water cut systems could restart without evidence of hydrate agglomeration.

## **6.10 REFERENCES**

Abivin P., H.I., Chaudemanche C., Argillier J.F., 2009. Dispersed Systems in Heavy Crude Oils. *Oil & Gas Science and Technology*, 64: 557-570.

Alapati, R., Lee, J. and Beard, D., 2008. Two field studies demonstrate that new LDHI chemistry is effective at high water cuts without impacting oil/water quality, *Offshore Technology Conference, OTC 19505*, Houston, Texas.

Arjmandi, M., 2007. Gas hydrate control by low dosage hydrate inhibitors, Ph.D. Thesis, Petroleum Engineering, Heriot-Watt University, Edinburgh.

Austvik, T., LI, X. and Gjertsen, L.H., 2000. Hydrate plug properties: formation and removal of plugs. *Annals of the New York Academy of Sciences*, 912(1): 294-303.

Azarinezhad, R., 2010. A chemical based wet cold flow approach for addressing hydrate flow assurance problems, PhD Thesis, Heriot-Watt University, Edinburgh

Behar, E., Delion, A.S., Sugier, A. and Thomas, M., 1994. Plugging Control of Production Facilities by Hydrates. *Annals of the New York Academy of Sciences*, 715(Natural Gas Hydrates): 94-105.

Colombel, E., Gateau, P., Barré, L., Gruy, F. and Palermo, T., 2009. Discussion of agglomeration mechanisms between hydrate particles in water in oil emulsions. *Oil & Gas Science and Technology-Revue de l'IFP*, 64(5): 629-636.

Cowie, L., Bollavaram, P., Erdogmus, M., Johnson, T. and Shero, W., 2005. Optimal Hydrate Management and New Challenges in GoM Deepwater Using “Best in Class” Technologies, *OTC 17328*, *Offshore Technology Conference Houston, TX*, , pp. 2-5.

Dieker, L.E., Aman, Z. M., George, N. C., Sum, A. K., Sloan, E. D., 2009. Micromechanical adhesion force measurements between hydrate particles in hydrocarbon oils and their modifications. *Energy & Fuels*, 23(12): 5966-5971.

Erstad, K., 2009. The influence of crude oil acids on natural inhibition of hydrate plugs, PhD Thesis, University of Bergen, 85 pp.

Fadnes, F.H., 1996. Natural hydrate inhibiting components in crude oils. *Fluid Phase Equilibria*, 117(1-2): 186-192.

Fidel-Dufour, A., Gruy, F. and Herri, J.M., 2006. Rheology of methane hydrate slurries during their crystallization in a water in dodecane emulsion under flowing. *Chemical Engineering Science*, 61(2): 505-515.

Fotland, P., Askvik, K.M. and Slamova, E., 2011. Natural anti-agglomerants in crude oil: Isolation, identification and verification of inhibiting effect, *Proceedings of the 7th International Conference on Gas Hydrates (ICGH 2011)*, Edinburgh, Scotland, United Kingdom.

Frostman, L., 2000. Anti-Agglomerant Hydrate Inhibitors for Prevention of Hydrate Plugs in

Deepwater Systems, SPE 63122, Society of Petroleum Engineers, Houston, Texas.

Gao, S., 2009. Hydrate risk management at high watercuts with anti-agglomerant hydrate inhibitors. *Energy & Fuels*, 23(4): 2118-2121.

Greaves, D., Boxall, J., Mulligan, J., Sloan, E.D. and Koh, C.A., 2008. Hydrate formation from high water content-crude oil emulsions. *Chemical Engineering Science*, 63(18): 4570-4579.

Haghighi, H., Azarinezhad, R., Chapoy, A., Anderson, R. and Tohidi, B., 2007. HYDRAFLOW: Avoiding gas hydrate problems, SPE 107335, Presented at the SPE Europe/EAGE Annual Conference and Exhibition, London.

Herri, J. et al., 1999. Interest of in situ turbidimetry for the characterization of methane hydrate crystallization: Application to the study of kinetic inhibitors. *Chemical Engineering Science*, 54(12): 1849-1858.

Huo, Z., Freer E., Lamar M., Sannigrahi B., Knauss D. M., E. D. Sloan Jr., 2001. Hydrate plug prevention by anti-agglomeration. *Chemical Engineering Science*, 56: 4979–4991.

Kelland, M.A., 2006. History of the development of low dosage hydrate inhibitors. *Energy & Fuels*, 20(3): 825-847.

Kelland, M.A., Svartaas, T.M., Ovsthus, J., Tomita, T. and Mizuta, K., 2006. Studies on some alkylamide surfactant gas hydrate anti-agglomerants. *Chemical Engineering Science*, 61(13): 4290-4298.

Klomp, U., 2008. The World of LDHI: from conception to development to implementation, Proceedings of the 6th International Conference on Gas Hydrates (ICGH 2008), Vancouver, British Columbia, CANADA.

Lachance, J.W., Dendy Sloan, E. and Koh, C.A., 2008. Effect of hydrate formation/dissociation on emulsion stability using DSC and visual techniques. *Chemical Engineering Science*, 63(15): 3942-3947.

Le Ba, H., Cameirao, A., Herri, J.M., Darbouret, M., 2010. Chord length distributions measurements during crystallization and agglomeration of gas hydrate in a water-in-oil emulsion: Simulation and experimentation. *Chemical Engineering Science*, 65(3): 1185-1200.

Leporcher, E., Peytavy, J., Mollier, Y., Sjoblom, J. and Labes-Carrier, C., 1998. Multiphase transportation: hydrate plugging prevention through crude oil natural surfactants, SPE 49172, New Orleans, Louisiana.

Mehta, A., Hebert, P., Cadena, E. and Weatherman, J., 2002. Fulfilling the promise of low dosage hydrate inhibitors: journey from academic curiosity to successful field implementation, OTC 14057, Offshore Technology Conference, Houston, Texas.

Moradi, M., Alvarado, V. and Huzurbazar, S., 2011. Effect of Salinity on Water-in-Crude Oil Emulsion: Evaluation through Drop-Size Distribution Proxy. *Energy & Fuels*, 25: 260–268.



Nagashima, K., Orihashi, S., Yamamoto, Y. and Takahashi, M., 2005. Encapsulation of saline solution by tetrahydrofuran clathrate hydrates and inclusion migration by recrystallization. *The Journal of Physical Chemistry B*, 109(20): 10147-10153.

Palermo, T., Arla, D., Borregales, M., Dalmazzone, C. and Rousseau, L., 2005. Study of the agglomeration between hydrate particles in oil using differential scanning calorimetry (DSC). 5th International Conference on Gas Hydrates, Trondheim, Norway, 1: 332–339.

Palermo, T. and Maurel, P., 1999. Investigation of hydrates formation and hydrates transportation with and without dispersant additives under multiphase flow conditions, Multiphase'99, 9th International Conference on Multiphase, 9th International Conference on Multiphase. Cannes, pp. 567-582.

Palermo, T., Mussumeci, A. and Leporcher, E., 2004. Could hydrate plugging be avoided because of surfactant properties of the crude and appropriate flow conditions?, OTC 16681, Presented in the Offshore Technology Conference, Houston, Texas.

Plegue, T.H., Frank, S.G., Fruman, D.H. and Zakin, J.L., 1986. Viscosity and colloidal properties of concentrated crude oil-in-water emulsions. *Journal of Colloid and Interface Science*, 114(1): 88-105.

Plegue, T.H., Frank, S.G., Fruman, D.H. and Zakin, J.L., 1989. Concentrated viscous crude oil-in-water emulsions for pipeline transport. *Chemical Engineering Communications*, 82: 111-122.

Pleguea T. H. , F.S.G.b., Frumanc D. H. and Zakin J. L., 1986. Viscosity and colloidal properties of concentrated crude oil-in-water emulsions. *Journal of Colloid and Interface Science*, 114(1): 88-105

Pleguea T. H. , F.S.G.b., Frumanc D. H. and Zakin J. L., 1989. CONCENTRATED VISCOUS CRUDE OIL-IN-WATER EMULSIONS FOR PIPELINE TRANSPORT *Chemical Engineering Communications*, 82(1): 111 - 122

Sinclair, A.R., 1970. RHEOLOGY OF VISCOUS FRACTURING FLUIDS. *Journal of Petroleum Technology*, 22(JUN): 711-&.

Sinquin, A., Palermo, T. and Peysson, Y., 2004. Rheological and flow properties of gas hydrate suspensions. *Oil & Gas Science and Technology*, 59: 41–57.

Sjöblom, J., Ovreivoll, B., Jentoft, G.H., Lesaint, C., Palermo, T., 2010. Investigation of the Hydrate Plugging and Non-Plugging Properties of Oils. *Journal of dispersion science and technology*, 31(8): 1100-1119.

Sloan, E.D., 2005. A changing hydrate paradigm--from apprehension to avoidance to risk management. *Fluid Phase Equilibria*, 228: 67-74.

Steinborn, R. and Flock, D., 1983a. The rheology of heavy crude oils and their emulsions. *Journal of Canadian Petroleum Technology*, 22(5): 38-52.

Steinborn, R. and Flock, D.L., 1983b. THE RHEOLOGY OF HEAVY CRUDE OILS AND THEIR EMULSIONS. *Journal of Canadian Petroleum Technology*, 22(5): 38-52.

Yana, Y., Pala, R. and Masliyah, J., 1991. Rheology of oil-in-water emulsions with added solids *Chemical Engineering Science*, 46(4): 985-994

York, D. and Firoozabadi, A., 2009. Effect of Brine on Hydrate Antiagglomeration. *Energy & Fuels* 23: 2937–2946.

Zaki, N.N., Ahmed, N.S. and Nassar, A.M., 2000. Sodium lignin sulfonate to stabilize heavy crude oil-in-water emulsions for pipeline transportation. *Petroleum Science and Technology*, 18(9-10): 1175-1193.

Zanota, M.L., Dicharry, C. and Graciaa, A., 2005. Hydrate plug prevention by quaternary ammonium salts. *Energy & Fuels*, 19(2): 584-590.

## **CHAPTER 7    EXPERIMENTAL STUDY USING A SATURATED FLOW LOOP**

### **7.1 INTRODUCTION**

Gas hydrate formation blockage is a critical issue that must be addressed early in the design process for offshore production systems. A promising alternative technique to mitigate and solve hydrate blockage problems in production pipelines would be to allow hydrates to form, but in a controlled way, in order to transport a dispersed slurry in the flow line. Knowledge of the rheological behaviour of hydrate suspensions would contribute to a better understanding of underlying mechanisms to transport oil and gas through a pipeline over long distances with low risk of hydrate blockage. Studies of the rheological properties of hydrate slurry are either performed in viscometers where torque values are converted to viscosity values, or in pipelines/flow loops where pressure drops are continuously measured through the pipeline. To measure hydrate transportability and to mimic field conditions, pressure drop measurements in flow loops are the better method of the two. Because of the scarcity of real field data on properties of hydrate slurry flows and hydrate plug formation, flow loops have become the next best way to simulate actual pipeline conditions. However, flow loop experiments require an extensive amount of samples, and hence experimental design matrices are reduced to a minimum. The possibility of generating sufficient data for a reliable description of the rheological behaviour of hydrate slurries is therefore limited.

In Chapter 6, the small scale helical tube viscometer calibrated was used to measure the viscosity of hydrate slurries at constant RPM. A large number of experiments were carried out to investigate the effect of AA concentration, salt, mixer speed, water cut, etc. on the rheological behaviour of water/oil/hydrate mixtures in high water cut systems. Due to its small size, this small scale apparatus required minimal amounts of oil for testing and less time and manpower for operation. It was therefore possible to generate reliable data to study the rheological behaviour of hydrate slurries in high water cut systems. One of the challenging problems of developing a small scale apparatus is that the results from small scale apparatus may not be transferable to the large scale oilfield pipe flow.

In this chapter several flow loop experiments were conducted to characterize the rheological behaviour of hydrate slurry flow by pressure drop measurements taken from the flow loop. The major objectives of this study are to investigate the following aspects of the rheological behaviour of hydrate slurry flow in high water cut systems in real pipelines:

- The effect of AA concentration
- The effect of salt in the presence of AA
- The effect of pump speed/ shear rate
- The effect of water cut

Finally, the pressure drop measurements from the flow loop were related to the viscosity measurements from the small scale helical tube viscometer.

## **7.2 EXPERIMENTAL EQUIPMENT**

All the experiments in this study were carried out in the saturated flow loop described in detail in Chapter 4.

## **7.3 MATERIALS**

The materials used in this study are similar to those used in the small scale experiments. One crude oil, named as oil (A), was used as the liquid hydrocarbon phase. The main chemical characteristics of this crude oil are given in Table 5.1 and the oil composition is given in Table A.1.

Experiments were conducted at two different high water cuts, i.e. 60 and 80 %. Deionised water mixed with 5 wt. % of salt ( $\geq 99\%$  anhydrous NaCl (Aldrich)) and different AA1 concentrations (a commercial water-soluble AA) was used as aqueous phase. A typical natural gas was used in all experiments (composition given in Table A.4).

## **7.4 OPERATIONAL PROCEDURE**

A summary of the standard operating procedure is as follows:

- Evacuate the flow loop and the storage tank using the vacuum pump to a pressure of about 0.05-0.1 bars.
- Load the required mass of crude oil and water into the saturation tank using the liquid injection pump.
- Recirculate the liquid through both loop and tank for few hours at high motor speed at room temperature (around 20 °C) in order to create a homogenous water-oil emulsion.
- Set off-stream the storage tank and recirculate the water-oil emulsion through the flow loop only, at the chosen pump speed.
- Set the John Crane oil seal pressure to at least 10% or 5 bars above operating pressure.
- Charge the required amount of gas into the flow loop at constant ambient temperature and bring the flow loop to operating pressure.
- Stabilize the flow loop for at least 3 hours to verify saturation of liquid phase with gas and to check for leaks.
- Initiate the experiment by simultaneously starting the data acquisition and setting the cooling system to the temperature planned for the experiment.
- Set the gas booster pump to the operating pressure.
- Inject gas to the flow loop to keep the pressure constant during the cooling and hydrate formation process.
- Once hydrate starts to form, continue the gas injection until the desired hydrate volume fraction or the equipment limit (i.e. when the pressure difference between suction and discharge is a maximum of 20 bars) is reached.
- Dissociate hydrates by setting a heating ramp to a temperature of 20 °C.
- Depressurize, drain and clean the flow loop.

## 7.5 RESULTS AND DISCUSSION

Experiments were performed at five different test conditions and in high water cut. The test matrix for these experiments is shown in Table 7.1. AA concentration, motor speed, salt concentration and water cut were varied in the experiments. Materials and test conditions selected were similar to those in the small scale experiments; to compare the results obtained using the high pressure autoclave cell with the flow loop results.

**Table 7. 1 Test matrix for flow loop experiments in high water cut.**

Test #	AA (wt. %)	NaCl (wt. %)	Water cut (vol. %)	Motor speed (RPM)	Pressure (bar)	Emulsion type <sup>a</sup>
1	0.6	0	60	300	68	O/W
2	0.6	5	60	300	68	O/W
3	0.6	5	60	150	68	O/W
4	1	5	60	150	68	O/W
5	1	5	80	150	68	O/W

a: Type of emulsion before hydrate onset

### 7.5.1 Effect of AA Concentration

From the small scale experiments, it was observed that hydrate transportability in high water cut systems significantly improved with increasing AA concentrations and that it was more pronounced for AA concentrations below 1 wt. %. Flow loop experiments were conducted at constant motor speed of 150 RPM, for two different AA concentrations 0.6 and 1 wt. % at 60% water cut (Tests 3 and 4). Figure 7.1 shows the total pressure drop measured between the discharge and suction of the Moineau pump as a function of the hydrate volume fraction. In this case, similarly to the viscosity increases observed in the small scale experiments, as hydrate formed in the flow loop, a substantial increase in the total pressure drop across the circulating pump was immediately measured. This was attributed to the phase inversion from oil-in-water to water-in-oil emulsions (Figure 7.1). It is clear that after phase inversion point with increasing hydrate content in the system, the pressure drop firstly increases gradually and then rises faster. The rate of increase in the pressure drop is higher in the case of the lower AA concentration (Test 3). This result can be attributed to the formation of bigger hydrate aggregates, trapping more liquid phase among the hydrate particles. In the test with 0.6 wt. % AA, large pressure drop fluctuations were observed for a hydrate volume fraction higher than 0.3. These large fluctuations in the measured pressure drops may be an indication of the formation of partial plugs that move and then stop in the pipe until enough pressure builds up to move them again (Hernandez O.C., 2006). However, increasing the AA concentration to 1 wt. %, significantly

improved the hydrate transportability, as hydrate volume fraction increased up to 0.43, with no evidence of gas hydrate plugging.

From Figure 7.2, it is clear that the test with the higher AA concentration resulted in higher water conversion. The figure indicates a sharp increase in water conversion followed by a plateau. The reason for these plateau trends can be explained as follows. When hydrate starts to form, it is believed that, i) a thin layer of hydrate quickly covers the water droplet's surface and prevents the hydrate forming components from making contact with the water trapped inside the droplets, ii) the salinity of the aqueous phase is continuously increased due to hydrate formation, hence the hydrate equilibrium curve is shifting towards a lower temperature (and therefore reducing further the driving force for hydrate formation).

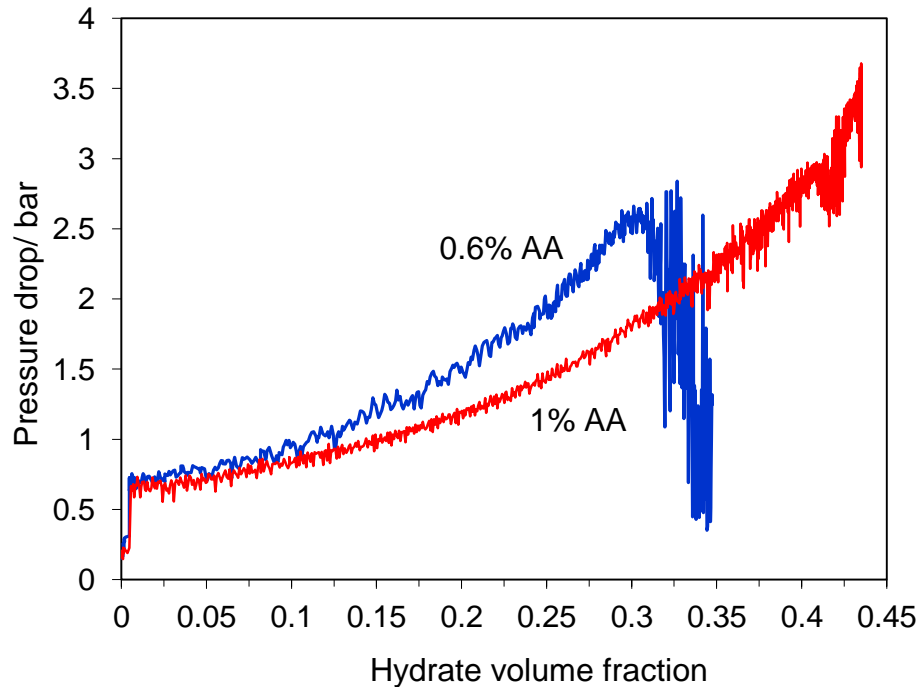


**Figure 7. 1 Pressure drop across the Moineau pump as a function of the hydrate volume fraction for different AA concentrations: Tests 3 and 4 with 60% water cut and pump speed of 150 RPM.**

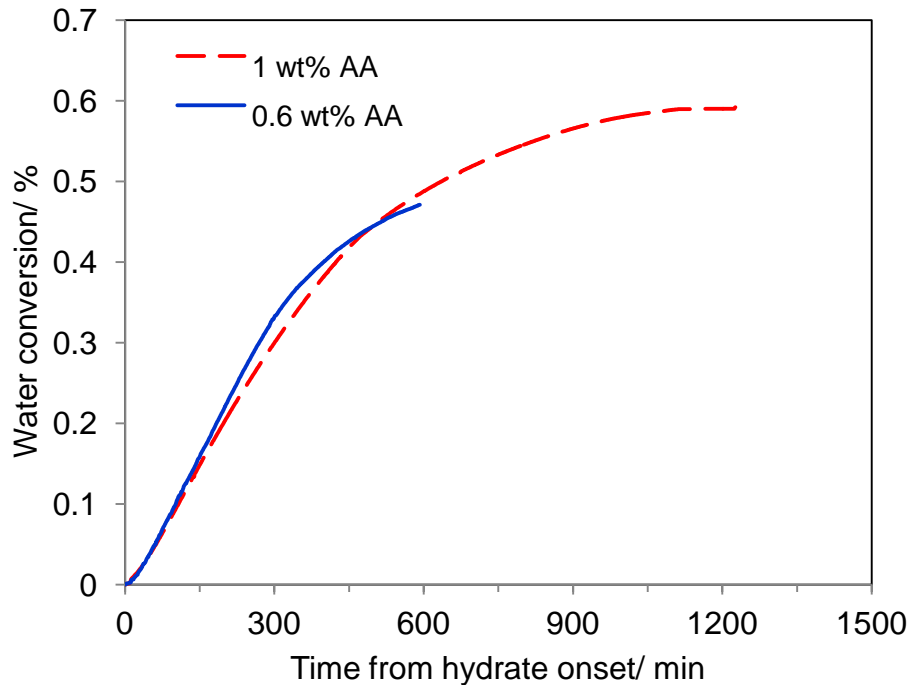


**Figure 7. 2 Water conversion rate for systems with different AA concentrations: Tests 3 and 4 with 60% water cut and pump speed of 150 RPM.**

### 7.5.2 Effect of Salt on AA Performance

A flow loop experiment was conducted with an aqueous phase containing 0.6 wt. % AA and without salt (Test 1). As hydrates formed in the flow loop, a substantial increase in pressure drop was measured due to phase inversion (Figure 7.3). Then the pressure drop increased gradually with increasing hydrate content but at a hydrate volume fraction of about 0.16 the measured pressure drop decreased sharply and then started to fluctuate, due to the deposition of hydrates inside the pipeline (Hernandez O.C., 2006). The results indicate that without salt, this type of AA (AA1) at this concentration was not able to prevent hydrate deposition after the hydrate volume fraction reaches a certain value.

Figure 7.4 shows the effect of salinity on the performance of AA compared with the results of experiments conducted with 0.6 wt. % AA with and without salt. It is clear that adding 5 wt. % salt significantly improved the performance of this AA. One can see that the presence of salt reduces pressure drop considerably during hydrate formation. Another phenomenon taking place is the elimination of the hydrate deposition at high hydrate volume fractions. Test 1, without salt, resulted in hydrate deposition when the hydrate volume fraction approached 0.16, while in the



test in the presence of 5 wt. % salt, it was possible to circulate hydrate as slurry up to a fraction of 0.32 without any indication of hydrate deposition. These results are consistent with our small scale results, which showed that the performance of AA and the hydrate transportability significantly improved with increasing NaCl concentration.

Moreover, Figure 7.5 shows that the presence of salt in the system resulted in a reduction in the rate of water conversion. This can be due to:

- Lower sub-cooling induced by the presence of salt, therefore reducing the driving force for hydrate formation
- Increase in salt concentration in the remaining free water, due to the fact that hydrates exclude salts.

Additionally, it has been widely reported in the open literature that commercial AAs do not perform as well in fresh water (salt free) (Kelland, 2006), as hydrate particles may form large and very sticky hydrate aggregates.

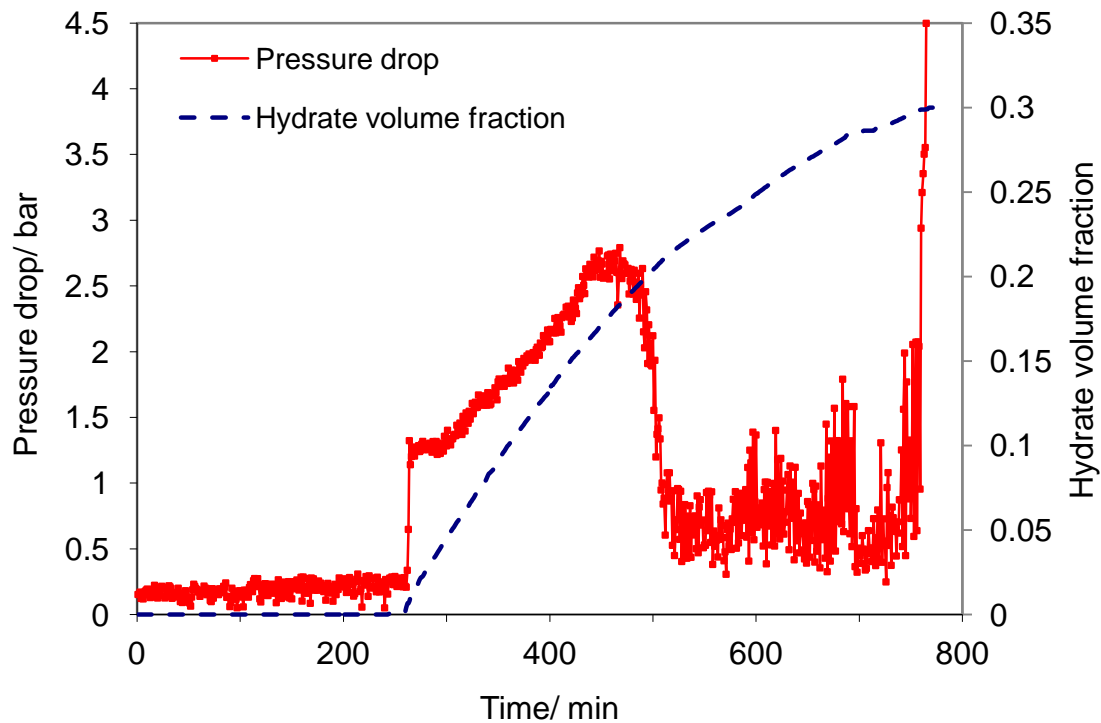


**Figure 7. 3 Pressure drop across the Moineau pump and the rate of hydrate formation during the test without salt: Test 1 with 60% water cut, 0.6 wt. % AA and pump speed of 300 RPM.**

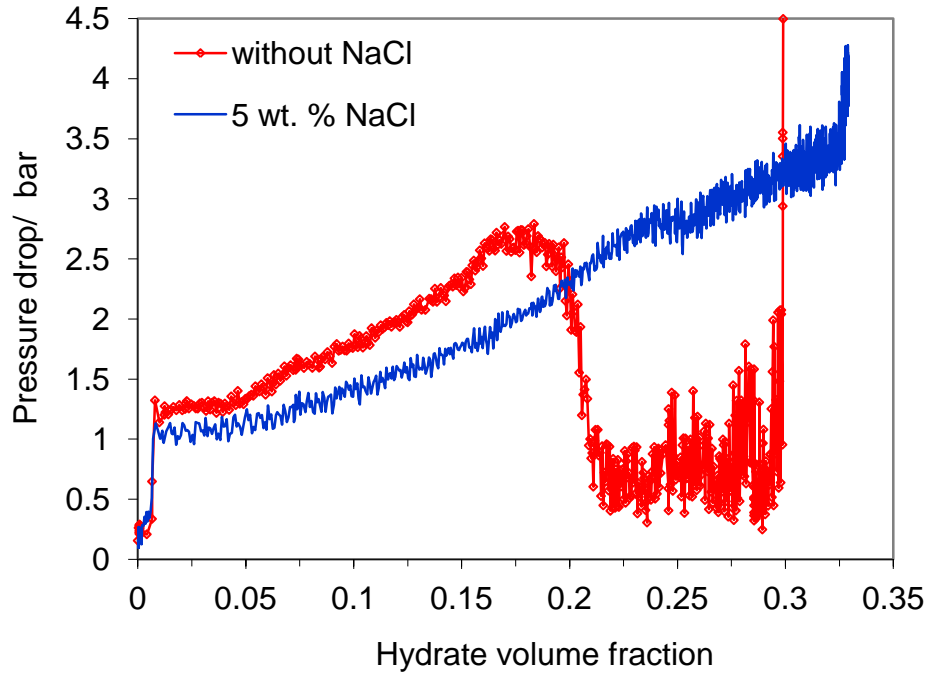


**Figure 7. 4 Pressure drop across the Moineau pump as a function of the hydrate volume fraction for tests without and with 5 wt. % salt: Tests 1 and 2 with 60% water cut and pump speed of 300 RPM.**

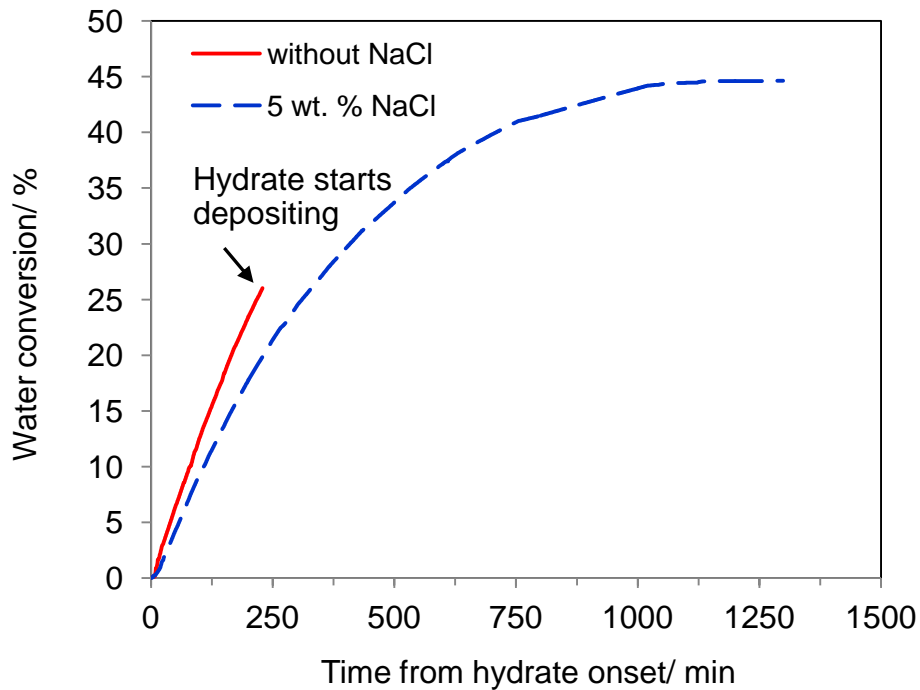


**Figure 7. 5 Water conversion rate for systems with different salt contents: Tests 1 and 2 with 60% water cut and pump speed of 300 RPM.**

### 7.5.3 Effect of Pump Speed/ Shear Rate

Another parameter studied was the effect of flow conditions. Our small scale investigations revealed that in addition to AA, salt and natural surfactants, a change in the shear rate can also influence hydrate slurry transportability (Chapter 6.6). The effect of shear rate was more pronounced at AA concentrations lower than 1 wt%.

Flow loop experiments showed that in the presence of 5 wt. % NaCl the performance of AA was significantly improved, as hydrate slurries were transportable to higher hydrate volume fractions. However, for the test with 0.6 wt. % AA (Test 3) hydrates were deposited on the pipe wall at high hydrate volume fractions (Figure 7.1). Figure 7.6 shows that hydrate deposition could be eliminated by increasing the pump speed or the slurry shear rate. In Test 2, with pump speed of 300 RPM, some small fluctuations on pressure drop can be observed from hydrate volume fractions beyond 0.25, which can be attributed to the formation of large hydrate lumps. However, it is clear that the slurry flow is still moving without a hydrate deposition problem. In general, it seems that the hydrate deposition tendency disappears in the high pump speed test, as more energy is available to disperse the hydrate particles in the liquid phase inside the flow loop. In fact, hydrate particle aggregation can be prevented by high shear, while low shear encourages particle aggregation and plugging (Sjöblom et al., 2010). These results are also in good agreement with our small scale findings.

It can thus be suggested that flow assurance operators may be able to manage AA consumption by applying a suitable shear rate to reduce the risk of hydrate plugging of pipelines.

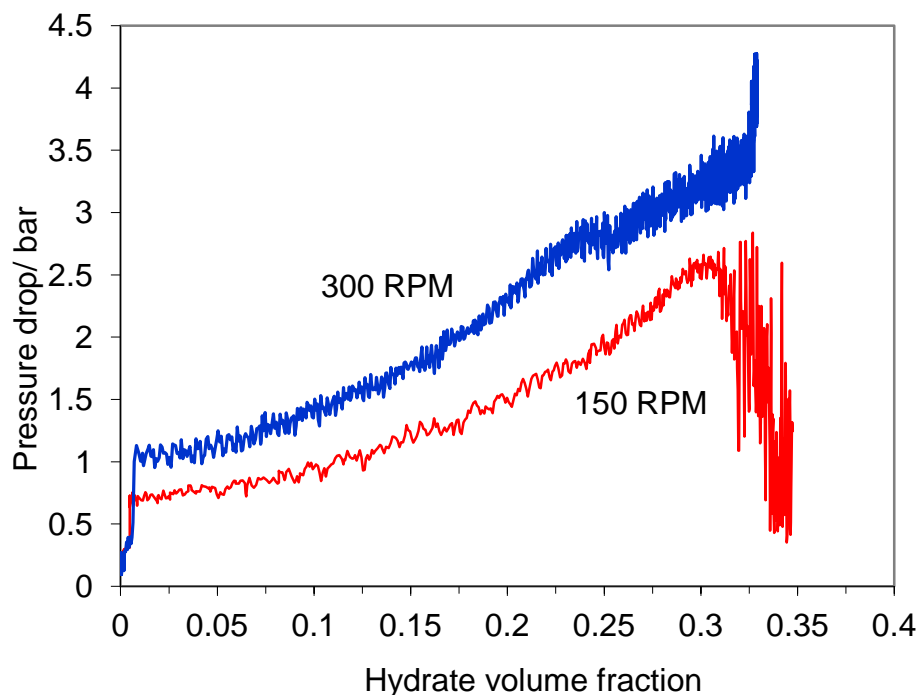


**Figure 7. 6 Pressure drop across the Moineau pump as a function of the hydrate volume fraction for different pump speeds: Tests 2 and 3 with 60% water cut and 0.6 wt. % AA.**

#### 7.5.4 The Effect of Water Cut

From the small scale experiments, it was observed that, depending on the water cut and the composition of the aqueous phases, the morphology of the water-oil emulsion may be altered during hydrate formation.

The experimental results of Test 4 (60% water cut) show that shortly after hydrate onset, the pressure drop across the circulating pump rapidly increased; however, this phenomenon was not observed for the test at 80% water cut (Test 5), as seen in Figure 7.7. Similar trends were observed in the small scale experiments, where the apparent viscosities jumped at the onset of the hydrate formation process for the 60% water cut experiments. This behaviour was attributed to the phase inversion from oil-in-water to water-in-oil emulsion. After the phase inversion, the pressure drop gradually increased with further hydrate formation and the water-in-oil emulsion became more stable due to the reduction in the aqueous phase (Figure 7.7). In the case of very high water cut test (80% water cut), due to some technical problems with the main pump, it was not possible to continue the test after reaching about 20 vol. % hydrates. However, the result revealed that similarly to the small scale experiments, phase inversion did not occur with

conversion of some of the water phase into hydrates and the pressure drop remained low during hydrate formation, even though the hydrate content reached about 20 % of the total volume.

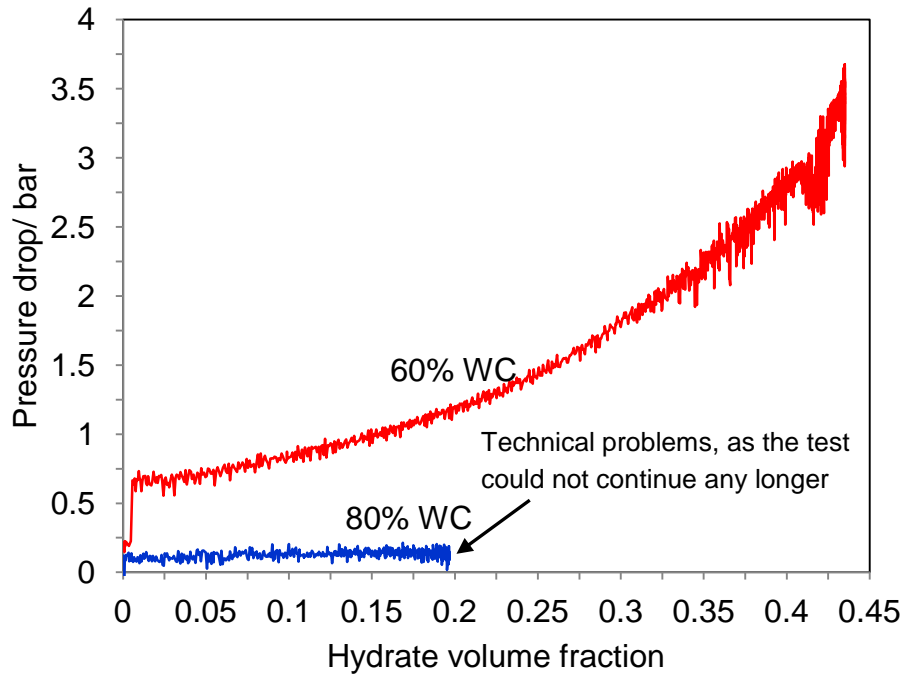


**Figure 7. 7 Pressure drop across the Moineau pump as a function of the hydrate volume fraction for different water cut: Tests 4 and 5 with 1 wt. % AA and pump speed of 150 RPM.**

### 7.5.5 Comparison of Flow Loop and Small Scale Results

One of the main objectives of this study was to relate the small scale viscosity measurements carried out with the high pressure autoclave cell and the pressure drop measurements from the flow loop. To compare these results, pressure drop and viscosity ratio parameters are defined as:

$$H = \frac{\Delta P}{\Delta P_{inv}} \quad \text{for flow loop}$$

$$V = \frac{\mu}{\mu_{inv}} \quad \text{for small scale experiments}$$

where  $H$  refers to the ratio between the pressure drop during hydrate formation,  $\Delta P$ , and pressure drop at the inversion point,  $\Delta P_{inv}$ .  $V$  is the ratio between the apparent viscosity of the water/oil/hydrate mixture during hydrate formation,  $\mu$ , and that at the inversion point,  $\mu_{inv}$ .

Figure 7.8 shows the pressure drop ratios calculated from the flow loop data plotted with the small scale viscosity ratios, as a function of the hydrate volume fraction. The test conditions and materials are similar for both systems and the concentration of AA is 0.6 wt. %. It is obvious that the trend of the pressure drop in the flow loop agrees well with viscosity trend in the small scale cell, for hydrate volume fractions up to 0.3. Figure 7.9 also shows the flow loop and small scale results for the test with 1 wt. % AA. Similar to the test with 0.6 wt. % AA, there is a good agreement between the trends of pressure drop and apparent viscosity of both systems up to 0.3 of hydrate volume fraction. However, beyond 0.3 hydrate volume fraction (the test with 1 wt. % AA), the increase in viscosity in the small scale experiment is much higher than the rate of pressure drop increase in the flow loop. This difference can be attributed to the effect of the circulating pump, which may prevent normal hydrate agglomeration growth when the volume of hydrate in the system is high. The gap between the rotor and the stator is very small and thus can affect the size of hydrate aggregates when they pass through the circulating pump. However, in the high pressure autoclave cell there is no limitation on the space for hydrate agglomeration growth and aggregates can grow naturally, in a similar way to what happens in real pipelines.

In order to convert flow loop pressure drop measurements into viscosity values, a correlation relating the measured pressure drops to viscosity values was developed, as shown in Figure 7.10. The data set includes viscosity values between 250 cP and 800 cP, collected from Figure 7.8, for a flow loop pump speed of 150 RPM. Since the water cut was high, the viscosity of the water-in-oil emulsion is inherently high, even at the beginning of hydrate formation. Therefore, the correlation can convert pressure drop measurements to viscosity only for a limited range of the measured pressure drops.

Further experiments with different crude oil, water cut and pump speed are required in order to develop various calibration curves to relate flow loop pressure drops to the viscosity values over a wide range of the measured pressure drop by flow loop.

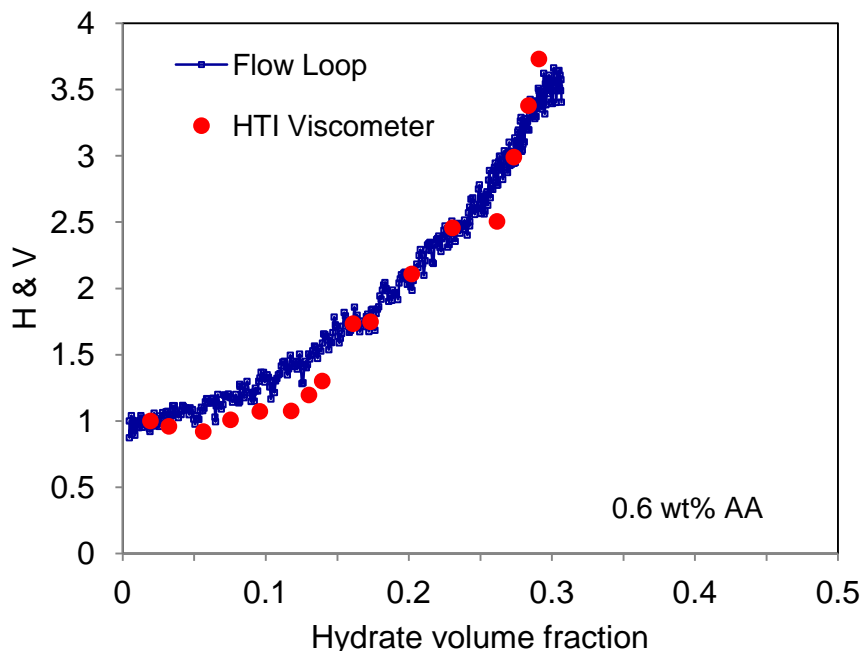


**Figure 7. 8 Comparison of small scale and flow loop test with 60% WC, 0.6 wt. % AA, and 5 wt. % salt. Flow loop pump speed and high pressure autoclave cell mixer speed were kept constant during the tests at 150 RPM and 200 RPM respectively.**

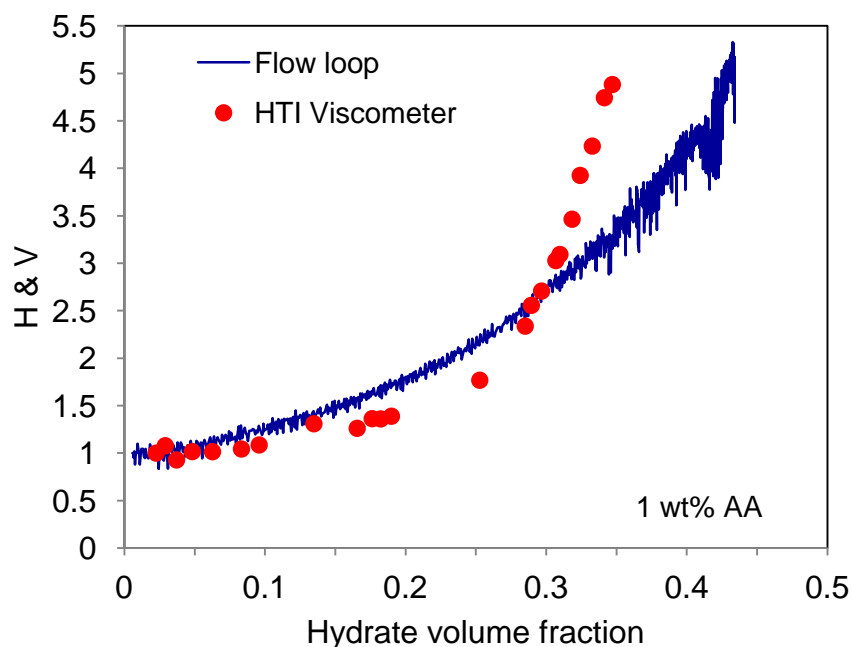


**Figure 7. 9 Comparison of small scale and flow loop test with 60% WC, 1 wt. % AA and 5 wt. % salt. Flow loop pump speed and high pressure autoclave cell mixer speed were kept constant during the tests at 150 RPM and 200 RPM respectively.**

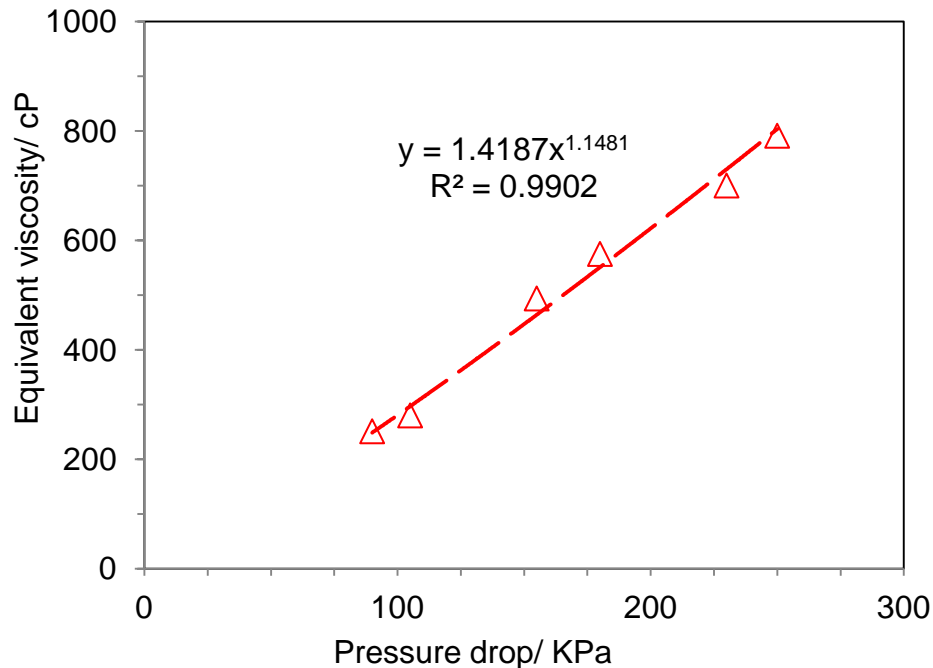


**Figure 7.10 Calibration curve for flow loop to convert pressure drop to viscosity for a constant pump speed of 150 RPM.**

## 7.6 CONCLUSIONS

The rheological behaviour of hydrate slurry flow in high water cut systems has been studied using a saturated flow loop. A total of 5 tests with crude oil (A) as the liquid hydrocarbon phase were reported in this study. The following conclusions have been drawn from the results obtained with the flow loop:

1. An increase in the measured pressure drops occurred almost immediately after hydrate formation for all tests performed at 60% water cut. Similar trends were observed for apparent viscosity of mixtures for the tests with 60% water cut at the small-scale tests. These increases have been attributed to phase inversion of O/W emulsion to W/O emulsion.
2. Pressure drops in the test with 0.6 wt. % AA are greater than in the test with 1 wt. %. This can be attributed to the formation of larger hydrate aggregates in the low AA concentration test.
3. The AA used in this study did not perform so well in freshwater as hydrates deposited on the pipe wall when hydrate volume fraction approached 0.16. However, adding salt



reduced the measured pressure drop considerably during hydrate formation and significantly improved hydrate transportability in the flow loop.

4. At low pump speed test (150 RPM) hydrate particles deposited on the pipe wall at high hydrate volume fractions, while this was not observed for the high pump speed test (300 RPM).
5. The magnitude of pressure drop measurements from the flow loop agrees well with viscosity values from the small scale.
6. A correlation was developed for a limited range of the measured pressure drop by flow loop to relate pressure drops to the viscosity values.

## **7.7 REFERENCES**

Hernandez O.C., 2006. Investigation of Hydrate Slurry. Flow in Horizontal Pipelines. PhD Dissertation, University of Tulsa.

Kelland, M.A., 2006. History of the development of low dosage hydrate inhibitors. *Energy & Fuels*, 20(3): 825-847.

Sjöblom, J., Ovrevoll, B., Jentoft, G.H., Lesaint, C., Palermo, T., 2010. Investigation of the Hydrate Plugging and Non-Plugging Properties of Oils. *Journal of dispersion science and technology*, 31(8): 1100-1119.

## **CHAPTER 8 BIMODAL MODEL FOR PREDICTING THE EMULSION-HYDRATE MIXTURE VISCOSITY IN HIGH WATER CUT SYSTEMS**

### **8.1 INTRODUCTION**

Gas hydrate blockages cause an outstanding flow assurance challenge for oil and gas production with high water cut because hydrate inhibition with traditional techniques often becomes economically and logistically unpractical. In deepwater productions where subcooling is generally too high for kinetic hydrate inhibitors (KHIs), it has been heightened the need to use AAs to help in transporting the fluid produced without a risk of pipeline blockage. As a result, predicting the apparent viscosity of the hydrate slurry is of great importance, since understanding the apparent viscosity is the key to manage the transportability of hydrate slurry and the associated pressure drop (pump requirement).

The viscosity of hydrate slurry is of great interest in various research areas both applied and fundamental. Most of the existing predictive models for calculating viscosity of hydrate slurry use the liquid hydrocarbon phase as the continuous phase and the relative viscosity is defined as the ratio of hydrate slurry viscosity to oil viscosity. This has been found to be almost correct for low water cut systems, where most or all of the water phase is converted into hydrate particles and the continuous phase is mainly liquid hydrocarbon. However, the experimental results given in the previous chapters showed that, in the case of high water cut systems, there can always be a free water phase in a system that produces a three phase flow of water, oil and hydrate particles, where the water-oil emulsion behaviour has a significant role on the viscosity of the mixture. The study of the rheological behaviour of such systems is important for transporting hydrate slurries without the risk of hydrate plugging. Little work has been conducted in this area to date.

In this chapter, a model to predict the viscosity of water-oil emulsion in the presence of hydrate particles in high water cut systems using a bimodal mixture concept is proposed. In the model, water-oil emulsion and hydrate particles in the liquid continuous phase are treated separately as unimodal models. In addition, a modification has been applied to the Mills (1985) model to calculate the viscosity of unimodal hydrate suspensions. The model has been validated using the experimental data reported in Chapter 6 for high water cut systems in the presence of different

AA concentrations. The predictions of the proposed model are in good agreement with the experimental data for both oil-in-water and water-in-oil hydrate mixtures.

## 8.2 APPLICATION OF THE BIMODAL MODEL TO PREDICT THE VISCOSITY OF A WATER/OIL/HYDRATE MIXTURE

The rheological behaviour of a water/oil/hydrate mixture is shown to be characterized by a bimodal model that represents the mixture made up of hydrate particles as a coarse sized fraction and liquid droplets as a fine sized fraction. According to the model, these coarse and fine fractions behave independently of each other, as will be explained in the following sections.

### 8.2.1 Bimodal Suspensions

A bimodal suspension can be regarded as a system consisting of two different sized particles, as the larger particles are suspended in a continuous fluid containing the smaller particles (Eveson et al., 1951). A considerable amount of literature has been published on this issue indicating that in bimodal suspensions the small particles behave essentially as a suspending medium toward the large sized particles (Farris, 1968; Yan et al., 1991b). Farris (1968) was one of the first investigators to develop a model to predict the viscosity of multimodal suspensions based on geometric argument. For simplicity he firstly made a bimodal model by adding the large particles to the suspension of small ones. The small particles behaved as a fluid towards the large ones when the relative size of coarse particles is sufficiently greater than fine particles. The equation (Equation 8.1) given by Farris (1968) for a bimodal suspension is

$$\frac{\mu_{SUSP}(\varphi_L, \varphi_S)}{\mu_f} = \left[ \frac{\mu_s(\varphi_S)}{\mu_f} \right] \times \left[ \frac{\mu_L(\varphi_L)}{\mu_f} \right] \quad (8.1)$$

where  $\mu_{SUSP}$  is the bimodal suspension viscosity containing large and small particles.  $\mu_f$  indicates the viscosity of the suspending medium (pure fluid) and the  $\mu_L$  and  $\mu_s$  indicate the unimodal suspension viscosity of large and small particles. In Equation 8.2  $\varphi_L$  denotes the volume fraction of large particles in the total suspension volume and in Equation 8.3  $\varphi_s$  denotes the volume fraction of small particles in the pure fluid plus small particles:

$$\varphi_L = \frac{V_L}{V_L + V_S + V_f} \quad (8.2)$$

$$\varphi_S = \frac{V_S}{V_S + V_f} \quad (8.3)$$

where  $V_L$ ,  $V_S$  and  $V_f$  are the volume of large and small particles and pure fluid, respectively.

Although Farris' model was developed for suspensions of solid-solid particles, the concept can be applied for liquid-solid particles suspended in a continuous liquid which is immiscible with the liquid droplets. Numerous experimental studies have attempted to explain the rheological behaviour of water-oil emulsion in the presence of solids (Pal and Masliyah, 1990; Yaghi, 2001; Yan and Masliyah, 1993; Yan et al., 1991a; Yan et al., 1991b). The most illustrative work was performed by Yan et al. (1991b) who studied the rheological properties of model suspensions with bimodal particle size distribution. They analyzed the results of viscosity measurements of oil in water emulsion with the addition of solid particles. From their experimental work they observed that it is possible to consider the mixture as a bimodal suspension. Their findings showed that in a ternary system consisting of water/oil/solid mixture, when the size ratio of solid particles to the oil droplets is greater than 3, the viscosity of the mixture can be predicted from the viscosity of unimodal oil in a water emulsion and unimodal solid particles in a water phase, as the behaviour of the oil droplets is completely independent of the solid particles. This finding was in agreement with Farris (1968), who stated that the small particles act as a suspending medium towards the larger particles.

Yan et al. (1991b) revealed that in the water/oil/solid mixture, where the solids were larger in size than the dispersed liquid droplets (by at least 3 times), it is possible to correlate the rheological data of the emulsion and solids by assuming that the solid addition is made into a homogeneous fluid of oil in water emulsion. Therefore, the mixture can be treated as a bimodal system that acts as two separated unimodal systems. In other words, the viscosity of the water/oil/solid mixture, which is a ternary system, can be regarded as the viscosity of its binary components, i.e., oil in water emulsion and solid in water suspension. Yan et al. (1991b) extended this concept of a bimodal system to experimentally develop a model to predict the viscosity of a water/oil/solid mixture. They used three different types of oil as the dispersed liquid phases, and in all experiments the size ratio of the solid to the oil droplets was larger than three. Due to the dependency of the rheological behaviour of the emulsion-solid mixtures on

shear rate, the shear rate was kept constant during the experiments. They gathered a large amount of viscosity measurement data for ternary systems and were able to derive the following equation (Equation 8.4.):

$$\mu_{OWS}(\beta_o, \varphi_s) = \frac{\mu_{SW}(\varphi_s) \times \mu_{OW}(\beta_o)}{\mu_w} \quad (8.4)$$

where  $\mu_{OWS}$ ,  $\mu_{WS}$ ,  $\mu_{OW}$  and  $\mu_w$  denote the viscosities of the solid/oil/water mixture, unimodal suspension of the solid particles, oil in water emulsion and pure water phase, respectively. It should be noted that Yan et al. (1991b), similarly to Farris (1968), distinguished between volume fraction of oil droplets,  $\beta_o$ , and volume fraction of solid particles,  $\varphi_s$ , based on the following equations:

$$\beta_o = \frac{V_o}{V_o + V_w} \quad (8.5)$$

$$\varphi_s = \frac{V_s}{V_s + V_w + V_o} \quad (8.6)$$

where  $V_s$ ,  $V_o$  and  $V_w$  are the volume of the solid particles, oil droplets and water phase, respectively. From Equations 8.5 and 8.6 it is clear that for determination of  $\beta_o$ , the solid particles were excluded from the water phase; however, for  $\varphi_s$  all phases were taken into account. Equation 8.4 can be written in the following different forms:

$$\frac{\mu_{OWS}(\beta_o, \varphi_s)}{\mu_{SW}(\varphi_s)} = \frac{\mu_{OW}(\beta_o)}{\mu_w} = \psi_1(\beta_o) \quad (8.7)$$

$$\frac{\mu_{OWS}(\beta_o, \varphi_s)}{\mu_{OW}(\beta_o)} = \frac{\mu_{SW}(\varphi_s)}{\mu_w} = \psi_2(\varphi_s) \quad (8.8)$$

$$\frac{\mu_{OWS}(\beta_o, \varphi_s)}{\mu_w} = \frac{\mu_{OW}(\beta_o)}{\mu_w} \times \frac{\mu_{SW}(\varphi_s)}{\mu_w} \quad (8.9)$$

From Equation 8.7 we can see that the ratio of the mixture viscosity to the unimodal suspension viscosity of solid particles is equal to the unimodal relative viscosity of pure emulsion (free of

solid), which is just a function of volume fraction of the oil droplets,  $\beta_o$ . Based on Equation 8.8, normalize mixture viscosity with respect to pure emulsion viscosity is equal to relative viscosity of pure solid suspension in water. The second term of Equation 8.8 demonstrates that this normalized mixture viscosity is only a function of the solid volume fraction and is independent of the dispersed oil droplets. The interesting points in the last terms of Equations 8.7 and 8.8 are that they strongly indicate that a bimodal suspension system can be regarded as two separated unimodal systems, i.e. solid in water mixture and oil in water emulsion. This concept is very helpful to predict the viscosity of water/oil/solid mixtures. Equation 8.9 clearly demonstrates that the relative viscosity of the mixture is calculated by multiplying the unimodal relative viscosity of the pure emulsion and the unimodal relative viscosity of the pure solid suspension.

Later, Pal. et al. (1992) conducted an experimental study to investigate the applicability of Equation 8.4 to evaluate the effect of added water droplets on the rheological behaviour of clay in oil suspensions. The size of the clay solid particles were about one order of magnitude smaller than the water droplets as it was assumed that the water droplets see the solid particles in oil suspension as a homogeneous fluid. The authors were able to derive an equation similar to Equation 8.4 for predicting the viscosity of the ternary clay/oil/water mixture as follows:

$$\frac{\mu_{wso}(\beta_s, \varphi_w)}{\mu_o} = \frac{\mu_{wo}(\varphi_w)}{\mu_o} \times \frac{\mu_{so}(\beta_s)}{\mu_o} \quad (8.10)$$

where  $\varphi_w$  and  $\beta_s$  denote the volume fraction of water in the total mixture and the clay volume fraction on a water free basis, respectively.

### 8.2.2 Unimodal Suspension -Viscosity of Hard-Sphere Suspensions

In very dilute solid suspensions the relative viscosity,  $\eta_{RS}$  (the ratio of the viscosity of the suspension,  $\mu_s$ , to the viscosity of the continuous fluid,  $\mu_c$ ) increases linearly as the suspension concentration increases. Einstein (1906) was the first person who considered the effect of the volume fraction of solid particles,  $\varphi_s$ , on the relative viscosity of the suspension by Equation 8.11:

$$\eta_{RS} = \frac{\mu_s}{\mu_c} = 1 + 2.5\varphi_s \quad (8.11)$$

where  $\varphi_s < 0.02$ . However, at moderate and high solid concentrations, the viscosity increases nonlinearly with  $\varphi_s$ . Numerous studies have attempted to explain the relative viscosity at concentrated suspensions. Roscoe (1952) extended Equation 8.11 to higher concentrations by incorporating interaction between hard spheres. He made the assumption that a certain amount of liquid immobilizes around the contact point of particles, which increases effective concentration by a factor of 1.35:

$$\eta_{RS} = \frac{\mu_s}{\mu_c} = (1 - 1.35\varphi_s)^{-2.5} \quad (8.12)$$

Krieger (1959) also derived a semi-empirical equation for high concentrate hard-sphere systems:

$$\eta_{RS} = \frac{\mu_s}{\mu_c} = \left(1 - \frac{\varphi_s}{\varphi_{\max}}\right)^{-[\lambda]\varphi_{\max}} \quad (8.13)$$

where  $[\lambda]$  is the intrinsic viscosity ( $[\lambda] = 2.5$  for hard spheres), and  $\varphi_{\max}$  is the maximum packing fraction (the critical volume fraction relative to the transition threshold between the fluid state and the solid state).

Another equation that has been widely used to study the relative viscosity of concentrated suspensions was developed by Mills (1985). This equation gives good agreement with experimental data for the hard spheres with only hydrodynamic interactions:

$$\eta_{RS} = \frac{\mu_s}{\mu_c} = \frac{1 - \varphi_s}{\left[1 - \frac{\varphi_s}{\varphi_{\max}}\right]^2} \quad (8.14)$$

where  $\varphi_{\max}$  is taken as the approximately random close packing concentration of mono-dispersed spheres, regarded as equal to  $4/7$ .

### 8.2.3 Unimodal Suspension -Viscosity of Pure Emulsion

In general, the relative viscosity of a unimodal water-oil emulsion depends on a number of factors, such as the volume fraction of the dispersed phase, shear rate (if non-Newtonian), temperature, viscosity of the continuous and dispersed phases and the nature and concentration of the emulsifying agents. There is a large volume of published studies describing the role of dispersed phase volume fraction on the relative viscosity of unimodal water-oil emulsion,  $\eta_E$ , i.e. the ratio of the emulsion viscosity  $\mu_E$  to the viscosity of the pure continuous phase  $\mu_c$ . The



Taylor (1932) equation was the first equation that took into account the dispersed volume fraction, viscosity of the dispersed droplets and continuous phases in very dilute emulsions. The equation is given by:

$$\eta_E = 1 + \frac{(5K + 2)}{2(K + 1)} \beta_d \quad (8.15)$$

where  $\beta_d$  is the volume fraction of the dispersed liquid droplets and  $K$  is the ratio of dispersed-phase viscosity,  $\mu_d$ , to continuous-phase viscosity,  $\mu_c$ :

$$K = \frac{\mu_d}{\mu_c} \quad (8.16)$$

In this equation, the interactions between droplets have a negligible effect and the equation is only valid for very low concentrations. The Taylor equation (Equation 8.15) can be reduced to the Einstein (1906) Equation (Equation 8.11) as long as the dispersions are spherical solid particles where the  $K$  ratio tends to infinity. Several attempts have been made to develop an appropriate equation for emulsions containing high concentrations of dispersed droplets, but there has always been at least an unknown parameter that needs to be determined experimentally. For example, the equation below shows Pal and Rhodes' (1985) correlation for the relative viscosity of an emulsion

$$\eta_E = \left[ 1 + \frac{\beta_d / R}{1.187 - (\beta_d / R)} \right]^{2.5} \quad (8.17)$$

where the parameter  $R$  is the dispersed phase volume fraction, for which the relative viscosity  $\eta_E$  equals 100 and is used as a fitting parameter that must be determined experimentally for every emulsion system.

Pal (2000) has also developed an equation to predict the relative viscosity of emulsions consisting of nearly spherical droplets. He found that the presence of surfactants in the system causes a significant amount of the continuous-phase liquid to become attached to the droplet surface. Starting from Taylor's (1932) equation (Equation 8.15) and using this concept, Pal (2000) derived a viscosity equation for concentrated emulsions. His equation is given by:

$$\left[ \frac{\mu_E}{\mu_c} \right]^{-2/5} \left[ \frac{2(\mu_E / \mu_c) + 5K}{2 + 5K} \right]^{-3/5} = 1 - K_0 \beta_d \quad (8.18)$$

where  $K_0$  is a tuning factor that needs to be defined experimentally for every system. This factor takes into account the presence of adsorbed surfactants on the surface of the droplets. The value of  $K_0$  is constant for a certain emulsion system; however, it may not be identical for different emulsion systems. This factor depends mainly on the following parameters: a) the nature of the surfactant b) the concentration of the surfactant c) the chemical nature of the dispersed and continuous phases.

#### **8.2.4 Development of a New Viscosity Equation for the Relative Viscosity of Hydrate Slurry**

As mentioned previously, in the case of dilute suspensions, the real solid volume fraction is only taken into account for predicting relative viscosity. For concentrated suspensions many models have been reported in the literature for taking into account the swelling of the real volume of particles, which is believed to occur due to the immobilised fluid around the contact point of the particles. In the case of hydrate slurry, the viscosity of suspension is higher than those of suspensions of solid spheres at the same true concentration. It can be explained that hydrate particle clusters grow due to the capillary adhesive forces presented between the particles, resulting in the formation of bigger aggregates. To study the rheology of hydrate slurry, several theoretical models have been proposed to take the hydrate agglomeration into account (Camargo and Palermo, 2002; Colombel et al., 2009; Fidel-Dufour et al., 2006; Palermo et al., 2005). In these models, it is believed that the main reason for unexpected hydrate swelling can be due to formation of hydrate fractal aggregates (Colombel et al., 2009; Leba et al., 2010). Figure 8.1 shows a volume of liquid phase (water and liquid hydrocarbons) captured within the hydrate aggregates and their apparent volume fraction is higher than the volume fraction of elementary particles. It is assumed that, at each time step, the whole volume of each water droplet converts to hydrate (assuming the equilibrium conditions). But, when one studies the rheological behaviour of hydrate slurry during hydrate formation, it is observed that in high water cut systems it can cause some deviations due to the presence of unconverted water inside the particles. During hydrate formation, based on the shell model, hydrate firstly forms on the exterior of the water droplets and the unconverted water remains within the hydrate shells (Turner et al., 2009; Turner, 2005). For a predictive model, what is important is the volume of aggregated hydrate particles, i.e. the volume fraction of hydrate shells and occluded water inside of them and the trapped fluid among particles (Figure 8.1).

In this work all the contributions from different factors are gathered into one parameter: the effective volume fraction. It can then be possible to apply the rules of solid suspensions to predict the relative viscosity of the hydrate slurry. We assume that the effective hydrate volume fraction,  $\varphi_{eff}$ , is related to the true hydrate volume fraction,  $\varphi$ , as:

$$\varphi_{eff} = \left( \frac{1}{1-\gamma} \right) \varphi \quad (8.19)$$

where  $\gamma$  is the fraction of total volume of an aggregate not occupied by hydrate shells.

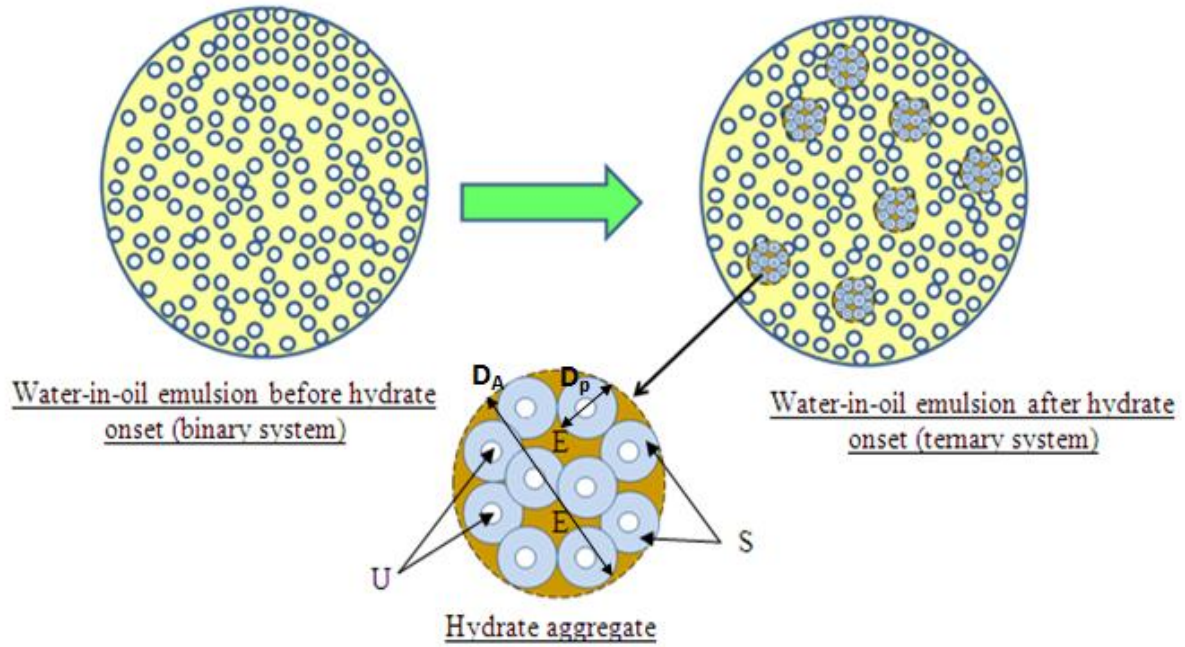


**Figure 8. 1** Conceptual model of a hydrate aggregate enclosed by the dashed circle; the hydrate shells covering the hydrate particles, denoted by “S”; unconverted water inside hydrate particles, denoted by “U” and emulsion trapped in the void space of the fractal structure, denoted by “E”.  $D_A$  denotes the hydrate aggregate diameter and  $D_p$  denotes the hydrate particle diameter

Replacing the term  $(1/(1-\gamma))$  in the above equation by the trapped liquid factor,  $K_v$ , one can write:

$$\varphi_{eff} = K_v \varphi \quad (8.20)$$

The value of  $K_v$  depends on the size of the aggregate, which is determined by the balance between adhesive and viscous forces among particles (Camargo and Palermo, 2002). The aggregate diameter is also believed to be a function of shear rate, oil viscosity, and oil–water

interfacial tension (Turner et al., 2009). Consequently, the value of  $K_v$  may vary from one hydrate slurry system to another, which mostly depends on the composition of liquid hydrocarbon and surfactant concentration in the system.

In the model to predict the relative viscosity of unimodal hydrate slurry, the hydrate volume fraction in Equation 8.14 is replaced with the effective hydrate volume fraction from Equation 8.20 as follows:

$$\eta_{RS} = \frac{\mu_s}{\mu_c} = \frac{1 - K_v \phi}{\left[1 - \frac{K_v \phi}{\phi_{\max}}\right]^2} \quad (8.21)$$

The value of  $K_v$  is determined by tuning the predicted mixture viscosity of the bimodal model with experimental data.

### 8.3 MODEL DESCRIPTION

Numerous studies have attempted to predict the rheological behaviour of hydrates in a continuous liquid phase as hydrate slurry. So far, however, there has been very little discussion about the rheological behaviour of emulsion-hydrate mixtures. It is recognized that the rheological behaviour of water-oil emulsion has a significant effect on the behaviour of hydrate slurry flow. Therefore, a model for predicting viscosity of emulsions with added hydrate particles needs to be developed, addressing the rheological behaviour of hydrate slurry in high water cut systems. The proposed approach in this study is a combination of Pal's model (Equation 8.18) for pure emulsion, a new modified form of the Mills model (Equation 8.21) for unimodal hydrate suspensions and the Yan model (Equation 8.4), to link the viscosities of pure emulsion and unimodal hydrate suspension to predict the viscosity of a water/oil/hydrate mixture.

In the Yan (1991b) model, the main assumption is that the size ratio of the solid particles to the oil droplets is larger than 3. The size of the agglomerated hydrate particles, which is determined by the force balance between inter-particle adhesive and shear forces, depends on many parameters, such as interfacial tension between water and oil phases, shear rate and oil composition. There is a large volume of published studies that confirms that hydrate particles can stick together during hydrate formation and create much bigger aggregates (Leba et al.,

2010; Palermo et al., 2005; Pauchard and Palermo, 2005) (Figure 8.1). The surface of hydrate particles is inherently hydrophilic, and thus, the presence of water droplets between hydrate particles creates a strong capillary force, which would hold the hydrate particles together. It has also been observed that a volume of liquid phase containing water and oil phases can be captured within these aggregates (Austvik et al., 2000). Recently Leba et al. (2010) have investigated the agglomeration phenomenon of hydrate particles. They observed that hydrate particles attached together to form large aggregates in the presence of certain concentration of AA. Leba and co-workers (2010) explained that hydrate aggregates have a fractal structure and can be characterized by their fractal dimension which is a measure of the way by which hydrate particles are fitted together in the 3D space. They concluded that hydrate aggregates are constructed from initial hydrate particles with numbers of particles from 200 to 1500, depending on lengths of time of the hydrate crystallization.

It has been indicated that, for similar systems, the rheological behaviour of hydrate slurry changes with AA concentration (Gao, 2009; York and Firoozabadi, 2009). The main function of AAs is to produce dispersed hydrate particles in the hydrate slurry. The performance of an AA depends on many parameters, including, mainly, the type of AA, water cut, AA concentration, and composition of the liquid hydrocarbon phase. It is believed that the quality of AA gets worse with increasing water cut (Gao, 2009; York, 2008) because the inter-particle interactions among hydrate particles become more important (Anklam et al., 2007). Studies of the effect of AA on hydrate transportability in high water cut systems have shown that, in high water cut systems in the presence of AA, system plugging may occur due to hydrate agglomeration (Azarinezhad, 2010; Gao, 2009; York, 2008). Gao (2009) conducted several experiments to investigate the effect of AA concentration on hydrate transportability in high water cuts from 30% to 80%. His results showed that transportability of hydrate slurry strongly depended on AA concentration. He also presented several photographs that exhibited hydrate particles aggregated in the presence of AA concentrations even up to 3%. York (2008) used two different types of AA to study the effect of salt on the performance of AAs. Although at low water cut systems, with a certain concentration of AA and salt, the systems were not plugged, they observed that, in high water cut systems, AAs could not prevent hydrate agglomeration at all. The effect of AA in high water cuts is an important new area that requires further research. Therefore, the following simplifying assumptions were used in the calculations:

- i. Primary hydrate particles stick together to form hydrate aggregates as the diameter of aggregates are at least three times bigger than that of the dispersed droplets
- ii. Hydrate aggregates are considered as coarse particles and water/oil dispersed droplets in the emulsion are considered as fine particles

To calculate the viscosity of pure emulsion at each time step from Equation 8.18, we need to know the values of  $K_0$  and  $\beta_d$ . The amount of oil and surfactants in the system during hydrate formation are constant and only gas is injected to form hydrate particles. It can be assumed that the oil composition is constant during the test; therefore, the value of  $K_0$  is constant during the experiment. From Equation 8.18 and the viscosity of pure emulsion before hydrate onset,  $\mu_{E0}$ , the value of  $K_0$  can be calculated. During hydrate formation, the water phase steadily converts into hydrate particles, resulting in the reduction of the volume fraction of the water phase in the emulsion. The volume fraction of the dispersed phase,  $\beta_d$ , can be given by:

$$V_{Wi} = V_{W_0} - V_{WCon} \quad (8.22)$$

$$\beta_d = \frac{V_{Wi}}{V_o + V_{Wi}} \quad \text{for water in oil emulsions} \quad (8.23)$$

or

$$\beta_d = \frac{V_o}{V_o + V_{Wi}} \quad \text{for oil in water emulsions} \quad (8.24)$$

where  $V_{Wi}$  is the volume of the liquid water phase in the emulsion for each time step (i),  $V_{W_0}$  is the volume of the initial water phase in the system (before hydrate onset) and  $V_{WCon}$  is the total water converted into hydrate at time step (i).

Like the Yan et al. (1991b) model, the hydrate/water/oil system is regarded as a bimodal suspension system, consisting of two different unimodal suspensions, pure hydrate suspension and pure emulsion. The general form of Equation 8.4 is used to link the viscosity of two unimodal suspensions for any type of water-oil emulsion, as follows:

$$\mu_{OWH}(\beta_d, \phi_H) = \frac{\mu_{HC}(\phi_H) \times \mu_E(\beta_d)}{\mu_C} \quad (8.25)$$

where  $\mu_{OWH}$ ,  $\mu_{HC}$ ,  $\mu_E$  and  $\mu_C$  denote the viscosities of the bimodal suspension mixture, pure hydrate suspension, pure emulsion and continuous liquid phase, respectively. The hydrate particle concentration,  $\phi_H$ , and distributed droplet concentration,  $\beta_d$ , are defined as follows:

$$\beta_d = \frac{V_d}{V_d + V_C} \quad (8.26)$$

$$\phi_H = \frac{V_H}{V_H + V_d + V_C} \quad (8.27)$$

where  $V_H$ ,  $V_C$  and  $V_d$  are volumes of the hydrate phase, liquid continuous phase and distributed droplet phase, respectively.

## 8.4 RESULTS AND DISCUSSION

As stated previously, at each time step, using the Pal model (Equation 8.18) for the unimodal water-oil emulsion system, the viscosity of pure oil-water emulsion is first calculated, based on the water volume fraction in the emulsion (solid free). Then the viscosity of the pure hydrate suspension in the suspending medium is predicted, using the new derived equation (Equation 8.21) based on the volume fraction of hydrate particles in the total volume. The bimodal viscosity of the water/oil/hydrate mixture is finally calculated using the general form of Yan (1991b) model (Equation 8.25). Depending on system conditions, different values of  $K_v$  were used to achieve the best fit to the experimental viscosity data.

The model is validated using the experimental data collected from Chapter 6 for high water cut systems in the presence of different AA concentrations and liquid hydrocarbon compositions. Table 8.1 gives further details on the various oil/water/hydrate mixtures which have been considered in this study.

**Table 8. 1 Summary of oil/water/hydrate slurry systems considered in the present work**

Test No.	Initial water cut	AA (wt. %)	Liquid hydrocarbon phase	Type of emulsion
1	50	1	Oil (A)	W/O
2	70	1	Oil (A)	W/O
3	60	0.15	Oil (A)	W/O
4	60	0.3	Oil (A)	W/O
5	60	0.6	Oil (A)	W/O
6	60	1	Oil (A)	W/O
7	60	2	Oil (A)	W/O
8	80	0.3	Oil (A)	O/W
9	80	0.6	Oil (A)	O/W
10	80	1	Oil (A)	O/W
11	80	2	Oil (A)	O/W
12	60	1	Oil (B)	W/O
13	60	2	Oil (B)	W/O

#### 8.4.1 Comparison of Existing Hard-Sphere Models with Experimental Data

Some classical models (Krieger and Dougherty, 1959; Mills, 1985; Roscoe, 1952) to calculate the viscosity of solid particles dispersed in a continuous phase were used to correlate our experimental data. In these models hydrates are only considered as solid inert particles, without interactions with the continuous phase (i.e.  $\phi_{eff}$  is considered to be equal to  $\phi$ ). As can be seen in Figures 8.2 and 8.3, these models deviate from the experimental data (Tests 1 and 2). From these Figures, it is clear that the experimental values fall significantly above the predicted values and the deviation between the experimental and predicted values varies from one system to another. This discrepancy is caused by the fact that considering hydrates as solid spheres, for calculating the viscosity of hydrate suspension, fails to take into account the effect of the hydrate particle agglomeration, in which the liquid phase will be trapped among particles. These comparisons emphasize that there is a need to use the Equation 8.21 for calculating hydrate slurry viscosity, taking into account the effect of the hydrate aggregate growth.



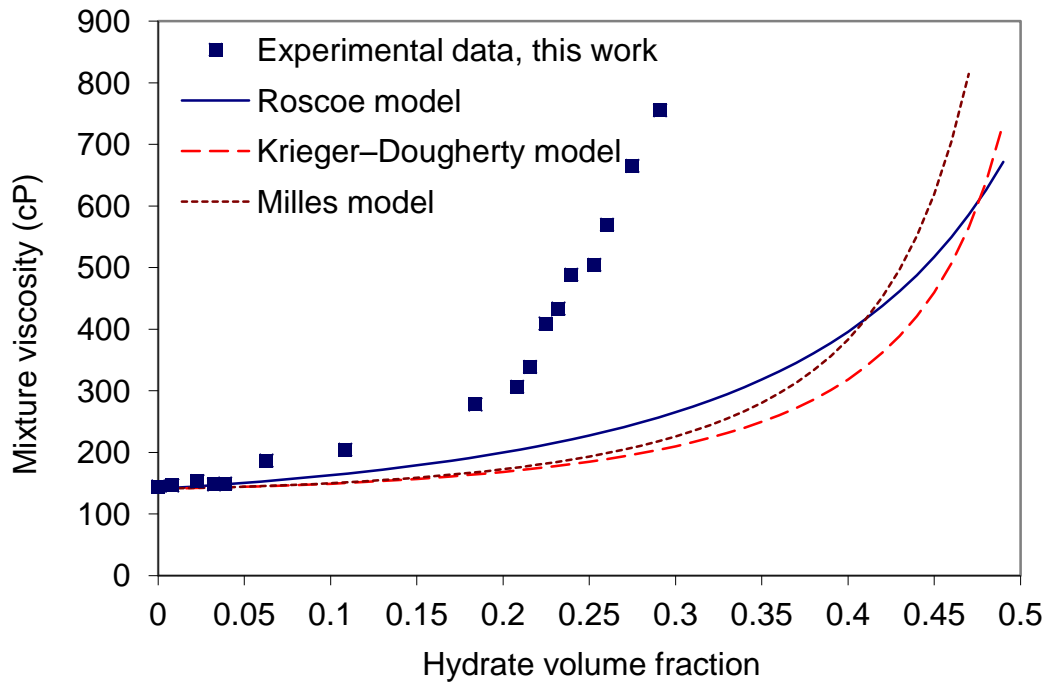


**Figure 8. 2 Comparison between experimental data and existing models for solid spheres: Test 1, 50% water cut and 1 wt. % AA, water-in-oil (A) emulsion.**

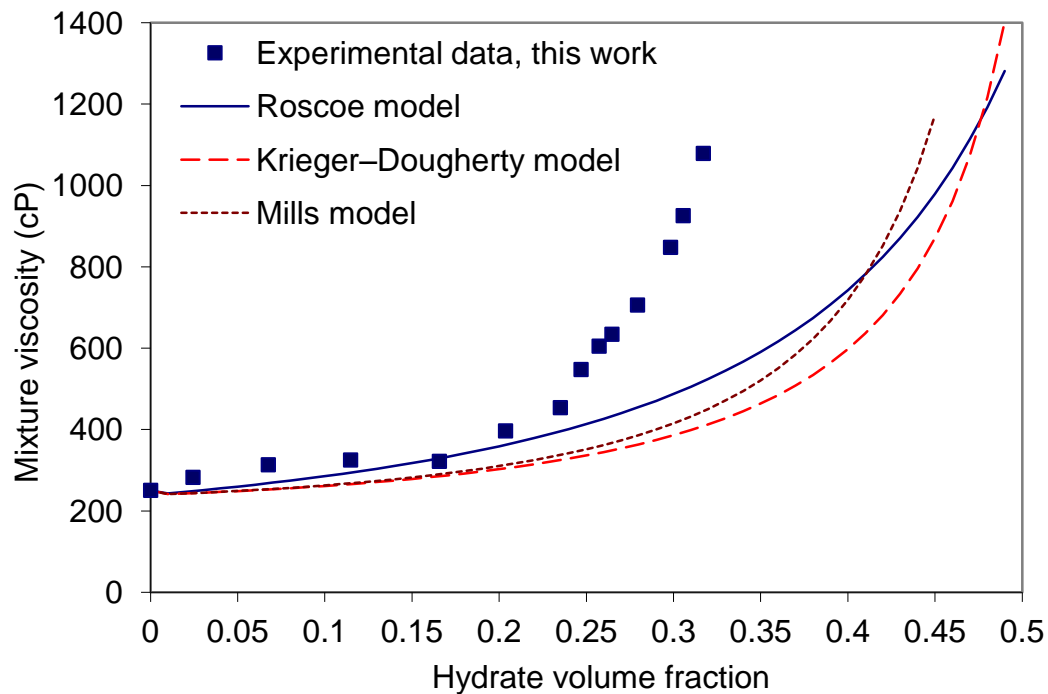


**Figure 8. 3 Comparison between experimental data and existing models for solid spheres: Test 2, 70% water cut and 1 wt. % AA, water-in-oil (A) emulsion.**

### **8.4.2 Effect of Anti-Agglomerant Concentrations**

Experimental results from Chapter 6 showed that AAs play an important role in management of the hydrate slurry viscosity in high water cut systems. Hydrate transportability was improved with increasing AA concentration in the water-oil emulsion and the performance of AA was affected by the liquid hydrocarbon composition. It was indicated that, at low AA concentrations when there is no adequate AA concentration in the system, as the water droplets were converted into the hydrate particles, the flow regime did not follow a regular pattern. These trends can be attributed to the agglomeration tendency of hydrate particles, resulting in the formation of large aggregates which trapped large amounts of the liquid phase within the aggregates themselves. However, with increasing AA concentration, the fluctuations in viscosity measurements significantly reduced and they followed a regular trend.

The model was used to predict the apparent viscosities of water/oil/hydrate mixtures for different AA concentrations by tuning the trapped liquid factor,  $K_v$ . The coefficient of multiple determinations ( $R^2$ ) is used to evaluate the accuracy of the fitted model. If the coefficient of multiple determinations is 1, it provides an excellent response to the input parameters and if the residual error increases, the multiple determination coefficients reduce in the range between 0 and 1. The model has been applied for five different AA concentrations (0.15, 0.3, 0.6, 1.0 and 2.0 wt. %) studied for water-oil (A) emulsion with 60% water cut, as seen in Table 8.1.

Figures 8.4 to 8.7 show the experimental data and the calculated values of the model as a function of hydrate volume fraction. It is clear that the system with low AA concentration displays a more rapid increase in the mixture viscosity as hydrate concentration increases. It has been shown that AA, because of its ability to reduce the adhesive force between hydrate particles, keeps the hydrate aggregates small and well dispersed throughout the mixture (Anklam et al., 2008; Taylor et al., 2008). Hence, with increasing AA concentration the capillary adhesive force between water and hydrocarbon phases decreases, resulting in a reduction in the size of hydrate aggregates. At very low AA concentration (0.15 mass% of AA), the model was unable to predict the increase in mixture viscosity observed. Possible explanations for the initial deviation from the model prediction are due to the presence of a high strength capillary force among the hydrate particles, forming bigger lumps containing large amounts of the liquid phase (Figure 8.4). These may break up in a random manner because of the application of shear force during hydrate formation, but the mixture is not easily transportable.

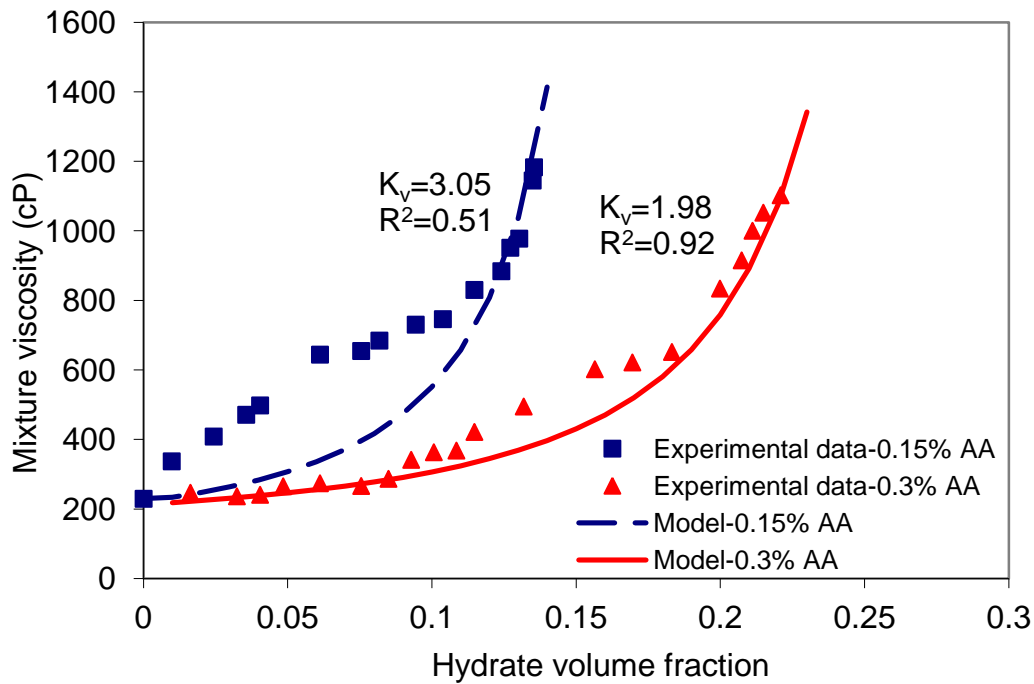


**Figure 8. 4 Comparison between experimental data and proposed model for Tests 3 and 4, 60% water cut, water-in-oil (A) emulsion.**

At higher hydrate concentration, with the reduction in the space between the hydrate lumps, they stick together, which leads to a change in the rheological behaviour of the mixture into a paste, or to visco-elastic behaviour as the mixture viscosity sharply approaches infinity. The value of the trapped liquid factor,  $K_v$  was set to 3.05 in an attempt to match the increase in the mixture viscosity, but  $R^2$  was equal to 0.51, which is still very far from 1. However, as shown in Figure 8.4, by setting the value of  $K_v$  to 1.98 the model could predict the experimental data of Test 4 with 0.3 wt. % AA ( $R^2=0.92$ ). This shows that the system could control the mixture viscosity at a range of hydrate volume fraction, but the hydrate aggregates are still too large and the system was plugged when hydrate volume fraction approached to 0.20.

For Tests 5, 6, and 7, with the same conditions as Tests 3 and 4 but with higher AA concentrations, good fits were found between the model predictions and the experimental data, as the values of  $R^2$  are 0.96, 0.99 and 0.99 for tests with 0.6, 1.0 and 2.0 wt. % AA, respectively (Figures 8.5 to 8.7). Additionally, the value of  $K_v$  has reduced significantly with AA concentration. These results indicate the expected reduction of the amounts of the liquid trapped

among hydrate particles and consequently the size of hydrate aggregates, with increasing AA concentration.

Figures 8.8 to 8.11 show the results for Tests 8-11 for 80% water cut and different AA concentrations ranging from 0.3 to 2.0 wt. % (Table 8.1). The experimental results from Chapter 6 showed that in these tests, due to the high water cuts, the systems were oil in water emulsions throughout the experiments. These systems, in the presence of adequate AA concentrations, were able to transport higher hydrate volume fractions due to the existence of massive amounts of aqueous phase as continuous phase and thus the emulsion viscosity remains low for a wide range of hydrate volume fractions during the experiment. The prediction from the model is not good for low AA concentration (0.3 mass% of AA), as the value of  $R^2$  is equal to 0.76 (Figure 8.8). In this case, the value of  $K_v$  is very large, i.e., 2.45, due to the high volume of liquid trapped within the hydrate agglomerates. However, with increasing AA concentration (resulting in a reduction of the hydrate aggregate size) the ability of the system to control the mixture viscosity at a wide range of hydrate volume fractions increased and could fit quite well with the experimental data (Figures 8.9 to 8.11). It is obvious that the model is also applicable for oil in water systems, as it agrees well with the experimental data at high AA concentrations.

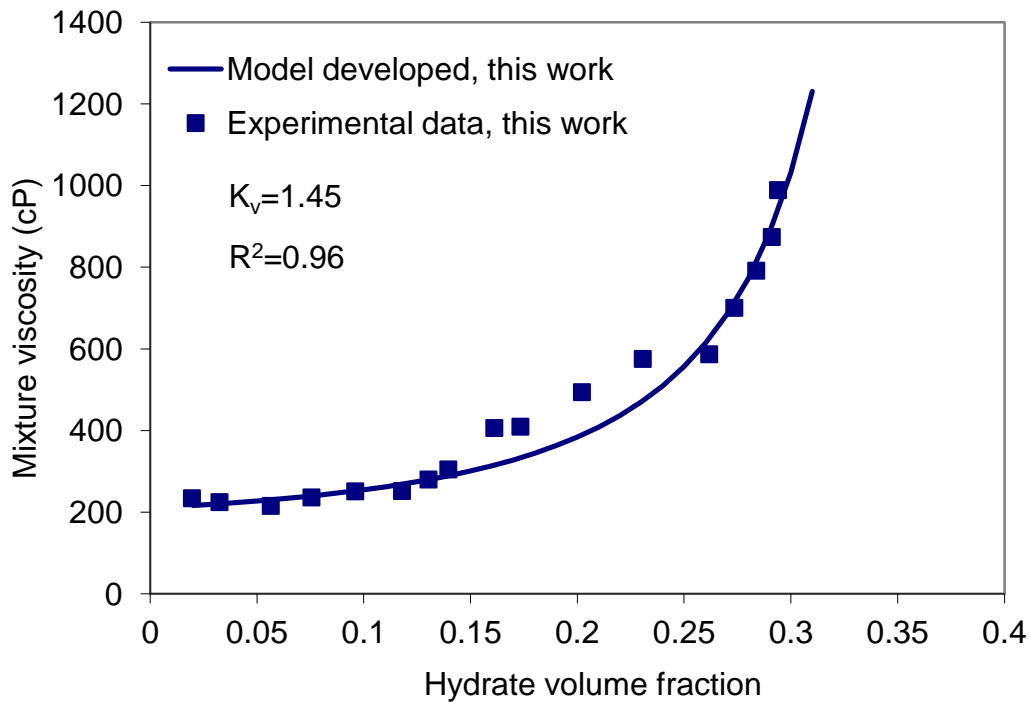


**Figure 8. 5 Comparison between experimental data and proposed model for Test 5, 60% water cut and 0.6 wt. % AA, water-in-oil (A) emulsion.**

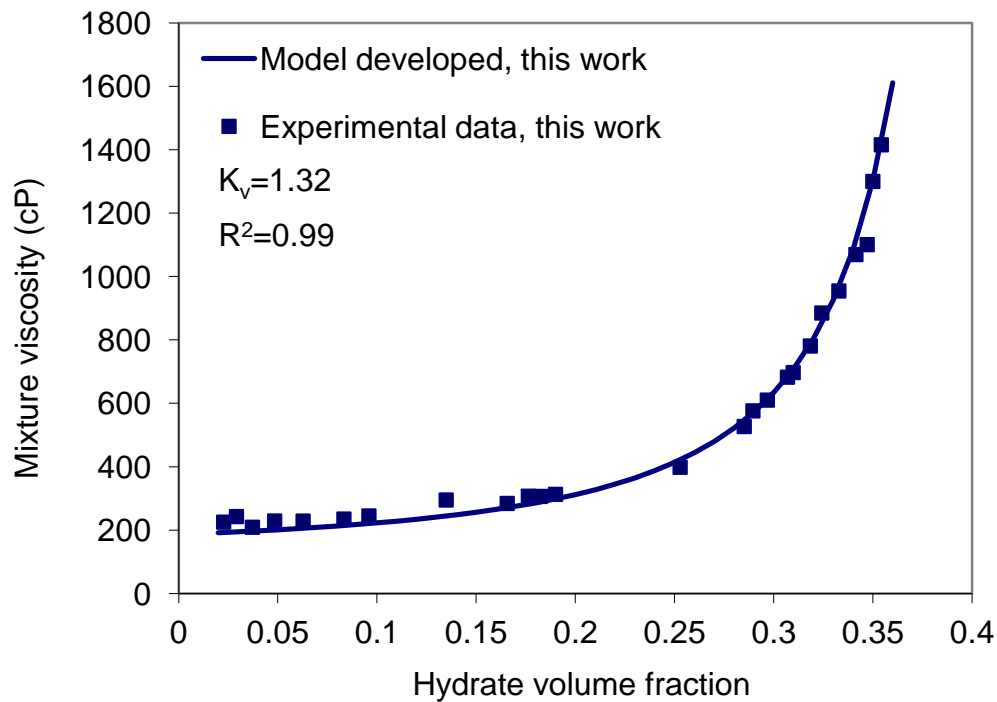


**Figure 8. 6 Comparison between experimental data and proposed model for Test 6, 60% water cut and 1 wt. % AA, water-in-oil (A) emulsion.**

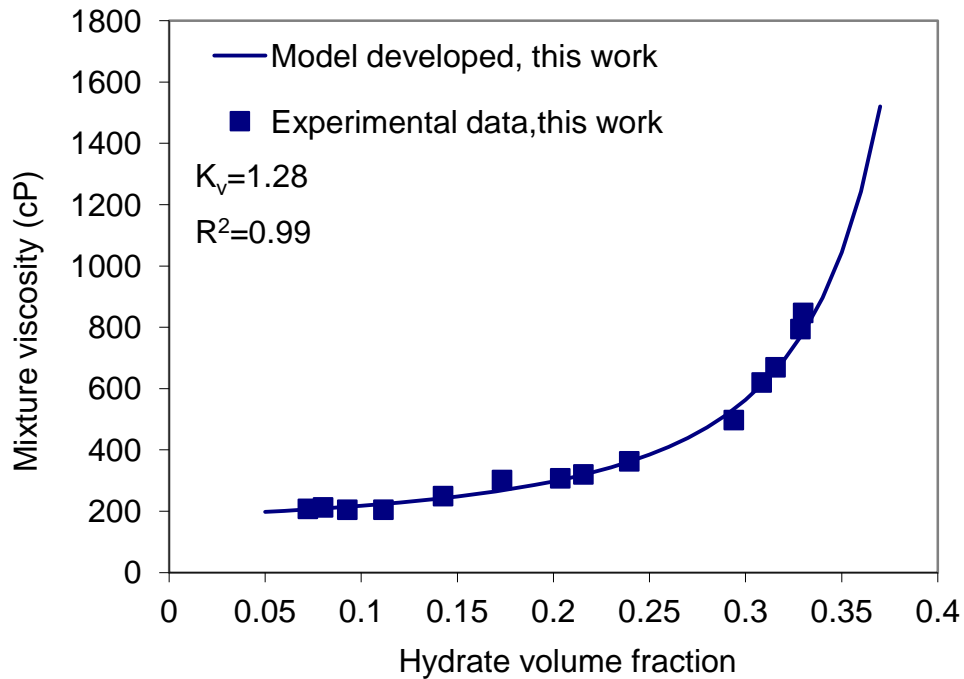


**Figure 8. 7 Comparison between experimental data and proposed model for Test 7, 60% water cut and 2 wt. % AA, water-in-oil (A) emulsion.**

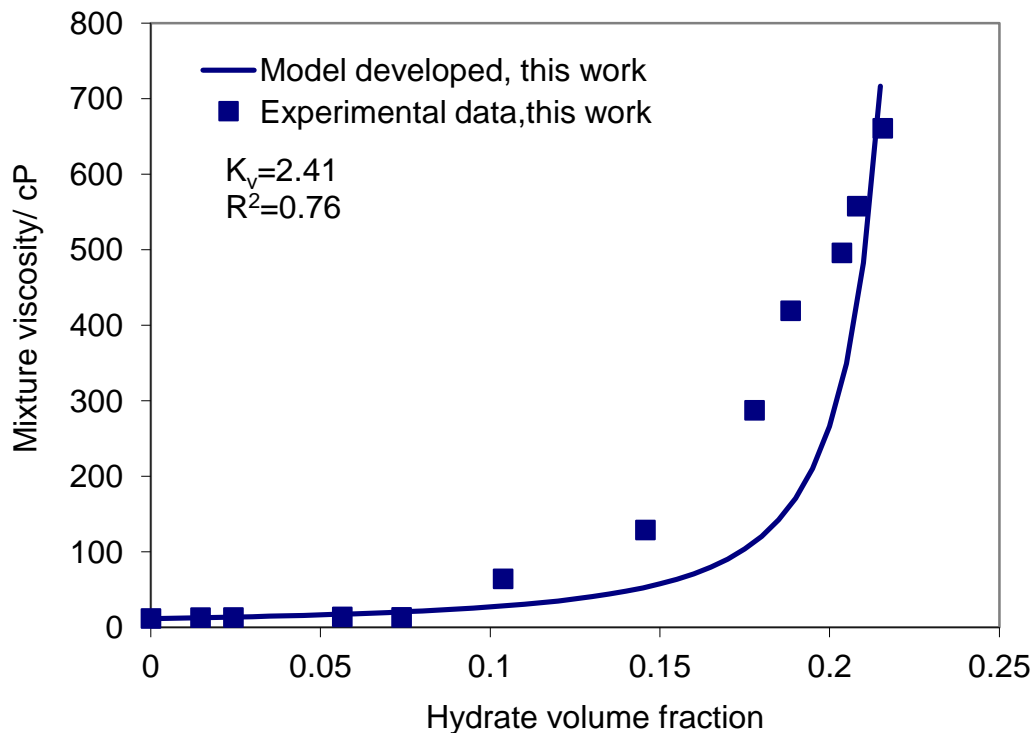


**Figure 8. 8 Comparison between experimental data and proposed model for Test 8, 80% water cut and 0.3 wt. % AA, oil (A) -in-water emulsion.**

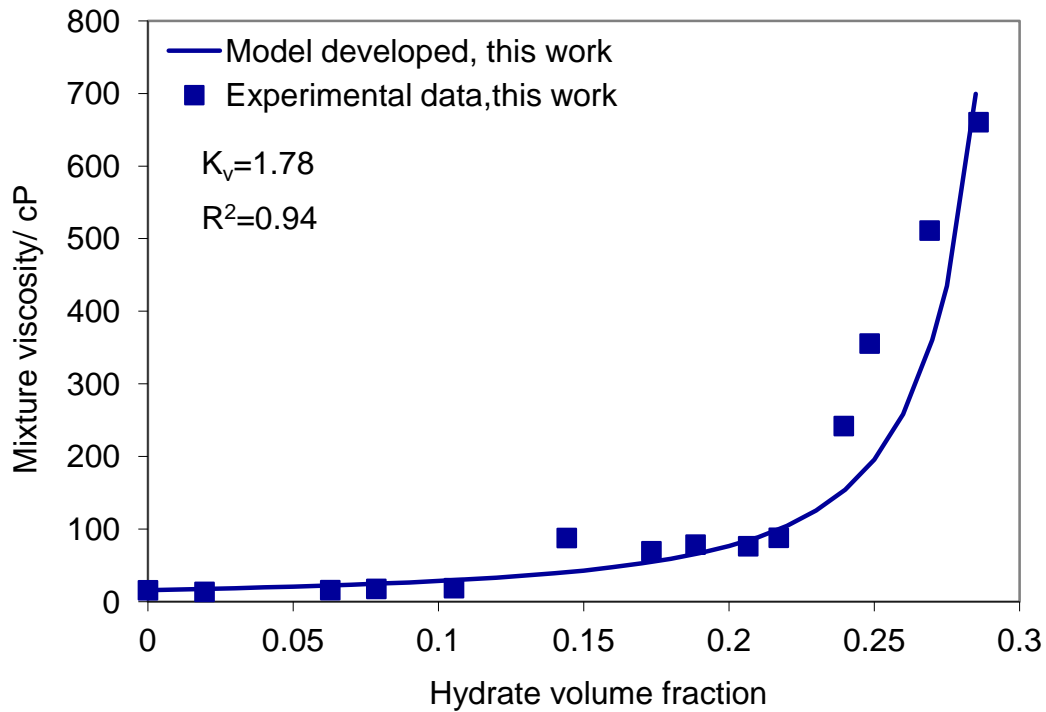


**Figure 8. 9 Comparison between experimental data and proposed model for Test 9, 80% water cut and 0.6 wt. % AA, oil (A) -in-water emulsion.**

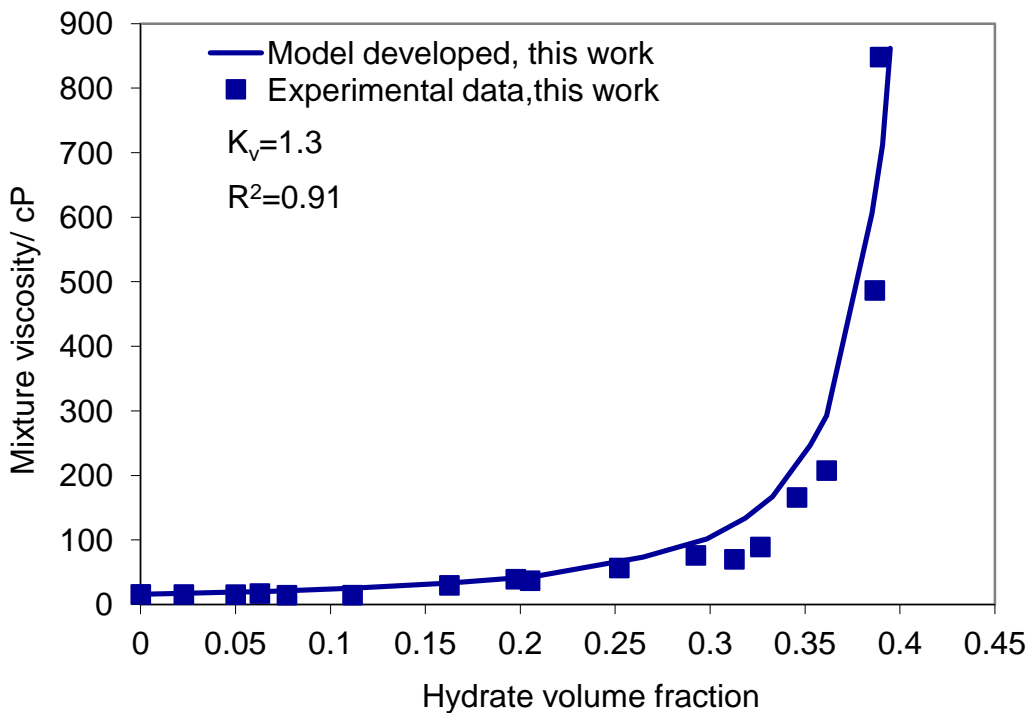


**Figure 8. 10 Comparison between experimental data and proposed model for Test 10, 80% water cut and 1 wt. % AA, oil (A) -in-water emulsion.**

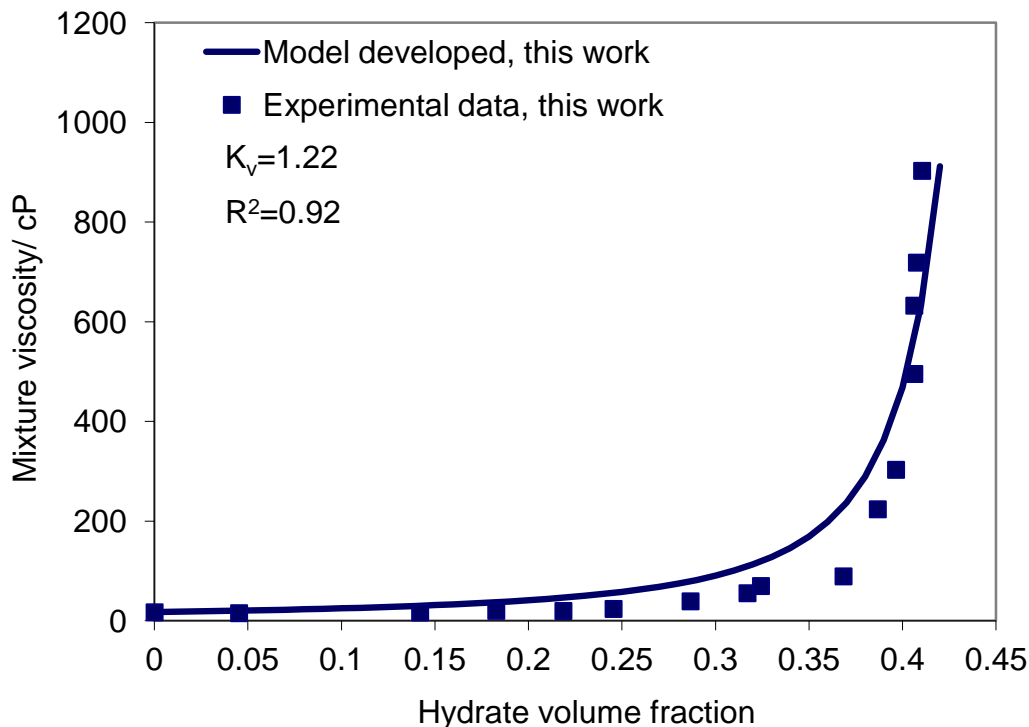


**Figure 8. 11 Comparison between experimental data and proposed model for Test 11, 80% water cut and 2 wt. % AA, oil (A) -in-water emulsion.**

#### 8.4.3 Effect of Liquid Hydrocarbon Compositions

Comparison of the rheological behaviour of hydrate slurry in high water cut systems of two crude oils with different natural surfactant contents indicated that the required concentration of AA to manage hydrate transportability is strongly dependent on the presence of natural surfactants in the liquid hydrocarbon phase (Chapter 6). It was concluded that for the same test conditions and similar AA concentrations the systems containing higher natural surfactants (water-oil (A) emulsions) have higher potential for transporting hydrate particles than systems with lower natural surfactant contents (water-oil (B) emulsions). Production of large hydrate aggregates, including a liquid phase, was supposed to be responsible for the significant differences observed in transportability of different systems. The model was used to predict the apparent viscosities, by setting the  $K_v$  parameter to fit the experimental data.



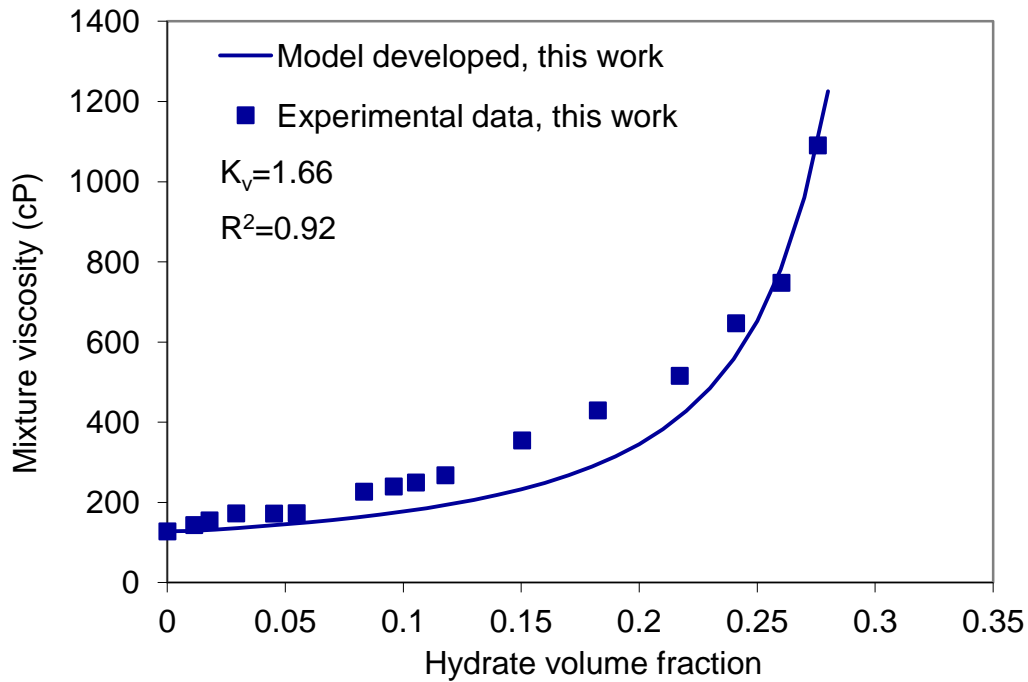


**Figure 8. 12 Comparison between experimental data and proposed model for Test 13, 60%water cut and 1 wt. % AA, water-in-oil (B) emulsion.**

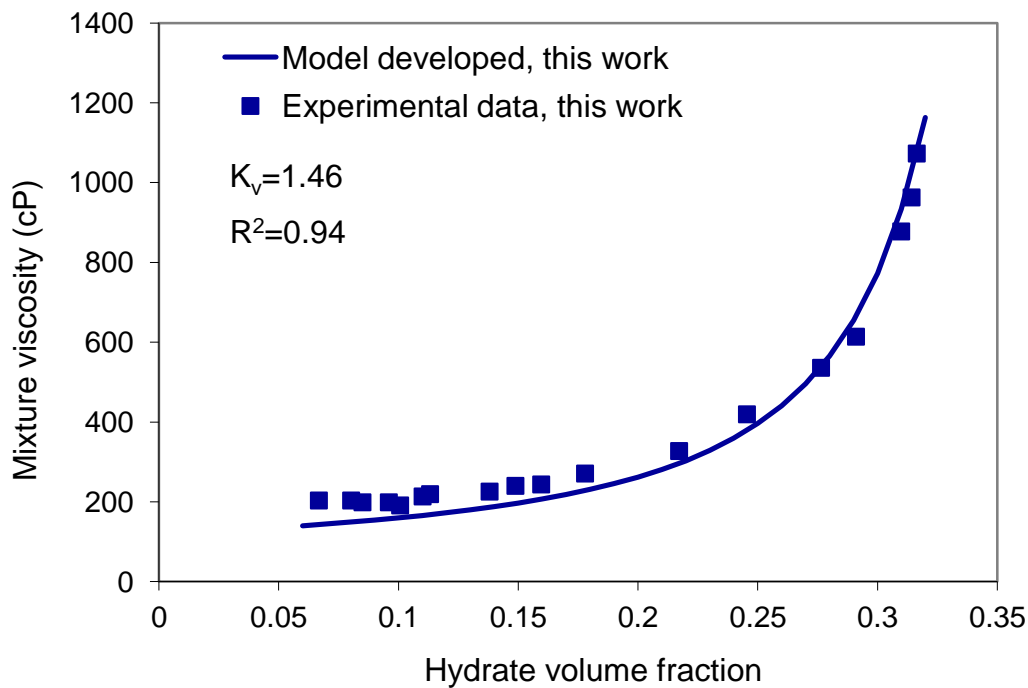


**Figure 8. 13 Comparison between experimental data and proposed model for Test 13, 60% water cut and 2 wt. % AA, water-in-oil (B) emulsion.**

Figure 8.12 shows the apparent viscosity predictions from the model for Test 12 (Table 8.1) as a function of the hydrate volume fractions. To get the best fit to the experimental data, a trapped liquid factor ( $K_v$ ) of 1.66 was used. From the figure, it is apparent that the value of the viscosity data are somewhat above the predicted viscosities, which shows that larger amounts of liquids have been trapped within hydrate aggregates compared to the model predictions.

Comparison of prediction models for the tests with different oil compositions and 1.0 wt % AA, Figures 8.6 and 8.12, shows that a larger trapped liquid factor ( $K_v$ ) was required for the test with water-oil (B) emulsion, to tune the model to the experimental data, than for the water-oil (A) emulsion. It can therefore be suggested that the size of the hydrate aggregates is larger in the water-oil (B) emulsion test, which is most probably due to the lower amounts of natural surfactant (asphaltenes and resins) in the crude oil (B). A recent study by Dieker (2009) reports that presence of asphaltene in the liquid hydrocarbon phase significantly reduces adhesive force between hydrate particles and thus it can act as a co-surfactant to produce transportable hydrate slurry in the attendance of commercial AAs.

For Test 13, with the same conditions as Test 12 but higher AA concentration (2.0 wt. %), Figure 8.13 shows that the best fit was found with a trapped liquid factor ( $K_v$ ) of 1.46. Even though the initial experimental data are slightly above the predicted viscosity values, the model was able to fit well with the data from hydrate volume fractions above 0.1. Comparisons between the two Figures 8.12 and 8.13 shows that with increasing AA concentration, not only does the trapped liquid factor ( $K_v$ ) significantly decrease, but it results in a regular trend of viscosity increases.

#### **8.4.4 Correlation for the Trapped Liquid Factor, $K_v$**

The oil and gas industry has a great interest in predicting hydrate slurry viscosity in order to reduce the risk of hydrate plugging. Predicting the mixture viscosity is a key parameter to manage the value of AA concentration required to produce transportable hydrate slurries. As pointed out before, the trapped liquid factor ( $K_v$ ) is an important parameter to predict viscosity of water/oil/hydrate mixtures. The value of  $K_v$  varies with AA concentration, within a certain oil and gas system. A summary of  $K_v$  values for all the mixtures in this study is given in the Table 8.2. Using the  $K_v$  parameters predicted for high water cut systems at different AA

concentrations, a correlation between the trapped liquid factor ( $K_v$ ) and the AA concentration was found, as shown in Figures 8.14 and 8.15. The figures show plots of  $K_v$  against AA concentration for 60% and 80% water cut systems. It is clear that the value of  $K_v$  decreases and finally levels off with increasing the concentration of AA, at a limit about 1.25 for the systems tested in this study. The best equation that can fit is:

$$K_v = M^{-B} + 0.25 \times M \quad (8.28)$$

where M stands for AA concentration (wt. % of aqueous phase) and B is an empirical parameter that can depend on several factors such as the composition of the liquid hydrocarbon phase, AA performance, salt concentration, etc. Although  $K_v$  reaches a constant value for high AA concentrations, Equation 8.28 can be used to calculate the value of  $K_v$  and consequently mixture viscosity for optimizing AA consumption (usually below 1.0-2.0 wt. %).

**Table 8. 2 Calculated  $K_v$  and  $R^2$  for the systems presented in this work**

Test No.	Trapped liquid factor ( $K_v$ )	Coefficient of multiple determination ( $R^2$ )
1	1.55	0.96
2	1.33	0.98
3	3.05	0.51
4	1.98	0.92
5	1.45	0.96
6	1.32	0.99
7	1.28	0.99
8	2.41	0.76
9	1.78	0.94
10	1.3	0.91
11	1.22	0.92
12	1.66	0.92
13	1.46	0.94

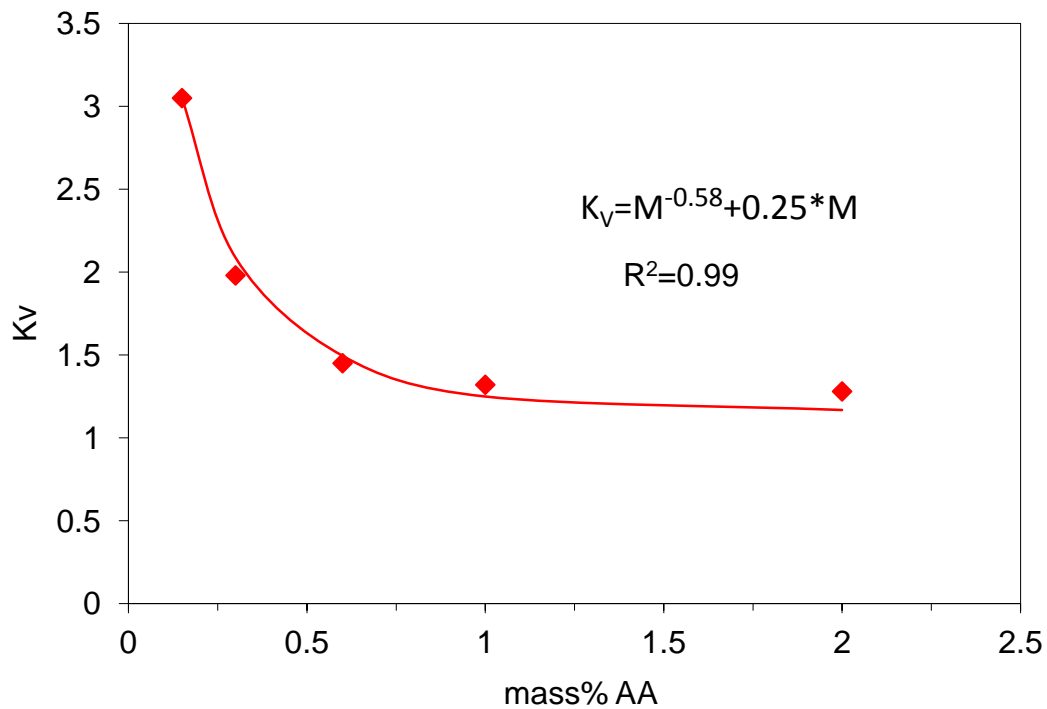


**Figure 8. 14 Trapped Liquid factor,  $K_v$  as a function of AA concentration for 60% water cut, Tests 3-7, water-in-oil (A) emulsion.**

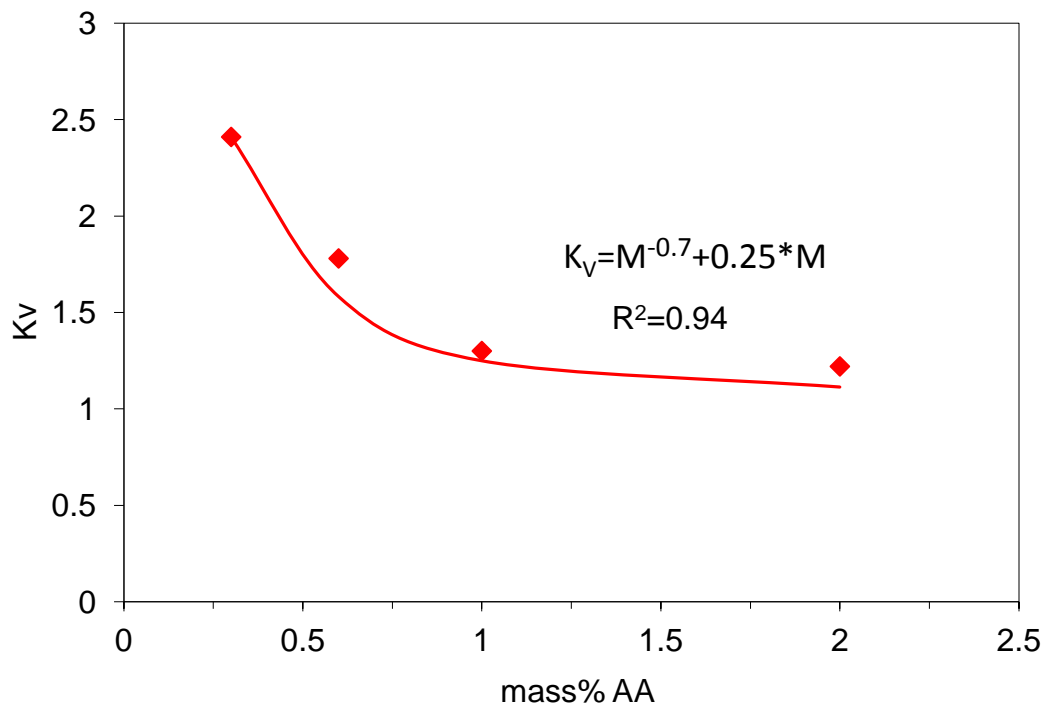


**Figure 8. 15 Trapped liquid trapped factor,  $K_v$  as a function of AA concentration for 80% watercut, Tests 8-11, oil (A) -in-water emulsion.**

## **8.5 CONCLUSIONS**

For water-oil emulsions in the presence of hydrate particles, a bimodal model has been developed to predict the viscosity of a water/oil/hydrate mixture. The model considers the viscosity of the mixture, which is a ternary system, as the viscosity of its binary components, i.e. water-oil emulsion and hydrate suspension. Additionally, a new modified form of Mills' (1985) equation is suggested to describe the viscosity of a hydrate suspension. A good agreement was found between the model and the experimental mixture viscosity data, using the trapped liquid factor,  $K_v$ , as tuning parameter. For very low AA concentrations ( $\leq 0.3$  mass %), possibly due to the presence of large hydrate aggregates, the model was unable to predict the mixture viscosity accurately. However, increasing the AA concentration resulted in a significant reduction in the trapped liquid factor  $K_v$  and gave very good agreement with the experimental data. For the tests with crude oil (A), which has a high concentration of natural surfactants (asphaltenes and resins), lower  $K_v$  was needed to tune the model compared to the tests conducted with crude oil (B), which has a low concentration of natural surfactants. The model also fits the mixture viscosity data for both oil-in-water-hydrate mixtures and water-in-oil-hydrate mixtures, remarkably well. The trapped liquid factor  $K_v$  was not constant for the tests with different AA concentrations, but it approached a constant value at high AA concentrations. For the crude oil (A) and AA used in this study the value of  $K_v$  approached 1.25 with increasing AA concentration.

A correlation for the value of  $K_v$  as a function of AA concentration was derived, in which  $K_v$  is inversely proportional to the AA concentration. The proportionality constant, B is an empirical parameter that can depend on several factors such as the composition of the liquid hydrocarbon phase, AA performance, salt concentration, etc. This correlation could be useful to manage the consumption of AA in different oil and gas production systems.

## **8.6 REFERENCES**

Anklam, M.R., York, J.D., Helmerich, L. and Firoozabadi, A., 2007. Effects of anti-agglomerants on the interactions between hydrate particles. *AIChE J.*, 54: 565-574.

Anklam, M.R., York, J.D., Helmerich, L. and Firoozabadi, A., 2008. Effects of antiagglomerants on the interactions between hydrate particles. *Aiche Journal*, 54(2): 565-574.

Austvik, T., LI, X. and Gjertsen, L.H., 2000. Hydrate plug properties: formation and removal of plugs. *Annals of the New York Academy of Sciences*, 912(1): 294-303.

Azarinezhad, R., 2010. A chemical based wet cold flow approach for addressing hydrate flow assurance problems, PhD Thesis, Heriot-Watt University, Edinburgh

Camargo, R. and Palermo, T., 2002. Rheological properties of hydrate suspensions in an asphaltenic crude oil, 4th International Conference on Gas Hydrates, Yokohama Symposia, Yokohama, Japan, pp. 19-23.

Colombel, E., Gateau, P., Barré, L., Gruy, F. and Palermo, T., 2009. Discussion of agglomeration mechanisms between hydrate particles in water in oil emulsions. *Oil & Gas Science and Technology-Revue de l'IFP*, 64(5): 629-636.

Dieker, L.E., Aman, Z. M., George, N. C., Sum, A. K., Sloan, E. D., 2009. Micromechanical adhesion force measurements between hydrate particles in hydrocarbon oils and their modifications. *Energy & Fuels*, 23(12): 5966-5971.

Einstein, A., 1906. Effect of Suspended Rigid Spheres on Viscosity. *Ann. Phys*, 4: 289.

Eveson, G., Ward, S.G. and Whitmore, R., 1951. Classical colloids. Theory of size distribution; paints, coals, greases, etc. Anomalous viscosity in model suspensions. *Discuss. Faraday Soc.*, 11: 11-14.

Farris, R., 1968. Prediction of the viscosity of multimodal suspensions from unimodal viscosity data. *Journal of Rheology*, 12: 281.

Fidel-Dufour, A., Gruy, F. and Herri, J.M., 2006. Rheology of methane hydrate slurries during their crystallization in a water in dodecane emulsion under flowing. *Chemical Engineering Science*, 61(2): 505-515.

Gao, S., 2009. Hydrate risk management at high watercuts with anti-agglomerant hydrate inhibitors. *Energy & Fuels*, 23(4): 2118-2121.

Krieger, I.M. and Dougherty, T.J., 1959. Concentration Dependence of the Viscosity of Suspensions. *Trans. Soc. Rheol.*, 3: 137- 152.

Le Ba, H., Cameirao, A., Herri, J.M., Darbouret, M., 2010. Chord length distributions measurements during crystallization and agglomeration of gas hydrate in a water-in-oil emulsion: Simulation and experimentation. *Chemical Engineering Science*, 65(3): 1185-1200.

Mills, P., 1985. Non-Newtonian behaviour of flocculated suspensions. *Journal de Physique Lettres*, 46(7): 301-309.

Pal, R., 2000. Viscosity-concentration equation for emulsions of nearly spherical droplets. *Journal of Colloid and Interface Science*, 231(1): 168-175.

Pal, R. and Masliyah, J., 1990. Rheology of oil in water emulsions with added solids. *The Canadian Journal of Chemical Engineering*, 68(1): 24-28.

Pal, R. and Rhodes, E., 1985. A novel viscosity correlation for non-Newtonian concentrated emulsions. *Journal of Colloid and Interface Science*, 107(2): 301-307.

Palermo, T., Arla, D., Borregales, M., Dalmazzone, C. and Rousseau, L., 2005. Study of the agglomeration between hydrate particles in oil using differential scanning calorimetry (DSC). 5th International Conference on Gas Hydrates, Trondheim, Norway, 1: 332–339.

Pauchard, V. and Palermo, T., 2005. Transformation of a concentrated oil/water emulsion into a gel due to slight hydrates formation, In: *Proceedings of the Fifth International Conference on Gas Hydrates*, Trondheim, Norway.

Roscoe, R., 1952. The viscosity of suspensions of rigid spheres. *British Journal of Applied Physics*, 3: 267.

Taylor, C.J., Dieker, L.E., Miller, K.T., Koh, C.A. and Sloan, E.D., 2008. Hydrate Particles Adhesion Force Measurements: Effects Of Temperature, Low Dosage Inhibitors, and Interfacial Energy, 6th International Conference on Gas Hydrates (ICGH 2008), Vancouver, British Columbia, CANADA.

Taylor, G.I., 1932. The viscosity of a fluid containing small drops of another fluid. *Proceedings of the Royal Society of London. Series A, Containing Papers of a Mathematical and Physical Character*, 138(834): 41-48.

Turner, D., Miller, K. and Sloan, E., 2009. Direct conversion of water droplets to methane hydrate in crude oil. *Chemical Engineering Science*, 64(23): 5066-5072.

Turner, D.J., 2005. Clathrate hydrate formation in water-in-oil dispersions, *Colorado School of Mines*, 220 pp.

Yaghi, B.M., 2001. Viscosity behavior: Correlation of water-in-oil emulsions in presence of solids. *Petroleum Science and Technology*, 19(7): 847-861.

Yan, Y. and Masliyah, J.H., 1993. Effect of oil viscosity on the rheology of oil in water emulsions with added solids. *The Canadian Journal of Chemical Engineering*, 71(6): 852-858.

Yan, Y., Pal, R. and Masliyah, J., 1991a. Rheology of oil-in-water emulsions with added solids. *Chemical Engineering Science*, 46(4): 985-994.

Yan, Y., Pal, R. and Masliyah, J., 1991b. Viscosity correlations for emulsion--solids mixtures as bimodal systems. *Chemical Engineering Science*, 46(7): 1823-1828.

York, D. and Firoozabadi, A., 2009. Effect of Brine on Hydrate Antiagglomeration. *Energy & Fuels* 23: 2937–2946.

York, J.D., 2008. Experimental and theoretical developments in hydrate anti-agglomeration, Ph.D. thesis, Yale University, 207 pages pp.



## **CHAPTER 9 CONCLUSIONS AND RECOMMENDATIONS**

### **9.1 INTRODUCTION**

In this thesis the rheological behaviour of hydrates slurries in high water cut systems was investigated using comprehensive experiments and unique model. The thesis has been divided into three main parts as follows:

- 1) Experimental study to investigate the morphology of water-oil emulsions
- 2) Rheological study of water/oil/hydrate mixtures using HTI viscometer and flow loop
- 3) Bimodal model to predict apparent viscosity of water/oil/hydrate mixture

### **9.2 CONCLUSIONS**

#### **9.2.1 Experimental Study to Investigate Morphology of Water-Oil Emulsions**

AAs have been widely used in the oil and gas production to produce transportable hydrate slurries in the pipelines, but their effects on the morphology of water-oil emulsions before hydrate formation or during hydrate formation have rarely been considered. This study was undertaken to investigate the effect of AA and salt on the morphology of water-oil emulsions. The most important obvious finding to emerge from this study is that:

- Type of emulsion plays an important role in stability of emulsions, as W/O emulsions exhibit much higher stability compared to O/W emulsions.
- Crude oil (A) with higher asphaltene content exhibited higher W/O emulsion stability and AA did not affect its stability, but addition of AA reduced the W/O emulsion stability of the crude oil (B) with low asphaltene content.
- In the case of O/W emulsions, adding water soluble AA significantly improved the stability of the emulsions, for both medium and tight emulsions
- Untreated W/O emulsions behaved as a thick paste at very high water cuts and no phase inversion was observed, as the extra water formed a separate phase. However,

adding a small concentration of AA (0.15-0.3 wt. %) completely changed the emulsion behaviour and resulted in phase inversion.

- Phase inversion point measurement tests showed that droplet hold-up (oil droplets) in the continuous phase (aqueous phase) at the phase inversion point increases with addition of AA, but addition of AA decreases the droplet hold-up (water droplets) when continuous phase is liquid hydrocarbon.
- The morphology of emulsions may change during the hydrate formation process, which strongly depends on the type of the initial emulsion, AA concentration, initial water cut and the nature of the liquid hydrocarbon phase.
- The findings of this study suggest that when the water phase is converted into hydrate, it comes out from the water-oil emulsion and forms a separate solid phase in the system, changing the initial binary water-oil emulsion to a ternary water/oil/hydrate mixture
- The results of this investigation show that crude oil (A) (a natural surfactant-rich crude oil) with O/W emulsion morphology converted to W/O emulsion at lower hydrate volume fractions than oil (C) (an oil poor in natural surfactants) during the hydrate formation process.

### **9.2.2 Rheological Study of Water/Oil/Hydrate Mixtures Using HTI Viscometer and Flow Loop**

A comprehensive set of experiments were conducted using the HTI viscometer to investigate the rheological property of hydrate slurries in high water cut systems. The following conclusions can be drawn from this part of study:

- Addition of a small amount of AA to the W/O emulsions significantly lowers the apparent viscosity of the system before hydrate formation and also during hydrate formation process.
- The findings show that the morphology of water-oil emulsion has a significant effect on hydrate transportability in high water cut systems, as water continuous emulsions can transport more hydrates compared to oil continuous emulsions at sufficient AA concentration.

- A higher AA performance was achieved in the crude oil which exhibited higher W/O emulsion stability. For example, loose W/O emulsion (oil (C)) needed 1 wt% AA to transport around 0.22 of the hydrate volume fraction while for the medium (oil (B)) and tight (oil (A)) W/O emulsions only 0.6 and 0.3 wt% AA were required to transport the same hydrate volume fraction. It was attributed to the presence of natural surfactants (asphaltenes and resins) in the crude oil which are able to reduce adhesive force between hydrate particles (Dieker et al., 2009). Therefore, natural surfactants can act as co-surfactants to improve the effectiveness of commercial AAs.
- AAs with different physicochemical properties result in different rheological behaviour of hydrate slurries. The results suggest that it is possible to produce transportable hydrate slurry in high water cut systems, within a certain range of hydrate volume fraction, using a suitable and efficient AA.
- Blending of oil (C) (with loose W/O emulsion) with an appropriate volume of the rich asphaltenic crude oil (A) (with tight W/O emulsion) significantly improved the performance of AA in the system. This result is very important because it indicates that an appropriate blend of a loose and tight emulsion oil can behave similarly to a medium or tight emulsion and result in large savings in AA consumption
- In this study using viscosity measurements showed that gas hydrate formation and dissociation process has a destabilizing effect on highly stable W/O emulsion (oil (A)) at 70% water cut.
- The presence of NaCl has a positive effect on the performance of the AA (AA1) used in this study, as the ability of the systems to transport hydrate particles improved with addition of NaCl concentration. However, the effect of NaCl on the AA performance almost levelled off after 5 wt. % NaCl.
- In high water cut systems with the presence of an efficient AA, as long as the hydrate volume fraction in the system is below the critical point, it will restart without evidence of hydrate agglomeration after a long period of shut-in

Additionally, a saturated liquid flow loop system was used to further investigate the rheological behaviour of hydrate slurry flow in high water cut systems in the real pipelines. In

total, five tests with crude oil (A) as the liquid hydrocarbon phase were conducted in this study. The following conclusions have been drawn from the results obtained with the flow loop:

- An increase in the measured pressure drops occurred almost immediately after hydrate formation for all tests performed at 60% water cut. Similar trends were observed for apparent viscosity of mixtures for the tests with 60% water cut. These increases have been attributed to phase inversion of oil-in-water emulsion to water-in-oil emulsion.
- Pressure drops in the test with 0.6 wt.% AA are greater than in the test with 1 wt.%. This can be attributed to the formation of larger hydrate aggregates in the low AA concentration test.
- The AA used in this study did not perform so well in freshwater as hydrates deposited on the pipe wall when hydrate volume fraction approached 0.16. However, adding salt considerably reduced the measured pressure drop during hydrate formation and significantly improved hydrate transportability in the flow loop.
- At low pump speed test (150 RPM) hydrate particles deposited on the pipe wall at high hydrate volume fractions, while this was not observed for the high pump speed test (300 RPM).
- The magnitude of pressure drop measurements from the flow loop agrees well with viscosity values from the small scale.
- A correlation was developed for a limited range of the measured pressure drop by flow loop to relate pressure drops to the viscosity values.

### **9.2.3 Proposed model to predict apparent viscosity of water/oil/hydrate mixture**

Experimental results from rheological study of hydrate slurry (Chapter 6) showed that agglomeration of hydrate particles has been responsible for viscosity increases of high water cut systems during hydrate formation. These results also suggested that when water phase in water-oil emulsions converts to hydrate particles, they aggregate and forms separate solid phase in the system, as the binary water and oil emulsion alter to a ternary water/oil/ hydrate system. To predict the viscosity of water/oil/hydrate mixtures in high water cut systems, a bimodal model was proposed. The model considers the viscosity of the mixture, as the viscosity of its binary components, i.e. water-oil emulsion and hydrate suspension. Additionally, a new modified form

of Mills' (1985) equation is suggested to describe the viscosity of a hydrate suspension. A good agreement was found between the model and the experimental mixture viscosity data, using the trapped liquid factor,  $K_v$ , as tuning parameter. For very low AA concentrations ( $\leq 0.3$  mass %), possibly due to the presence of large hydrate aggregates, the model was unable to predict the mixture viscosity accurately. However, increasing the AA concentration resulted in a significant reduction in the trapped liquid factor  $K_v$  and gave very good agreement with the experimental data. For the tests with crude oil (A), which has a high concentration of natural surfactants (asphaltenes and resins), lower  $K_v$  was needed to tune the model compared to the tests conducted with crude oil (B), which has a low concentration of natural surfactants. The model also fits the mixture viscosity data for both oil-in-water-hydrate mixtures and water-in-oil-hydrate mixtures, remarkably well.

The trapped liquid factor  $K_v$  was not constant for the tests with different AA concentrations, but it approached a constant value at high AA concentrations. For the crude oil (A) and AA (AA1) used in this study the value of  $K_v$  approached 1.25 with increasing AA concentration.

A correlation for the value of  $K_v$  as a function of AA concentration was derived, in which  $K_v$  is inversely proportional to the AA concentration. The proportionality constant, B is an empirical parameter that depends on several factors such as the composition of the liquid hydrocarbon phase, AA performance, salt concentration, etc. This correlation could be useful to manage the consumption of AA in different oil and gas production systems.

### 9.3 RECOMMENDATIONS

Based on the results of this study, the following recommendations can be made:

- The biodegradation of crude oil results in the formation of carboxylic acid compounds or naphthenic acids (Sinquin et al., 2007). Recent studies have shown that the acidic fractions in the crude oils contain natural hydrate inhibiting components (Dieker et al., 2009; Fotland et al., 2011). These acidic fractions can change the wettability of hydrate surfaces from water-wet to oil-wet and prevent gas hydrate agglomeration. The effect of natural surfactants such as asphaltene and resins on emulsion stability, performance of AAs and hydrate transportability was investigated using crude oils with low TANs (Total Acid Number) in this study. It is

suggested to investigate the effect of acidic fractions (by providing high acid crude oils) on the performance of AAs and the rheological property of hydrate slurries in high water cut systems using the HTI set-up and flow loop system.

- The rheological properties of hydrate slurries investigated in this study were at water cuts up to 80%. It would be useful to conduct further tests with gas systems, i.e. systems with water without liquid hydrocarbon phase. So, it will be possible to investigate the hydrate particle distribution and hydrate slurry transportability in the pure water phase with the presence of different AA concentrations.
- The oil blending tests were carried out only at oil ratio 20/80 (20 vol. % oil (A) and 80 vol. % oil (C)). It would be useful to conduct further experiments in different ratios and different oil compositions.
- Additional experiments with different crude oils are suggested to evaluate the effect of hydrate formation and dissociation on emulsion stability in high water cut systems.
- It would be beneficial to determine the size and distribution of hydrate agglomerates during hydrate formation process. Measuring the size of hydrate agglomerates for various systems with different AA concentrations and oil compositions would also provide more confidence on the rheological behaviour and modelling of hydrate slurries.
- This investigation developed for the first time a bimodal model to predict apparent viscosity of water/oil/hydrate mixtures in which hydrate aggregates in water-oil emulsions were under gas saturated conditions (no free gas phase is present). The model can be extended to consider free gas phase in a new model with combination of the calculated viscosity of bimodal model as the liquid phase with the free gas phase using the existing models in the literature, e.g., for stratified liquid-gas flow or the homogeneous model for dispersed gas-liquid flow.

## **9.4 REFERENCES**

Dieker, L.E., Aman, Z. M., George, N. C., Sum, A. K., Sloan, E. D., 2009. Micromechanical adhesion force measurements between hydrate particles in hydrocarbon oils and their modifications. *Energy & Fuels*, 23(12): 5966-5971.

Fotland, P., Askvik, K.M. and Slamova, E., 2011. Natural anti-agglomerants in crude oil: Isolation, identification and verification of inhibiting effect, *Proceedings of the 7th International Conference on Gas Hydrates (ICGH 2011)*, Edinburgh, Scotland, United Kingdom.

Mills, P., 1985. Non-Newtonian behaviour of flocculated suspensions. *Journal de Physique Lettres*, 46(7): 301-309.

Sinquin, A., Arla, D., Prioux, C., Peytavy, J. L., Glenat, P., 2007. Gas Hydrate Formation and Transport in an Acidic Crude Oil: Influence of Salt and pH†. *Energy & Fuels*, 22(2): 721-728.

